The Role of Platelets in the Regulation of Pulmonary Infection and Host Defence

O'Shaughnessy, Blaze Georgia

Awarding institution:
King's College London

The Role of Platelets in the Regulation of Pulmonary Infection and Host Defence

Blaze Georgia O'Shaughnessy

A thesis submitted for the degree of Doctor of Philosophy

Experiments described in this thesis were performed in:

The Sackler Institute of Pulmonary Pharmacology

Institute of Pharmaceutical Science

King's College London

Abstract

Background. The implication of platelets in inflammatory disorders, such as asthma, has become increasingly more apparent. Following an inflammatory insult, platelets modulate inflammation by a number of distinct mechanisms, including pulmonary-leukocyte recruitment and release of platelet specific mediators. However, little is known regarding the role of platelets in the regulation of pulmonary infection. Pulmonary colonisation of bacteria, including *Pseudomonas aeruginosa (P.aeruginosa)* and *Staphylococcus aureus (S.aureus)* presents a therapeutic challenge due to antimicrobial resistance (AMR).

Objectives. In this study, the effect of experimentally induced platelet depletion was investigated on infection and inflammatory parameters in a murine model of pulmonary infection. A new approach in targeting AMR was also tested, using a novel antibiotic enhancer compound, HT61.

Methods. C57/B16 mice were experimentally depleted of platelets, 24 hours prior to infection with either sham, *P.aeruginosa* or *S.aureus* embedded agar beads. Bronchoalveolar lavage (BAL) fluid and lungs, kidney and spleen were analysed for inflammatory cells and bacterial load respectively. The role of platelet purinergic receptors was also assessed. *In vitro* assays were performed to investigate the effect of bacteria on platelet function, through measurements of platelet-leukocyte complexes and mediator release. Additional *in vivo* experiments were performed to test enhancer compound, HT61.

Results. Infection induced pulmonary platelet recruitment ($p<0.01$) in addition to a mild state of thrombocytopenia ($p<0.05$). Evidence of platelet activation was detected in infected mice through increased levels of platelet-derived mediators Platelet Factor-4 (PF-4) and Regulated upon activation, normal T-cell expressed and secreted (RANTES) in BAL fluid and platelet-neutrophil complexes ($p<0.01$) in blood. In mice depleted of circulating platelets, there was evidence of systemic bacterial dissemination and weight loss was increased compared to mice with normal platelet levels. Furthermore, pulmonary neutrophil recruitment was significantly reduced 24 hours post infection in mice depleted of circulating platelets. These results were reproduced following inhibition of the $P2Y_{14}$ receptor and use of the ATP/ADP hydrolysing agent, Apyrase.
HT61 as a singular treatment showed no inhibition of *P.aeruginosa* or *S.aureus* bacterial load, however, in combination with Tobramycin an enhanced reduction in bacterial load was observed for two strains of *P.aeruginosa* ($p<0.05$) when compared to treatment with either drug alone.

Conclusions. Here it is demonstrated that infection induces platelet activation and accumulation in the lungs. Mice depleted of circulating platelets or treated with Apyrase or a $P2Y_{14}$ receptor antagonist demonstrated increased weight loss and increased systemic infection, this therefore suggests that in addition to the role played by neutrophils, platelets also have a distinct role in the host defence against bacterial infection.

Furthermore, I demonstrated an enhancement of Tobramycin's efficacy when administered in combination with HT61, highlighting a potential novel treatment to target AMR.

Acknowledgements

I wish to express my sincere gratitude to several people without whom this PhD would not have been possible.

First and foremost, I would like to thank my supervisors Professor Clive Page and Dr. Simon Pitchford. Clive, thank you for believing in me and supporting me over the course of the last few years. I have been incredibly lucky to have you as my supervisor and I have learnt a great deal from you. Simon, thank you for your continued support and guidance throughout my project, your advice has always been invaluable. I would also like to thank my 'everyday supervisor' and good friend- Richard Amison. Working with you has been an absolute pleasure and I could not have asked for a better supervisor. We have laughed together, (I have) cried and I will never forget our hilarious conversations during experiments! Your support, particularly in these last few months, really has carried me through so I am eternally grateful. Thank you also to the other members of the Sackler Institute, particularly Steph, Simon and Sajeel, I have absolutely loved working with all of you and what a team we make!

Next, I would like to thank my boyfriend, Joe. Without sounding too cliché you have been my absolute rock recently and in no way would this PhD have been possible without you. You continually amaze me with your willingness to listen to me talking gobbledygook about platelets and your encouragement with everything I do in life. You have made these last few years so much easier and I can only hope I can repay you somehow in the future.

A special thank you to my Mum and sister for your support. Mum, since I was tiny you have always encouraged me and supported me, and being the most hard working, driven person I know, you have inspired me to take the same approach to life. Thank you for always being there, I owe you so much! Amber, since moving to Singapore you have still been the most

caring, attentive and supportive sister, offering to proofread my thesis and countless phone calls to check up on me. Speaking to you always brightens up my day so thank you so much for being the best sister I could wish for. Also thank you to Tom Olney for supporting me and being the older brother I never had, you make me feel so at ease with your career advice and I always feel way better after speaking with you!

To my Dad and step mum, Rachel- coming home throughout my PhD has been a breath of fresh air. Even if it is supplying me with a much needed gin and tonic and giving me puppies to walk, it has been a wonderful break at times and very much helped to alleviate stress, so thank you for that and your continued support with everything I do.

Finally, a big thank you to all of my friends for your support over the last few years, particularly, Livvy O'Neill for always being there for me since we were little 11-year olds! Having a best friend like you has made my PhD so much easier.

You have all helped in so many ways I can't even describe and I couldn't have done it without all of you, thank you!

Publications Arising from Thesis

- Amison RT, **O'Shaughnessy BG**, Arnold S, Cleary SJ, Nandi M, Pitchford SC, Bragonzi A, Page CP. Platelet Depletion Impairs Host Defence to Pulmonary Infection with Pseudomonas aeruginosa in Mice. *Am J Respir Cell Mol Biol,* 2018, 58 (3): 331-340

- Amison RT, Arnold S, **O'Shaughnessy BG**, Cleary SJ, Ofoedu J, Idzko M, Page CP, Pitchford SC. Lipopolysaccharide (LPS) induced pulmonary neutrophil recruitment and platelet activation is mediated via the P2Y1 and P2Y14 receptors in mice. *Pulm Pharmacol Ther,* 2017, 45: 62-68

- Page CP, **O'Shaughnessy BG**, Barnes P. Pathogenesis of COPD and Asthma, *Handb Exp Pharmacol,* 2017, 237: 1-21

- **O'Shaughnessy BG**, Amison RT, Hu Y, Coates A, Page CP. The Small Quinolone Compound HT61 Enhances Bactericidal Activity of Tobramycin against *Pseudomonas Aeruginosa* and Methicillin Resistant Staphylococcus Aureus *in vitro* and *in vivo (Manuscript in preparation)*

- Cleary SJ, Hobbs C, Amison RT, Arnold S, **O'Shaughnessy BG**, Lefrançais E, Mallavia V, Looney MR, Page CP, Pitchford SC. Platelet recruitment to lungs of mice following LPS inhalation does not require interaction with neutrophils, PSGL-1 or P-selectin *(Manuscript in preparation)*

- **O'Shaughnessy BG**, Amison RT, Coates A, Page CP. Assessing the synergistic effect of the enhancer compound HT61 on Tobramycin activity in a murine lung infection model, *European Respiratory Journal*, 2017, 50 (suppl 61) OA4837

Contents

List of Abbreviations

ACD- Acid Citrate Dextrose

ADP- Adenosine diphosphate

ALI- Acute Lung Injury

AMP- Adenosine Monophosphate

AMR- Antimicrobial Resistance

AnGAP- Anion Gap

ANOVA- One-way Analysis of Variance

ARDS- Acute Respiratory Distress Syndrome

ASPA- Animal (Scientific Procedures) Act

ATP- Adenosine Triphosphate

BAL- Bronchoalveolar Lavage

BCS- Body Conditioning Score

BSA- Bovine Serum Albumin

β-TG- Beta-Thromboglobulin

Ca^{2+}- Calcium

CF- Cystic Fibrosis

cfu- Colony Forming Units

CI- Chemotactic Index

ClfA- Clumping Factor A

ClfB- Clumping Factor B

CLR- C Type Lectin Receptors

COPD- Chronic Obstructive Pulmonary Disease

CTAP-3- Connective Tissue Activating Peptide

DAB- Diaminebenzidine

DMSO- Dimethyl Sulfoxide

DTS- Dense Tubular System

E.coli- *Escherichia coli*

ELISA- Enzyme Linked Immunosorbent Assay

EPS- Extracellular Polymeric Substance

ESAM- Endothelial Cell-Specific Adhesion Molecule

FB-A- Fibrinopeptide A

FB-B- Fibrinopeptide B

FITC- Fluorescein Isothiocyanate

fMLP- N-Formylmethionine-leucyl-phenylalanine

FnBPA- Fibronectin Binding Protein A

FnBPB- Fibronectin Binding Protein B

GP- Glycoprotein

GPCR- G Protein Coupled Receptor

H and E- Haematoxylin and Eosin

Hb- Haemoglobin

$HCO3^-$-Hydrogen Carbonate

Hct- Haematocrit

HEK- Human Embryonic Kidney

h.p.i- Hours Post Infection

H.pylori- *Helicobacter pylori*

HRP- Horse Radish Peroxidase

IACUC- Institutional Animal Care and Use Committee

IBD- Irritable Bowl Syndrome

ICAM 2- Intracellular Adhesion Molecule 2

Ig- Immunoglobulin

IFNγ- Interferon Gamma

IL- Interleukin

i.m- Intramuscular

i.p- Intraperitoneal

Isd- Iron-Regulated Surface Determinant

i.v- Intravenous

JAM- Junctional Adhesion Molecule

KC- Chemokine Receptor Ligand KC (CXCL1)

KCl- Potassium Chloride

K.pneumoniae- *Klebsiella pneumoniae*

LAD- Leukocyte Adhesion Deficiency

LFA1- Lymphocyte function-associated antigen 1

LPS- Lipopolysaccharide

LPxTG- Leucine-Proline-x-Threonine-Glycine

MAdCAM 1- Mucosal Vascular Addressin Cell Adhesion Molecule 1

MDC- Macrophage Derived Chemokine

MFI- Mean Fluorescence Intensity

$MgCl_2$- Magnesium Chloride

MIP-1α- Macrophage Inflammatory Protein- 1α

MMP- Matrix Metalloproteinases

mL- Millilitres

MRSA- Methicillin- resistant *Staphylococcus aureus*

MS- Multiple Sclerosis

MSSA- Methicillin- susceptible *Staphylococcus aureus*

$NaHCO_3$- Sodium Hydrogen Carbonate

$Na_2HPO_4.12H_2O$- Sodium Dihydrogen Phosphate Dodecahydrate

NAP-2- Neutrophil activating peptide-2

NaOH- Sodium Hydroxide

NET- Neutrophil Extracellular Trap

ng- Nanograms

NK- Natural Killer

NLR- NOD like Receptor

o.a- Oropharyngeal

OCS- Open Canalicular System

OD- Optical Density

ONC- Overnight Culture

***P.aeruginosa*-** *Pseudomonas aeruginosa*

PAF- Platelet Activating Factor

PAMP- Pathogen Associated Molecular Pattern

PBP- Platelet Basic Protein

PBP- Penicillin Binding Protein

PBS- Phosphate Buffered Saline

PCO2- Partial Pressure Carbon Dioxide

PCR- Polymerase Chain Reaction

PCV- Packed Cell Volume

PDGF- Platelet Derived Growth Factor

PE- Phycoerythrin

PECAM- Platelet Endothelial Cell Adhesion Molecule

PF-4- Platelet Factor- 4

PGE_1- Prostaglandin E1

PI- Propidium Iodide

PKC- Protein Kinase C

PLC- Phospholipase C

PMC- Polymononuclear Cell

PMP- Platelet Microbicidal Protein

PPP- Platelet Poor Plasma

PRP- Platelet Rich Plasma

PRR- Pathogen Recognition Receptors

PSGL-1- P-selectin Glycoprotein Ligand 1

RA- Rheumatoid Arthritis

RANTES- Regulated on Activation, Normal T- cell Expressed and Secreted

RGD- Arginine Glycine Aspartate

RLR- RIG-1 like Receptors

RPM- Rotations Per Minute

S.aureus*- *Staphylococcus aureus

SDF-1α- Stromal Cell Derived Factor 1α

SEM- Standard Error of the Mean

***S.gordonii*-** *Streptococcus gordonii*

***S.pneumoniae*-** *Streptococcus pneumoniae*

***S.pyogenes*-** *Streptococcus pyogenes*

***S.sanguinis*-** *Streptococcus sanguinis*

NaCl- Sodium Chloride

TARC- Thymus Activated on Regulated Chemokine

Tβ-4- Thymosin β-4

TCO2- Total Carbon Dioxide

TGFB- Transforming Growth Factor Beta

TLR- Toll-like Receptor

TNFα- Tumour Necrosis Factor Alpha

TRAP- Thrombin Receptor Activating Peptide

TSA- Tryptic Soy Agar

TSB- Tryptic Soy Broth

TxA_2- Thromboxane

UDP- Uridine Diphosphate

UTP- Uridine Triphosphate

VCAM-1- Vascular Cell Adhesion Protein 1

VEGF- Vascular Endothelial Growth Factor

VLA4- Very Late Antigen 4

vWF- Von Willebrand Factor

w/v- Weight Per Volume

µL- Microliters

List of Tables

Chapter I: Introduction

Chapter II: Materials and Methods

List of Figures

Chapter I: Introduction

Chapter II: Materials and Methods

Chapter III: Results I

Chapter IV: Results II

Chapter V: Results III

Chapter VI: Discussion

Chapter I

Introduction

1.1 Pulmonary infection with *Pseudomonas aeruginosa* and *Staphylococcus aureus*

1.1.1 *Pseudomonas aeruginosa*

P.aeruginosa is a highly motile, gram-negative bacterium, preliminarily identified by its distinctive grape-like odour and white, pearlescent appearance of colonies. *P.aeruginosa* is a versatile bacterium able to grow in soil and aqueous environments, in addition to on plant and animal tissue (Stover et al., 2000) (Gellatly and Hancock, 2013). *P.aeruginosa* is a major opportunistic pathogen, accounting for between 17-26% of all nosocomial infections (Nanvazadeh et al., 2013) and it typically establishes itself in the respiratory, urinary and gastrointestinal tracts of immunodeficient individuals, with infection prevalent in patients with severe burns, acute leukaemia, urinary-tract infections in catheterised patients and in patients who have received organ transplants (Di Lorenzo et al., 2015) (Stover et al., 2000) (Nanvazadeh et al., 2013) (Gellatly and Hancock, 2013). *P.aeruginosa* is now recognised as a major colonising pathogen in the pathophysiology of cystic fibrosis (CF) (Di Lorenzo et al., 2015) (Van Heeckeren et al., 1997), with *P.aeruginosa* infection established in 70-80% of CF patients (Lyczak et al., 2002). *P.aeruginosa* is also the predominant cause of morbidity and mortality in CF patients (Stover et al., 2000).

P.aeruginosa can exist in non-mucoid and mucoid forms; non-mucoid strains initially colonise the lung, causing transient pulmonary infections in early life (Di Lorenzo et al., 2015) (Friedl et al., 1992), followed by the predominance of the mucoid form in the subsequent course of disease. Mucoid strains are frequently isolated from the respiratory tracts of patients with CF and chronic obstructive pulmonary disease (COPD) (Friedl et al., 1992), and these strains produce large quantities of viscous polysaccharide. Mucoid strains of *P.aeruginosa* persist in the lung forming biofilms (Patrauchan et al., 2007). This establishes a chronic, persistent

infection (Di Lorenzo et al., 2015) (Costerton et al., 1999), associated with incessant cycles of airway obstruction and chronic inflammation, leading to the progressive loss of respiratory function (Gibson et al. , 2003) (Dhooghe et al., 2014).

1.1.2 Biofilm Formation

Several species of bacteria possess the ability to become associated with one another and irreversibly adhere to wet, solid surfaces to form a coat, called a biofilm (Klausen et al., 2003). A biofilm may be defined as a highly organised, structured community of bacterial cells embedded in a self-producing matrix of extracellular polymeric substance (EPS) (Bjarnsholt, 2013). Biofilms preferentially develop on both living surfaces, in the case of endocarditis, and inert, non-living surfaces, such as on medical devices and sequestra of dead bone (Costerton et al., 1999). Furthermore, biofilms can be present in natural, industrial or hospital environments.

P.aeruginosa is a bacterium that can form a structured consortium of bacteria on moist surfaces, acting as a protective mechanism of growth in a hostile environment. Biofilm formation is a major survival mechanism of *P.aeruginosa* and aides evasion of the host defences (Bjarnsholt, 2013). It has been suggested that mucoid forms of *P.aeruginosa* can form a biofilm on host tissues and epithelial surfaces during chronic infections, particularly in the CF lung (Gellatly and Hancock, 2013) (Friedl et al., 1992) (Dötsch et al., 2012). Biofilms are a hallmark of *P.aeruginosa* chronic infection, and the incessant cycles of infection and inflammation experienced by patients with long term pulmonary colonisation by *P.aeruginosa* exemplifies most biofilm infections (Costerton et al., 1999).

Nasal carriage of the gram-positive *S.aureus* allows bacteria to disseminate to other parts of the body, where it is either removed by the immune system of the host, or attaches to extracellular matrix proteins of the host to form a multi-layered, heterogeneous biofilm (Archer et al., 2011). *S.aureus* infections possess the ability to rapidly develop multiple-antibiotic resistance, and transform acute, transient infections into ones of a recurrent, chronic nature (Archer et al., 2011).

Biofilm formation is a sequential process, involving several different phases (**Figure 1.1**). Initially, bacteria migrate towards a nutrient rich surface (Klausen et al., 2003). This is followed by the attachment phase; whereby motile and non-motile subpopulations of bacteria attach to the solid surface. This reversible interaction is mediated by van der Waals and electrostatic forces, and reinforced by host and tissue-specific adhesins, such as flagella and pili (Kaplan, 2010). Maturation and clonal growth follows the attachment phase, where microcolonies differentiate into 'true' biofilms of EPS encased communities (Costerton et al., 1999). During this phase, the motile bacterial subpopulation spread out along the substratum and non-motile bacteria form a microcolony (Bjarnsholt, 2013). Immobilised aggregates of bacteria begin to spontaneously secrete EPS, composed of nucleic acids, polysaccharide and macromolar components. This forms a matrix, which attracts motile bacteria and forms mushroom-like shaped structures (Bjarnsholt, 2013) (Klausen et al., 2003). The final stage of biofilm development is the detachment of sessile bacteria from the biofilm, and dispersal into the environment to colonise new areas (Kaplan, 2010) (Costerton et al., 1999).

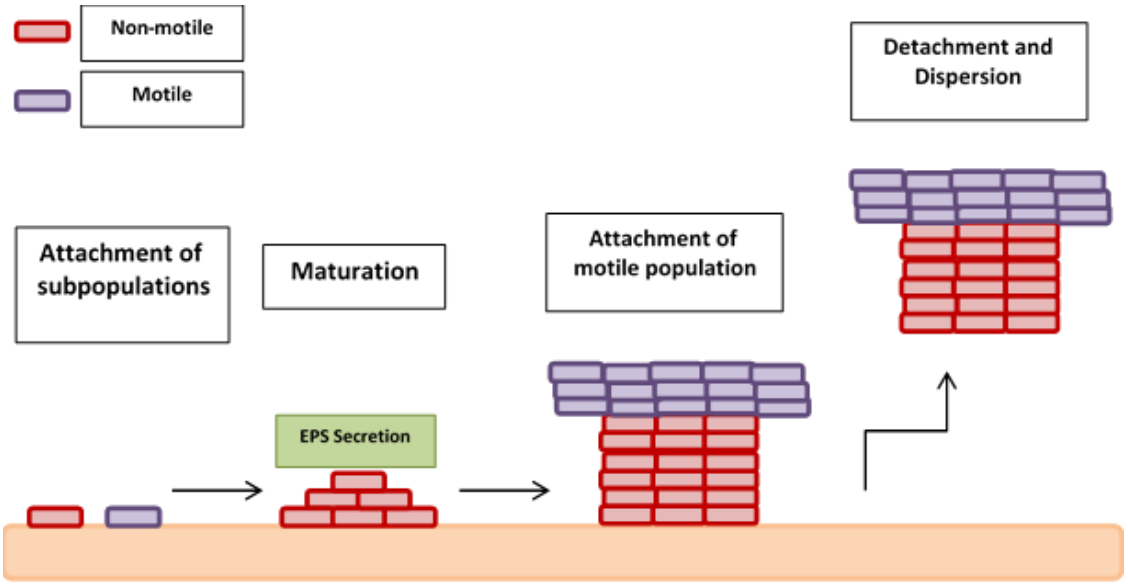

Figure 1. 1 The Process of Biofilm Formation

Sessile bacteria present in biofilms are significantly less susceptible to antimicrobial agents than their planktonic (non-attached, free swimming) counterparts (Gellatly and Hancock, 2013) (Archer et al., 2011), due to the heterogeneous subpopulations of bacteria contained within them (Stewart, 2002). Antibiotic therapy often alleviates the symptoms of pulmonary infection, yet fails to eradicate the infection within a biofilm community (Costerton et al., 1999). One potential mechanism of biofilm resistance to antimicrobial agents is the inability of antimicrobials to penetrate the entire depth of the biofilm, with components of the matrix slowing down the diffusion rate of antibiotics and host defence molecules (Gellatly and Hancock, 2013) (Stewart, 2002) (Costerton et al., 1999). Furthermore, mature biofilms are highly heterogeneous; microenvironments established within the biofilm are exposed to different physiochemical characteristics, such as varying gradients in pH, O_2, nutrients and waste material (Batoni et al., 2016) (Archer et al., 2011), where these factors may impact the activity of antimicrobial agents. Biofilm embedded bacteria possess many advantages over

planktonic bacteria, including the ability to evade multiple clearance mechanisms produced by the host and synthetic sources. Biofilm embedded bacteria are resistant to clearance strategies by antimicrobial agents, shear stress, host phagocytic elimination and host radical and protease defences (Archer et al., 2011). This has been demonstrated in the literature, whereby *P.aeruginosa* planktonic and young biofilm cells were susceptible to killing by Tobramycin and Piperacillin, resulting in total eradication. In contrast, older *P.aeruginosa* biofilm cells were reduced to approximately 20% of the total population and regrowth of the organism occurred following antibiotic therapy (Anwar et al., 1992). This demonstrates the reduced susceptibility of biofilm embedded bacteria to antimicrobial agents.

Biofilm-associated infections result in chronic disease and the progression of a biofilm is now recognised as a major mediator in infection. The high intrinsic and inducible resistance of biofilms to antimicrobials contributes towards their resilience, and consequently, the prevention and management of biofilm- associated infections represents a serious therapeutic challenge (Nanvazadeh et al., 2013). In this context, experimental models could be established to investigate the potential anti-biofilm activity of antimicrobial agents, as the majority of research groups investigate this *in vitro,* which is perhaps not truly representative of the pathophysiological processes involved in biofilm formation in chronic disease.

1.1.3 Staphylococcus aureus

S.aureus is a non-motile, gram-positive coccus bacterium, that forms distinctive irregular grape-like clusters. *S.aureus* is a commensal bacterium, which grows on the skin and nasal mucus membrane, and in the human population, 20-25% have become persistently colonised (Archer et al., 2011). However, *S.aureus* is also a leading cause of infection in humans, causing

a wide array of diseases, ranging from minor skin and soft tissue infections, to the more life-threatening, septicaemia, endocarditis, toxic shock syndrome and pneumonia (Diep et al., 2006) (Hu, 2013).

Methicillin was introduced to the clinic in 1959 to treat *S.aureus* infections (Stapleton and Taylor, 2007). Two years later however, in the United Kingdom, it was reported that isolates of *S.aureus* had acquired resistance to Methicillin (Enright et al., 2002). Methicillin-resistant *Staphylococcus aureus* (MRSA) is now one of the most common pathogens implicated in both hospital and community-acquired infections (Hu, 2013) (Enright et al., 2002) (Diep et al., 2006); frequently associated with infections in health care facilities, sports facilities, clinics and the community, and in patients presenting to the intensive care unit (Green et al., 2012).

Formerly, MRSA infections were acquired exclusively in hospitals. Prior exposure of patients to healthcare associated risk factors, such as previous antibiotic therapy, surgery, admission to an intensive care unit and exposure to an MRSA colonised patient, increased the likelihood of MRSA colonisation (Chambers, 2001). However, the prevalence of MRSA infections has dramatically increased due to the emergence of community-acquired strains of MRSA in healthy individuals (Diep et al., 2006). Colonisation of the lower respiratory tract by *S.aureus* and MRSA can occur in chronic pulmonary diseases, such as COPD (Defres et al., 2009), or due to breaches in natural defences, such as endotracheal intubation (Defres et al., 2009). The most commonly reported MRSA infections in patients include septic shock (56%), pneumonia (32%), endocarditis (19%), bacteraemia (10%) and cellulitis (1%) (Green et al., 2012), and these infections are now associated with significant increases in length of hospital stay, cost of treatment and mortality rate (Klevens et al., 2007) (Archer et al., 2011) (Green et al., 2012).

1.2 Antibiotic Resistance

1.2.1 An Introduction to Antibiotic Resistance

During the era of antibiotic discovery (1940-1960), more than 15 different classes of antibiotics were developed and produced (Hu et al., 2010) (Martens and Demain, 2017). These antibiotics typically target multiplying bacteria (Hu, 2007), yet are inefficient at killing non-multiplying bacteria or persister cells (Hu et al., 2010) (Martens and Demain, 2017) thus resulting in only the partial clearance of the total bacterial population (**Figure 1.2**). A more prolonged duration of antibiotic therapy is therefore often required to control bacterial infections, increasing the possibility of emergence of resistance (Hu et al., 2010). The reduced efficacy of current antibiotics in combination with a steady decline in the discovery of novel compounds (Martens and Demain, 2017) has exacerbated the emergence of antibiotic resistance. Inappropriate antibiotic use by humans is a significant driver of this problem, for example misuse and overuse of antibiotics, poor management of childhood and hospital-acquired infections, and use of antibiotics in agriculture to prevent disease in livestock (Laxminarayan, 2014).

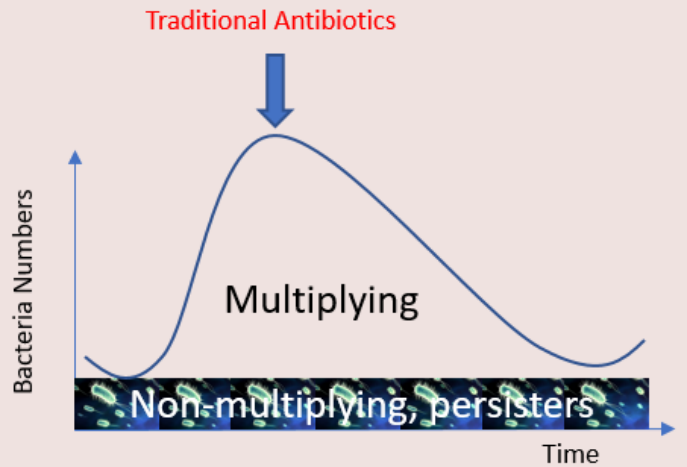

Figure 1. 2 The Action of Traditional Antibiotics

Figure adapted from:
http://www.ukpharmsci.org/2012resourcepack/PDFPresentations/TCS1_1540_Prof_Anthony_Coates.pdf:
Prof Anthony Coates, St George's University of London, Antibiotic Discovery

As a result of a significant increase in resistance, infectious disease is now the second leading cause of mortality in the world, with drug-resistant bacteria killing ~25,000 people per year in Europe (Martens and Demain, 2017). Some infections that were previously susceptible to antibiotics, such as *Neisseria gonorrhoeae* with penicillin, are now entirely resistant (Laxminarayan, 2014). This exemplifies the critical requirement for a novel approach towards antibiotic discovery and use, in addition to the conservation of current antimicrobials.

Colistin remains the last line of defence against many gram-negative bacteria, due to their resistance to multiple antimicrobial agents. However, as a likely consequence of increased Colistin use, Colistin-resistant bacteria have now been reported (Giani et al., 2015). This research reports a large nosocomial outbreak of 93 bloodstream infections with Colistin-resistant *Klebsiella pneumoniae (K.pneumonaie).* This clearly highlights the critical requirement for novel antimicrobial agents in the clinic, which show efficacy against multiple drug resistant bacteria.

1.2.2 Mechanisms of Antibiotic Resistance

P.aeruginosa is a versatile and adaptable microorganism, able to evade the activity of antimicrobial agents. The emergence of mutator variants in chronic infections further increases its adaptability and development of resistance to antimicrobials (Cabot et al., 2016). *P.aeruginosa* exhibits the highest rates of resistance towards fluoroquinolones, with resistance to ciprofloxacin ranging from 33-34% of all isolates (Flamm et al., 2004), in comparison to Aminoglycoside and β-lactam antibiotics (Tobramycin: 12-16%, Ceftazidime: 12-15%) (Flamm et al., 2004). Multidrug resistant strains of *P.aeruginosa* represent a more serious therapeutic challenge, displaying resistance to three or more classes of antibiotics (Flamm et al., 2004). Recent research has reported that 24.9% of *P.aeruginosa* strains, isolated from wounds, blood and respiratory tracts of patients, displayed multidrug resistance (Flamm et al., 2004), highlighting the ongoing concern for isolates exhibiting antimicrobial resistance.

During the course of chronic pulmonary infection in patients with CF, *P.aeruginosa* strains develop mutants that differ both phenotypically and genotypically to the initial infecting strain (Bragonzi et al., 2009). The major resistance mechanism in chronic *P.aeruginosa* infections, such as CF, is the production of high levels of β-lactamase (Campbell et al., 1997) (Zaidenstein et al., 2018). β-lactamases are cephalosporinase enzymes, which are encoded by an inducible AmpC gene and are responsible for the metabolism of β-lactam antibiotics. In wild type *P.aeruginosa* strains, AmpC cephalosporinase is expressed at low levels, however the pathway is induced following exposure to β-lactam antibiotics (Cabot et al., 2016). Mutation to constitutive high level β-lactamase production occurs spontaneously and this mediates resistance to β-lactam antibiotics (Colom et al., 1995). The genetic events

underlying the overproduction of the enzyme in resistant clinical isolates have not been elucidated, however it is reported that the enhancement of β-lactamase levels may occur either through the acquisition of a secondary β-lactamase, amplification of the gene encoding the chromosomal β-lactamase or mutations in the regulatory genes that control the expression of the β-lactamase gene (Campbell et al., 1997) (Colom et al., 1995).

The outer membrane of *P.aeruginosa* contains water filled protein channels, called porins (Bajaj et al., 2017). These channels play an important role in the transportation of nutrients, ions, vitamins and proteins through biological membranes (Bajaj et al., 2017) (Ochs et al., 1999). Additionally, certain classes of hydrophilic antibiotics are transported across the membrane via porins, for example OprD is responsible for the transportation of carbapenems, including Imipenem (Ochs et al., 1999). Research has reported that two predominant types of imipenem-resistant mutants are observed in the clinic, both involving the porin channel, OrpD (Ochs et al., 1999). Firstly, OrpD-mediated resistance occurs as a result of deletions in the OrpD coding region and the upstream promoter region. Secondly, bacteria displaying multiple antibiotic resistance to both imipenem, quinolones and chloramphenicol show a marked reduction in the expression of OprD in the outer membrane (Ochs et al., 1999) (Cabot et al., 2016). A loss of function and inactivation of the membrane porin channels prevent antimicrobial agents from crossing bacterial membranes and further contribute to the complexity and concern about antimicrobial resistance. In addition to the production of inducible AmpC cephalosporinases and the reduced permeability of the outer membrane, *P.aeruginosa* expresses constitutive and inducible efflux pumps which further contribute to the genetic antibiotic resistance machinery of *P.aeruginosa* (Cabot et al., 2016).

Similarly, *S.aureus* has the ability to rapidly develop resistance towards antimicrobial agents through the acquisition of resistance genes or through chromosomally encoded resistance mechanisms. Methicillin is a β-lactam antibiotic, which acts by inhibiting penicillin-binding proteins (PBPs). β-lactam antibiotics function to inhibit the transpeptidation domain of PBPs, thus interfering with the cross-linking reaction. Without the cross-linking of peptidoglycan, the cell wall is weakened, resulting in leakage of the bacterial cell contents and cell death (Stapleton and Taylor, 2007). PBPs are involved in the synthesis of a mesh-like structure, called peptidoglycan, which is an essential component of the Staphylococcal cell wall. There are four native subtypes of PBPs in *S.aureus*, PB1, PB2, PB3 and PB4, which are essential for the growth and survival of the bacteria (Pereira et al., 2007). These PBPs have different molecular weights; with high molecular weight PBPs possessing two protein domains, one involved in transpeptidation and the other involved in transglycosylation (Stapleton and Taylor, 2007). Furthermore, these PBPs elicit different susceptibilities to antimicrobials, most likely a reflection of differential PBP affinity (Georgopapadakou and Liu., 1980).

Resistance to Methicillin in *S.aureus* is, in part, conferred through the expression of a foreign PBP, called PBP2a, which is encoded by the *mecA* gene (García-Álvarez et al., 2011) (Pereira et al., 2007). Synthesis of PBP2a is regulated and usually expressed low at basal levels, however synthesis is enhanced if mutations occur in the regulatory genes (Stapleton and Taylor, 2007). In contrast to the native PBPs, PBP2a shows an extremely low affinity for most β-lactam antibiotics, consequently PBP2a can take over the transpeptidase function of cell wall synthesis in the presence of therapeutic levels of methicillin, which would usually inhibit the function of other PBPs (Pereira et al., 2007) (García-Álvarez et al., 2011).

The emergence of mutant forms of *P.aeruginosa* and *S.aureus,* which display reduced susceptibility to antimicrobial agents and possess a wide array of resistance mechanisms, demonstrate that a novel approach for the discovery of antibiotics is critical to allow the continuation of the antibiotic era.

1.2.3 Antibiotic Enhancer Compounds

Within a bacterial population, both multiplying and non-multiplying bacteria co-exist (Hu et al., 2010). Antibiotics are typically developed to target the multiplying subpopulation of bacteria and all commercially available antibiotics currently work via this mode of action (Hu et al., 2010). However, these agents are either inactive or only partially active against non-multiplying or slow multiplying bacteria (Belley et al., 2009). Consequently, this leads to the partial death of the total target population, requiring repeated doses of antibiotics and in turn, enhancing the emergence of resistance (Hu et al., 2010). Furthermore, in some cases, it is not feasible to significantly enhance doses of antibiotics as a result of their toxic side effects (Hu et al., 2010).

One potential strategy for eradicating bacterial infection is by targeting the non-multiplying population of bacteria, thereby swiftly removing the total target bacterial population and in turn, shortening the duration of therapy. Shortening antibiotic treatment regimens has the added benefit of reducing side effects for patients, reducing cost of treatment and slowing the emergence of antibiotic resistance (Coates and Hu, 2008). Enhancer compounds have been developed as a strategy to provide improved treatments for infectious diseases, which act by restoring sensitivity of resistant bacteria to currently commercially available antibiotics. Furthermore, enhancer compounds target both multiplying and non-multiplying bacteria (Hu,

2013). Hu and colleagues have developed such a drug, the antibiotic enhancer, HT61, a small quinolone derived compound as an exemplar of this novel approach.

The activity of HT61 was tested and compared to commercially available antibiotics, including Amoxicillin and Levofloxacin and it was demonstrated that HT61 as a singular treatment was more active against non-multiplying Methicillin-susceptible *Staphylococcus aureus* (MSSA), producing a 7 log CFU/ml reduction in bacteria, when compared to currently available antibiotics, which failed to exhibit any activities against non-multiplying bacteria (Hu et al., 2010). Intriguingly, HT61 was less active against multiplying *S.aureus*, when compared to commercially available antibiotics, and despite showing activity against non-multiplying gram-positive bacteria, had no activity against gram-negative bacteria, including *P.aeruginosa* (Hu et al., 2010).

With the aim of restoring sensitivity to drug resistant bacteria, experiments were performed using HT61 in combination with commercially available antibiotics. Intriguingly, time-kill analysis reported an enhancement of the activity of older generation antibiotics (gentamicin, neomycin and chlorhexidine) when used in combination with HT61 (Hu, 2013) against MRSA and MSSA, eradicating the total bacterial population by 2-8 hours.

It was elucidated that the compound acts on the bacterial cell membrane, causing cell depolarisation and the release of the intracellular contents of the cell, leading to bacterial destruction (Hubbard et al., 2017). In addition, the cell wall structure was nicked in the presence of high concentrations of HT61 (Hu et al., 2010), allowing greater cellular access to the antibiotic. Furthermore, it is postulated that HT61 by disrupting the membrane, the membrane-embedded enzymes that are involved in anaerobic metabolism are disrupted. Therefore, non-multiplying bacteria are required to activate their anaerobic metabolic

pathways when they are oxygen deprived and consequently become susceptible to killing by compounds that poison the respiratory chain (Hu, 2013). It has been reported elsewhere in the literature that antimicrobial combinations that display *in vitro* synergistic effects may be more effective in eradicating infections in patients, for example against Tobramycin resistant strains of *P.aeruginosa* (Chan and Zabransky, 1987). These observations have also been supported by other studies, which have demonstrated the enhancement of the activity of Doxycycline with ianthelliformisamine derivatives against resistant gram-negative bacteria (Pieri et al., 2014).

These studies highlight the potential beneficial effects of using combination treatments and enhancer compounds to target drug-resistant bacteria and to eradicate infection.

1.3 Platelets

1.3.1 Platelet Development and Production

The platelet is an anucleated, specialised component of the blood, which primarily functions as a regulator of haemostasis in response to vascular injury. It is well documented that circulating platelets have a characteristic discoid shape under normal resting conditions (Hartwig et al., 2003) and an approximate size of 1-3 µm (Machlus and Italiano, 2013). Platelets are present at high concentrations in the human blood, typically ranging from 1.5-4.0 x 10^8 platelets/mL, and once released into the circulation, have a typical lifespan of 8-10 days (Thon and Italiano, 2012). Whilst the precise mechanism remains unclear, platelets derive from the fragmentation of megakaryocytes and (Radley and Scurfield, 1980) were the first to postulate that long pro-platelet extensions from megakaryocytes were linked to the

production and release of platelets. In order to maintain adequate platelet levels, approximately 10^{11} platelets are replenished daily from megakaryocytes residing in the bone marrow (Hartwig et al., 2003).

The development and production of platelets is a complex process and can be arbitrarily divided into two main phases (Hartwig et al., 2003) (Machlus and Italiano, 2013). The first phase occurs over a period of days and requires megakaryocyte specific growth factors (Hartwig et al., 2003). During this phase, the cytoplasm of the megakaryocytes becomes enlarged and is filled with cytoskeletal proteins and platelet specific granules (Thon and Italiano, 2012) (Machlus and Italiano, 2013). The second phase of platelet development is much more rapid and is completed within hours. During the second phase, it has been proposed that the cytoplasm of the megakaryocyte remodels itself into multiple long, branching extensions, termed pro-platelets (Richardson et al., 2005) (Hartwig et al., 2003). In this case, platelets form at the tip of the pro-platelet extensions, extruding outwards from the cell body of the megakaryocyte. Prior to the release of mature platelets into the circulation, nascent platelets must be packaged and assembled with platelet organelles and granules (Machlus and Italiano, 2013). Pro-platelets function as the assembly line of platelet production, with the shaft of the pro-platelet serving as a track to transport the organelles and granules from the regions of synthesis within the megakaryocyte to the pro-platelet (Thon and Italiano, 2012) (Machlus and Italiano, 2013). This transportation process is bidirectional, culminating at the end of the pro-platelet (Thon and Italiano, 2012), where the platelet organelles and granules can be assembled and packaged, thus completing platelet maturation prior to their subsequent release (Kosaki, 2005) (Leven and Yee, 1987) (Tablin et al., 1990). The process of megakaryopoiesis and platelet production occurs over a time period of approximately 5 days in humans (Machlus and Italiano, 2013), and intriguingly, a single

megakaryocyte can form 10-20 pro-platelet extensions (Machlus and Italiano, 2013) and give rise to 1,000-3,000 platelets (Thon and Italiano, 2012).

It remains unclear as to where this process occurs as platelets have been shown to be produced from megakaryocytes within the pulmonary circulation (Trowrridge et al., 1982) (Martin et al., 1983), which is suggestive of the occurrence of thrombopoiesis in an additional organ asides from the bone marrow. Indeed, the formation of pro-platelets from megakaryocytes isolated from humans, mice and guinea pigs has been demonstrated *in vitro* (Cramer et al., 1997) (Leven and Yee., 1987) (Tablin et al., 1990) (Radley and Haller, 1983). Moreover, the release of platelets from pro-platelet tips has been demonstrated using intravital microscopy in mice (Junt et al., 2007) and pro-platelets extending into the sinusoidal blood vessels of bone marrow has been observed (Zhang et al., 2012). Asides from animal models, in the clinic it has been reported that platelet production from megakaryocytes can increase by as much as 20-fold under conditions of peripheral demand and inflammation (Bozza et al., 2009). Significant increases in pulmonary megakaryocytes have been detected in patients with acute lung injury, acute respiratory distress syndrome (ARDS) and in patients dying from burns, and in addition, platelet life span and platelet turnover rates are altered in these patients (Mandal et al., 2007).

The experimental and clinical evidence demonstrating enhanced platelet production and megakaryopoiesis in the lung is suggestive of a potential role for platelets as effector cells in a variety of pulmonary disorders (Weyrich and Zimmerman, 2013).

1.3.2 Platelet Ultrastructure

Platelets have a complex structure, containing a number of distinguishable structural elements that allow them to function as regulators of haemostasis, angiogenesis and innate immunity. The plasma membrane of the platelet is composed of a phospholipid bilayer, comprising of cholesterol, glycolipids and glycoproteins, and further contains a plethora of densely packed receptors that are requisite in signaling and intracellular trafficking of the platelet (Thon and Italiano, 2012). In addition, the plasma membrane contains membrane foldings, which are the entrances to a system of internal membranes called the open canalicular system (OCS) (Hartwig, 2013) (Bearer et al., 2002). The OCS is a network of membrane channels that run throughout the platelet, which has several functions. The OCS allows for the selective entry of external elements into the platelet and serves as a conduit into which platelet granules fuse and release their contents (Hartwig, 2013). Studies have demonstrated that following platelet activation, degranulation occurs most often into the OCS, with granule contents subsequently released through pores into the extracellular space (Stenberg et al., 1984). Furthermore, the OCS may facilitate filopodia formation and cell spreading following platelet adhesion to an activating surface and acts as a storage site for plasma membrane glycoproteins (Thon and Italiano, 2012). The dense tubular system (DTS) of the platelet is a closed-channel network of residual endoplasmic reticulum, which is involved in calcium ion (Ca^{2+}) sequestration (Bearer et al., 2002).

Also contained within the platelet are a vast array of different organelles, including mitochondria, peroxisomes, lysosomes and granules, which contain a large number of biologically active molecules (Bearer et al. 2002). The mediators contained within platelet granules are implicated in the regulation of haemostasis, inflammation and infection, and are

requisite in determining platelet function following activation (Smyth et al., 2009). Platelet granular contents are listed in **Table 1.1**.

Platelets contain three main types of granule within their cytoplasm, α-granules, dense (δ) granules and lysosomal (λ) granules. Previous published research has demonstrated that thrombin stimulation of platelets results in the release of preformed mediators from platelet α-granules (Stenberg et al., 1984), thus highlighting that platelet activation leads to granular release. Platelet α-granules are the largest (approximately 0.2-0.5 μm in diameter) and most abundant granule (50-80 per platelet) (King and Reed, 2002) (Yun et al., 2016). The α-granules contain mediators requisite in platelet adhesion during vascular repair and haemostatic functions. The α-granules store matrix adhesive proteins (fibrinogen, fibronectin, thrombospondin, vitronectin and von- Willebrand Factor (vWF)), and have glycoprotein (GP) and platelet adherence receptors embedded in their membranes (P-selectin, GPIb-IX-V, integrin αIIβ3), which promote adhesion between platelets and the matrix (Hartwig, 2013) (Thon and Italiano, 2012).

In contrast to α-granules, platelets contain considerably less dense granules, with approximately 3-9 present in human platelets (King and Reed, 2002). Dense granules are approximately 0.15 μm in diameter and they function primarily to enhance platelet activation through the secretion of additional platelet agonists. Dense-granules contain a variety of haemostatically active molecules, including adenosine triphosphate (ATP), adenosine diphosphate (ADP), serotonin and Ca^{2+} (Hartwig, 2013) (Yun et al., 2016), which upon platelet activation promote aggregation. Furthermore, they contain a large array of chemokines, including Macrophage Inflammatory Protein-1α (MIP-1α) and Regulated on Activation,

Normal T Cell expressed and Secreted (RANTES), which can amplify platelet activation and induce platelet and leukocyte migration (Smyth et al., 2009).

The third type of platelet secretory granules are lysosomal granules, which contain glycosidases, acid proteases, and cationic proteins, including collagenase and β-glucuronidase, which may possess bactericidal activity and aid in pathogen clearance (Yun., 2016) (Jenne et al., 2013).

α-granules	Dense granules	Lysosomal granules
Multimerin	***ADP * ~ #***	***Acid Proteases***
Adhesive glycoproteins	***ATP * ~***	Cathespin D
von Willebrand factor *	***Calcium * ~ #***	Cathespin E
Fibrinogen * #	***Serotonin * ~ #***	Carboxypeptidase A
von Willebrand factor propeptide	***Pyrophosphate***	Carboxypeptidase B
Fibronectin * #	***GDP ****	Prolinecarboxypeptidase
Thrombospondin-1 * #	***Magnesium***	Collagenase #
Vitronectin * ~		Acid Phosphatase
	Other secreted or released proteins	Arylsulphatase
Coagulation factors	Protease nexin I *	
Factor V *	Gas6 *	***Glycohydrolases***
Protein S *	Amyloid b-protein precursor	Heparinase
Factor XI *	Tissue factor pathway inhibitor	β-*N*-acetyl-glusaminase
	Factor XIII *	β-glucuronidase #
Mitogenic factors	α_1-Protease inhibitor	β-galactosidase
Platelet-derived growth factor * ~ #	Complement I inhibitor * ~	α- glucosidase
Transforming growth factor-b ~ #	High molecular weight kininogen	
Endothelial cell growth factor ^	α_2-Macroglobulin *	
Epidermal growth factor	Vascular permeability factor	
Insulin-like growth factor I	Interleukin-1β ~	
	Histidine-rich glycoprotein	
Angiogenic factors		
Vascular endothelial growth factor ^	***Chemokines***	
Platelet factor 4 (inhibitor) ~ ^	MIP-1α (CCL3) ~	
	RANTES (CCL5) ~	
Fibrinolytic inhibitors	MCP-3 (CCL7) ~	
α_2-Plasmin inhibitor * #	Gro-α (CXCL1) ~	
Plasminogen activator inhibitor-1 *	Platelet factor 4 (CXCL4) * ~ #	
	NAP-2 (CXCL7) * ~	
Albumin	ENA-78 (CXCL5) ~	
Immunoglobulins *	Interleukin-8 (CXCL8) ~ ^	
Granule membrane-specific proteins	TARC (CCL17) ~	
P-selectin (CD62P) * ~		
GMP 33		
GPIb/IX/V *		
GPIIb/IIIa *		
GPIV *		

* Granular contents involved in haemostasis
~ Granular contents involved in inflammation
^ Granular contents involved in angiogenesis
# Granular contents involved in antimicrobial defence

Table 1. 1 Platelet Granular Constituents

Adapted from (Smyth et al., 2009) (Yeaman, 1997) (Jenne et al., 2013)

The cytoskeleton defines the discoid shape of the resting platelet and maintains cell integrity, under the shear forces generated by the blood flow (Thon and Italiano, 2012). The cytoskeleton is composed of a spectrin-based skeleton, a microtubule coil and a network of cross-linked actin filaments and supports the OCS and platelet plasma membrane (Hartwig, 2013) (Bearer et al., 2002). Under normal resting conditions, granules are located within close proximity to the OCS membranes. Upon platelet activation, the α and dense-granules may fuse with the plasma membrane and secrete their pre-formed mediators (**Table 1.1**) via the OCS, to be delivered precisely at the site of vascular injury (Thon and Italiano, 2012). This process enables platelets to play important roles in the functional modulation of leukocytes and other circulating platelets (Smyth et al., 2009).

1.4 Mechanisms of Platelet Activation

Under normal physiological conditions, circulating platelets must sustain the high fluid shear forces generated by the blood flow over the endothelium, without becoming prematurely activated. Platelet activation leading to aggregation is a well-defined role of platelets in the regulation of haemostasis, following injury to damaged endothelium (Brass, 2010). In this instance, platelets must recognise vascular injury, cease motion, adhere to the vessel wall and aggregate to one another to form a stable platelet plug (Brass, 2010). Additionally, over stimulation of platelet aggregation results in the formation of platelet thrombi (Andrews and Berndt, 2004). This occurs when diseases or drugs interfere with the mechanisms involved in unwarranted platelet activation, resulting in the accumulation of platelets where it is not required (Brass, 2010).

Conversely, platelets have also been shown to play an important role in the modulation of the inflammatory response (Hechler and Gachet, 2015) (Pitchford, 2007) (Semple and Freedman, 2010) (Amison et al., 2015) (Gresele et al., 1993) (Boilard et al., 2010). Platelets are thought to be implicated in various autoimmune, allergic and infectious diseases, including asthma, COPD, rheumatoid arthritis (RA) and sepsis (Pitchford et al., 2008) (Gawaz et al., 1995) (Gresele et al., 1993) (Johansson et al., 2011) (Bunescu et al, 2004)(Ferroni et al., 2000). Interestingly, in regards to platelet activation in the context of inflammation, activation induced by inflammatory stimuli is not associated with subsequent platelet aggregation. Indeed, it has been demonstrated that in patients with asthma a mild haemostatic defect is seen (Kowalska et al., 2000) (Brown et al., 2013).

Quiescent platelets express a plethora of cell surface receptors, including G-Protein Coupled Receptors (GPCRs) (Purine receptors, Thromboxane receptors, Thrombin receptors and Chemokines receptors) (Brass, 2010), Ionotropic receptors ($P2X_1$), Toll-like receptors (TLR2, TLR4 and TLR9) (Clark et al., 2007) (Kerrigan and Cox, 2010) (Middleton et al., 2016), integrins (αIIbβ3), immunoglobulin receptors (FcεRI) and glycoprotein receptors (GPVI) (Walsh et al., 2015). Furthermore, platelets express a wide array of adhesion molecules (P-selectin, P-selectin glycoprotein ligand-1 (PSGL-1), CD40 and CD40L (Pitchford, 2007) (Yeaman, 2010) (Hechler and Gachet, 2015) (Mangin et al., 2004). Platelets can become activated by a number of inflammatory agents, such as bacteria, viruses and chemokines, as well as in response to endogenous agonists, such as ADP and thrombin. Stimulation of these receptors may result in different products of platelet activation, such as platelet granule secretion (Stenberg et al., 1984), platelet chemotaxis (Czapiga et al., 2005) (Kraemer et al., 2010), leukocyte recruitment (Pitchford et al., 2003) and pathogen recognition (Ali et al., 2017).

Although there are some shared intracellular signalling cascades leading to platelet granule secretion, it is now recognised that there is a divergence in platelet function whereby platelet activation is distinct following activation with inflammatory stimuli in comparison to aggregatory stimuli (Maccia et al., 1977) (Thompson et al., 1984)(Amison et al., 2018). For example, the purinergic ligand, ADP can activate platelets by signalling through the purinergic $P2Y_1$ receptor (Gachet, 2006) (Leon et al., 2008). This receptor is mediated via stimulation of Gαq, which induces PLC-β activation, catalysing the production of inositol-1,4,5-triphosphate (IP_3) and Diacyl-glycerol (DAG). IP_3 triggers Ca^{2+} mobilisation from intracellular stores, whilst DAG causes the activation of PKC. This initiates platelet shape change, granule release and transient aggregation (Mangin et al., 2004) (Amison et al., 2018) (Fabre et al., 1999).

Similarly, activation of the CCR4 receptor by Macrophage derived Chemokine (MDC) and Thymus and Activation-Regulated Chemokine (TARC), and activation of the CXCR4 receptor by Stromal Derived Factor 1α (SDF-1α), is mediated by Gαq intracellular pathways and induces a transient intracellular rise in cytosolic Ca^{2+} in washed platelet preparations (Abi-Younes et al., 2001) (Abi-Younes et al., 2000). However, whilst stimulation of the $P2Y_1$ receptor with ADP induces transient platelet aggregation with a subthreshold dose of ADP (100nm) (Fabre et al., 1999), co-activation with SDF-1α and MDC stimulates platelet chemotaxis (Kraemer et al., 2010) (Amison et al., 2015). This therefore highlights that there are multiple mechanisms controlling platelet function, which dictates the type of the response (Walsh et al., 2015).

Further evidence supports this divergence in platelet function, since platelet activation induced by inflammatory stimuli can be inhibited pharmacologically, without interfering with platelet aggregation (Amison et al., 2015). The rho family of GTP binding proteins, commonly known as Rho-GTPases (including RhoA, Rac1 and cdc42), are regulators of platelet function,

and are important in adhesion, activation and motility of leukocytes (Amison et al., 2018). Rho-GTPases are involved in the amplification of the intracellular signaling pathways following activation of platelet cell surface receptors (Aslan and McCarty, 2013), which in turn moderates platelet function. It is thought that RhoA contributes towards platelet shape change upon activation and has been implicated in the motility of leukocytes (Aslan and McCarty, 2013), however RhoA activity is insufficient for full platelet aggregation in response to ADP (Amison et al., 2018). Furthermore, it has been suggested that Rac1 controls platelet lamellipodia formation and plays a minor role in platelet aggregation (Qian et al., 2012), and Cdc42 is associated with platelet granule secretion (Aslan and McCarty, 2013).

(Amison et al., 2018) showed differences in the signaling of $P2Y_1$ receptors depending on the stimulation present, for example low doses of ADP (0.1μM) induced inflammatory effects through the small GTPase RhoA, but not through induction of the canonical pathway via PLC (Amison et al., 2018). Conversely, high doses of ADP (10μM) induced platelet aggregation (Amison et al., 2018). Other GTPases, such as Rac1 are requisite for leukocyte recruitment in lipopolysaccharide (LPS)-induced airway inflammation (Qian et al., 2012). As the $P2Y_1$ specific agonist MRS2365 binds to the same site as ADP, albeit with a much lower affinity, it is possible that this difference in effect on platelet function through $P2Y_1$ is a result of biased agonism (Amison et al., 2018) (Amison et al., 2015).

However, despite these specific functions of Rho-GTPases and the canonical pathway in platelet activation, it is now thought that there is a cross-talk amongst integrins, GPCRs and Rho proteins to modulate platelet function in cytoskeletal regulation, aggregation, secretion, thrombus formation and other cellular processes (Aslan and McCarty, 2013).

Platelets undergo dynamic morphological alterations upon exposure to biological stimuli or agonists, changing from a resting discoid shape into more rounded structures. Platelet shape change occurs following exposure to sub-threshold concentrations of platelet agonists, which cannot result in either aggregation or adhesion (Shin et al., 2017). Under normal resting physiological conditions, the discoid shape of the platelet is maintained through inhibition of actin polymerisation and sequestration of actin monomers by monomer binding proteins, such as profilin and thymosin-β4 (Hartwig, 1992) (Bearer et al., 2002). Platelet shape change occurs via reorganisation of actin filaments within the cytoskeleton. Firstly, platelets become rounded as actin filaments are fragmented, and spectrin networks composed of filamin A, Gp1b/IX and spectrin are released (Paul et al., 1999) (Shin et al., 2017) (Hartwig, 1992). The membranes of the platelets then protrude outwards, forming lamellipodia and filopodia, resulting from actin filament assembly (Winokur and Hartwig, 1995). As previously described, platelet activation leading to shape change is mediated via a Gαq dependent mechanism (Zheng et al., 2015) (Paul et al., 1999) (Gachet, 2006)(Lapetina and Siegel, 1983) (**Figure 1.3**).

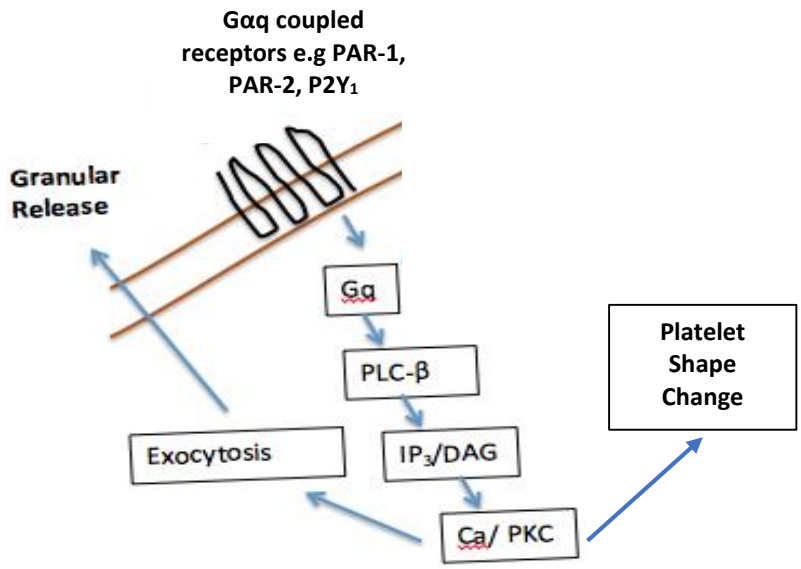

Figure 1. 3 Induction of Platelet Shape Change and Granule Secretion via Gαq Coupled Receptors

Breakdown of the cytoskeleton maintaining the discoid shape under resting conditions is regulated by Gelsolin and Cofilin (Hartwig, 1992) (Li et al., 2002) (Winokur and Hartwig, 1995) (Bearer, 1991). These are actin binding proteins that severe and cap actin filaments in the presence of Ca^{2+}, and subsequently release actin monomers (Shin et al., 2017). This unlocks the membrane cytoskeleton and allows deformation of the membrane, allowing the production of new structures within the platelet (Shin et al., 2017). The actin monomers can then bind to Arp2/3 complex (actin related protein 2/3) stimulating actin assembly (Li et al., 2002). In addition, actin sequestering proteins, profilin and thymosin-β4, carry actin monomers to the barbed end of filopodia enabling filament elongation. CapZ then recaps the barbed filament ends to complete assembly (Bearer, 1991). This newly formed actin cytoskeleton results in the final activated platelet shape- round, small structures with long, thin filopodia extending outwards from the platelet (Hartwig, 1992).

Platelet shape change is one of the first measurable physiological responses following platelet activation (Lapetina and Siegel, 1983). Although, for continued platelet activation a vast number of signalling and adhesion molecules (**Table 1.1**) are released from the platelet granules (Smyth et al., 2009). Platelet activation results in the release of contents from dense granules via exocytosis. Dense granules store an array of haemostatically activate mediators, such as ADP, ATP and Ca^{2+} (King and Reed, 2002) (Jenne et al., 2013). Additional mediators are released from platelet dense granules, such as serotonin, which has been shown to play an important role in neutrophil rolling and adhesion (Duerschmied et al., 2013).

Previous studies have demonstrated the redistribution of platelet α-granule contents (Fibrinogen, Platelet Factor 4) following platelet stimulation with thrombin (Stenberg et al., 1984), demonstrating platelet α-granules release upon activation. Platelet activation inducing granular release is mediated through stimulation of Gαq receptors (**Figure 1.3**) (Gachet, 2006). These mediators play a significant role in innate immunity, either by modulating the expression of platelet adhesion receptors interacting with leukocytes, or by releasing cytokines that affect leukocyte function (Yun et al., 2016). Platelet factor-4 (PF-4) is one of the most abundant proteins within α-granules and has a broad range of activities linked to innate immunity, such as promoting phagocytosis, respiratory burst and the secretion of cytokines (Kasper et al., 2007). RANTES is also found in large quantities in platelet α-granules and mediates monocyte recruitment (Von Hundelshausen et al., 2005). Platelets express P-selectin, which is rapidly mobilised to the platelet surface upon activation and has a requisite role in the interactions between platelets, leukocytes and endothelial cells via its counter ligand PSGL-1 (Frenette et al., 2000). P-selectin/PSGL-1 interactions are critical mediators in the formation of platelet-leukocyte complexes, allowing tethering and rolling along the

endothelium and the subsequent recruitment of platelet-leukocyte complexes (Pitchford et al., 2003).

Furthermore, platelets have been identified as the single largest source of CD40L, which interacts with CD40 located on neutrophils (Pitchford et al., 2017). The engagement of CD40L with CD40 induces a pro-inflammatory phenotype, characterised by the release of pro-inflammatory cytokines and an increased expression of adhesion molecules (intercellular adhesion molecule-2 (ICAM-2), and vascular cell adhesion molecule-1 (VCAM-1)) (Vowinkel et al., 2007) (Danese et al., 2004).

Platelet shape change and the secretion of mediators from platelet granules contributes to activation pathways and allows platelets to function as regulators of haemostasis, thrombosis and innate immunity.

1.5 A Proposed Divergence in Platelet Function

1.5.1 The Role of Platelets in Haemostasis and Thrombosis

Platelets have a well-established role in haemostasis and platelet activity is primarily associated with the initiation of platelet activation and aggregation in response to vascular injury. The basic function of platelets is to bind to endothelial cells of damaged blood vessels, aggregate to form a stable platelet plug and prevent excessive bleeding. Similarly, the role of platelets in thrombosis has been well established. Thrombosis is considered to be a pathological process, where clot formation results from inappropriately triggered or dysregulated haemostasis (Kuijpers et al., 2004) (Middleton et al., 2016). In this instance, activated platelets aggregate at the site of the atherosclerotic plaque or endothelial cell

erosion, stimulating thrombus formation and promoting atherothrombotic disease (Yun et al., 2016)

The haemostatic response can be characterised by three distinct phases, initiation, extension and stabilisation (Brass, 2010). During the initiation phase, platelets are activated by collagen or thrombin and adhere to the damaged vessel wall (Brass, 2010) (Kuijpers et al., 2004). Platelets bind to collagen fibres, which forms a complex with vWF. This complex subsequently interacts with exposed GPIbα on the surface of circulating platelets (Tsuji et al., 1997). The interaction of platelets and collagen fibres, mediated by vWF, slows platelet progression along the vessel and triggers inside-out activation of the integrin $\alpha_{IIb}\beta_3$ (Kuijpers et al., 2004). Platelet activation also results in the secretion of thromboxane A2 (TXA_2) and ADP from dense granules, alongside increased expression of adhesion molecules, including P-selectin and PSGL-1 (Li et al., 2010). This creates a monolayer of activated platelets along the damaged endothelium (Rivera et al., 2009).

During the secondary extension phase, circulating platelets adhere to this platelet monolayer resulting in their activation and the further release of platelet agonists, Thrombin, ADP and TXA_2. These all activate PLCβ via Gq resulting in an increase in cytosolic levels of Ca^{2+} (Li et al., 2010) (Brass, 2010). This activates integrin $\alpha_{IIb}\beta_3$ via inside-out signalling, which enables interaction with fibrinogen and the formation of cohesive interactions between adjacent platelets. (Rivera et al., 2009) (Brass, 2010). Interactions between adjacent platelets and platelets with the endothelium are then strengthened via interactions between fibrinogen/fibrin or vWF with $\alpha_{IIb}\beta_3$, GPVI or GPIb-IX-V (Andrews and Berndt, 2004) (Li et al., 2010).

The third stabilisation phase is characterised by activated platelets within the plug coming into close contact with one another to form a cross-linked fibrin network, preventing premature platelet disaggregation. This enables paracrine signalling of platelet molecules and occurs through outside-in signalling, predominantly mediated by integrin αIIbβ3 (Rivera et al., 2009). This results in the formation of a haemostatic plug composed of activated platelets embedded within a cross-linked fibrin mesh, stable enough to withstand the shear forces generated by the flow of blood (Brass, 2010).

1.5.2 The Role of Platelets in Inflammation

1.5.2.1 The Role of Platelets in Inflammatory Disorders

In addition to their roles in haemostasis and thrombosis, platelets have been described as important mediators in inflammatory disorders. Evidence now suggests that platelets are potent and versatile immune and inflammatory effector cells, with the ability to perform recognition and signaling functions, transfer biologic information and orchestrate complex physiological and pathological inflammatory responses (Middleton et al., 2016) (Middleton et al., 2018). Platelets have been implicated in several pro-inflammatory disorders, including asthma, COPD, irritable bowel disease (IBD), RA, ARDS and acute lung injury (ALI) (Pitchford et al., 2003) (Joseph et al., 2001) (Bunescu et al, 2004) (Gresele et al., 1993) (Vowinkel et al., 2007) (Ortiz-Muñoz et al., 2014) (Lax et al., 2017).

Platelets contribute to inflammatory disorders via several mechanisms. Firstly, platelets have been reported to directly migrate to the site of inflammation (Pitchford et al., 2003) (Pitchford et al., 2005), where they release pro-inflammatory mediators from their granules

(**Table 1.1**), contributing to chronic inflammatory events inducing tissue remodelling and altering tissue architecture (Pitchford et al., 2004) (Idzko et al, 2015). Secondly, platelets can directly interact with inflammatory leukocytes, 'priming' them for efficient migration to the site of inflammation. Therefore, platelets are critical links between the innate and adaptive immune system (Pitchford, 2007) (Middleton et al., 2016) (Bozza et al., 2009) (Semple and Freedman, 2010) (Langer and Chavakis, 2009) (Amison et al., 2012).

Evidence has suggested an alteration in platelet function and character in the clinic in patients with allergic inflammatory diseases, including asthma, allergic rhinitis and atopic dermatitis (Pitchford., 2007), as measured by alterations in platelet secretion, expression of surface molecules, aggregation and adhesion to the endothelium (Idzko et al., 2015). In addition, elevated levels of platelet-derived activation markers have been detected in patients with asthma following allergen provocation, with increased levels of Beta-Thromboglobulin (β-TG), PF-4, RANTES, platelet activating factor (PAF) and P-selectin (Pitchford., 2007) (O'Sullivan et al., 2005) (Idzko et al., 2015). Moreover, patients with atopic asthma have also been reported to have a shorter platelet lifespan in the circulation (4.7 days), when compared to healthy individuals (8.9 days) (Taytard et al., 1986), suggestive of continuous platelet activation in this disease. This clearly highlights a role for platelets in the modulation of inflammatory disorders, which is distinct from haemostasis and thrombosis.

1.5.2.1 Pulmonary Platelet Recruitment

Platelets were previously regarded as static cells that do no move once they adhere to a matrix (Kraemer et al., 2010). However, once recruited from the circulation platelets possess

all of the molecular assets required for cell migration (Gaertner et al., 2017). More recently, platelet migration towards both allergic and bacterial stimuli has been demonstrated *in vitro,* towards N-formyl-methionyl-leucyl-phenylalanine (fMLP) (Czapiga et al., 2005), LPS (Ortiz-Muñoz et al., 2014), SDF-1α (Kraemer et al., 2010) and MDC (Kowalska et al., 2000). This highlights that platelets are indeed motile cells and suggests that platelet migration may be modulated by mediators involved in inflammation and infection. Through the use of experimental models, platelets have been found in extravascular lung tissue of allergic mice, mediated by an IgE/FcεRI-dependent mechanism (Idzko et al., 2015) (Pitchford et al., 2008). Similarly, intratracheal LPS administration has been shown to induce pulmonary platelet sequestration (Ortiz-Muñoz et al., 2014) and platelet recruitment into lung alveoli (Lax et al., 2017). This is consistent with findings in the clinic, whereby platelets obtained from allergic donors have demonstrated migration *in vitro* when exposed to the allergen to which the patient was sensitised (Idzko et al., 2015). Similarly in other inflammatory diseases, platelets have been found extravascularly in the synovial fluid of patients with arthritis (Boilard et al., 2010) and in ischemia and reperfusion (Kraemer et al., 2010) (Rainger et al., 2015). This evidence therefore suggests that mediators involved in inflammation and infection may be capable of inducing platelet activation and migration.

Once recruited to inflamed tissue, platelets participate in the innate immune response and contribute directly to tissue remodeling in chronic inflammation. Studies have implicated a direct role for platelets in airway remodelling and chronic inflammation, by the release of platelet-derived mediators, including growth factors (transforming growth factor b (TGFB), vascular endothelial growth factor (VEGF) and platelet derived growth factor (PDGF)) and matrix metalloproteinases (MMP1, MMP2, MMP3 and MMP14) (Pitchford et al., 2004). This

platelet activation has been shown to persist long after the initial allergen challenge, suggesting a potential role for platelets in chronic airway remodeling associated with asthmatic patients (Kowal et al., 2006). Similarly, increased platelet activation has been shown to correlate with changes in lung architecture, as measured by basement membrane thickening, myofibroblast proliferation and bronchial smooth muscle growth (Pitchford, 2007). This is further demonstrated in studies where platelet depletion in a mouse model of allergic inflammation decreased epithelial thickening, smooth muscle thickening, and sub-epithelial reticular fiber deposition (Pitchford et al., 2004).

1.5.2.2 The Role of Platelets in Inflammatory Leukocyte Recruitment

In addition to platelet recruitment alone, research suggests that platelets can influence leukocyte recruitment towards both allergic and infectious stimuli (Page and Pitchford, 2013) (Pitchford et al., 2017) (Kornerup et al., 2010) (Ortiz-Muñoz et al., 2014) (Lax et al., 2017). Activated platelets displaying adhesion molecules (CD40L, P-selectin) are able to interact with counter ligands expressed on leukocytes (CD40, PSGL-1) within the circulation, forming platelet-leukocyte complexes (Langer and Chavakis, 2009) (Page and Pitchford, 2013). These complexes are important for subsequent leukocyte activation, tethering, rolling and migration into inflamed tissue (Kornerup et al., 2010) (Wang et al., 2007) (Lukacs et al., 2002) (Pitchford et al., 2005). The heightened occurrence of platelet-leukocyte complexes in circulating blood has been reported in a vast array of inflammatory, infectious and autoimmune diseases, including asthma, COPD, RA, bacteremia and sepsis (Ferroni et al., 2000) (Gresele et al., 1993) (Pitchford et al., 2003)(Pitchford et al., 2005) (Johansson et al., 2011) (Gawaz et al., 1995) (Russwurm et al., 2002) (Bunescu et al., 2004). The formation of

platelet-leukocyte complexes as seen in the clinic has also been replicated in numerous animal models of acute inflammation (Lukacs et al., 2002) (Pitchford et al., 2003) (Pitchford et al., 2005) (Tamagawa-Mineoka et al., 2009) (Bins et al., 2014) (Pan et al., 2015) (Amison et al., 2015), underpinning a role for platelets in leukocyte recruitment.

The importance of platelets in the recruitment of leukocytes in the acute inflammatory response has been demonstrated previously in literature (Kornerup et al. 2010) (Pitchford et al., 2003)(Pan et al., 2015) (Amison et al., 2017) (Coyle et al., 1990). For example, recent observations have indicated that platelet depletion results in the abolition of allergen induced eosinophilia (Pitchford et al., 2003) (Amison et al., 2015), and platelet activity is important for LPS-induced neutrophil recruitment (Pan et al., 2015) (Riffo-Vasquez et al., 2016) (Amison et al., 2017)**.** This further demonstrates platelet-facilitated leukocyte accumulation.

P-selectin is a glycoprotein expressed by platelets, which is rapidly translocated from platelet α-granules to the plasma membrane of the platelet upon platelet activation (Mauler et al., 2016). Here, P-selectin recognises its counter ligand PSGL-1, expressed on the surface of polymononuclear cells (PMC), initiating the interaction between platelets and leukocytes and increasing circulating platelet-leukocyte complexes (Joseph et al., 2001) (Kornerup et al., 2010) (Pitchford et al., 2003) (Jawien et al., 2002). These interactions support contact-dependent activation of leukocytes and subsequent activation of integrins (αMβ2 and α4β1) (Johansson and Mosher, 2013). This leads to increased adhesion of leukocytes to the vascular endothelium and facilitates the extravasation of leukocytes into inflamed tissue (Jawien et al. 2002).

Indeed, the importance of P-selectin in mediating leukocyte recruitment has been demonstrated experimentally using both P-selectin knockout mice and P-selectin blocking

agents (de Stoppelaar et al., 2015) (Mauler et al., 2016), which demonstrate platelet dependence of leukocyte rolling, intravascular crawling and diapedesis *in vivo* (Langer and Chavakis, 2009) (Wang et al., 2007). This has been further confirmed through reinfusion of thrombocytopenic mice with platelets treated with the P-selectin blocking antibody RB40.34 (Pitchford et al., 2005). When treated platelets were reinfused, allergen induced eosinophilia remained suppressed unlike vehicle treated platelets.

P-selectin-PSGL-1 interactions tether leukocytes to the endothelium from rapidly flowing blood. The sequential formation and dissolution of these interactions enables the subsequent rolling of platelet-leukocyte complexes along the endothelium (Alon et al., 1996) This process does not require leukocyte activation and is mediated by endothelial derived selectins (P-selectin, E-selectin and L-selectin). The importance of leukocyte rolling in the recruitment of leukocytes is highlighted by a rare congenital disorder called leukocyte adhesion deficiency II (LAD II), where patients cannot produce functional selectin ligands and consequently display defects in neutrophil rolling and recruitment, leading to severe recurrent bacterial infections (Langer and Chavakis, 2009).

Whilst it is important to note that P-selectin-PSGL-1 interactions are important in leukocyte adhesion and recruitment to inflamed tissue, other molecules are implicated. The mediators involved are dependent upon both the cell types involved and the mediators expressed and released on the platelet surface. It has been reported that activated platelets are a rich source of soluble CD40L (Vowinkel et al., 2007) (Vanichakarn et al., 2008), which has been shown to interact with its receptor CD40 expressed on neutrophils (Vanichakarn et al., 2008). Studies have demonstrated that the engagement of CD40L with its receptor stimulates the release of pro inflammatory cytokines, chemokines and the increased expression of adhesion

molecules, including selectins and ICAM-2 (Vowinkel et al., 2007). This increased expression of adhesion molecules amplifies the signals involved in the recruitment of leukocytes to inflamed tissue and may contribute to the perpetuation of the inflammatory response. The importance of CD40-CD40L interactions has been highlighted in the literature, which described an attenuated recruitment of leukocytes and platelets in CD40 or CD40L knockout mice in a model of acute inflammation (Vowinkel et al., 2007).

Contact dependent activation, in addition to activation of leukocytes by chemokines secreted from the inflamed tissue, leads to inside-out integrin activation of leukocytes (Johansson and Mosher, 2013). Integrin adhesion molecules and their counter ligands (ICAM-2/ Lymphocyte function-associated antigen 1 (LFA1) (Diacovo et al., 1994) (Kuijper et al., 1998), Very Late Antigen 4 (VLA4)/ VCAM-1, $\alpha_4\beta_7$/ mucosal vascular addressin cell adhesion molecule 1 (MAdCAM 1) and junctional adhesion molecules (JAM 1-3)) (Chavakis et al., 2004) (Woodfin et al., 2007) provide firm adhesion to the endothelium and support paracellular and transcellular diapedesis of platelet-leukocyte complexes to inflamed tissue. Further important adhesion molecules involved in leukocyte recruitment include the platelet-endothelial cell adhesion molecule-1 (PECAM-1) (Berman and Muller, 1995) (Woodfin et al., 2007) and endothelial cell adhesion molecule (ESAM) (**Figure 1.4**). Intriguingly, the involvement of these interactions in mediating leukocyte recruitment has been demonstrated using antagonists, which was reported to significantly attenuate neutrophil recruitment into inflamed tissue (Chavakis et al., 2004).

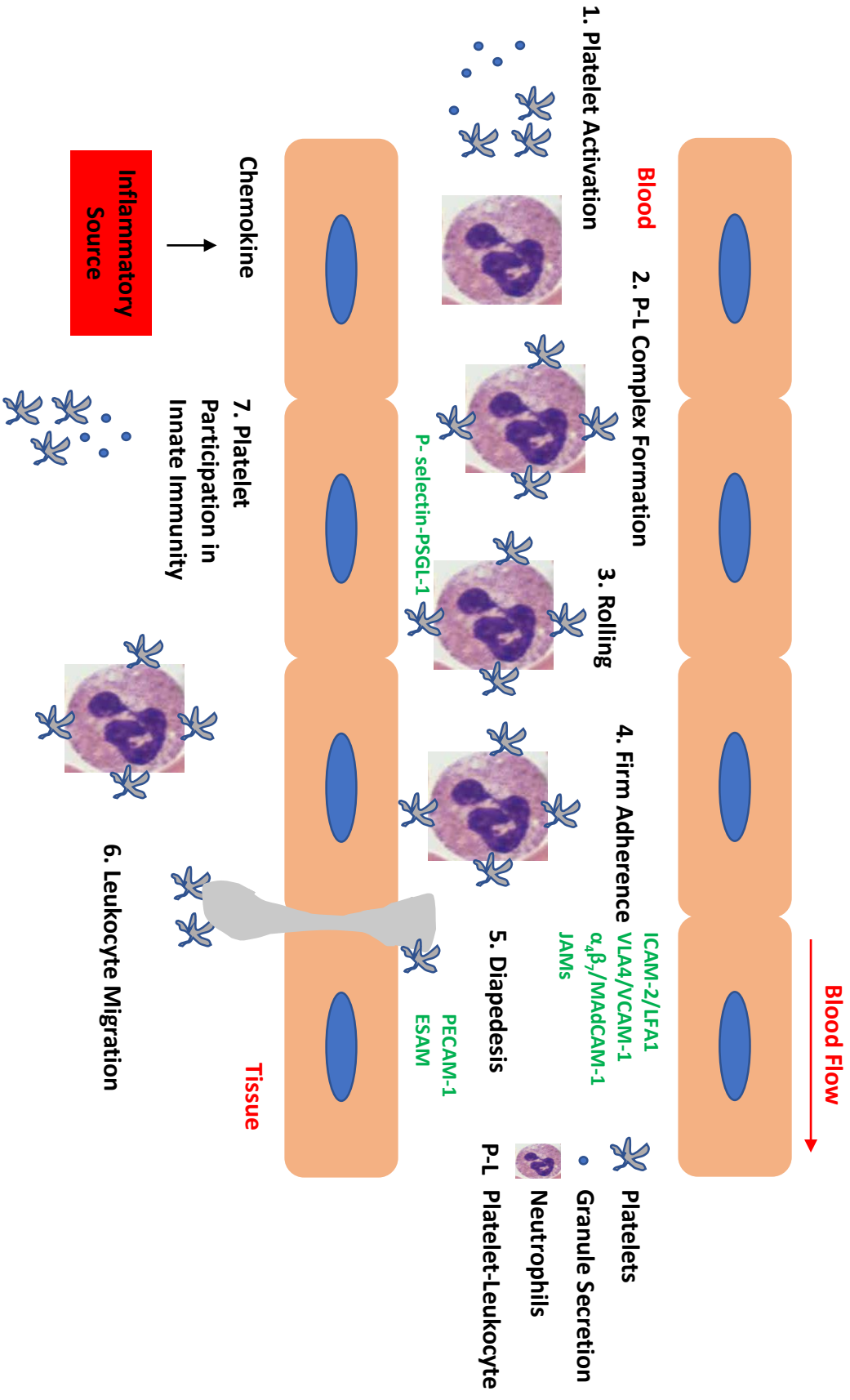

Figure 1. 4 Involvement of Platelets in Leukocyte Recruitment to Inflamed Tissue

1.5.3 The Role of Platelets in Infection

1.5.3.1 The Inflammatory Response to Bacterial Infection

The innate immune system and its primary cellular components, including macrophages, neutrophils, natural killer (NK) and dendritic cells (**Figure 1.5**), play a pivotal role in the activation of the inflammatory response to infection. Pulmonary bacterial infections, including CF, are characterised by chronic airway inflammation and consequently patients present to the clinic with diminished lung function (Pillarisetti et al., 2011) (Cigana et al., 2018).

Innate immune mechanisms detect bacterial infections through their characteristic pathogen associated molecular mechanisms (PAMPs), which triggers the appropriate response against that particular infection (Kurup and Tarleton, 2013). PAMPs are usually components of the bacterial cell wall, including LPS (gram-negative), lipopeptides (gram-positive), peptidoglycan, flagellin and bacterial DNA (Elson and Daubeuf, 2007). PAMPs are recognised by complement, and the complement components C3b and iC3b (Frank and Fries, 1991) (Gaboriaud et al., 2003) subsequently label the particles in a process termed opsonisation. Phagocytes are then able to recognise opsonised bacterial components by the expression of complement (C1q and C3) and Fc receptors (Frank and Fries, 1991) (Van Amersfoort et al., 2003). In addition, phagocytes express pattern recognition receptors (PRRs) (TLRs, NOD-like receptors (NLRs), RIG-1 like receptors (RLRs), C type lectin receptors (CLRs)) on their cell surface, which enables the recognition and phagocytosis of opsonised bacteria. The bacterial epitopes may then be presented on the cell surface via MHC class II to initiate the adaptive immune response.

Pathogens or immunogenic particles initiate the release of an array of pro-inflammatory mediators from macrophages, including tumour necrosis factor (TNF-α), interleukin (IL) 1β

and IL-6, and induce vascular and physiological changes (Kawakami et al., 1983) (Broug-Holub et al., 1997) (Huang et al., 2008) (Bhakdi et al., 1991). Neutrophils respond to these inflammatory stimuli by intravascular aggregation, adhering to the endothelium and migrating towards the inflammatory source (Bray et al., 1981) (Schiffmann et al., 1975) (Gaertner et al., 2017). Neutrophils further augment the inflammatory cascade by the production of additional inflammatory mediators, including leukotriene-β4, PAF and TNFα (Camussi and Tetta, 1989). Once activated, neutrophils express CD14, CD11/CD18, complement and Fc receptors, enabling phagocytosis of either bacterial fragments or whole bacteria (Van Amersfoort et al., 2003) (Gaertner et al., 2017).

Neutrophils produce and secrete microbicidal agents from internal granules, including oxygen free radicals and lysozyme, which facilitate their role in host defence (Chatham and Blackburn, 1993). In addition to their more traditional role in phagocytosis, activation of neutrophils causes the release of dense web-like structures of DNA, called neutrophil extracellular traps (NETs). These NETs contain proteolytic activity that can trap and destroy invading microorganisms (Caudrillier et al., 2012) (Clark et al., 2007) (McDonald et al., 2012).

The innate immune response leads to the activation of the acquired immune system. It is reported that IL-12 is a key modulator of immune function (Wolf et al., 1994). Antigen presenting cells present bacterial epitopes to naive T-cells, resulting in the activation of T-cells and the differentiation of naïve T-cells into Th1 cells (**Figure 1.5**). This leads to the production of pro-inflammatory cytokines, including interferon gamma (IFN-γ) (Wolf et al., 1994) (Cooper et al., 1995) (O'Sullivan et al., 1995), which promotes cell mediated immunity directed towards intracellular pathogens (Wurster et al., 2002). Exposure to allergen induces IL-4 production and causes activation of the transcription factor STAT6, which promotes Th2 cell

differentiation (Kaplan et al., 1996) (**Figure 1.5**). Th2 cells produce IL-4, IL-5 and IL-13, which activate mast cells and eosinophils (Wurster et al., 2002) to mediate allergic reactions, asthma and anti-parasitic infections. A summary of the innate and acquired immune responses to bacterial infection is shown in **Figure 1.5.**

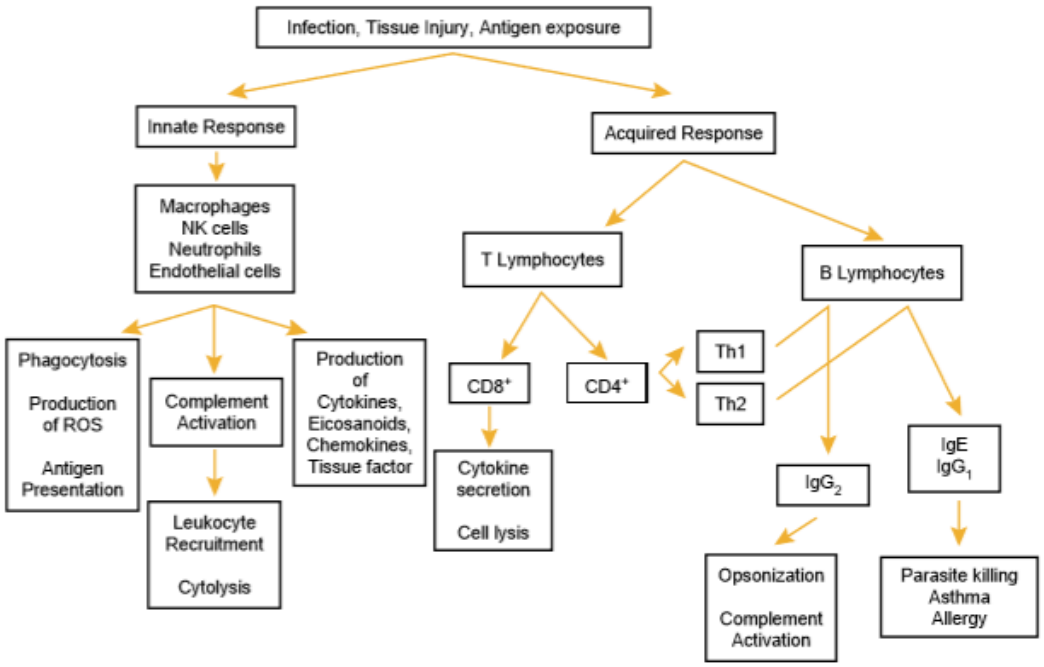

Figure 1. 5 The Innate and Acquired Immune Responses to Infection

(Sherwood and Toliver-Kinsky, 2004)

1.5.3.2 Platelet Activation and Thrombocytopenia in Infectious Diseases

Asides from their well-established role in haemostasis, recently a role for platelets in the regulation of the immune response has become increasingly more apparent. Platelets are the first and most abundant inflammatory cell type recruited in response to injury or infection

(Kerrigan, 2015) (Gaertner et al., 2017). Furthermore, platelets interact with various inflammatory cells and regulate adhesion and extravasation (Pitchford et al., 2003) (Smyth et al., 2009) (Hurley et al., 2016) (Ortiz-Muñoz et al., 2014) (Kornerup et al., 2010) (Amison et al., 2017), suggesting a role for platelets in orchestrating the immune response to infection.

The involvement of platelets in the regulation of the immune response to infection was initially identified in 1901, whereby platelets were observed to 'clump' in response to *Vibrio cholerae* in rabbits (Levaditi, 1901). This has since been validated in the clinic, whereby increases in the expression of platelet activation markers in patients with numerous infectious diseases has been documented (Gawaz et al., 1995) (Gawaz et al., 1997) (Ogura et al., 2001) (O'Sullivan et al., 2005) (Papapanagiotou et al., 2009). It has been demonstrated that CF patients have increased circulating activated platelets when compared to healthy individuals, as determined by increases in platelet-monocyte and platelet-neutrophil complexes, and platelet P-selectin surface expression, (O'Sullivan et al., 2005). Similarly, platelet activation has been detected in patients presenting to the clinic with sepsis (Gawaz et al., 1995) (Gawaz et al., 1997) (Ogura et al., 2001). In these patients, circulating platelet-neutrophil complexes are increased in early stage sepsis, yet decrease following multiple organ dysfunction, suggesting the platelet-neutrophil complexes migrate towards the damaged organs (Russwurm et al., 2002) (Peters et al., 2003) (Gawaz et al., 1997). This finding is consistent in animal models of bacterial induced sepsis, indicating that platelet-neutrophil complexes decrease during late stage sepsis (Hurley et al., 2016). Similarly in other bacterial infections, including periodontitis, platelet activation has been shown to correlate with the severity of disease (Papapanagiotou et al., 2009).

Indeed, the finding of platelet activation in response to bacterial infection has been replicated in numerous experimental models of pulmonary infection, as measured by increases in platelet granular secretion and platelet-neutrophil complex formation (Youssefian et al., 2002) (Hurley et al., 2016) (Gawaz et al., 1995) (Ogura et al., 2001) (de Stoppelaar, 2014)(de Stoppelaar et al., 2015). Gram-positive species of bacteria (*S.aureus* and *Streptococcus pyogenes (S.pyogenes*)) have been shown to induce platelet activation, as measured by elevated P-selectin surface expression and fibrinogen release (Youssefian et al., 2002), in addition to increased platelet-neutrophil complex formation and the accumulation of platelet aggregates (Hurley et al., 2016). Similarly, gram-negative species of bacteria have been shown to induce platelet activation in a model of gram-negative pneumonia derived sepsis, whereby *K.pneumoniae* induced PF-4 secretion from platelet granules (de Stoppelaar, 2014). These findings clearly suggest a role for platelets in response to bacterial infection.

Thrombocytopenia is a common finding in patients admitted to the intensive care unit with sepsis (de Stoppelaar, 2014) (Shannon, 2015) (Greco et al., 2017) and this is associated with a poor prognosis and worsened outcome (Xiang et al., 2013) (Yeaman, 2014) (Claushuis et al., 2016). Studies have reported that the level of thrombocytopenia correlates to illness severity. For example, findings by (Hui et al., 2011) have demonstrated that the occurrence of thrombocytopenia during critical illness appeared to increase the risk of death and was often correlated to sepsis and organ dysfunction in patients admitted to the intense care unit. Furthermore, additional studies have demonstrated that patients with thrombocytopenia presented more commonly with severe sepsis and 30-day mortality was significantly elevated (Gafter-Gvili et al., 2011). Other studies have suggested that thrombocytopenia can also be used as an independent predictor of organ damage and mortality in critically ill patients (Hurley et al, 2016).

There are several proposed mechanisms to elucidate infection induced thrombocytopenia. Firstly, bacteria induces platelet activation and activated platelets have shown shortened survival (4.7 days) in comparison to platelets from healthy individuals (8.9 days) (Taytard et al., 1986) in atopic asthma. Furthermore, platelet activation induced by interactions with bacteria causes platelet granular secretion, irreversible platelet aggregation (Youssefian et al., 2002) (Clawson and White, 1971) and increased platelet accumulation at the site of infection (Hurley et al., 2016) (Kerrigan and Cox, 2010) (Yeaman, 2014). Reports have suggested that bacterial components, such as peptidoglycan and their secreted toxins can induce platelet apoptosis and cytotoxic effects (Kraemer et al., 2012), further contributing to the observed thrombocytopenia during bacterial infection. Other plausible mechanisms which induce thrombocytopenia during infection are the enhancement of platelet phagocytosis by macrophages (Guo et al., 2009) and the sequestration of platelets in the spleen (Aster, 1966).

Animal models of experimentally induced thrombocytopenia have been developed to further investigate the protective role of platelets in host defence against infection. In these models, experimentally induced thrombocytopenia has been associated with worsened infection in rabbits and mice, as measured by enhanced mortality and bacterial load and the exacerbation of sepsis and organ failure (Sullam et al., 1993) (Xiang et al., 2013) (de Stoppelaar, 2014)(van den Boogaard et al., 2015) (Ali et al., 2017). The depletion of circulating platelets has been shown to dramatically impair host defence against infection, increasing mortality in LPS induced endotoxemia (Xiang et al., 2013) and *K.pneumonaie* (de Stoppelaar, 2014), *Streptococcus pneumoniae (S.pneumoniae)* and *Escherichia coli* (*E.coli)* derived sepsis models (van den Boogaard et al., 2015) (Xiang et al., 2013). Thrombocytopenia has been associated with a higher bacterial burden in a rabbit model of *Streptococcal* endocarditis (Sullam et al., 1993) and has been shown to exacerbate bacterial sepsis and organ failure in numerous other

models (Xiang et al., 2013) (Van den Boogaard et al., 2015) (de Stoppelaar, 2014). Intriguingly, the protective effect of platelets have been restored upon platelet reinfusion, improving survival and protection against septic shock (Xiang et al., 2013). These data implicate a role for platelets in the protection against infection and suggest that platelet transfusion may be an effective method of treating severely septic patients.

1.5.3.3 Platelet-Bacteria Interactions

Platelets express an array of constitutive and inducible receptors that allow them to sense PAMPs and respond to signals of infection (Kurup and Tarleton, 2013) (**Figure 1.6**). Platelets are able to interact with bacteria via three main mechanisms: Direct binding, whereby a bacterial surface protein binds to a platelet surface receptor (Kerrigan et al., 2002) (Miajlovic et al., 2010), indirect binding, mediated by a protein that can bind to both platelets and bacteria (e.g. fibrinogen) (Loughman et al., 2005) (Siauw et al., 2006), or the binding of platelets to bacterial secretory product (e.g. cysteine proteinases) (Ståhl et al., 2006) (Lourbakos et al., 2001). The sequence of events involved in platelet-bacteria interactions involves four subsequent steps: contact, platelet shape change, early aggregation and irreversible aggregation (Clawson and White, 1971a).

Bacteria display considerable variation in their ability to interact with platelets, with the subsequent effect on platelet function determined by the receptors involved in bacterial recognition and both the species and concentration of bacteria present (Dewitte et al., 2017) (Yeaman, 1997a). For example, *S.aureus* and *S.pyogenes* have been shown to induce rapid

and complete platelet aggregation, whilst *E.coli* induces platelet aggregation much less rapidly (Clawson and White, 1971b) (Clawson and White, 1971a).

Similarly, the bacteria to platelet ratio has a direct correlation with the velocity and extent with which platelet aggregation occurs (Bayer et al., 1995) (Yeaman et al., 1992). Platelet aggregation induced by bacteria is an 'all or nothing' response, whereby a sub-threshold concentration of bacteria does not induce platelet aggregation (Arman et al., 2014). Unlike with classical platelets agonists, following interaction there is a distinct pause or 'lag' prior to platelet aggregation induced by bacteria, with a higher concentration of bacteria shortening the lag time to aggregation (Arman et al., 2014). A short lag time is indicative of a direct interaction between platelets and bacteria, yet a long lag time is indicative of an indirect interaction (Kerrigan, 2015). Literature has reported that some bacteria, including *Helicobacter pylori (H.pylori)*, can induce platelet aggregation with a short lag time of 2-5 minutes (Byrne et al., 2003) (Kerrigan et al., 2002), whilst other bacteria, including *Streptococcus gordonii (S.gordonii)*, can induce platelet aggregation with a long lag time of 12-18 minutes (Loughman et al., 2005) (Kerrigan et al., 2007).

1.5.3.3.1 Toll-Like Receptors

Murine and human platelets constitutively express low levels of TLR2, TLR4 and TLR9 on their surface (Andonegui et al., 2005) (Cognasse et al., 2005) (Aslam et al., 2016), suggesting that platelets can detect and bind infectious agents (**Figure 1.6**). The expression of these TLRs is significantly increased upon platelet activation (Scott and Owens, 2008). Studies have indicated that PAMPs are detected via TLRs (Takeuchi et al., 1999) and this is a pivotal component of the immune response to infection. Indeed, it has been demonstrated that LPS

from gram-negative bacteria evokes platelet activation and secretion by a TLR4-mediated process, whilst the platelet response to LPS was diminished using platelets isolated from TLR4 knockout mice (Zhang et al., 2009). Furthermore, engagement of TLR4 by LPS has been shown to induce platelet degranulation, enhancing ATP release and P-selectin expression, in addition to inducing the secretion of cytokines, microbicidal proteins and kinocidins (Zhang et al., 2009) (Cognasse et al., 2008). Conversely, additional studies reported that LPS did not induce platelet aggregation, nor the expression of the activation marker P-selectin (Ward et al., 2005). It is therefore evident that the ability of platelet TLR4 to induce aggregation in response to LPS remains controversial and requires further investigation.

Evidence has reported that the actions of LPS on platelet activation mediated by TLR4 may in fact be indirect. It has been suggested that LPS induced platelet activation by TLR4 primes platelets for efficient neutrophil binding and activation (Clark et al., 2007), leading to NETosis and the subsequent trapping of bacteria within the vasculature.

Platelet TLR2 also plays a significant role in the recognition of PAMPs associated with gram-positive bacteria, including lipoproteins (Takeuchi et al., 1999). Gram-positive bacteria, including *S.pneumoniae,* have been shown to induce platelet aggregation and dense granule secretion in a TLR2-dependent manner (Keane et al., 2010). This was further demonstrated using blocking agents, whereby pre-treatment of platelets with an inhibitory monoclonal antibody against TLR2 antibody abolished bacterial-induced platelet secretion and aggregation (Keane et al., 2010). These data highlight the importance of TLR2 and TLR4 in platelet interactions with gram-positive and gram-negative bacteria respectively. They further suggest that platelets possess the capacity to augment the antimicrobial function of other immune cells.

1.5.3.3.2 FcγRIIa receptors

Platelets express a large number of functional FcγRIIa receptors (400-2000 per platelet) (Karas et al., 1982), which are thought to be involved in platelet interactions with bacteria (Dewitte et al., 2017) (**Figure 1.6**). FcγRIIa is a low affinity receptor that binds to IgG (Karas et al., 1982) and plays a significant role in linking the innate and adaptive immune systems. The platelet FcγRIIa receptor can recognise immune complexes and other IgG coated targets (Middleton et al., 2016) (Arman et al., 2014), providing direct mechanisms for immune interaction and effector activities. Subsequent receptor stimulation triggers Ca^{2+} mobilisation, platelet activation and the release of platelet derived mediators (PF-4, P-selectin), which further amplifies the platelet response to bacteria (Arman et al., 2014). Furthermore, it has been suggested that IgG immune complexes that bind to FcγRIIa can be internalised by platelets (Worth et al., 2006). A number of reports suggest that the binding of bacteria to FcγRIIa is mediated via an indirect mechanism, whereby bacterial proteins use IgG to cross-link to platelet FcγRIIa (Tilley et al., 2013) (Naito et al., 2006). Bacteria-induced platelet aggregation is generally inhibited by antibodies that target the FcγRIIa receptor, with the blockade of FcγRIIa preventing aggregation induced by numerous bacterial species (Kerrigan et al., 2002) (Shannon et al., 2007) (Byrne et al., 2003). It has also been suggested that the activation of other platelet receptors by bacteria often requires the simultaneous involvement of the FcγRIIa receptor for an effective platelet response (Hamzeh-Cognasse et al., 2015). This suggests a direct link between the FcγRIIa receptor and the mechanisms of platelet aggregation induced by bacteria. Platelets are the richest source of FcγRIIa, therefore they play a pivotal role in the ability of platelets to interact with bacteria and in their subsequent antibacterial response (Hamzeh-Cognasse et al., 2015).

1.5.3.3.3 Integrin $\alpha_{IIb}\beta_3$

Integrin $\alpha_{IIb}\beta_3$ (GPIIbIIIa) is expressed exclusively on platelets and megakaryocytes and primarily acts as a fibrinogen receptor (Bennett, 2005). $\alpha_{IIb}\beta_3$ facilitates the bridging of fibrinogen and cross-linking of platelets in haemostasis, although this platelet receptor has also been implicated in mediating the interactions between platelets and bacteria (Dewitte et al., 2017) (Deppermann et al., 2016) (**Figure 1.6**). The binding sites of ligands, including fibrinogen, to this receptor is thought to be mediated by the recognition of an arginine-glycine-aspartate (RGD) peptide sequence (Kerrigan, 2015). A number of bacteria have also been shown to express surface proteins that can bind directly to $\alpha_{IIb}\beta_3$, independent of fibrinogen (Kerrigan, 2015). A common feature of these interactions is the presence of regions rich with RGD repeats in the bacterial protein mediating the binding (Kerrigan, 2015). For example, *S.aureus* expresses iron-regulated surface determinant (Isd) proteins, which have been shown to directly bind to platelet $\alpha_{IIb}\beta_3$ in the absence of fibrinogen (Arman et al., 2014)**.** Furthermore, platelet adhesion and aggregation induced by *S.aureus* were significantly attenuated following incubation with either an anti- $\alpha_{IIb}\beta_3$ antibody, Tirofiban, an RGD-sequence inhibitor or using a strain defective in the expression of IsdB (Miajlovic et al., 2010).

Bacteria are also capable of indirect binding to platelet $\alpha_{IIb}\beta_3$ using a plasma protein, such as fibrinogen, to bridge itself to the platelet (Deppermann and Kubes, 2016). Different species of bacteria express different proteins which enable binding to the plasma protein. For example, *S.aureus* expresses clumping factor B (ClfB), fibronectin-binding protein A (FnBPA), fibronectin-binding protein B (FnBPB) and clumping factor A (ClfA) (Arman et al., 2014). These bacterial proteins are characterised by an RGD-sequence and a C-terminal containing a leucine-proline-x-threonine-glycine (LPxTG) motif, which anchors the protein to the cell wall

of the bacteria (Kerrigan, 2015) (Signas et al., 1989). Following binding to fibrinogen, the bacteria is then cross-linked to the platelet via $\alpha_{IIb}\beta_3$. In order to induce full platelet aggregation by indirect binding, a co-stimulus is required, which is provided by the bacteria binding IgG and cross-linking to the platelet FcγRIIa receptor (Arman et al., 2014).

1.5.3.3.4 GPIbα

GPIbα is a membrane glycoprotein expressed exclusively on platelets and megakaryocytes (Lopez, 1994). Although it primarily functions as the platelet receptor for vWF, a number of different species of bacteria have been shown to express serine-rich repeats (SRR), which can bind directly to platelet GPIbα (Arman et al., 2014). For example, *Streptococcus sanguinis* (*S.sanguinis*) and *S.aureus* express the SRR proteins termed SrpA and SraP respectively, which can bind directly to GPIbα (Plummer et al., 2005) (Siboo et al., 2005) (**Figure 1.6**). In the same way that fibrinogen acts as a bridge between bacteria and platelets when indirectly binding to $\alpha_{IIb}\beta_3$, vWF may be used as an intermediary to facilitate the interactions between bacteria and platelet GPIbα. For example, protein A (SpA) from *S.aureus* binds to vWF for indirect adhesion to platelets (O'Seaghdha et al., 2006), and similarly vWF is used by *H.pylori* to interact with platelets (Byrne et al., 2003). The involvement of this receptor in mediating the interaction with bacteria has been underpinned clinically, whereby platelets obtained from patients lacking expression of GPIbα in Bernard Soulier Syndrome fail to aggregate in response to *H.pylori* (Byrne et al., 2003).

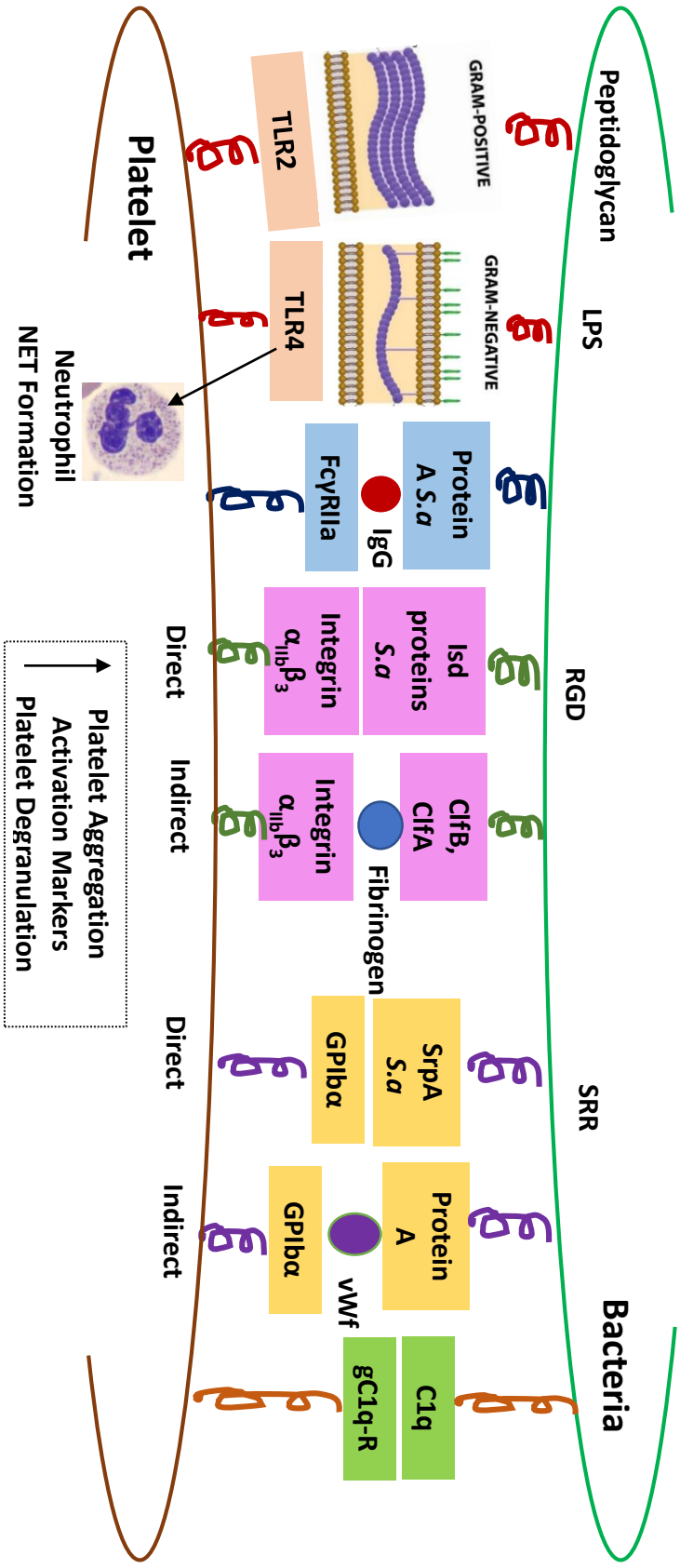

Figure 1. 6 A Summary of Direct and Indirect Interactions Between Platelets (TLR, FcγRIIa, $\alpha_{IIb}\beta_3$, GPIbα, complement) and Bacteria

1.5.3.3.5 Complement

The complement receptor gC1q-R is expressed at low levels on platelets under normal resting conditions, however it becomes upregulated upon platelet activation (Peerschke et al., 2003). Complement proteins interact with bacteria through both the classical and alternative complement pathways (Hamzeh-Cognasse et al., 2015) (**Figure 1.7**). The classical pathway is initiated following the formation of immune complexes, after IgG or IgM bind to bacteria (Sarma and Ward, 2011). The C1 complex, consisting of C1q, C1r and C1s molecules, then binds to the immune complex inducing the activation of C1s and C1r. C1s then subsequently cleaves C4 and C2 to form the C3 convertase, C4bC2a. C4bC2a further cleaves C3 to release C3a and C3b. C3b acts to amplify complement activation and is involved in phagocytosis. Furthermore, C3b complexes with the C3 convertases to form the C5 convertases, C3bBbC3b and C4bC2aC3b. The C5 convertases cleave C5 to form C5a and C5b. The membrane attack complex (C5b-9) is then initiated by C6 and C7 binding to C5b, followed by the binding of C8 and C9 binding. This complex forms a pore in cell membranes and results in cell lysis (Sarma and Ward, 2011) (**Figure 1.7**).

The alternative pathway is initiated by carbohydrates, lipids and proteins on non-self surfaces (**Figure 1.7**) (Sarma and Ward, 2011). C3 is hydrolysed to form C3b, which binds to bacteria. Factor B is then recruited to C3b, followed by Factor D, which cleaves Factor B to form the C3 convertase C3bBb (Sarma and Ward, 2011).

Bacteria coated with the complement factor C1q are able to interact with and bind to platelet gC1q-R (Hamzeh-Cognasse et al., 2015), where it has been shown that SpA from *S.aureus* can bind directly to platelet gC1q-R (Nguyen et al., 2000).

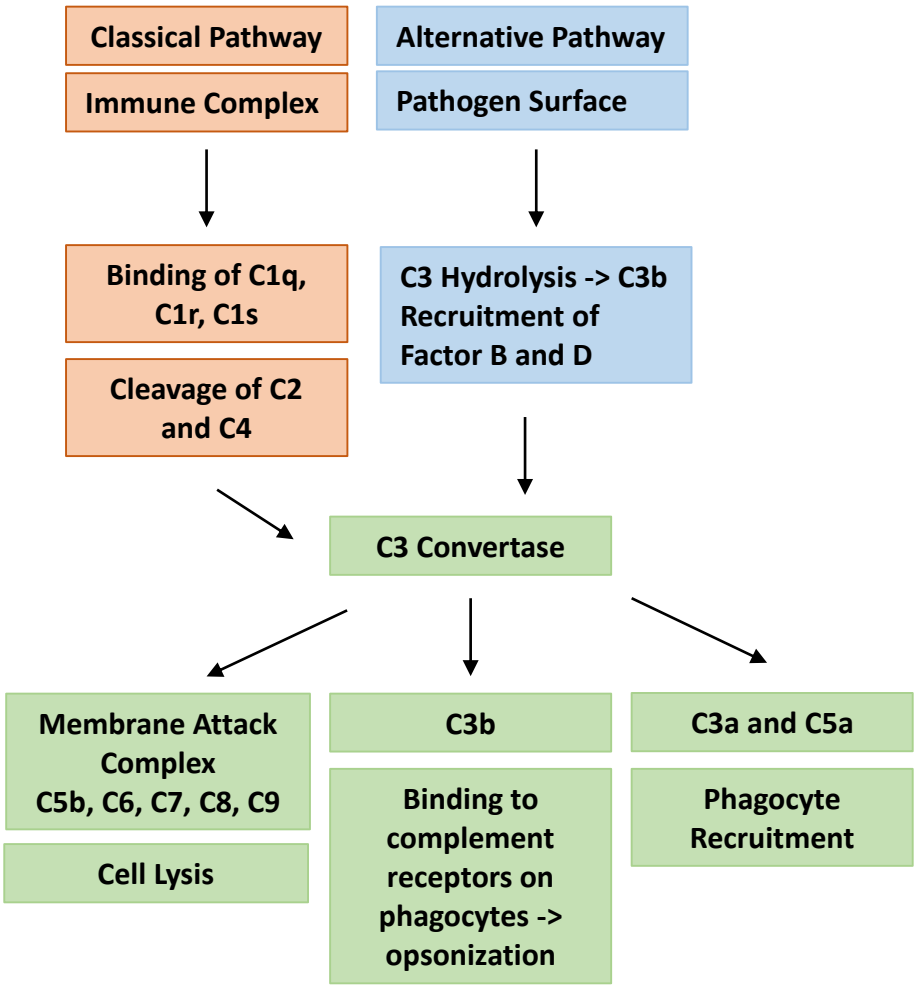

Figure 1. 7 An Overview of the Main Components and Actions of Complement

Platelet aggregation induced by ClfA and ClfB from *S.aureus* are also thought to be mediated by complement, since its inactivation by heating the sera or removing complement proteins using zymosan has been shown to inhibit platelet activation and aggregation (Loughman et al., 2005) (Miajlovic et al., 2007). Consequently, this implicates the complement receptor gC1q-R in mediating the interactions between platelets and bacteria (**Figure 1.6**).

These data suggest that platelets possess a vast array of cell surface receptors, which facilitate their interactions with bacteria (**Figure 1.6**). It is evident that different bacterial species have different mechanisms by which they interact with platelets and vary in their ability to adhere to and aggregate platelets. However, the overall resulting effect on platelet function induced by bacteria is determined by the magnitude of stimulation and the duration of contact between the platelets and bacteria (Yeaman and Bayer, 1999).

1.5.3.4 Platelet Purinergic Receptors in Inflammation and Infection

Platelets express a family of receptors, which are activated by the purines, ADP, ATP, uridine 5'-diphosphoglucose (UDP) and uridine 5'-triphosphoglucose (UTP) (Scrivens and Dickenson, 2006) (Chambers et al., 2000). 4 receptor subtypes are known to be expressed on the platelet surface, 3 from the G-protein coupled receptor family, $P2Y_1$, $P2Y_{12}$ and $P2Y_{14}$ and 1 from the ionotropic P2X family, $P2X_1$ (Storey et al., 2002) (Dovlatova et al., 2008) (**Figure 1.8**). The $P2X_1$ receptor is a ligand gated ion channel, which is activated by endogenous ATP, resulting in the rapid influx of Ca^{2+} ions (Murugappan and Kunapuli, 2006). In contrast, the $P2Y_1$ receptor subtype is stimulated by endogenous ADP triggering activation of the $G_{\alpha q}$/ phospholipase C pathway (Gachet, 2006). Similarly, the $P2Y_{12}$ receptor is activated by endogenous ADP and is coupled to G_i. Signalling via this G-protein negatively regulates the membrane bound adenylyl cyclase (Kauffenstein et al., 2001). $P2Y_{14}$ receptors are thought to be coupled to G_i and are activated by uridine diphosphate (UDP) and UDP-glucose (Dovlatova et al., 2008), although signalling downstream of the $P2Y_{14}$ receptor remains to be elucidated in platelets.

The role of platelet purinergic receptors in platelet aggregation ($P2X_1$, $P2Y_1$, $P2Y_{12}$) has been well documented (Gachet, 2006) (Léon et al., 2003) (Storey et al., 2000), however more

recently the implication of these receptors and their purine ligands in inflammatory processes has become much more apparent (Storey et al., 2002) (Leon et al., 2008) (Klinkhardt et al., 2002) (Amison et al., 2018c) (Amison et al., 2015). Various cell types involved in innate immunity and inflammation express the purinergic P2 receptor subtype, which have been shown to be involved in the modulation of inflammation and the immune response.

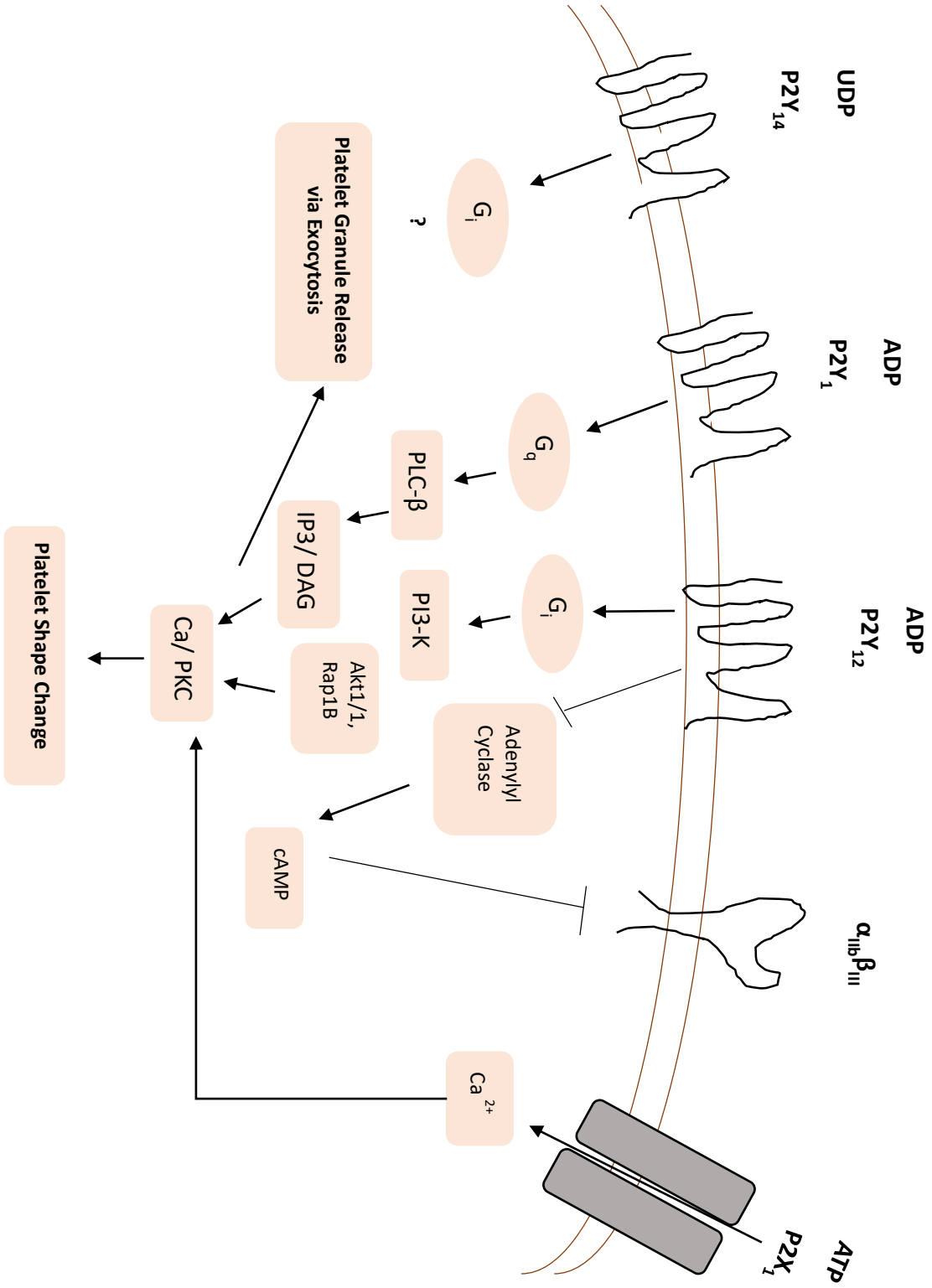

Figure 1. 8 An Overview of Platelet Purinergic Signalling and Effects

Asides from the ability of platelet purinergic receptors to modulate platelet function in the context of haemostasis, stimulation of the platelet purinergic receptors, by ADP or ATP has been shown to induce platelet activation, resulting in aggregation, granule secretion, adhesion molecule upregulation and interactions with inflammatory cells (Fabre et al., 1999) (Léon et al., 2003) (Storey et al., 2000) (Cattaneo et al., 2004) (Hechler et al., 2003). Indeed, a number of studies have demonstrated the ability of purinergic receptor stimulation to induce increases in P-selectin expression, platelet-leukocyte complex formation and in contributing to leukocyte activation and recruitment (Léon et al., 2003) (Storey et al., 2002) (Amison et al., 2017) (Amison et al., 2015). This is suggestive of the ability of platelet purinergic receptors to modulate platelet function that is relevant to inflammation.

ADP induced activation of platelet $P2Y_1$ receptors triggers the activation of PLCβ via G_q (Gachet, 2006), leading to the generation of the second messengers IP_3 and DAG from PIP_2 (**Figure 1.8**). Elevated levels of IP_3 result in calcium mobilisation and release from intracellular stores (Lian et al., 2005). Ca^{2+} promotes rearrangement of the actin cytoskeleton to induce platelet shape change. Furthermore, DAG triggers PKC activation, which in combination with elevated levels of intracellular Ca^{2+}, results in the secretion of platelet granules (Walker and Watson, 1993). Indeed, the inhibition of $P2Y_1$ has been shown to reduce platelet activation and inflammation in a number of studies. For example, pulmonary neutrophil recruitment induced by intranasal LPS administration was inhibited in mice following administration of a $P2Y_1$ antagonist, MRS2500 (Amison et al., 2017), whilst blockade of $P2Y_1$ also reduced P-selectin expression and the incidence of circulating platelet-leukocyte complexes (Léon et al., 2003) (Amison et al., 2015).

The platelet $P2Y_{12}$ receptor is coupled to G_i, with activation of the G-protein negatively regulating adenylyl cyclase. Under normal resting conditions, adenylyl cyclase catalyses the production of cyclic adenosine monophosphate (cAMP), which locks the platelet integrin αIIbβ3 in an inactive conformation preventing platelet aggregation (Kauffenstein et al., 2001). However, upon $P2Y_{12}$ receptor activation and subsequent inhibition of adenylyl cyclase, the decrease in intracellular cAMP levels removes this 'break' on the platelet integrin αIIbβ3 activation, thus enabling platelet aggregation (Kauffenstein et al., 2001) (Gachet, 2006). Furthermore, activation of the platelet $P2Y_{12}$ receptors amplifies platelet aggregation, since its activation also stimulates the secretion of platelet dense granules resulting in the local generation of thrombin and TXA_2 (Storey et al., 2000).

The $P2Y_{12}$ receptor is an attractive therapeutic target for anti-thrombotic agents and its antagonism has demonstrated clear anti-thrombotic effects, decreasing P-selectin expression and platelet aggregation induced by a variety of stimuli (Storey et al., 2002) (Léon et al., 2003) (Kauffenstein et al., 2001).

In the context of inflammation, literature has shown mixed actions of the platelet $P2Y_{12}$ receptor. Some groups have highlighted that antagonism of the platelet $P2Y_{12}$ receptor, using Clopidogrel, has demonstrated attenuation of circulating inflammatory mediators, decreased exposure of P-selectin and CD40L and diminished formation of platelet-leukocyte complexes (Gachet, 2012) (Cattaneo, 2015) (Steinhubl et al., 2007) (Liverani et al., 2016). Recent findings also implicate the $P2Y_{12}$ receptor in acute inflammation in sepsis, where platelets play an important role by enhancing pulmonary infiltration of neutrophils, exacerbating tissue damage (Asaduzzaman et al., 2009) (de Stoppelaar et al., 2015). Whilst, other published literature has demonstrated that LPS induced systemic inflammation becomes more severe

in the absence of $P2Y_{12}$ receptors (Liverani et al., 2014) and $P2Y_{12}$ antagonism using Clopidogrel was shown to potentiate inflammation in a rat model of peptidoglycan-polysaccharide induced arthritis (Garcia et al., 2011).

In contrast, literature using a murine model of allergic airway inflammation has suggested that the antagonism of $P2Y_{12}$ had no significant effect in pulmonary leukocyte recruitment, yet significantly reduces bleeding time and *ex vivo* platelet aggregation to ADP (Amison et al., 2017). This would indicate a dichotomy in platelet activation during inflammation when compared to purinergic receptor involvement in haemostatic processes, however the conflicting results in the literature show a clear need to further investigate the role of the $P2Y_{12}$ receptor in inflammatory conditions.

More recently, platelets have also been shown to express the purinergic $P2Y_{14}$ receptor on their surface (Dovlatova et al., 2008), which is activated by UDP glucose and related sugar nucleotides (Scrivens and Dickenson, 2006). It has been suggested that the $P2Y_{14}$ receptor is coupled to G_i proteins (Moore et al., 2003) (Dovlatova et al., 2008), since UDP-glucose stimulated signalling was completely blocked following pre-treatment of human embryonic kidney (HEK) 293 cells with pertussis toxin (Chambers et al., 2000). Furthermore, UDP glucose has been shown to stimulate significant increases in intracellular Ca^{2+} in a variety of cell lines, which again was sensitive to pertussis toxin (Scrivens and Dickenson, 2006). This is further suggestive of the $P2Y_{14}$ receptor coupling to G_i proteins.

The physiological function of $P2Y_{14}$ remains unknown at present, however the $P2Y_{14}$ receptor appears to be redundant in platelet aggregation unlike the other platelet P2 receptors (Amison et al., 2017) (Dovlatova et al., 2008). This receptor subtype has demonstrated an ability to mediate cell migration in other cell types, including stem cells (Lee et al., 2003), in

addition to stimulating pro-inflammatory cytokine release (IL-8), inducing dendritic cell maturation (Scrivens and Dickenson, 2006) and inhibiting T-lymphocyte proliferation (Scrivens and Dickenson, 2005), clearly indicating an involvement of the $P2Y_{14}$ receptor in modulating inflammatory processes. Moreover, the expression of $P2Y_{14}$ has been shown to increase in rat brain and spleen following provocation with LPS (Moore et al., 2003). Others (Amison et al., 2017) have demonstrated that $P2Y_{14}$ receptor activation affects platelet function by stimulating platelet-induced neutrophil chemotaxis *in vitro* and in mediating pulmonary neutrophil recruitment in mice, in response to LPS challenge (Amison et al., 2017). In these studies, administration of a $P2Y_{14}$ antagonist significantly inhibited pulmonary neutrophil recruitment induced by intranasal LPS, whilst the haemostatic responses (platelet aggregation and bleeding times) remained unaltered.

The $P2X_1$ receptor is an ATP-gated, non-selective cation channel (Gachet, 2006). Studying the involvement of $P2X_1$ in platelet activation has proved difficult due to rapid desensitisation of the receptor following stimulation. However, this can be prevented through the hydrolysis of excess ATP using Apyrase (Mahaut-Smith et al., 2011) (Sun et al., 1998). ATP stimulation of the $P2X_1$ receptor has been shown to increase cellular permeability to Ca^{2+} (Sun et al., 1998), resulting in significant increases in intracellular Ca^{2+} levels following activation (Mahaut-Smith et al., 2011). The influx of Ca^{2+} can trigger reversible platelet shape change, movement of secretory granules without secretion and low level inside-out activation of αIIbβ3 integrin (Mahaut-Smith et al., 2011) (Toth-Zsamboki et al., 2003). Furthermore, it has been reported that activation of the $P2X_1$ receptor with ATP plays an important role in facilitating neutrophil chemotaxis (Lecut et al., 2009).

In other studies, it was shown that inhibition of the $P2X_1$ receptors in a model of LPS-induced inflammation had no impact on pulmonary neutrophil recruitment (Amison et al., 2017). Interestingly, these studies demonstrated that antagonism of the $P2X_1$ receptor significantly increased bleeding times and *ex vivo* platelet aggregation in response to ADP. This further highlights a potential dichotomy in platelet activation during inflammation versus haemostasis.

It is evident that purinergic receptor signalling can mediate inflammatory processes, therefore it is reasonable to suggest that these receptors are likely to be activated in response to infection. In the lung, it is reported that purinergic receptors regulate the rate of mucus clearance (Homolya et al., 2000), surfactant secretion (Rice et al., 1995) and pulmonary vasodilation (Hamada et al., 1998). Whilst these receptors are also important in the modulation of inflammation, including the release of cytokines and leukocyte chemotaxis and adhesion (Geary et al., 2005)

A role for purinergic receptors in response to infection with *P.aeruginosa* has also been detailed. These studies have demonstrated that pulmonary *P.aeruginosa* infection of $P2Y_1$ and $P2Y_2$ deficient mice significantly decreased survival when compared to wild type mice (Geary et al., 2005). It is thought that the mechanism for the impaired survival of mice in these studies was related to an attenuation of the inflammatory cascade and impaired alveolar wall integrity (Geary et al., 2005).

Finally, additional studies have indicated that purinergic receptor signalling via $P2X_7$ is involved in modulating infectious processes in bacterial Chlamydia infections, protozoal infections, including Leishmania and Toxoplasma, and viral infections, including hepatitis B and C (Swartz et al., 2015) (Miller et al., 2011). However, this receptor is not expressed on the

platelet surface, suggesting that whilst platelet P2 receptors are involved in this process, their effects are not solely related to platelets.

1.5.3.5 Effects of Bacteria on Platelet Function

The consequences of the interactions between platelets and bacteria significantly influence the balance between infection and immunity. It has recently been described that platelets are involved in the earliest detection of microbial pathogens (Gaertner et al., 2017) (Kerrigan, 2015) and possess structures and functions of host defence effector cells. Numerous reports have suggested that platelets possess both direct antimicrobial functions, acting as a source of an array of antimicrobial peptides (Yang et al., 2015) (Yeaman, 2010) (Krijgsveld et al., 2000) (Tang et al., 2002) (Kraemer et al., 2011) (Dewitte et al., 2017) (Ali et al., 2017) and directly internalising bacteria (Youssefian et al., 2002), and also indirect antimicrobial functions by enhancing the immune functions of other cells, for example enhancing NET formation from neutrophils and the phagocytic capacity of macrophages (Clark et al., 2007) (Caudrillier et al., 2012) (Yeaman, 1997) (Ali et al., 2017) (**Figure 1.9**).

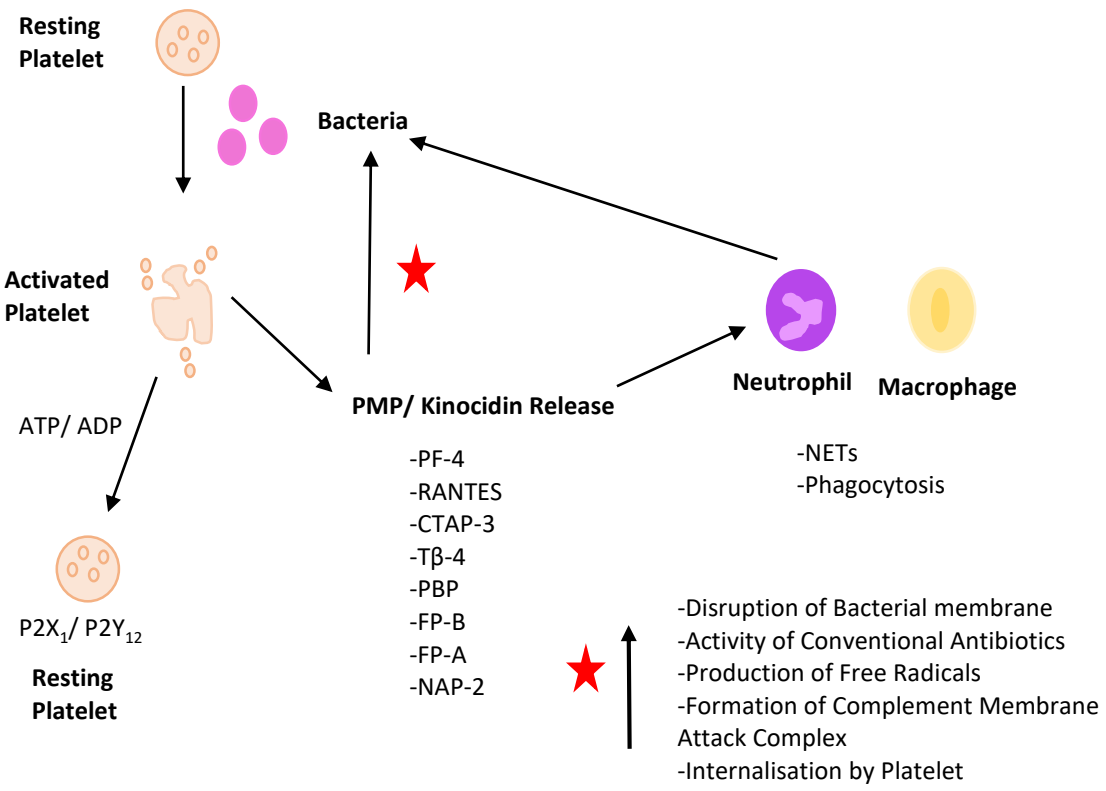

Figure 1. 9 An Overview of the Direct and Indirect Antimicrobial Functions of Platelets

The release of antimicrobial proteins (PF-4, RANTES, connective tissue activating peptide 3 (CTAP-3), platelet basic protein (PBP), thymosin β-4 (Tβ-4), fibrinopeptide B (FP-B), and fibrinopeptide A (FP-A)) from both human and rabbit platelet α-granules has been demonstrated *in vitro*, following stimulation with thrombin (Krijgsveld et al., 2000) (**Figure 1.9**). This releasate, termed platelet microbicidal proteins (PMPs), are reportedly involved in the clearance of pathogens including *viridans streptococci*, *S.aureus*, *E.coli* and *Candida albicans* (Krijgsveld et al., 2000) (Tang et al., 2002) (Yeaman, 1997a). Furthermore, platelets have been shown to release a subset of PMPs, termed kinocidins, which directly kill pathogens and mediate leukocyte chemotaxis (Yount and Yeaman, 2006) (Yount et al., 2007). Thus

demonstrating that platelet-derived microbicidal proteins and kinocidins are capable of orchestrating the immune response to infection.

Kinocidins are classified according to their chemokine nomenclature, for example the CXC chemokines, including PF-4, PBP, CTAP-3 and neutrophil activating peptide 2 (NAP-2), are termed α- kinocidins due to their CXC-chemokine motif. In contrast, β- kinocidins, including RANTES, contain a CC-chemokine motif (Yeaman, 2010) (Yeaman et al., 1997) (Krijgsveld et al., 2000). Mature PMPs and kinocidins are subject to further cleavage after their release from platelets and their products also possess strong antimicrobial activity. For example, the N-terminal of the kinocidins PF-4 is cleaved to give rise to CTAP-III, β-TG and NAP-2 (Yeaman, 2014), generating additional antimicrobial peptides.

PMPs and kinocidins are rapidly released from platelets into the blood stream in response to bacterial invasion via a sequential process. Firstly, bacteria induced platelet activation results in platelet degranulation and the release of PMPs, kinocidins and ADP/ATP (Trier et al., 2008) (**Figure 1.9**). Studies have suggested that PMPs and kinocidins are released if the platelet-bacteria (*S.aureus)* ratio is above 10:1, highlighting the importance of platelet recognition and interactions with bacteria (Trier et al., 2008). The ADP/ATP released from platelets subsequently activates platelet purinergic receptors ($P2X_1$ and $P2Y_{12}$) on adjacent platelets, further amplifying the release of PMPs and kinocidins from successive platelets (Yeaman, 2010) (**Figure 1.9**). The association between purinergic receptors and PMPs/kinocidins has been underpinned using Apyrase and $P2X_1$ and $P2Y_{12}$ receptor antagonists, whereby the release of PMPs from platelets was diminished (Trier et al., 2008).

Studies have indicated that human derived PF-4 and RANTES display antimicrobial activity against *E. coli* and *S.aureus* (Y. Tang et al., 2002). Similarly, the levels of PMPs and kinocidins

released from human platelets have been reported to increase dramatically (4-6 fold) in an infectious setting *in vivo* (Lorenz and Brauer, 1988) (Mezzano et al., 1992). In this instance, plasma levels of PF-4 increased in septicaemia (Lorenz and Brauer, 1988) and other bacterial infections, including *Streptococcal* nephritis (Mezzano et al., 1992). Furthermore, research has indicated that platelet antimicrobial peptides are detectable within human wounds and blister fluid (Tang et al., 2002), demonstrating that platelets can play a protective role in preventing and limiting infection. Intriguingly, in patients with inherited platelet disorders, including Wiscott–Aldrich Syndrome, May–Hegglin Anomaly and Gray-Platelet Syndrome, where there is an abnormality in platelet function, a strong correlation exists between morbidity and mortality due to *S.aureus* and other infections (Yeaman, 2010). This study suggests that normal platelet function and a threshold platelet count is an important barrier to infection. This protective role of platelets in infection has highlighted the potential beneficial effect of platelet transfusions in infection and sepsis (Yeaman, 2010).

Additional studies have also demonstrated the antimicrobial activity of platelet rich plasma (PRP) and other additional plasma preparations in periodontal disease (Yang et al., 2015) (Drago et al., 2013). These studies showed that PRP interfered with *Porphyromonas gingivalis* and *Aggregatibacter actinomycetemcomitans* attachment (Yang et al., 2015) and inhibited the growth of *Enterococcus faecalis, Candida albicans*, *Streptococcus agalactiae* and *Streptococcus oralis* isolated from the oral cavity (Drago et al., 2013).

In vitro studies exposing rabbit derived PMPs to bacterial cells have revealed that PMPs target and disrupt bacterial cytoplasmic membranes (Yeaman, 1997) (**Figure 1.9**), resulting in ultrastructural damage and subsequent bactericidal and bacteriolytic effects. PMPs have also been shown to potentiate the antimicrobial effects of conventional antibiotics against

infection with *S.aureus* (Asensi and Fierer, 1991) (**Figure 1.9**), for example β-lysin and ampicillin interact synergistically *in vitro* to inhibit *Listeria monocytogenes,* thus demonstrating a potential therapeutic use of PMPs in patients with bacterial infections.

In addition to the release of PMPs and kinocidins, platelets contribute to other host defence effector functions. Platelets have been shown to release free radicals, such as superoxide anion, hydrogen peroxide and hydroxyl radicals, when stimulated by certain bacteria (Yeaman, 2010) (**Figure 1.9**). Moreover, studies have shown that platelets interact with components of the complement system to mediate complement fixation. For example, platelets are capable of regulating the generation of the membrane attack complex (Polley et al., 1981) (Zimmerman and Kolb, 1976) (**Figure 1.9**). Complement receptors expressed on the platelet surface subsequently bind to bacteria exhibiting this complex, which triggers platelet activation and degranulation (Polley and Nachman, 1983). Furthermore, platelet proteases can cleave C5 to C5a, therefore providing a positive chemotactic stimuli for the recruitment of macrophages and neutrophils (Weksler and Coupal, 1973) (**Figure 1.9**).

Platelet migration and scanning of the vascular surface for invading pathogens precedes the collection and internalisation of deposited bacteria, clearing pathogens from the blood stream (Gaertner et al., 2017) (Youssefian et al., 2002). Studies performed by (Youssefian et al., 2002) demonstrated the engulfment of *S.aureus* by platelets that displayed classical signs of activation, including GPIb, P-selectin expression and fibrinogen release. It was proposed that the engulfing vacuole was formed by plasma membrane invagination following platelet activation. GPIb was not detected within the engulfing vacuole, suggested that its clearance from the platelet plasma membrane facilitates platelet shape change and initiates the contractile events required for bacteria internalisation. These studies also demonstrated the

fusion of platelet α-granules with the engulfing vacuole, resulting in the interaction of bacteria with the granular secretory products (Youssefian et al., 2002). Other research has proposed that platelets function as 'covercytes,' with platelet pseudopods surrounding bacteria until the organism is enclosed in a vacuole consisting of extracellular space surrounded by plasma membrane (White, 2005) (**Figure 1.9**).

In addition to platelets possessing direct antimicrobial functions, it has been suggested that platelets potentiate the antimicrobial mechanisms of leukocytes (Tang et al., 2002) (Clark et al., 2007) (Ali et al., 2017) (Caudrillier et al., 2012). It has been suggested that the interaction between platelets with monocytes and neutrophils provides a plausible mechanism by which platelets participate in antimicrobial defence. A wide array of platelet secretory products, including PF-4, PAF, PDGF, act as positive chemotactic stimuli for monocytes and neutrophils (Nachman and Weksler, 1972). Studies using experimental models have demonstrated that injection of PF-4 and PDGF rapidly induces neutrophil infiltration (Nachman and Weksler, 1972). Additionally, research performed by (Ali et al., 2017) suggested an indirect role of platelets in pathogen clearance through potentiation of phagocytic and killing capacity of macrophages (Ali et al., 2017) (**Figure 1.9**). In these studies, it was observed that activated platelets and their secreted products enhanced phagocytosis and restricted intracellular growth of *S.aureus* by macrophages. It was proposed that this process was mediated by platelet derived IL-1β, since its inhibition from platelets blocked phagocytosis and permitted *S.aureus* survival (Ali et al., 2017).

Other studies have suggested that PMPs that are active under mildly acidic conditions may augment the antimicrobial effect of leukocytes. It has been described that the ability of neutrophils to kill bacteria through non-oxidative mechanisms may be regulated by pH,

following engulfment by phagolysomes. Therefore, the acidic platelet (pH 5.5) releasate may amplify the direct antimicrobial mechanisms of neutrophils (Shafer et al., 1986) (Tang et al., 2002).

As previously described, emerging evidence has suggested that activated platelets induced the formation of NETS in ALI and sepsis (Caudrillier et al., 2012) (Clark et al., 2007) (**Figure 1.9**), further implicating platelets in the indirect mediation of the immune response to infection. These studies reported that under extreme conditions, such as severe sepsis, platelets via TLR4 function as a barometer for systemic infection. Bacteria induced platelet activation subsequently resulted in their rapid binding to sequestered neutrophils and induced the formation of NETS to ensnare bacteria in the circulation (Clark et al., 2007). The bacterial trapping capacity of these neutrophils is greatly augmented in the presence of platelets, with high concentration of LPS unable to induce NET formation directly, without the presence of platelets (Clark et al., 2007). Furthermore, the production of reactive oxygen species correlates to NET formation and interfering with platelet TXA_2 and MEK signalling significantly decreases NET formation (Caudrillier et al., 2012).

In summary, these studies provide evidence for platelets playing a key role in host defence against infection, mediated by both direct and indirect mechanisms. Platelets are the earliest and most abundant cell type present at sites of infection and can bind directly and indirectly to numerous microbial pathogens. Platelets can collect, bundle and internalise bacteria and release PMPs and kinocidins to facilitate microbial killing. They can also enhance the immune functions of other effector cells by NET formation and phagocytosis. Furthermore, thrombocytopenia has been shown to increase the susceptibility to infection (Yeaman, 1997). Therefore, the roles of platelets in infection towards *P.aeruginosa* and MRSA will be assessed

both in terms of their impact on inflammatory cell recruitment and direct interactions between platelets and bacteria.

1.6 Aims and Objectives

1) **To assess the inflammatory components in the response to infection and the involvement of platelets in this response.**

Neutrophil infiltration and inflammation are thought to contribute significantly to the pathophysiologic features of sepsis, CF and other bacterial infections. A murine model of pulmonary infection with *S.aureus* and *P.aeruginosa* will be established to investigate the inflammatory response induced by pulmonary bacterial infection.

To assess whether infection is associated with increased markers of platelet activation, measurements of platelet accumulation, granule secretion and the formation of platelet-neutrophil complexes will be quantified.

2) **To validate a model of pulmonary infection in animals experimentally depleted of circulating platelets to assess their role in the regulation of the infectious phenotype.**

Thrombocytopenia is a common feature in patients with sepsis, which is associated with a poor prognosis and worsened outcome. Similarly, numerous animal models have

demonstrated that thrombocytopenia dramatically impairs host defence. Therefore, the aims are:

1) To investigate whether experimentally induced platelet depletion in a murine model of pulmonary infection with *S.aureus* and *P.aeruginosa* is associated with a worsened phenotype.

2) To confirm whether the removal of circulating platelets enhances bacterial survival and subsequent mortality rates.

3) To determine whether thrombocytopenia amplifies increased permeability of alveolar and endothelial barriers in infection and permits the usual localised pulmonary infection to become systemic.

3) **Identify platelet signalling mechanisms involved in the regulation of the host response to *P.aeruginosa* and MRSA infection.**

Extending from the objects listed above, the involvement of TLR4 and purinergic receptors will be assessed on the bacterial and inflammatory parameters in a model of pulmonary infection with *P.aeruginosa* and MRSA.

4) **To determine whether a novel antibiotic enhancer compound attenuates bacterial infection with drug-resistant strains of *P.aeruginosa* and *S.aureus*.**

The reduced efficacy of current antibiotics in combination with a steady decline in the discovery of novel compounds have exacerbated the emergence of antibiotic resistance. One possible approach to provide improved treatment for infectious diseases is the use of enhancer compounds, which act by restoring sensitivity of resistant bacteria to currently available antibiotics. A novel antibiotic enhancer compound, HT61 will be utilised in a murine model of pulmonary infection with *S.aureus* and *P.aeruginosa* to determine whether there is any synergism associated using combination treatment with the conventional antibiotics, Tobramycin and Vancomycin.

Chapter II

Materials and Methods

2.1 Materials

ABC Vectastain kit	Vector Laboratories, CA, USA.
AB183345 (anti-CD42b)	Abcam plc, Cambridgeshire, UK.
AB68672 (Anti-Neutrophil Elastase Antibody)	Abcam plc, Cambridgeshire, UK.
Acid alcohol differentiation solution	Sigma-Aldrich LTD, Dorset, UK
Acid Citrate-Dextrose	Sigma-Aldrich LTD, Dorset, UK.
ADP	Sigma-Aldrich LTD, Dorset, UK.
Anti-GPIbα antibody #R300	Emfret Analytics, Wurzburg, Germany.
Apyrase	Sigma-Aldrich LTD, Dorset, UK.
ARC-66096	Tocris Bioscience, Bristol, UK
BA1000 (Biotinylated Goat Anti-Rabbit Secondary Antibody)	Vector Laboratories, CA, USA.
BD Falcon 24 well companion plate	Beckton Dickinson, Plymouth, UK.
BD Falcon Transparent 3µM PET insert	Beckton Dickinson, Plymouth, UK.
GelRed Nucleic Acid Stain	VWR International, Leicestershire, UK.
Bovine serum albumin	Sigma-Aldrich LTD, Dorset, UK.
Calcium	Sigma-Aldrich LTD, Dorset, UK.
Dimethyl sulfoxide	Sigma-Aldrich LTD, Dorset, UK.
DNA Ladder #15615-016	Invitrogen, Paisley, UK

DPX mounting medium	Thermo Fisher, Loughborough, UK.
EC8+ blood analyser cartridges	Point of Care Testing ltd, London, UK.
Eosin	Thermo Fisher, Loughborough, UK.
Evans Blue Dye	Sigma-Aldrich LTD, Dorset, UK.
FITC mouse anti-human CD41a #555466	BD Biosciences, Oxford, UK.
FITC mouse anti-rat IgG2b #553900	BD Biosciences, Oxford, UK.
FITC mouse IgG1 κ isotype control #555909	BD Biosciences, Oxford, UK.
FITC rat anti-mouse CD41 #553848	BD Biosciences, Oxford, UK.
Flow count flurospheres	Beckman Coulter Inc, Buckinghamshire, UK.
MRS2500	Tocris Bioscience, Bristol, UK
Murine Stromal cell derived factor 1	PeproTech EC, Ltd, London, UK.
NF279	Tocris Bioscience, Bristol, UK
Noble Agar	Scientific Laboratory Supplies, Nottingham, UK.
Formaldehyde	Thermo Fisher, Loughborough, UK.
Formamide	Sigma-Aldrich LTD, Dorset, UK.
Glucose	Thermo Fisher, Loughborough, UK
Haemotoxlyin	Sigma-Aldrich LTD, Dorset, UK

Heparin Sodium	Sigma-Aldrich LTD, Dorset, UK
HEPES	Sigma-Aldrich LTD, Dorset, UK.
Histoclear	National Diagnostics, Nottingham, UK.
HT61	Helperby Therapeutics, London, UK.
Hydrogen Peroxide	Sigma-Aldrich LTD, Dorset, UK
100% Industrial methylated spirit	Fisher Scientific, Loughborough, UK.
Isoflurane	Animal Care Ltd, York, UK.
i-STAT blood analyser (VetScan iSTAT 1 analyser 300A)	Abaxis, Union City, CA, USA
LIVE/DEAD BacLight Bacterial Viability #L7012	Thermo Fisher, Loughborough, UK.
Magnesium Chloride	Sigma-Aldrich LTD, Dorset, UK.
Mineral oil	Sigma Aldrich, Dorset, UK.
Mouse IgG isotype control #00751	Bioxcell, New Hampshire, USA.
Murine IL-6 Duoset ELISA, DY453	Bio-techne, Oxfordshire, UK.
Murine KC Duoset ELISA, DY406	Bio-techne, Oxfordshire, UK.
Murine PF-4 Duoset ELISA, DY595	Bio-techne, Oxfordshire, UK.
Murine RANTES Duoset ELISA, DY478	Bio-techne, Oxfordshire, UK.
Paraplast	Sigma-Aldrich LTD, Dorset, UK.
PCR Ready Mix Reaction Kit, R2648 20RXN	Sigma-Aldrich LTD, Dorset, UK.

PE rat anti-mouse Ly6g #551461	BD Biosciences, Oxford, UK.
PE rat IgG1 κ Isotype control #551979	BD Biosciences, Oxford, UK.
Phosphate buffered saline	Oxoid, Hampshire, UK.
Potassium Chloride	Sigma-Aldrich LTD, Dorset, UK.
PPTN Mesylate	Sigma-Aldrich LTD, Dorset, UK
Prostaglandin E_1	Sigma-Aldrich LTD, Dorset, UK.
Rat anti-mouse CD62P FITC #561923	BD Biosciences, Oxford, UK.
RPMI 1640 media	Sigma-Aldrich LTD, Dorset, UK.
0.9% Saline	Baxter Healthcare Ltd, UK.
Shandon™ Kwik-Diff™ staining kit	Thermo Fisher, Loughborough, UK.
Sodium Chloride	Thermo Fisher, Loughborough, UK.
Sodium Dihydrogen Phosphate Dodecahydrate	Thermo Fisher, Loughborough, UK
Sodium Hydrogen Carbonate	Sigma-Aldrich LTD, Dorset, UK.
Sodium Hydroxide	Sigma-Aldrich LTD, Dorset, UK.
Stromatol	Mascia Brunelli, Italy.
Tobramycin	Cayman Chemical Company, Mi, USA.
Thrombin receptor activating peptide	Tocris Bioscience, Bristol, UK
Tri-sodium citrate	Fisons Scientific Equipment, UK.
Trypticase soy broth	Oxoid, Hampshire, UK.

Turks solution	Merck KGaA, Germany.
Tween 20	Thermo Fisher, Loughborough, UK.
Urethane	Sigma-Aldrich LTD, Dorset, UK.
Vancomycin	Sigma-Aldrich LTD, Dorset, UK.
Xylene	Sigma-Aldrich LTD, Dorset, UK.

2.2 Animals

All animal experiments were approved by and conducted in accordance with the guidelines of the Animals (Scientific Procedures) Act (ASPA) 1986 (United Kingdom) with local ethical approval of King's College London, or according to protocols approved by San Raffaele Scientific Institute (Milan, Italy) Institutional Animal Care and Use Committee (IACUC) and adhered strictly to the Italian Ministry of Health guidelines for the use and care of experimental animals. Animals were housed under standard conditions of 22±2^{o}C and a 12:12 light: dark cycle. All animals were provided with food and water *ad libitum* and wood shavings, shredded paper and cardboard tubes were provided for environmental enrichment. All animals were provided with a minimum acclimatisation period of seven days upon arrival. Male, C57/Bl6J mice (20-25g, 8 weeks) were sourced from Envigo Laboratories (Cambridgeshire, UK). All animals were sacrificed through intra-peritoneal (*i.p.*) injection of 0.3mL 25% weight per volume (w/v) urethane to induce terminal anaesthesia.

2.3 Bacterial Strains

Three strains of the gram-negative bacterium *P.aeruginosa* were used in this study; RP73, a multi-drug resistant non-mucoid clinical strain, isolated 17.5 years after the onset of infection in a CF patient (Bragonzi et al., 2006), PAO1, the fully sequenced laboratory reference strain (Bragonzi et al., 2006) and NN2, a Tobramycin Resistant CF isolate, collected at the onset of chronic colonisation. (Bragonzi et al., 2006). A single strain of the gram-positive bacterium MRSA was used, USA300, which was isolated from a patient in 2000 and is the predominant cause of community acquired infections (Diep et al., 2006). Bacterial strains were kindly

provided by Dr. A. Bragonzi (Infection and Cystic Fibrosis Unit, San Raffaele Scientific Institute, Milan, Italy).

2.4 Bacterial Culture Preparation

48 hours prior to use, primary overnight cultures (ONC) for all strains were prepared by inoculating trypticase soy agar (TSA) plates (1.5% w/v agar and 3% w/v trypticase soy broth (TSB) in deionised water) with a stock cryo bead for 24 hours at 37^{o}C (Gallenkamp Hotbox size 2). 24 hours prior to use, secondary overnight cultures were prepared, inoculating 20mL TSB (3% w/v TSB in deionised water) with 2-3 colonies. Cultures were incubated for 16 hours at 37^{o}C, under shaking at 120 rotations per minute (rpm) (Sciquip mini incu shake).

2.5 *In vivo* Animal Studies

2.5.1 Preparation of Bacterial Embedded Agar Beads

The infectious and inflammatory profiles associated with bacterial infection were studied using a murine model of chronic pulmonary infection. Using a modified version of the method described by *Facchini et al* (Facchini et al., 2014), bacterial embedded agar beads were prepared *in vitro*, followed by direct instillation into the lungs. Bacterial ONCs were centrifuged at 2800 g (Heraeus Labofuge 400R) for 20 minutes at 4^{o}C. The pellet was resuspended in 1mL phosphate buffered saline (PBS). The bacteria were embedded into agar beads by mixing 1mL ONC with 9mL molten 1.5% w/v noble agar. This was then added into warmed mineral oil previously heated to 50^{o}C under stirring conditions using a IKA C-MAG

HS7 stir plate (speed setting 3 on plate, 6 minutes). The preparation was then cooled by slowly spinning (speed setting 1) on a stir plate, on ice for 35 minutes and subsequently centrifuged at 2,800 g for 30 minutes to remove any remaining mineral oil. The preparation was washed in sterile PBS and centrifuged at 2,800 g for 10 minutes, the supernatant was then discarded and the remaining pellet resuspended in sterile PBS to achieve a final volume of 20mL. A colony forming units (CFU) determination was performed on the bead slurry by homogenising a 3mL aliquot of the beads (Ultra Turrax T2, IKA WERKE). 1 in 10 serial dilutions (in saline) were performed using a 96 well plate and appropriate dilutions were plated onto TSA plates. The bead slurry was diluted with sterile PBS to obtain the desired CFU of either $2x10^7$ cfu/mL, $2x10^6$ cfu/mL or $2x10^5$ cfu/mL, to achieve a final dose of either $1x10^6$, $1x10^5$ or $1x10^4$ cfu/mouse. As a control, sterile, PBS embedded agar beads were prepared using the same protocol.

2.5.2 Establishing a Model of Pulmonary Infection with *P.aeruginosa* and MRSA

To define the optimum conditions for pulmonary infection with *P.aeruginosa* and MRSA, male C57/Bl6J mice were exposed to 3 different infection protocols. The infection protocols used 3 different inoculum levels with different bacterial strains (**Figure 2.1**). Mice were anesthetized with inhaled 3% isoflurane using an adaptable combination system with on-board oxygen concentrator rig (Burtons Vetinary). Animals were then inoculated with 50µL of either $2x10^7$ cfu/mL, $2x10^6$ cfu/mL or $2x10^5$ cfu/mL bacteria, strains *P.aeruginosa* RP73, PAO1, NN2 or MRSA USA300, via oropharyngeal (*o.a*.) dosing, achieving a final dose of $1x10^6$, $1x10^5$ or $1x10^4$ cfu/mouse. Sham control mice were inoculated with sterile PBS embedded agar beads via the *o.a.* route. Animals were weighed and assessed daily for signs of pain and

distress using the Body Condition Score (BCS), grading the animals from 5-1 (1: emaciated, 2: under conditioned, 3: well-conditioned, 4: over conditioned, 5: obese). Parameters assessed included animals showing reluctance to move, abnormal hunched posture, piloerection, dehydration detectable by skin tenting, lethargy and vocalisation on handling suggestive of pain. Animals that lost more than 20% of their body weight or received a BCS of less than 2 throughout the duration were humanely euthanised with 0.3mL Urethane, via *i.p* injection.

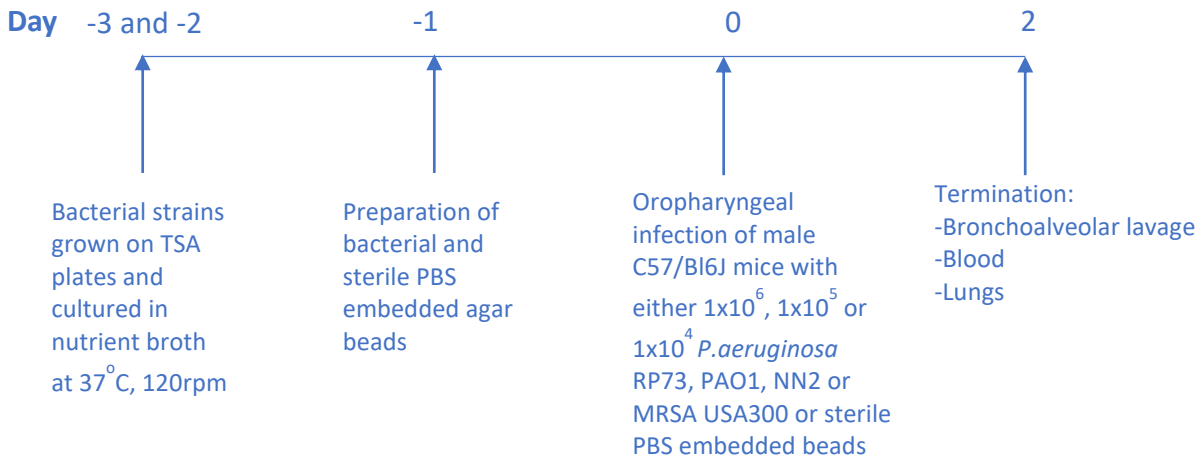

Figure 2.1 Protocol for Inducing Pulmonary Bacterial Infection in Mice

2.5.3 Whole Blood Platelet Quantification and Plasma Isolation

48 hours post infection (h.p.i), mice were terminally anaesthetised with 0.3mL 25% w/v Urethane via *i.p.* injection. Once suitably anaesthetised, 0.5-1mL blood was collected via cardiac puncture from animals anaesthetised with 0.3mL Urethane. Upon collection, blood was mixed with Acid Citrate Dextrose (ACD) at a ratio of 1-part ACD to 9-parts blood. For platelet quantification, whole blood was diluted in Stromatol (1:100) and quantified using an

improved Neubauer haemocytometer under a x40 objective and Leica DM 2000 LED upright microscope. The absolute platelet count was used to calculate the number of platelets/mL.

For plasma isolation, remaining whole blood was spun at 1700 g (Eppendorf centrifuge 5417R) for 10 minutes, and the supernatant collected and stored at -80^{o}C.

2.5.4 Bronchoalveolar Lavage

The trachea was exposed by blunt dissection and a small incision made. A 22-gauge cannula was inserted into the trachea and 3 aliquots of 0.5mL sterile PBS were injected into the lung. The resulting fluid was withdrawn using a 1mL syringe.

2.5.5 Total Leukocyte Quantification

Bronchoalveolar lavage (BAL) fluid was used to quantify total leukocytes. Each BAL sample was diluted 1:1 in Turk's solution. The total cell counts were then quantified using an improved Neubauer haemocytometer under a x20 objective and Leica DM 2000 LED upright microscope.

2.5.6 Differential Leukocyte Quantification

Cytospin slides (thermo scientific) were set up and a 100µL aliquot of each BAL sample was added. Samples were spun at 1000 rpm for 1 minute under slow acceleration (Shandon Cytospin 3) and allowed to air dry. Slides were subsequently stained using a Shandon™ Kwik-Diff™ staining kit and cover slipped using DPX mounting medium. Differential leukocyte

counts were quantified by counting 200 cells from a representative area of each slide, defined as 50 cells per field of view, and the percentage of neutrophils, lymphocytes, macrophages and eosinophils was determined. The total leukocyte count and the percentages of each cell type were used to determine the number of individual inflammatory leukocytes present in each BAL sample.

2.5.7 Colony Forming Unit Determination

48 h.p.i, lungs were aseptically removed and homogenized in 2mL sterile saline. Lung homogenates were serially diluted (in saline) using a 96 well plate and appropriate dilutions were plated onto TSA plates. Bacterial colonies were manually counted and the total pulmonary CFU was calculated.

2.5.8 The Effect of Tobramycin on Pulmonary Infection with *P.aeruginosa*

The optimum inoculum for pulmonary infection with *P.aeruginosa* was determined to be $1x10^6$ cfu/mouse, producing an infection and inflammatory profile analogous to the clinical setting. Therefore, experiments were performed to validate the murine model of pulmonary infection with *P.aeruginosa*, using a single dose of 0.2mL/ mouse of either vehicle (saline) Tobramycin at either 10, 50, 100, 200 or 300 mg/kg, at 24 h.p.i, via *i.p.* injection. Tobramycin doses for each *P.aeruginosa* strain are listed in **Table 2.1**. At 48 h.p.i, blood was taken, a BAL was performed and lungs were aseptically removed and processed as described in sections 2.5.3, 2.5.4 and 2.5.7 respectively.

Bacterial Strain	Tobramycin Dose (mg/kg)
P.aeruginosa RP73	50, 100, 300
P.aeruginosa PAO1	10, 50, 100
P.aeruginosa NN2	50, 100, 200

Table 2. 1 Tobramycin Doses for the Murine Model of Pulmonary Infection with *P.aeruginosa*

2.5.9 The Effect of Vancomycin on Pulmonary Infection with MRSA

The optimum inoculum for pulmonary infection with MRSA, strain USA300, was determined to be $1x10^6$ cfu/mouse. Experiments were performed to validate the murine model of pulmonary infection with MRSA, strain USA300, using a single dose of 0.2mL/ mouse of either vehicle (saline) or Vancomycin at either 50, 100 or 200 mg/kg, initiated at 24 h.p.i, via *i.p.* injection. At 48 h.p.i, blood was taken, a BAL was performed and lungs were aseptically removed and processed as described in sections 2.5.3, 2.5.4 and 2.5.7 respectively.

2.6 The Effect of Thrombocytopenia in a Murine Model of Pulmonary Infection with *P.aeruginosa* and MRSA

2.6.1 Establishing a Murine Model of Platelet Depletion

To investigate the role of platelets in the regulation of pulmonary infection, the depletion of circulating platelets was induced in a murine model of pulmonary infection with *P.aeruginosa* strain RP73. These experiments were performed with the assistance of collaborators at the

Infections and Cystic Fibrosis Unit, Division of Immunology, Transplantation and Infectious Diseases, IRCCS San Raffaele Scientific Institute, Milan, Italy. Male C57/Bl6 mice were anaesthetised and inoculated with *P. a.* strain RP73 embedded agar beads, at either $1x10^6$, $1x10^5$ or $1x10^4$ cfu/mouse as previously described in section 2.5.2. In other separate experiments, mice were infected with 1 x 10^5 cfu/mouse MRSA strain USA300. Sham control mice were inoculated with sterile PBS embedded agar beads. 24 hours prior to infection, platelet depletion was induced via intra-muscular (*i.m.*) injection with 50µL 1mg/kg of an anti-GPIbα platelet depleting antibody (in saline). Control mice were administered with 50µL IgG control antibody (*i.m.*) in saline. The following protocol (**Figure 2.2**) was used to investigate the role of platelets on pulmonary bacterial infection.

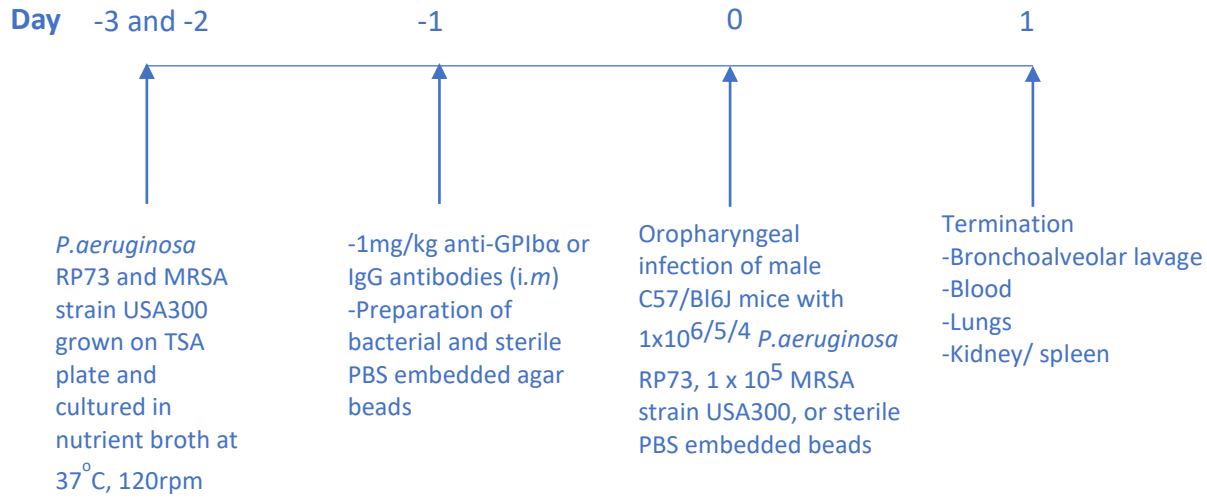

Figure 2. 2 A Protocol for Platelet Depletion: To Investigate the Effect of Platelet Depletion in a Murine Model of Pulmonary Bacterial Infection

24 h.p.i, platelet numbers were enumerated in whole blood, as described in section 2.5.3, to ensure adequate platelet depletion of ≥85%. A BAL of the lungs was performed and lungs were aseptically removed and processed as described in sections 2.5.4 and 2.5.7 respectively. Any incidence of mortality in mice depleted of platelets or in mice with normal circulating platelet levels was recorded.

2.6.2 The Effect of Platelet Depletion on Pulmonary Haemorrhage

In order to investigate whether administration of the platelet depleting anti-GPIbα antibody has any effect on pulmonary haemorrhage following infection with *P.aeruginosa* strain RP73, haemoglobin levels present in BAL fluid were quantified following administration of either the IgG control or anti-GPIbα antibodies. A 100µL aliquot of BAL fluid was taken and the absorbance was measured using a Spectramax 340PC microplate reader at 410nm, to detect haemoglobin.

In additional separate experiments, images of individual BAL fluid samples were taken to qualitatively analyse the haemoglobin levels present in BAL fluid, to determine whether administration of the platelet depleting anti-GPIbα antibody has any effect on pulmonary haemorrhage following infection with MRSA strain USA300.

2.6.3 Spleen and Kidney Harvest for Microbiological Analysis

To investigate whether experimentally induced platelet depletion had any effect on bacterial dissemination from the lungs to other peripheral organs, the kidney and spleen were removed

and homogenized in 2mL sterile saline. Homogenates were serially diluted using a 96 well plate and appropriate dilutions were plated onto TSA plates. Bacterial colonies were manually counted and the total kidney and spleen cfu were calculated.

2.6.4 Evaluation of Biochemical Markers of Metabolic Acidosis

Throughout experimentally induced platelet depletion experiments, core body temperature was monitored using rectal probe thermometry (Homeothermic Monitor, Harvard Apparatus).

24 hours following infection with $1x10^5$ cfu/mouse *P.aeruginosa* strain RP73, blood was collected, under anaesthesia, via cardiac puncture into heparin (100 units/mL) coated syringes. 65µl blood was transferred to EC8+ blood analyser cartridges and processed using a handheld i-STAT blood analyser (Abaxis VetScan iSTAT 1 analyser 300A) to quantify a panel of biochemical markers of metabolic acidosis used to detect organ dysfunction, including pH, urea, base excess, bicarbonate ions, pCO_2 and anion gaps.

In separate experiments, naïve mice were administered either 50µL of the IgG control or platelet depleting anti- GPIbα antibody. At 24 hours post treatment, the effects of platelet depletion on biochemical markers of metabolic acidosis were analysed as described above.

2.6.5 The Effect of Thrombocytopenia on Pulmonary Alveolar Integrity

Experiments were performed to investigate the effect of thrombocytopenia on pulmonary alveolar integrity, following infection with *P.aeruginosa* strain RP73. Thrombocytopenic mice

were infected with $1x10^5$ cfu/mouse as described in sections 2.5.2 and 2.6.1. 23 h.p.i 100µL 0.5% Evans Blue dye was administered via intra-venous (*i.v.*) injection. 24 h.p.i the right lobe of the lung was removed, weighed and added to 500µL Formamide. This was incubated at 65°C for 24 hours to extract the dye. At the same time point, the left lobe of the lung was removed and weighed to determine the 'wet weight'. This was subsequently incubated for 24 hours at 65°C. 24 hours post incubation, the left lobe lung samples were weighed, to determine the 'dry lung weight'. The right lobe lung samples were centrifuged at 1700 g for 5 minutes to remove remaining tissue fragments and absorbance values measured at 620nm (Jenway 6300 spectrophotometer). A standard curve was used to calculate nanograms (ng) Evans Blue dye per mg lung tissue for each sample.

2.7 Mechanisms of Platelet Involvement in Infection

2.7.1 The Role of Platelet TLR4 in the Regulation of Pulmonary Infection

To investigate the role of platelet Toll- like receptor 4 (TLR4) in infection, male TLR4 knockout mice (Riffo-Vasquez et al., 2012) and C57/BI6J wild type mice were infected with $1x10^5$ cfu/mouse as described in section 2.5.2 and sham control mice were inoculated with sterile PBS embedded agar beads. 24 h.p.i, a BAL of the lungs was performed as described in section 2.5.4, and lungs were removed and processed as described in section 2.5.7.

2.7.1.1 Polymerase Chain Reaction Analysis of Murine TLR4 cDNA

A mutation inducing loss of function was used to generate TLR4 knockout mice. DNA was extracted from tail clips of TLR4 knockout and C57/BI6J wild type mice. Tails clips were immersed in lysis buffer (100nM TRIS, 5mM EDTA, 0.4% SDS, 200nM NaCL, pH 8) and Proteinase K (diluted 1 in 100). Samples were subsequently heated overnight at 55^{o}C. The lysate was then centrifuged at 5,000 g for 1 minute in order to remove the insoluble fraction. Polymerase Chain Reaction (PCR) reaction mixture was then added to samples (components indicated in **Table 2.2**) and left at room temperature for approximately 10 minutes. TLR4 and wild type primer sequences used for DNA amplification are listed in **Table 2.3**.

Amount	Component	Final Concentration
25µl	Ready Mix	
0.5µl	Forward Primer	0.1-0.5µM
0.5µl	Reverse Primer	0.1-0.5µM
1µl	Template DNA (typically 10ng)	200pg/µL
23µl	Denucleated water	
50µl	**Total Volume**	

Table 2.2 Reaction Mixture Components and Final Concentrations Used

	primers	Ann temp	cycles	Final Primer conc u	Mg 2+	band size
TLR4	5′-cgt gta aac cag cca ggt ttt gaa ggc-3′	67	35	0.24	1.5	1200
WT	5′-tgt tgc cct tca gtc aca gag act ctg-3′					
TLR4	5′-tgt tgg gtc gtt tgt tcg gat ccg tcg-3′	67	35	0.24	1.5	1200
KO	5′-tgt tgc cct tca gtc aca gag act ctg-3′					

Table 2.3 TLR4 Knockout and Wild Type Primers using for DNA Amplification

The DNA present in each sample was subsequently amplified in a thermal cycler using 25 cycles of the protocol indicated in **Table 2.4**, Following DNA amplification, samples were placed on a hold cycle at 4^{o}C.

Cycling Parameter	**Temperature** (^{o}C)	**Time** (mins)
Denature Template	94	1
Anneal Primers	55	2
Extension	72	3

Table 2.4 Cycling Parameters Used for DNA Amplification.

Molten agarose gel solution was prepared (1.5% agarose in 1x TAE buffer- 40mM Tris, 20mM Acetate and 1mM EDTA pH 8), and heated until dissolved. GelRed stain was added into the molten gel solution (1:10,000) and mixed thoroughly. The gel was then allowed cooled, to solidify. Following the DNA amplification process, the samples or standard ladder were loaded onto the agarose gel. The gel was subsequently run at 100 volts for 30 minutes. The stained gel was viewed using a standard trans illuminator at 302nm and the gel was then imaged using an ethidium bromide filter.

2.7.2 The Role of Platelet Purinergic Receptors in the Regulation of Pulmonary Infection

The purine hydrolysing enzyme, Apyrase, was used to investigate the role of purines and purinergic receptors in the regulation of pulmonary infection. 30 minutes prior to infection, mice were treated with either vehicle (saline) or 100 units/mL Apyrase (0.1mL/mouse), via *i.v.* injection.

Additional separate experiments were performed to further investigate the role of specific platelet purinergic receptors ($P2Y_1$, $P2Y_{12}$, $P2X_1$ and $P2Y_{14}$). 30 minutes prior to infection, mice

were administered a single dose (0.1mL/mouse) of either vehicle control (saline), a $P2Y_1$ antagonist, MRS2500 (3mg/kg), a $P2Y_{12}$ antagonist, AR-C66096 (3mg/kg), a $P2X_1$ antagonist, NF-279 (3mg/kg) or a $P2Y_{14}$ antagonist, PPTN Mesylate (10mg/kg), via *i.v.* injection. A second dose of PPTN was administered at 6 h.p.i.

After drug treatments, mice were infected with $1x10^5$ cfu/mouse *P.aeruginosa* strain RP73, as described in section 2.5.2. Sham control mice were inoculated with sterile PBS embedded agar beads. At 24 h.p.i, blood was taken, a BAL was performed and lungs were aseptically removed and processed as described in sections 2.5.3, 2.5.4 and 2.5.7 respectively.

To investigate the effect of platelet purinergic receptors on bacterial dissemination from the lungs to the peripheral organs, the kidney and spleen were removed, as described in section 2.6.3.

2.8 Histological Analysis of Lung Tissue

2.8.1 Analysis of Infection Induced Pulmonary Neutrophil Recruitment

Lungs from sham and $1x10^6$ cfu/mouse *P.aeruginosa* strain RP73 infected mice, prepared as described in section 2.5.2, were inflated (0.5mL) and subsequently fixed in 20mL 10% Formaldehyde (in deionised water) for 24 hours. Lung tissue samples were paraffin fixed using a Shandon Citadel 2000 Tissue Processor and the following protocol was used **Table 2.5.**

Reagent	Time (minutes)
90% industrial methylated spirit (IMS)	120
100% IMS	360
Histoclear and IMS (1:1)	120
Histoclear	360
Paraplast	240

Table 2. 5 Protocol to Prepare Lung Tissues from Mice Infected with *P.aeruginosa*

Tissue samples were subsequently embedded into paraffin wax blocks and allowed to cool for 1 hour on a cold plate. Lungs were then sectioned, using a microtome (Microtom Heidelberg HM330), to 6µm slices onto superfrost plus slides and allowed to dry overnight. Sections were dewaxed in dewax xylene for 5 minutes and rehydrated in xylene and decreasing concentrations of ethanol for 1 minute at each concentration (100%, 90%, 70%, tap water). To block endogenous peroxidase activity, sections were immersed in 3% hydrogen peroxide in ethanol for 10 minutes and then washed 3 times with tap water. For antigen retrieval, a sodium citrate buffer (2.94g Tri-sodium citrate, 1L deionised water, 500µl tween 20) was prepared in a pressure cooker (Nordic ware) at pH 6.0 with 0.1M Sodium Hydroxide (NaOH). The sodium citrate buffer was heated on full power in a microwave (Kenwood) for 10-15 minutes, until the solution was at 100^{o}C. The rack of microscope slides was then placed into the buffer and the lid of the pressure cooker was tightened. The pressure cooker was heated in the microwave for a further 5 minutes. Once the pressure had equalised, the pressure cooker was placed under cold tap water to remove the retrieval buffer and to cool the slides. The remaining tap water was shaken off the slides and a ring was drawn around

each lung section using a hydrophobic pap pen. To block non-specific binding, 50µL 1% bovine serum albumin (BSA) blocking buffer (in PBS) was added to each lung section for 10 minutes, before blotting dry. Slides were stained for neutrophils using 50µL of an Abcam AB6872 anti-neutrophil elastase primary antibody (1:100 in 1% BSA in PBS) or 1% BSA in PBS for control sections and incubated for 2 hours at room temperature in a humidified chamber. The primary antibody was removed by washing sections 3 times in PBS, using a plastic squeeze dispensing wash bottle. 50µL of a secondary mouse-adsorbed biotinylated anti-rat rabbit secondary antibody (1:200 in 1% BSA in PBS) was added to sections for 1 hour. During this time, streptavidin (1:200 in 1% BSA in PBS) and biotinylated Horse Radish Peroxidase (HRP), (1:200 in 1% BSA in PBS) from an ABC Vectastrain kit, were mixed to form a complex. After 1 hour, the secondary antibody was removed by washing in PBS. The streptavidin + biotinylated (HRP) was added to sections for 1 hour at room temperature, before washing. A Diaminobenzidine (DAB) developing buffer was prepared (20mL DAB developing buffer 10x stock (1M TRIS pH 7.6), 180mL deionised water, 200µL 30% hydrogen peroxide and 1mL 50mg/mL DAB stock), and slides were developed in the DAB solution for 10 minutes before washing slides in tap water. Slides were counterstained with haematoxylin Gill's number 1 for 30 seconds, washed in tap water and immersed in acid alcohol differentiation solution for 10 seconds. Slides were then washed in tap water before dehydrating in increasing concentrations of ethanol (70%, 90%, 100%) and xylene, each for one minute. Following dehydration, slides were coverslipped using DPX mounting medium. Representative images of infected and control lung sections were captured using a Leica DM 2000 LED upright microscope, under a x40 objective.

2.8.2 Histological Analysis of Pulmonary Tissue with Haematoxylin and Eosin (H&E)

Experiments were performed to visualise the pulmonary inflammatory cell infiltrate following infection. Lungs from either sham control or infected ($1x10^6$ cfu/mL *P.aeruginosa* strain RP73) mice, as described in section 2.5.2, were formalin fixed, processed and embedded into paraffin wax blocks as described in section 2.8.1. Lungs were dehydrated in xylene and ethanol, as described in section 2.8.1 and immersed into tap water for 5 minutes. Slides were immersed in eosin for 10 seconds and subsequently washed in tap water 3 times. Slides were immersed in acid alcohol differentiation solution for 10 seconds, followed by washing in tap water. Samples were then immersed in haematoxylin Gill's number 1 for 30 seconds, followed by washing in tap water. Slides were immersed in acid alcohol differentiation solution a second time, dehydrated using ethanol and xylene, and coverslipped, as described in section 2.8.1. Representative images of infected and control lung sections were captured using a Leica DM 2000 LED upright microscope, under a x40 objective.

2.9 Evaluation of Inflammatory and Platelet Activation Markers Following Infection

Experiments were performed to investigate whether inflammatory markers, IL-6 and the chemokine receptor ligand KC (CXCL1), and platelet activation markers, PF-4 and RANTES, were significantly elevated following pulmonary bacterial infection. Plasma and BAL samples were taken from sham control, *P.aeruginosa* (RP73, PAO1 and NN2) and MRSA (USA300) infected mice, as described in 2.5.3 and 2.5.4. Murine IL-6, KC, PF-4 and RANTES in samples were measured using mouse Duoset enzyme linked immunosorbent assay (ELISA) kits, according to manufacturer's instructions (**Table 2.6**). 100µL of the capture antibody (in PBS (**Table 2.6**) was added to each well in a 96 well ELISA microplate and incubated overnight at

room temperature. Wells were washed three times with 400µL wash buffer (0.05% Tween 20 in PBS, pH 7.2-7.4) and blotted dry to remove any remaining wash buffer. Plates were blocked by adding 300µL of reagent diluent (1% BSA in PBS, pH 7.2-7.4) to each well, for 1 hour at room temperature. The plates were then washed again, as described previously. A seven-point standard curve of recombinant IL-6, KC, PF-4 and RANTES was prepared using 2-fold serial dilutions (in reagent diluent, **Table 2.6**), 100µL of sample or standard (diluted in reagent diluent) was added to wells and incubated for 2 hours at room temperature. Wells were washed again and 100µL of detection antibody (in reagent diluent, **Table 2.6**) was added to each well for 2 hours at room temperature. Wells were washed and 100µL of streptavidin-HRP (diluted in reagent diluent according to vial instructions) was added to each well for 20 minutes at room temperature, avoiding direct light. Plates were washed a final time and 100µL of substrate solution (1:1 mix of hydrogen peroxide and tetramethylbenzine) was added to each well for 20 minutes at room temperature, avoiding direct light. 50µL stop solution (2N H_2SO_4) was added to each well, whilst tapping gently to ensure thorough mixing. The optical density of each well was determined using a Spectramax 340PC microplate reader at 450nm.

Marker	**Capture Antibody** (µg/mL)	**7- Point Standard** (pg/mL)	**Detection Antibody** (ng/mL)
IL-6	2	1000 - 15.6	150
KC	2	1000 - 15.6	50
PF-4	2	2000 - 31.3	100
RANTES	2	2000 - 31.3	12.5

Table 2. 6 The Concentrations of Capture and Detection Antibodies and 7-point Standards: mouse Duoset enzyme linked immunosorbent assay (ELISA) kit

2.10 The Use of a Murine Model of Pulmonary Infection for Therapeutic Analysis

2.10.1 The Effect of HT61 Against Pulmonary Infection with *P.aeruginosa* and MRSA

Mice were anesthetised with inhaled isoflurane and inoculated with $1x10^6$ cfu/mouse bacterial embedded agar beads as described in section 2.5.2. Sham control mice were inoculated with sterile PBS embedded agar beads. 24 h.p.i, mice were administered with either 0.2mL/ mouse vehicle control (0.1% Dimethyl sulfoxide (DMSO)) or with a single dose of a small quinolone derived compound, HT61 at either 0.1, 1, 5 or 10 mg/kg HT61, via *i.p.* injection. HT61 doses for each bacterial strain are listed in **Table 2.7**.

Bacterial Strain	HT61 Dose (mg/kg)
P.aeruginosa RP73	0.1, 1, 5
P.aeruginosa PAO1	0.1, 1, 5
P.aeruginosa NN2	0.1, 1, 5
MRSA USA300	0.1, 1, 10

Table 2.7 HT61 Doses Used in the Murine Model of Pulmonary Infection with *P.aeruginosa* and MRSA

48 h.p.i, a BAL was performed and lungs were removed and processed, as described in sections 2.5.4 and 2.5.7 respectively.

2.10.2 The Effect of HT61 and Tobramycin/ Vancomycin Combination Treatment Against Pulmonary Infection with *P.aeruginosa* and MRSA

Experiments were performed to investigate whether combination therapies of HT61 with Tobramycin had any further effects on pulmonary bacterial load. Mice were anesthetised with inhaled isoflurane and inoculated with $1x10^6$ cfu/mouse bacterial embedded agar beads as described in 2.5.2. Sham control mice were inoculated with sterile PBS embedded agar beads. 24 h.p.i, mice were treated with either 0.2mL/ mouse vehicle (0.1% DMSO), 50, 100, 200 or 300 mg/kg Tobramycin (for *P.aeruginosa* strains), 100 mg/kg Vancomycin (for MRSA), 1 mg/kg HT61 (for all bacterial strains) or combination treatment, all administered via *i.p.* injection. Singular and combination treatment doses for each bacterial strain are listed in **Table 2.8.**

Bacterial Strain	**Tobramycin (T)** mg/kg	**Vancomycin (V)** mg/kg	**HT61 (H)** mg/kg	**Combination**	
				Tobramycin (T) or **Vancomycin** (V) (mg/kg)	**HT61** (mg/kg)
P.aeruginosa RP73	100, 300	X	1	100 T	1
P.aeruginosa PAO1	50	X	1	50 T	1
P.aeruginosa NN2	100, 200	X	1	100 T	1
MRSA USA300	X	100	1	50 V	1

Table 2. 8 Singular and Combination Treatment Doses for the Murine Model of Pulmonary Infection with *P.aeruginosa* and MRSA

48 h.p.i, a BAL was performed and lungs were removed and processed, as described in sections 2.5.4 and 2.5.7 respectively.

2.11 The Role of Platelets in the Regulation of Pulmonary Infection

2.11.1 Pulmonary Platelet Recruitment Following Infection with *P.aeruginosa* Strain RP73

Experiments were performed to determine whether platelets are recruited to the lung following bacterial infection. Lungs from sham control and $1x10^6$ cfu/mouse *P.aeruginosa* strain RP73 infected mice, were formalin fixed, processed and embedded into paraffin wax blocks as described previously (2.8.1). To assess platelet recruitment into different anatomical regions of the lung, sections were stained for platelets using a platelet specific anti-CD42b primary antibody (1:500), a Vector Laboratories BA100 biotinylated anti- rabbit secondary antibody (1:200), and an ABC Vectastain kit, as described in section 2.8.1.

2.12 *In vitro* Experiments

2.12.1 Murine Blood Collection

Male C57/BI6J mice were terminally anaesthetised with 0.3mL 25% w/v Urethane, via *i.p.* injection. 1mL citrated blood was collected via cardiac puncture, mixing with ACD at a ratio of 1-part ACD to 9-parts blood.

2.12.2 Murine Platelet Isolation

Platelet rich plasma (PRP) was collected from citrated blood by centrifugation at 100 g for 10 minutes at 23°C. Blood was then centrifuged again at 120 g for 5 minutes at 23°C and the remaining PRP collected. Prostaglandin E1 (PGE_1) (5µL 2.5mM) was added to the PRP, which was then centrifuged again at 900 g for 6 minutes. The resulting platelet pellet was resuspended in 200µL Tyrode's buffer (0.14M Sodium Chloride (NaCl), 0.003M Potassium Chloride (KCl), 0.0003M Sodium Dihydrogen Phosphate Dodecahydrate ($Na_2HPO_4.12H_2O$), 0.01M Sodium Hydrogen Carbonate ($NaHCO_{3)}$, 0.02M HEPES, 0.001M Magnesium Chloride ($MgCl_2$) and 0.005M Glucose, pH 7.3). Platelets were subsequently stained in Stromatol (1:100) and quantified on a Neubauer haemocytometer, under a x40 objective, using a Leica D 2000 led upright microscope. Platelets were diluted to a final working concentration of either $1x10^6$, $1x10^7$ or $1x10^8$ platelets/mL in Tyrodes buffer and treated with 2mM Ca^{2+} prior to use.

2.12.3 The Effect of Platelets on Growth of *P.aeruginosa* strain RP73 *in vitro*

Co-culture experiments were performed to investigate whether platelets can have a direct effect on bacterial growth. ONCs of *P.aeruginosa* strain RP73 were prepared, as described in 2.4, and diluted to a final working concentration of $1x10^6$ cfu/mL in TSB (OD_{600} 0.0031). Murine platelets were isolated, as described in section 2.12.2, and diluted to a final working concentration of $1x10^6$ platelets/mL in Tyrodes buffer. Platelets and bacteria were cultured at a volumetric ratio of 1:1, at 37°C, under shaking conditions at 120rpm. For CFU quantification, 20µL aliquots of the culture were taken periodically every 2 hours from 0 to 8

hours and 10-fold serial dilutions (in saline) were performed and plated onto TSA plates for 24 hours at 37^{o}C.

2.12.4 Platelet Bacterial Killing Assays

To further investigate whether platelets have a direct killing effect on bacteria, co-culture experiments were performed as described in 2.12.3, using a LIVE/DEAD *Bac*Light Bacterial Viability Kit, according to manufacturer's instructions. For these experiments, murine platelets were diluted to a final working concentration of either $1x10^6$, $1x10^7$ or $1x10^8$ platelets/mL in Tyrodes buffer. A culture with no platelets was prepared as a negative control. At each time point (0, 2, 4, 6 and 8 hours), 150µL aliquots were taken and centrifuged at 1700 g for 10 minutes and resuspended in 150µL deionised water. 100µL of each sample was added to black 96 well plates. 50µL 2.5uM SYTO9 (in deionised water) was added to each well, incubated for 15 minutes on ice and read at 488/20nm excitation, 528/20nm emission on a fluorescent plate reader (Synergy HT Bio-Tek). Samples were then counterstained using 50µL 15uM Propidium Iodide (PI) (in deionised water) for 15 minutes, and plates were read again at 488/20nm excitation, 645/20nm emission.

Other separate experiments were performed to ensure platelets remained viable throughout the duration of the co-culture experiments. At each time point (0, 2, 4, 6,8), 3 aliquots (50µL) of the $1x10^7$ platelet-bacteria co-culture were taken and stimulated with either vehicle control (saline), 100µM ADP or 10µM thrombin receptor activating peptide (TRAP) for 30 minutes at room temperature. After incubation, 1µL anti-CD41 Phycoerythrin (PE) and 1µL anti- CD62P Fluorescein Isothiocyanate (FITC) antibodies were added to each sample, and these were left to incubate for an additional 15 minutes at room temperature. Following incubation 500µL

PBS was added to each sample. CD62P events were quantified and analysed on a Beckman Coulter Cytomics FC 500 flow cytometer. Data was collected using FITC and PE fluorescent wavelengths at 515nm and 580nm respectively. Live gating was used to specifically identify CD62P positive events on cells positive for CD41, using forward and side scatter analysing 10,000 events. Events staining positive for both CD41 and CD62P were considered to represent P-selectin expressing platelets.

2.13 *Ex vivo* Animal Studies

2.13.1 Analysis of Platelet-Leukocyte Complexes Formation *ex vivo*

Male C57BIJ6 mice were anesthetised with inhaled isoflurane and inoculated with either sham or $1x10^6$ cfu/mouse *P.aeruginosa* RP73 bacterial embedded agar beads as described in section 2.5.2. 24 h.p.i, citrated blood was isolated via cardiac puncture. 2µL murine whole blood was treated with saturating concentrations of the platelet specific antibody, CD41-FITC (1:10 in saline) and the neutrophil specific antibody Ly6G-PE. Blood samples were incubated with the antibodies for 30 minutes, in the dark at room temperature. After the incubation period, 500µL lysis buffer (0.015M NH_4Cl, 0.001M $KHCO_3$, 0.00001M EDTA) was used to lyse erythrocytes. Platelet-leukocyte complexes were quantified and analysed on a Beckman Coulter Cytomics FC 500 flow cytometer as described in section 2.13.1. Live gating was used to specifically identify CD41 expressing platelets and Ly6G expressing neutrophils, using forward and side scatter analysing 10,000 events. Events positive for both CD41 and LY6G were considered to represent platelet-neutrophil complexes.

2.14 Human *in vitro* Studies

2.14.1 Human Platelet Isolation

Human citrated venous blood (20 mL) was isolated from the antecubital vein of healthy volunteers (who had not taken anti-platelet drugs for 10 days prior to donation), at a ratio of 1-part ACD: 9-parts blood. Blood was centrifuged at 120 g for 20 minutes at 25^{o}C and the resulting PRP was collected. PGE_1 was added to the PRP in excess (1:1000 into PRP) and centrifuged at 1300 g for 10 minutes at 25^{o}C. The supernatant or platelet poor plasma (PPP) was aspirated and the remaining platelet pellet resuspended in 1mL RPMI 1640 media. 10µL 2.5mM PGE_1 (1:100) was added to the platelet suspension and the final volume was made up to 10mL in RPMI 1640. The platelet suspension was centrifuged again at 1300 g for 10 minutes at 25^{o}C, before the supernatant was aspirated and the platelet pellet resuspended in 1mL RPMI 1640. Platelets were stained with Stromatol (1:100) and quantified using an improved Neubauer haemocytometer under a x40 objective and Leica DM 2000 LED upright microscope and diluted to a final working concentration of $1x10^8$ platelets/mL. Platelets were left for 45-60 minutes at 37^{o}C, to allow the PGE_1 to degrade prior to use. Platelets were then treated with 2mM Ca^{2+} for functional experiments and stimulated with 100nM ADP for chemotaxis experiments.

2.14.2 Bacteria Induced Platelet Chemotaxis *in vitro*

Wells on a BD Falcon 24 well companion plate were blocked for 1 hour using 1mL RMPI 1640 media + 1% BSA per well. After 1 hour, the blocking buffer was aspirated and individual wells

were washed using 1mL RPMI 1640 media. Cell culture inserts (BD Falcon transparent 3µm PET membrane for 24 well plate) were added to individual wells and 600µL *P.aeruginosa* strain RP73 was added to the bottom chamber at varying concentrations ($1x10^6$, $1x10^{5,}$ $1x10^4$ cfu/mL in RPMI 1640 media). 600µL 1µg/mL stromal cell derived factor 1α (SDF-1α) was added as a positive chemotactic control and 600µL RPMI 1640 media was added as a negative control. 250µL of washed platelets, isolated from human whole blood (ADP stimulated (100nM)) were added on top of the transwell inserts (**Figure 2.3**) and incubated for 90 minutes at 37^{o}C. After the incubation period, 50µL media from each of the bottom chambers was incubated with 2µL platelet specific CD41-FITC (1:10 in saline) antibody, for 30 minutes at room temperature in the dark. After 30 minutes, 500µL PBS and 50µL flow count flurospheres (Beckman Coulter) were added to 50µL of each sample. Flow count fluorospheres are a suspension of fluorospheres used to directly determine absolute counts on the flow cytometer. Samples were subsequently analysed and the platelets were quantified using a Beckman Coulter Cytomics FC 500 flow cytometer. Those that stained positively for the CD41 antigen were used as a measure of platelet migration.

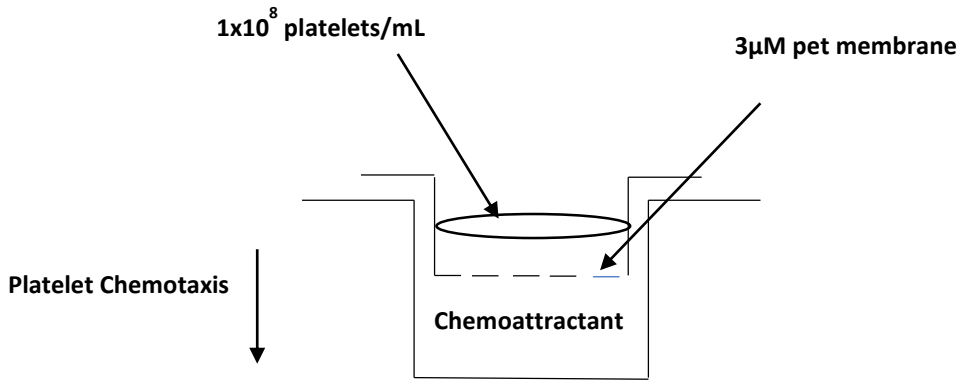

Figure 2. 3 Diagrammatic Representation of the Bacterial Induced Platelet Chemotaxis Apparatus

2.15 Statistical Analysis

Total lung CFU is expressed as log cfu. Total lung cfu and total and differential cell counts from BAL fluid taken from *in vivo* infection studies, and blood samples (circulating platelets and flow cytometry analysis) were expressed as mean ± standard error of the mean (SEM). A Sharipo-Wilk normality test was performed to confirm that values came from a Gaussian distribution of data. A parametric one-way analysis of variance (ANOVA), followed by a Bonferroni's multiple comparison post hoc test were used for comparisons of data sets. For immunohistochemistry and ELISA experiments, data were expressed as mean ± SEM and analysed using an unpaired Two-Tailed T-test. Survival curves were analysed using a Mantel-Cox test. For chemotaxis experiments, data was expressed as a chemotactic index (CI) ± SEM. Data was analysed using a one-way ANOVA, followed by a Bonferroni's multiple comparison test between groups. All data was analysed by GraphPad Prism 6.0 and significant differences

were accepted if $p<0.05$ was observed between individual groups, when compared to either sham or vehicle control groups.

Chapter III: Results I

Establishment and Validation of a Murine Model of Pulmonary Infection

3.1 Establishing a Murine Model of Pulmonary Infection with *P.aeruginosa* and MRSA

3.1.1 Establishing a Murine Model of Pulmonary Infection with *P.aeruginosa* strain RP73

Initial titration studies were performed to determine the optimum inoculum to establish a murine model of pulmonary infection with the multidrug resistant clinical strain of *P.aeruginosa,* RP73. Mice were exposed to 3 different concentrations ($1x10^4$, $1x10^5$ or $1x10^6$ cfu/mouse) of bacterial embedded agar beads and infection and inflammatory parameters were subsequently analysed.

Murine pulmonary infection was established with all 3 tested inoculum levels, with a significant increase in pulmonary bacterial load observed at 48 h.p.i when compared to sham controls (10^4: 3.94±0.20 log cfu, 10^5: 4.25±0.57 log cfu and 10^6: 4.76±0.17 log cfu, versus sham: 0.0±0.0 log cfu, $p<0.0001$, **Figure 3.1A**).

Infection with $1x10^6$ cfu/mouse *P.aeruginosa* strain RP73 induced a significant increase in pulmonary total leukocyte recruitment when compared to sham controls (10^6: $12.47±1.19x10^5$ cells/mL versus sham: $1.43±0.16x10^5$ cells/mL, $p<0.0001$, **Figure 3.1B**). This increase in total pulmonary leukocyte recruitment was characterised by a significant increase in neutrophils (10^6: $10.18±1.50x10^5$ cells/mL versus sham: $0.04±0.01x10^5$ cells/mL, $p<0.0001$, **Figure 3.1C**). In contrast, pulmonary infection with either $1x10^4$ or $1x10^5$ cfu/mL *P.aeruginosa* strain RP73 did not demonstrate any significant increase in either total leukocyte recruitment (10^4: $3.95±0.76x10^5$ cells/mL and 10^5: $4.33±0.36x10^5$ cells/mL, versus sham: $1.43±0.16x10^5$ cells/mL, **Figure 3.1B**) or neutrophil recruitment (10^4: $2.38±0.85x10^5$ cells/mL, 10^5: $2.84±0.53x10^5$ cells/mL, versus sham: $0.04±0.01x10^5$ cells/mL, **Figure 3.1B**) to the lungs, when compared to sham controls. No significant changes were observed with either macrophage

(10^4: 1.56±0.10x10^5 cells/mL, 10^5: 1.49±1.20x10^5 cells/mL and 10^6: 2.29±0.45x10^5 cells/mL, versus sham: 1.40±0.17x10^5 cells/mL, **Figure 3.1D**) or lymphocyte (10^4: 0.0±0.0x10^5 cells/mL, 10^5: 0.0±10.0x10^5 cells/mL and 10^6: 0.0±0.0x10^5 cells/mL, versus sham: 0.0±0.0x10^5 cells/mL) numbers at any tested inoculum.

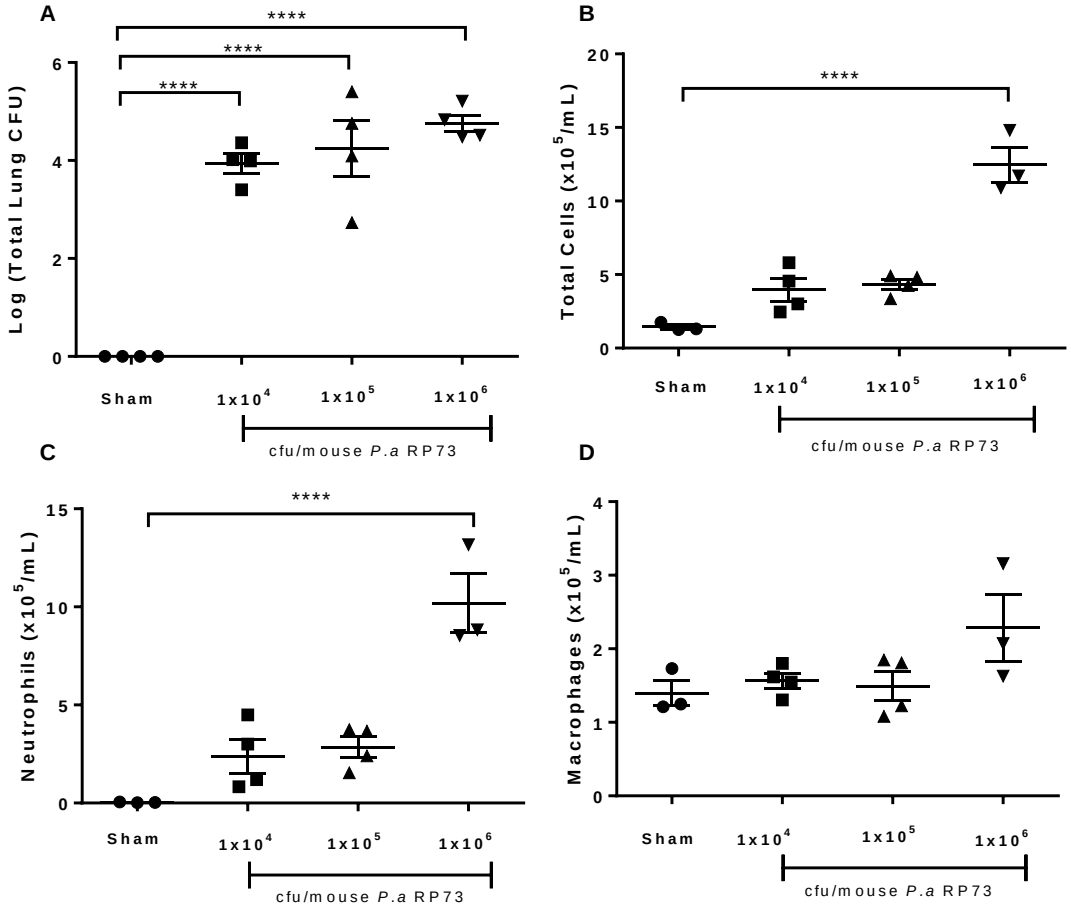

Figure 3.1 Effects of *P.aeruginosa* strain RP73 on Bacterial and Inflammatory Parameters of Pulmonary Infection

Mice were infected *(o.a)* with either sham or $1x10^4$, $1x10^5$, $1x10^6$ cfu/mouse RP73 embedded agar beads. A BAL of the lungs was performed for inflammatory cell quantification and lungs were aseptically removed, homogenised and plated for quantification of bacterial load at 48 h.p.i. (**A**) Pulmonary Bacterial Load, (**B**) Total Cells, (**C**) Neutrophils and (**D**) Macrophages, one-way ANOVA and Bonferroni's multiple comparisons post hoc test, **** $p<0.0001$ versus sham, n=3-4, data are presented as mean ± SEM.

3.1.1.1 Histological Analysis of Pulmonary Tissue Following Infection with *P.aeruginosa* strain RP73

Lung samples collected 24 h.p.i were stained with H&E to determine whether infection with *P.aeruginosa* strain RP73 had any significant effect on inflammatory cell recruitment, lung architecture and alveolar integrity.

Lung histopathology indicated gross differences in both the inflammatory cell type present and the density and distribution of cells, between *P.aeruginosa* infected and sham control animals. The H&E stain of *P.aeruginosa* infected animals indicated intra-alveolar inflammation and neutrophil accumulation (**Figure 3.2** iv-vi). Infection with *P.aeruginosa* induced alveolar damage and loss of alveolar integrity. In addition, representative images suggested evidence of haemorrhaging in the lungs and basement membrane thickening following infection (**Figure 3.2** iv-vi). Lung sections of sham control animals however showed preservation of normal lung architecture and little or no neutrophil recruitment. The predominant cell type in the lung parenchyma of sham control mice was macrophages, with no evidence of haemorrhaging or basement membrane thickening (**Figure 3.2** i-iii).

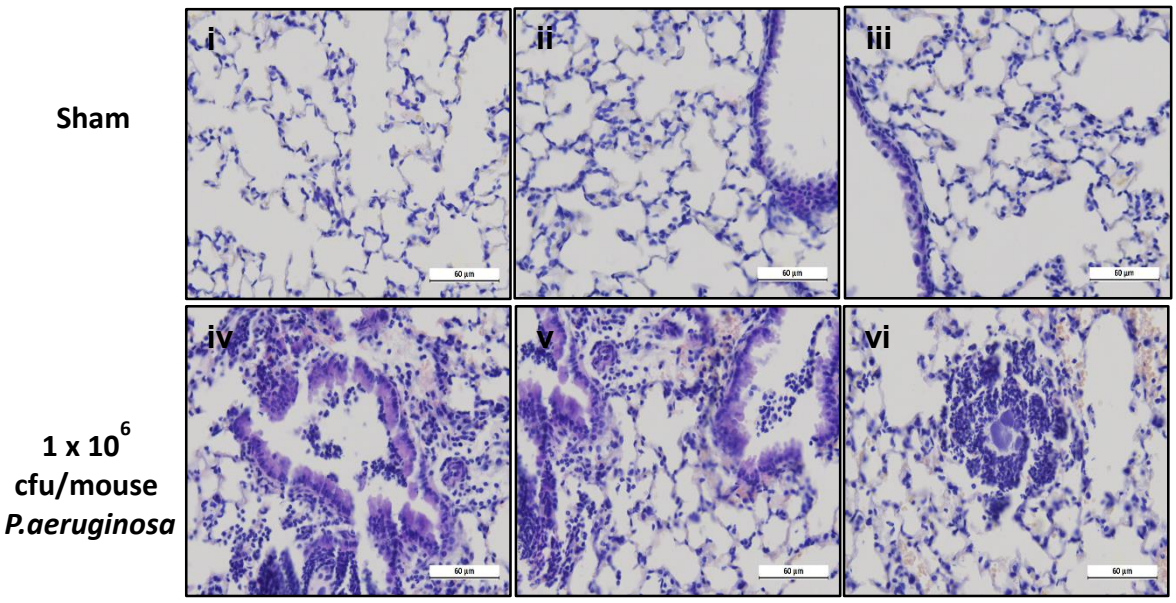

Figure 3.2 Effects of *P.aeruginosa* strain RP73 on Inflammatory Cell Recruitment, Lung Architecture and Alveolar Integrity

Mice were infected *(o.a)* with either sham or $1x10^6$ cfu/mouse RP73 embedded agar beads. At 24 h.p.i, lungs were removed, fixed in 10% formaldehyde and embedded into paraffin wax blocks. Tissue sections were stained with a Haematoxylin and Eosin stain. Representative images of lung parenchyma at x40 magnification from H&E stained lungs from (**i-iii**) sham control and (**iv-vi**) $1x10^6$ cfu/mL *P.aeruginosa* strain RP73 infected animals.

3.1.1.2 An Investigation into *P.aeruginosa* Strain RP73 Infection Induced Neutrophil Recruitment

Lung samples collected 24 h.p.i were stained with an anti-neutrophil elastase antibody to provide further evidence of neutrophil recruitment to the lungs post infection. Representative images of *P.aeruginosa* strain RP73 infected tissue sections indicated neutrophil accumulation and an increase in neutrophil recruitment into the airway lumen and alveolar spaces when compared to sham controls. Following quantification, a significant increase in neutrophil recruitment to the lungs was observed following infection with *P.aeruginosa* strain RP73 when compared to sham controls, as measured by the number of neutrophil elastase positive events per mm^2 of lung tissue ($1x10^6$ cfu/mL *P.aeruginosa* strain RP73: 39456±448.2 neutrophil elastase positive events/mm^2, versus sham: 2962±580.8 neutrophil elastase positive events/mm^2, **Figure 3.3A**). The percentage area of neutrophil elastase staining was also significantly increased following infection with *P.aeruginosa* strain RP73 when compared to sham controls ($1x10^6$ cfu/mL *P.aeruginosa* strain RP73: 8.99±1.5%, versus sham: 0.47±0.20%, **Figure 3.3B**), further highlighting infection induced neutrophil recruitment to the lungs.

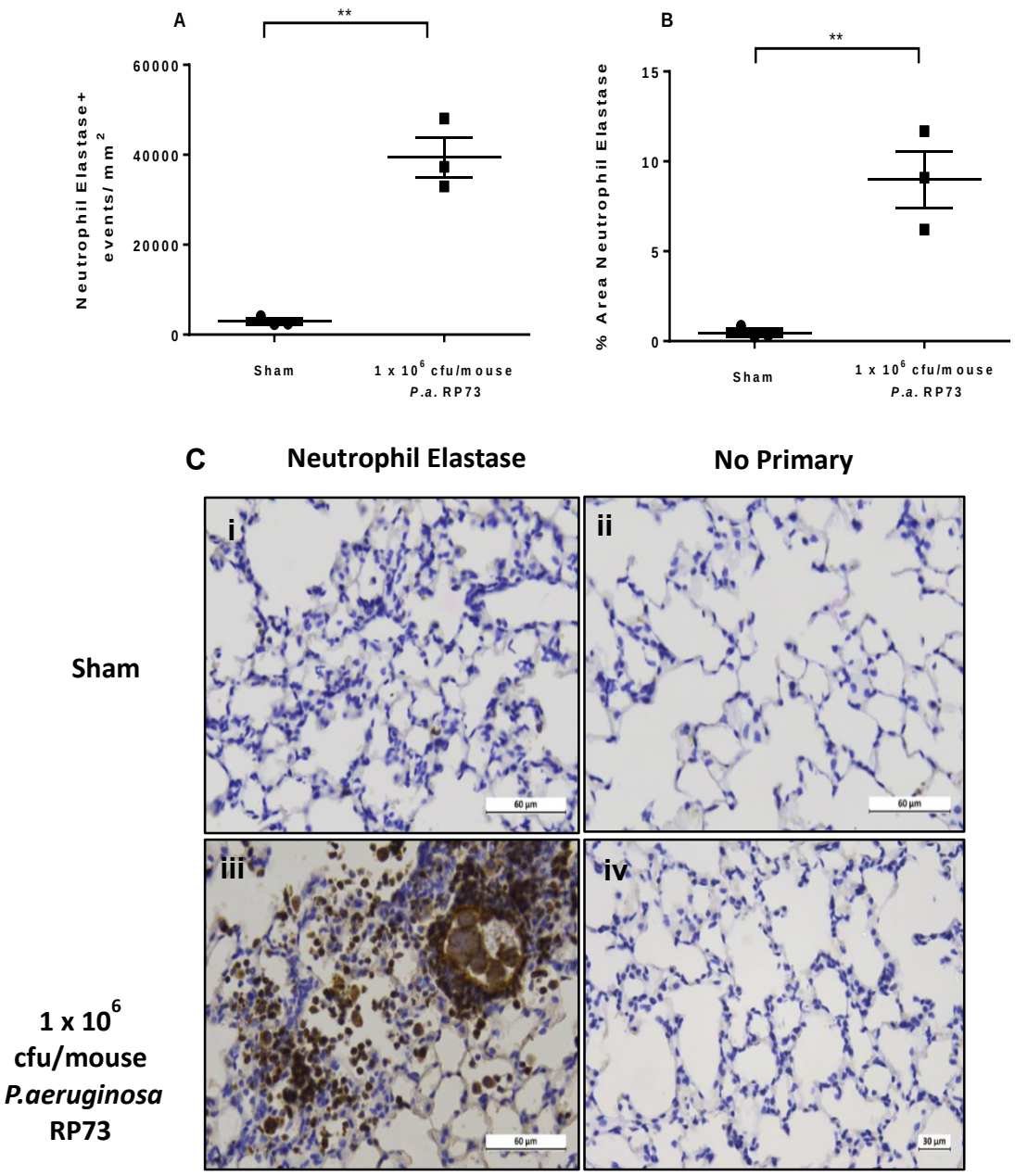

Figure 3.3 Effects of *P.aeruginosa* strain RP73 on Pulmonary Neutrophil Recruitment

Mice were infected *(o.a)* with either sham or $1x10^6$ cfu/mouse RP73 embedded agar beads. At 24 h.p.i, lungs were removed, fixed in 10% formaldehyde and embedded into paraffin wax blocks. Tissue sections were stained with an anti-neutrophil elastase antibody and analysed for quantification of (**A**) Neutrophil Elastase positive events per mm^2 and (**B**) Percentage area of neutrophil elastase. (**C**) Representative images of lung parenchyma at x40 magnification from (**i**) sham control and (**iii**) $1x10^6$ cfu/mL RP73 infected animals, (**ii**) and (**iv**) no addition of primary anti-neutrophil elastase antibody controls. Unpaired two-tailed t-test, **p<0.01 versus sham, n=3, data are presented as mean ± SEM.

3.1.2 Establishing a Murine Model of Pulmonary Infection with *P.aeruginosa* strain PAO1

Having established a murine model of pulmonary infection with *P.aeruginosa* strain RP73, experiments were performed to characterise additional gram-negative *P.aeruginosa* strains in the model. Mice were infected with 2 different concentrations ($1x10^5$ or $1x10^6$ cfu/mouse) of the laboratory reference strain, PAO1 embedded into agar beads and infection and inflammatory parameters were subsequently analysed.

The data obtained was comparable to that observed following infection with *P.aeruginosa* strain RP73, whereby infection was established with both tested inoculum levels. A significant increase in pulmonary bacterial load was observed at 48 h.p.i, when compared to sham controls (10^5: 4.87±0.30 log cfu and 10^6: 5.91±0.17 log cfu, versus sham: 0.0±0.0 log cfu, $p<0.0001$, **Figure 3.4A**).

Infection with $1x10^6$ cfu/mouse *P.aeruginosa* strain PAO1 induced significant recruitment of both total pulmonary leukocytes (10^6: 31.77±3.09$x10^5$ cells/mL versus sham: 1.82±0.23$x10^5$ cells/mL, $p<0.0001$**, Figure 3.4B**) and neutrophils (10^6: 29.57±3.12$x10^5$ cells/mL versus sham: 0.02±0.01$x10^5$ cells/mL, $p<0.0001$, **Figure 3.4C**) to the lungs. Conversely, pulmonary infection with $1x10^5$ cfu/mL *P.aeruginosa* strain PAO1 had no significant increase in total leukocyte recruitment (10^5: 4.46±0.53$x10^5$ cells/mL, versus sham: 1.82±0.23$x10^5$ cells/mL, **Figure 3.4B**) or neutrophil recruitment (10^5: 1.91±0.46$x10^5$ cells/mL, versus sham: 0.01±0.01$x10^5$ cells/mL, **Figure 3.4C**) to the lungs, when compared to sham controls.

Pulmonary infection with *P.aeruginosa* strain PAO1 had no significant effect on the recruitment of macrophages (10^5: 2.55±0.16$x10^5$ cells/mL and 10^6: 2.20±0.19$x10^5$ cells/mL, versus sham: 1.79±0.23$x10^5$ cells/mL, **Figure 3.4D**) or lymphocytes (10^5: 0.0±10.0$x10^5$ cells/mL

and 10^6: 0.0±0.0x10^5 cells/mL, versus sham: 0.0±0.0x10^5 cells/mL) to the lungs, with no significant increase observed in both infected groups compared to sham controls.

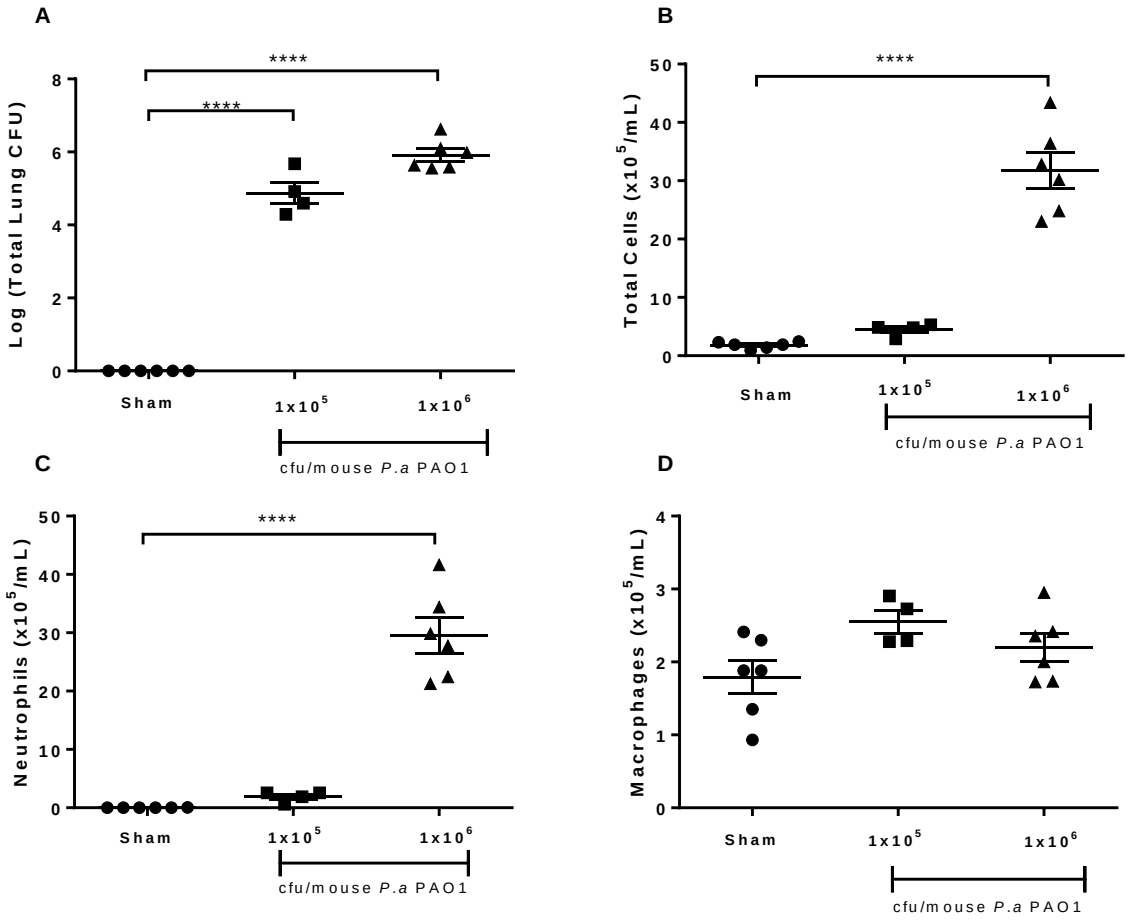

Figure 3.4 Effects of *P.aeruginosa* strain PAO1 on Bacterial and Inflammatory Parameters of Pulmonary Infection

Mice were infected (*o.a*) with either sham, 1x10^5 or 1x10^6 cfu/mouse PAO1 embedded agar beads. A BAL of the lungs was performed for inflammatory cell quantification and lungs were aseptically removed, homogenised and plated for quantification of bacterial load at 48 h.p.i. (**A**) Pulmonary Bacterial Load, (**B**) Total Cells, (**C**) Neutrophils and (**D**) Macrophages. One-way ANOVA and Bonferroni's multiple comparisons post hoc test, **** $p<0.0001$ versus sham, n=4-6, data are presented as mean ± SEM.

3.1.3 Establishing a Murine Model of Pulmonary Infection with *P.aeruginosa* strain NN2

Titration experiments were performed to characterise a Tobramycin resistant clinical isolate strain of *P.aeruginosa* in the murine model of pulmonary infection. Mice were infected with 3 different concentrations ($1x10^4$, $1x10^5$ or $1x10^6$ cfu/mouse) of *P.aeruginosa* strain NN2 embedded into agar beads and infection and inflammatory parameters were subsequently analysed.

Infection with $1x10^4$, $1x10^5$ and $1x10^6$ cfu/mouse induced a significant increase in pulmonary bacterial load at 48 h.p.i, when compared to sham controls (10^4: 1.35±0.57 log cfu, 10^5: 4.20±0.19 log cfu and 10^6: 6.41±0.05 log cfu, versus sham: 0.0±0.0 log cfu, $p<0.0001$, **Figure 3.5A**). In this strain, unlike RP73 and PAO1, a 0.41 log cfu increase was observed from the initial $1x10^6$ cfu/mouse inoculum.

Infection with both $1x10^5$ cfu/mouse and $1x10^6$ cfu/mouse induced significant recruitment of both total leukocytes (10^5: $32.05±2.86x10^5$ cells/mL, $p<0.01$ and 10^6: $76.9±8.65x10^5$ cells/mL, $p<0.0001$, versus sham: $2.74±0.51x10^5$ cells/mL, **Figure 3.5B)** and neutrophils (10^5: $28.25±3.34x10^5$ cells/mL, $p<0.01$ and 10^6: $74.15±8.77x10^5$ cells/mL, $p<0.0001$, versus sham: $0.0±0.0x10^5$ cells/mL, **Figure 3.5C**) to the lungs. However, no significant effects were observed on total leukocyte recruitment (10^4: $8.06±0.99x10^5$ cells/mL, versus sham: $2.74±0.51x10^5$ cells/mL, **Figure 3.5B**) or neutrophil recruitment to the lungs (10^4: $3.80±0.91x10^5$ cells/mL, versus sham: $0.0±0.0x10^5$ cells/mL, **Figure 3.5C**), following infection with $1x10^4$ cfu/mouse, when compared to sham controls.

Pulmonary infection with *P.aeruginosa* strain NN2 had no significant effect on the recruitment of macrophages (10^4: $4.28±0.30x10^5$ cells/mL, 10^5: $3.81±0.98x10^5$ cells/mL and 10^6:

2.76±1.61x10^5 cells/mL, versus sham: 2.74±0.51x10^5 cells/mL, **Figure 3.5D**) or lymphocytes to the lungs (10^4: 0.0±0.0x10^5 cells/mL, 10^5: 0.0±10.0x10^5 cells/mL and 10^6: 0.0±0.0x10^5 cells/mL, versus sham: 0.0±0.0x10^5 cells/mL), with no significant increase observed at any tested concentration, when compared to sham controls.

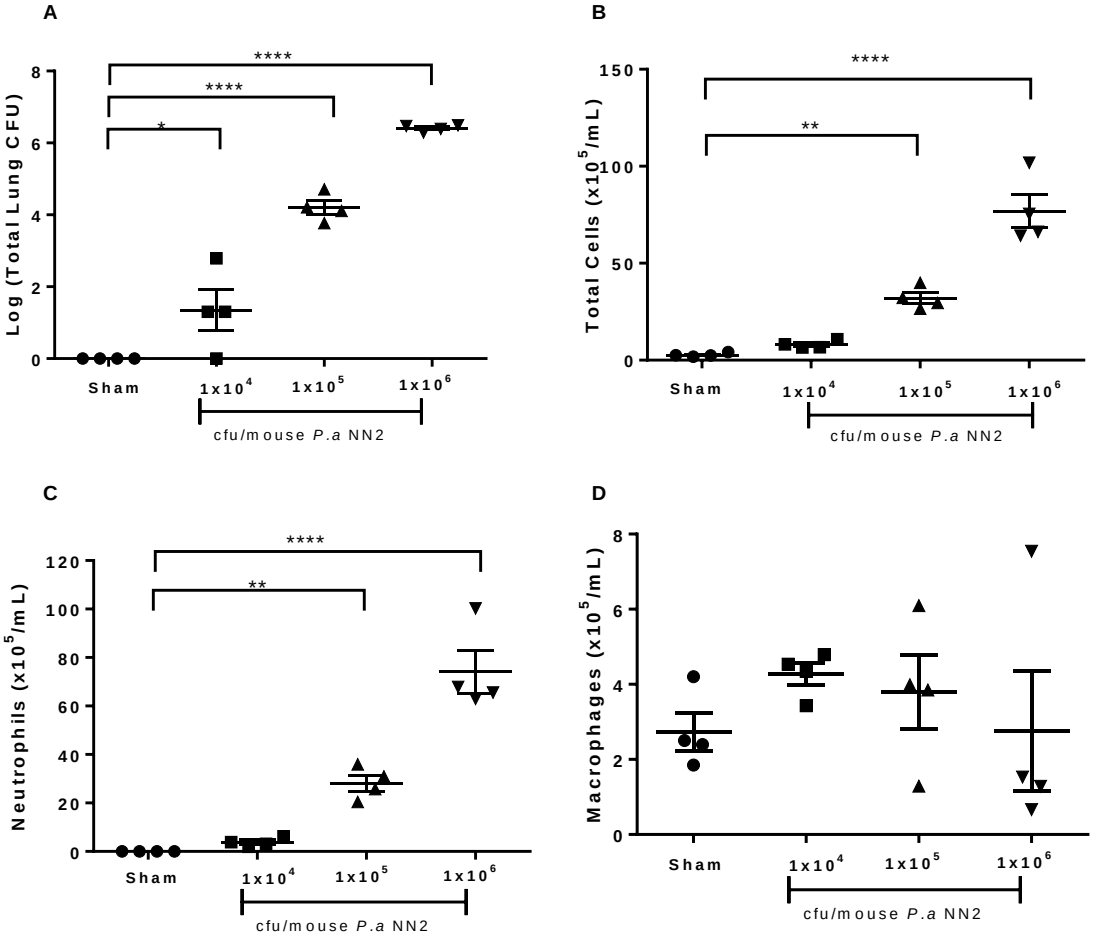

Figure 3.5 Effects of *P.aeruginosa* strain NN2 on Bacterial and Inflammatory Parameters of Pulmonary Infection

Mice were infected *(o.a)* with either sham or 1x10^4, 1x10^5, 1x10^6 cfu/mouse NN2 embedded agar beads. A BAL of the lungs was performed for inflammatory cell quantification and lungs were aseptically removed, homogenised and plated for quantification of bacterial load at 48 h.p.i. (**A**) Pulmonary Bacterial Load, (**B**) Total Cells, (**C**) Neutrophils and (**D**) Macrophages. one-way ANOVA and Bonferroni's multiple comparisons post hoc test, ** p<0.01, **** p<0.0001 versus sham, n=4, data are presented as mean ± SEM.

3.1.4 Establishing a Murine Model of Pulmonary Infection with MRSA strain USA300

Having established a murine model of pulmonary infection with the gram-negative bacterium, *P.aeruginosa*, additional experiments were performed to validate the model using a gram-positive bacterium, MRSA. Strain USA300 was used throughout this investigation, which is commonly associated with community acquired infections. Mice were infected with 3 different concentrations ($1x10^4$, $1x10^5$ or $1x10^6$ cfu/mouse) of USA300 embedded into agar beads and infection and inflammatory parameters were subsequently analysed.

Infection with $1x10^4$, $1x10^5$ and $1x10^6$ cfu/mouse induced a significant dose-dependent increase in pulmonary bacterial load recovered at 48 h.p.i compared to sham controls (10^4: 4.53±0.07 log cfu, 10^5: 4.86±0.03 log cfu and 10^6: 5.89±0.35 log cfu, versus sham: 0.0±0.0 log cfu, $p<0.0001$, **Figure 3.6A**).

MRSA, strain USA300, at any tested inoculum had no significant increase in total leukocyte recruitment to the lungs when compared to sham controls (10^4: 11.69±8.63x10^5 cells/mL, 10^5: 14.53±9.38x10^5 cells/mL and 10^6: 26.13±12.57x10^5 cells/mL, versus sham: 1.24±0.13x10^5 cells/mL, **Figure 3.6B**). However, infection with $1x10^6$ cfu/mouse significantly increased pulmonary neutrophil recruitment when compared to sham controls animals (10^6: 21.62±13.11x10^5 cells/mL, versus sham: 0.0±0.0x10^5 cells/mL, $p<0.01$, **Figure 3.6B**). Conversely, infection with $1x10^4$ cfu/mouse and $1x10^5$ cfu/mouse had no significant effect on neutrophil recruitment to the lungs when compared to sham controls (10^4: 1.05±0.53x10^5 cells/mL and 10^5: 4.33±2.68x10^5 cells/mL, versus sham: 0.0±0.0x10^5 cells/mL, **Figure 3.6B**).

Pulmonary infection with MRSA strain USA300 had no significant effect on the recruitment of macrophages (10^4: 10.64±8.10x10^5 cells/mL, 10^5: 10.20±6.70x10^5 cells/mL and 10^6: 4.51±0.61x10^5 cells/mL, versus sham: 1.23±0.13x10^5 cells/mL, **Figure 3.6D**) or lymphocytes to the lungs (10^4: 0.0±0.0x10^5 cells/mL, 10^5: 0.0±10.0x10^5 cells/mL and 10^6: 0.0±0.0x10^5 cells/mL, versus sham: 0.0±0.0x10^5 cells/mL), with no significant increase observed at any tested concentration, when compared to sham controls.

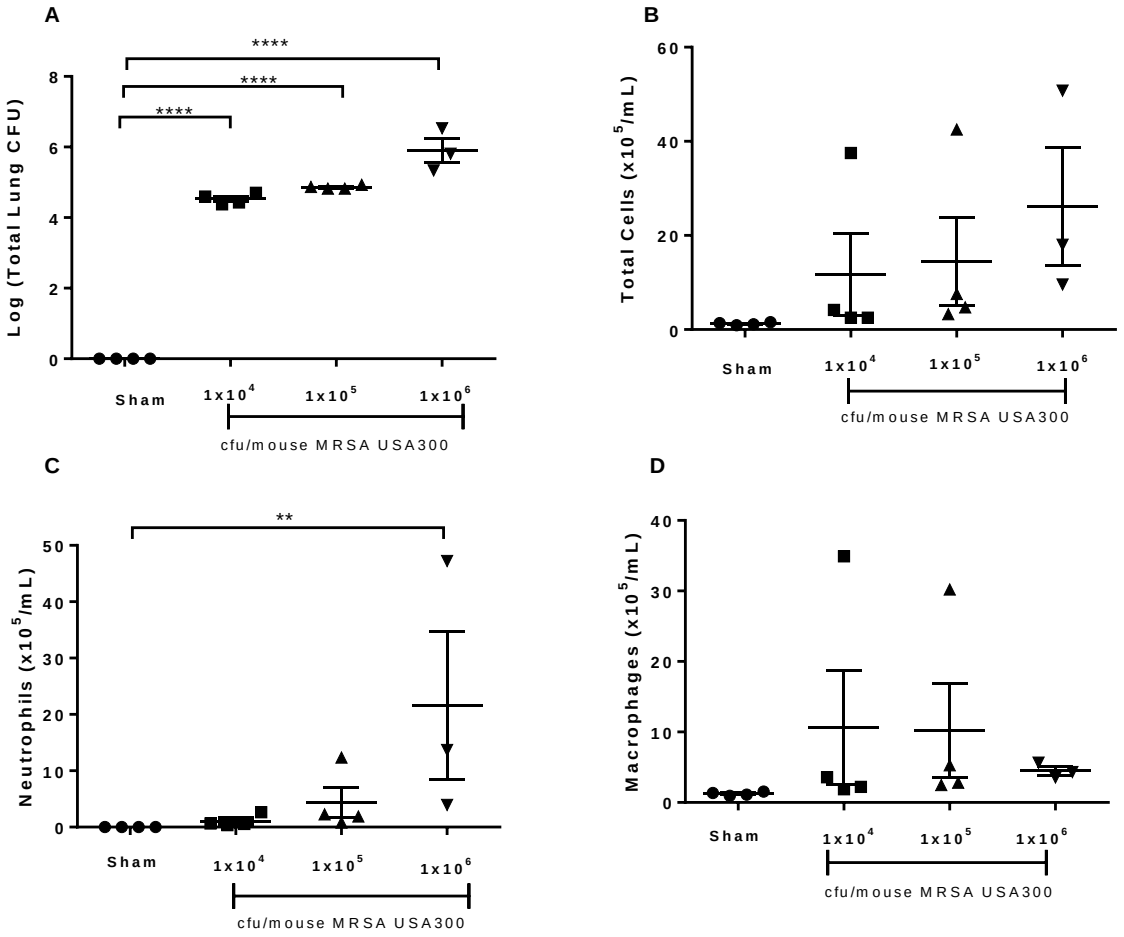

Figure 3.6 Effects of MRSA strain USA300 on Bacterial and Inflammatory Parameters of Pulmonary Infection

Mice were infected *(o.a)* with either sham or $1x10^4$, $1x10^5$, $1x10^6$ cfu/mouse MRSA embedded agar bead. A BAL of the lungs was performed for inflammatory cell quantification and lungs were aseptically removed, homogenised and plated for quantification of bacterial load at 48 h.p.i. (**A**) Pulmonary Bacterial Load, (**B**) Total Cells, (**C**) Neutrophils and (**D**) Macrophages. One-way ANOVA and Bonferroni's multiple comparisons post hoc test, ** $p<0.01$, **** $p<0.0001$ versus sham, n=4, data are presented as mean ± SEM.

3.2 Investigating the Effects of Infection on Inflammatory Markers in BAL Fluid and Blood Plasma

3.2.1 Quantification of IL-6 Levels in BAL Fluid Following Infection with *P.aeruginosa* or MRSA

IL-6 is a pro inflammatory cytokine produced transiently by activated macrophages, monocytes and T cells, in response to infection and tissue injuries (Tanaka et al., 2014). IL-6 may be used as an early marker of infection and has been used to predict mortality in critically ill patients with organ dysfunction (Takahashi et al., 2016). We therefore sought to investigate how infection with *P.aeruginosa* and MRSA influenced the concentration of IL-6 in a murine model of infection.

The concentration of IL-6 present in BAL fluid samples was significantly elevated following infection with $1x10^6$ cfu/mouse *P.aeruginosa* strain RP73 (RP73: 315.20±39.76 pg/mL, versus sham: 1.41±6.61 pg/mL, **Figure 3.7A**, $p<0.0001$), PAO1 (PAO1: 299.1±48.47 pg/mL, versus sham: -3.40±1.85 pg/mL, **Figure 3.7B**, $p<0.0001$) and NN2 (NN2: 477.1±48.62 pg/mL, versus sham: -4.95±0.85 pg/mL, **Figure 3.7C**, $p<0.0001$), when compared to sham controls. For PAO1 and NN2, the concentration of IL-6 present in the BAL fluid samples taken from sham controls was below the limit of detection.

Infection with $1x10^6$ cfu/mouse MRSA strain USA300 induced a significant increase in the concentration of IL-6 in BAL fluid samples, when compared to sham controls (MRSA: 83.61±16.22 pg/mL, versus sham: -4.23±0.38 pg/mL, **Figure 3.7D**, $p<0.0001$). The concentration of IL-6 present in the BAL fluid samples taken from sham controls was below the limit of detection.

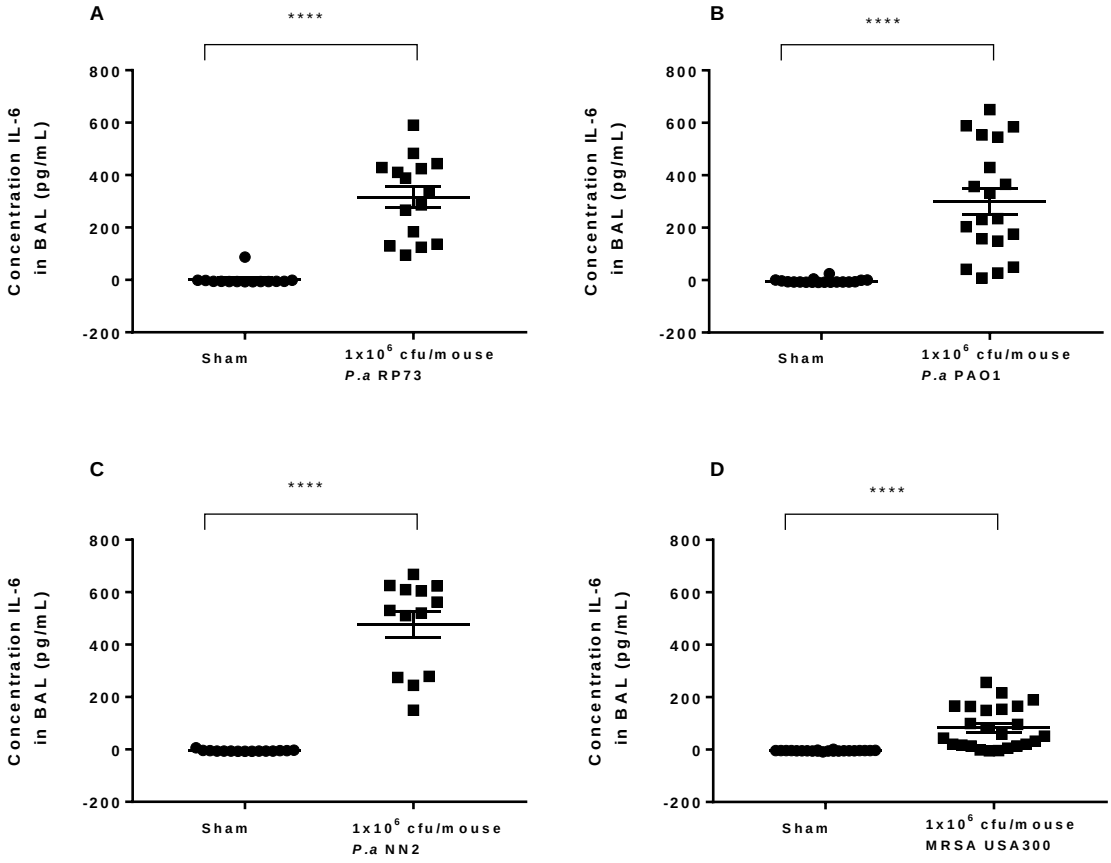

Figure 3.7 Effects of Infection with *P.aeruginosa* and MRSA on IL-6 Levels in BAL Fluid

Mice were infected *(o.a)* with either sham or $1x10^6$ cfu/mouse *P.aeruginosa* strain RP73, PAO1 or NN2 or MRSA strain USA300 embedded agar beads. At 48 h.p.i, a BAL of the lungs was performed. The concentration of IL-6 present in BAL fluid was measured using a murine IL-6 Duoset ELISA, DY453. **(A)** RP73, **(B)** PAO1, **(C)** NN2, **(D)** USA300, unpaired two-tailed t-test, ****p<0.0001 versus sham, n=13-24, data are presented as mean ± SEM.

3.2.2 Quantification of IL-6 Levels in Blood Plasma Following Infection with *P.aeruginosa* or MRSA

Infection with *P.aeruginosa* and MRSA induced a significant increase in the concentration of IL-6 at the site of infection in BAL fluid. Therefore, we sought to investigate whether infection with *P.aeruginosa* and MRSA would have a significant effect on the concentration of IL-6 in blood plasma.

The concentration of IL-6 present in plasma was significantly elevated following infection with $1x10^6$ cfu/mouse *P.aeruginosa* strain RP73 (RP73: 49.69±11.08 pg/mL, versus sham: -6.15±2.68 pg/mL, **Figure 3.8A**, $p<0.0001$), PAO1 (PAO1: 35.07±19.41 pg/mL, versus sham: -3.53±4.36 pg/mL, **Figure 3.8B**, $p<0.05$) and NN2 (NN2: 289.30±80.89 pg/mL, versus sham: -5.19±1.33 pg/mL, **Figure 3.8C**, $p<0.01$), when compared to sham controls. For all 3 of these *P.aeruginosa* strains, the concentration of IL-6 present in the plasma taken from sham controls was below the limit of detection. Although infection with all 3 strains of *P.aeruginosa* significantly increased the concentration of IL-6 in the plasma, the increase in the concentration of IL-6 in BAL fluid was greater at the site of the infection.

Infection with $1x10^6$ cfu/mouse MRSA strain USA300 had no significant effect on the concentration of IL-6 in plasma, when compared to sham controls (MRSA: -1.69±2.41 pg/mL, versus sham: 0.17±3.80 pg/mL, **Figure 3.8D**).

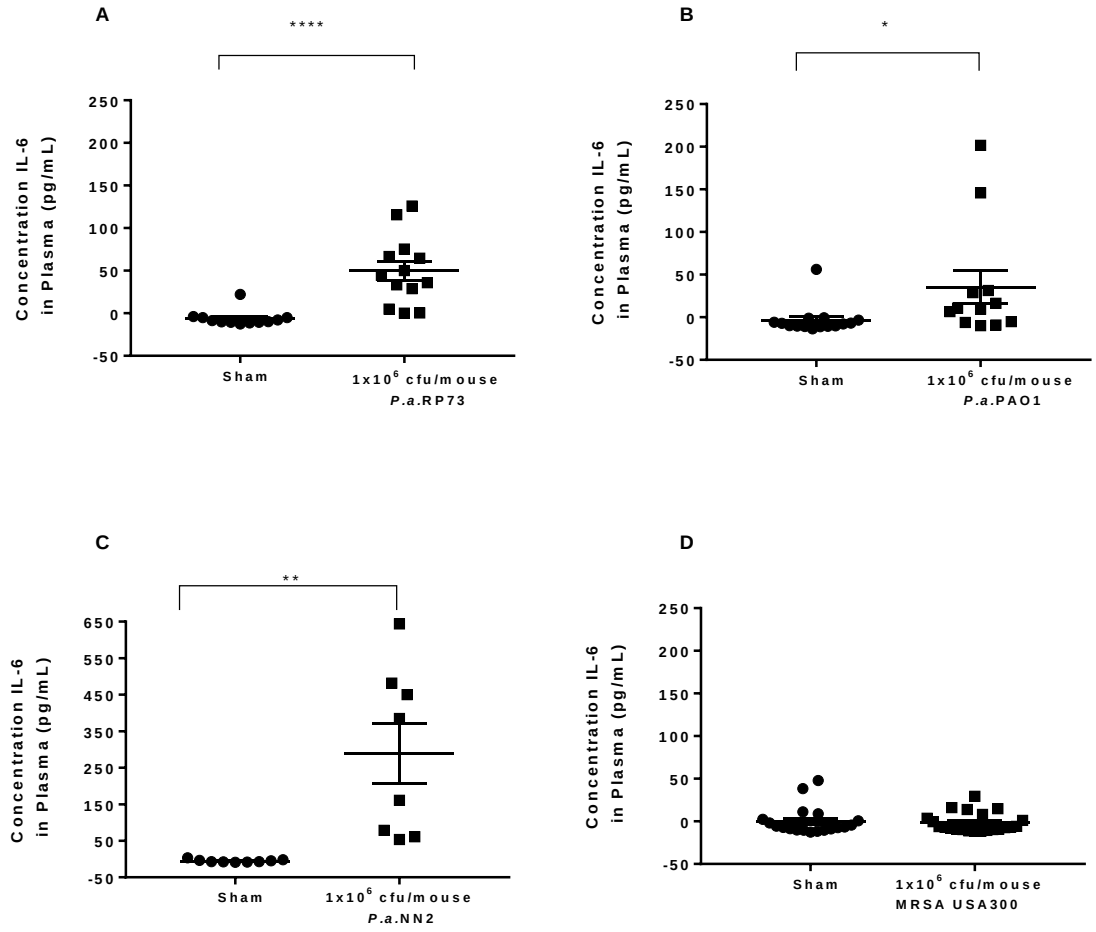

Figure 3.8 Effects of Infection with *P.aeruginosa* and MRSA on IL-6 levels in Blood Plasma

Mice were infected *(o.a)* with either sham or $1x10^6$ cfu/mouse *P.aeruginosa* strain RP73, PAO1 or NN2 or MRSA strain USA300 embedded agar beads. At 48 h.p.i, blood was taken via cardiac puncture and plasma was isolated. The concentration of IL-6 present in plasma was measured using a murine IL-6 Duoset ELISA, DY453. **(A)** RP73, **(B)** PAO1, **(C)** NN2, **(D)** USA300, unpaired two-tailed t-test, *p<0.05, **p<0.01, ****p<0.0001 versus sham, n=8-22, data are presented as mean ± SEM.

3.2.3 Quantification of KC Levels in BAL Fluid Following Infection with *P.aeruginosa* or MRSA

The murine chemokine KC (the murine analogue of human IL-8) plays a pivotal role in host defence against infection, by recruiting and activating circulating neutrophils to the site of infection, to participate in bacterial killing (Sawant et al., 2016). This has been demonstrated in several animal models, whereby KC has been shown to play a dual role in the host immune response by recruiting peripheral neutrophils and activating neutrophils to fight against infection, by the release of proteases and reactive oxygen species (Sawant et al., 2016). My earlier studies previously demonstrated infection induced pulmonary neutrophil recruitment and in this part of my work I investigated whether the concentration of KC was significantly elevated in response to bacterial infection.

As observed with the inflammatory marker IL-6, the concentration of KC present in BAL fluid was significantly elevated following infection with $1x10^6$ cfu/mouse *P.aeruginosa* strain RP73 (RP73: 208.60±35.77 pg/mL, versus sham: 8.94±6.23 pg/mL, **Figure 3.9A**, $p<0.0001$) PAO1 (PAO1: 201.10±65.54 pg/mL, versus sham: 12.81±6.48 pg/mL, **Figure 3.9B**, $p<0.01$) and NN2 (NN2: 356.00±53.59 pg/mL, versus sham: 26.39±8.12 pg/mL, **Figure 3.9C**, $p<0.0001$), when compared to sham controls.

Infection with $1x10^6$ cfu/mouse MRSA strain USA300 also induced a significant increase in the concentration of KC in BAL fluid samples, when compared to sham controls (MRSA: 133.70±44.25 pg/mL, versus sham: 20.39±6.67 pg/mL, **Figure 3.9D**).

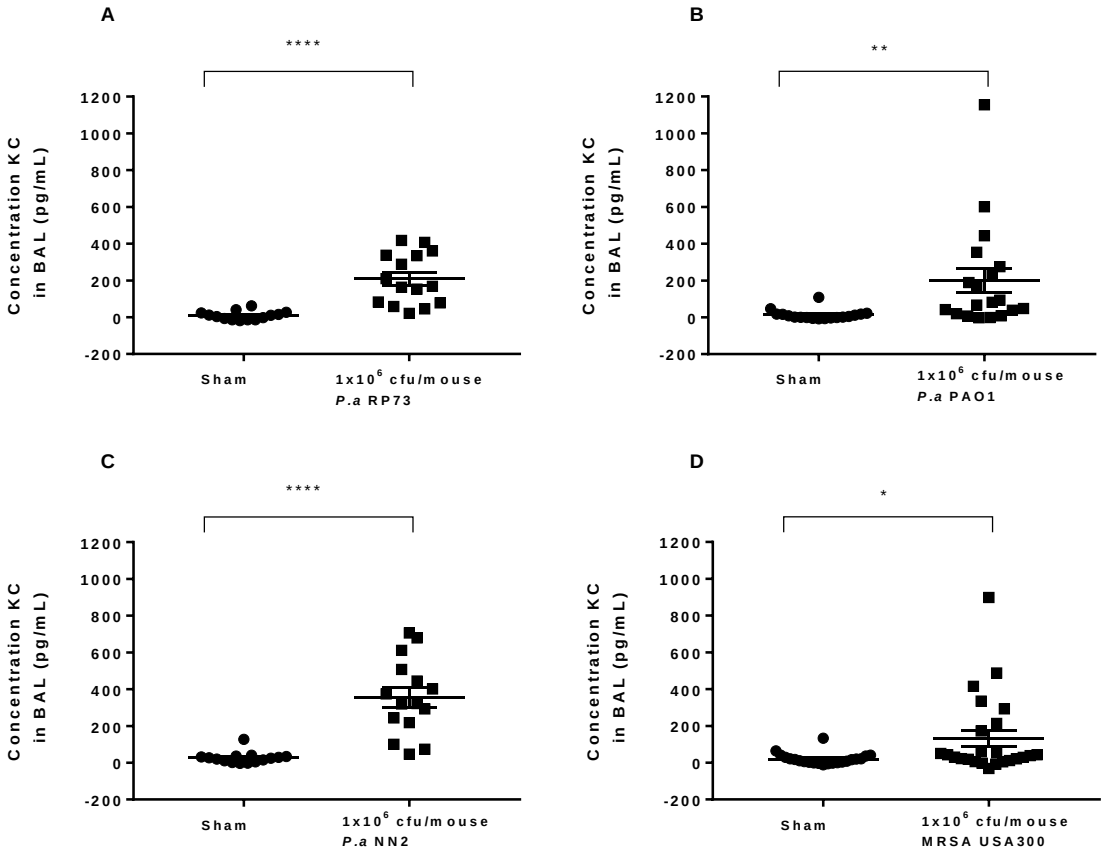

Figure 3.9 Effects of Infection with *P.aeruginosa* and MRSA on KC levels in Bal Fluid

Mice were infected *(o.a)* with either sham or $1x10^6$ cfu/mouse *P.aeruginosa* strain RP73, PAO1 or NN2 or MRSA strain USA300 embedded agar beads. At 48 h.p.i, a BAL of the lungs was performed. The concentration of KC present in BAL fluid was measured using a murine KC Duoset ELISA, DY406. **(A)** RP73, **(B)** PAO1, **(C)** NN2, **(D)** USA300, unpaired two-tailed t-test, *p<0.05, **p<0.01, ****p<0.0001 versus sham, n=14-22, data are presented as mean ± SEM.

3.2.4 Quantification of KC Levels in Blood Plasma Following Infection with *P.aeruginosa* or MRSA

Infection with *P.aeruginosa* and MRSA induced a significant increase in the concentration of KC at the site of infection in BAL fluid. Therefore, we sought to investigate whether infection with *P.aeruginosa* and MRSA would have a significant effect on the concentration of KC in blood plasma.

The concentration of KC present in blood plasma was significantly elevated following infection with $1x10^6$ cfu/mouse *P.aeruginosa* strain RP73 (RP73: 207.60±20.78 pg/mL, versus sham: 59.71±9.36 pg/mL, **Figure 3.10A**, $p<0.0001$) PAO1 (PAO1: 202.20±47.24 pg/mL, versus sham: 71.13±8.76 pg/mL, **Figure 3.10B**, $p<0.01$) and NN2 (NN2: 481.1±115.60 pg/mL, versus sham: 88.48±14.02 pg/mL, **Figure 3.10C**, $p<0.01$) when compared to sham controls.

Similar to the data obtained for the concentration of IL-6 in plasma, infection with $1x10^6$ cfu/mouse MRSA strain USA300 had no significant effect on the concentration of KC in plasma, when compared to sham controls (MRSA: 124.90±18.04 pg/mL, versus sham: 107.0±12.46 pg/mL, **Figure 3.10D**).

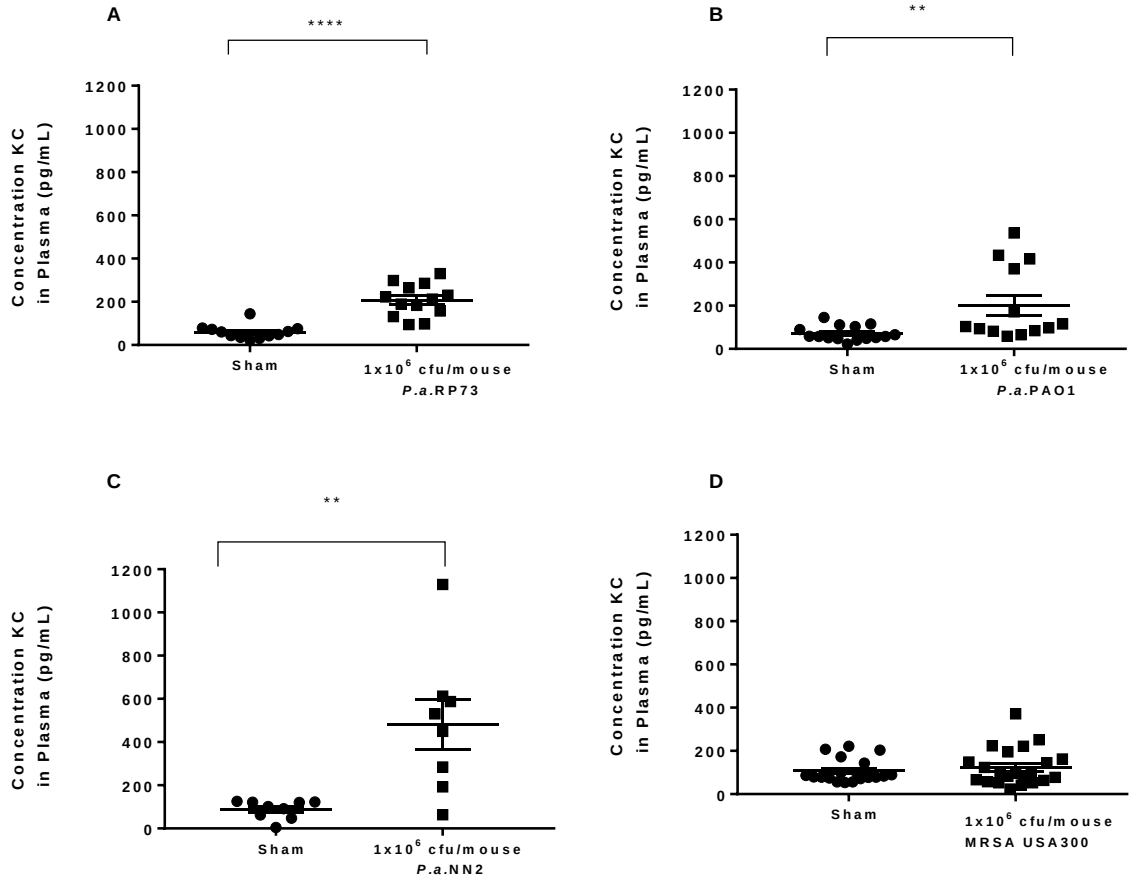

Figure 3.10 Effects of Infection with *P.aeruginosa* and MRSA on KC levels in Blood Plasma

Mice were infected *(o.a)* with either sham or $1x10^6$ cfu/mouse *P.aeruginosa* strain RP73, PAO1 or NN2 or MRSA strain USA300 embedded agar beads. At 48 h.p.i, blood was taken via cardiac puncture and plasma was isolated. The concentration of KC present in plasma was measured using a murine KC Duoset ELISA, DY406. **(A)** RP73, **(B)** PAO1, **(C)** NN2, **(D)** USA300, unpaired two-tailed t-test, **p<0.01, ****p<0.0001 versus sham, n=8-22, data are presented as mean ± SEM.

3.3 Validation of the Murine Model of Pulmonary Infection with *P.aeruginosa* and MRSA, using Tobramycin and Vancomycin

3.3.1 Validation: Assessing the Ability of Tobramycin to Reduce Bacterial Load Post Infection with *P.aeruginosa* strain RP73

Having established the optimum inoculum for pulmonary infection with 3 different strains of the gram-negative bacterium, *P.aeruginosa*, additional experiments were performed to validate the model with the conventional antibiotic, Tobramycin. Mice were infected with $1x10^6$ cfu/mouse *P.aeruginosa* strain RP73 (a multidrug resistant strain) and the effects of Tobramycin (either 50, 100, or 300 mg/kg/day, *i.p.*) on infection and inflammatory parameters were subsequently analysed.

Infection with RP73 induced a significant increase in pulmonary bacterial load in vehicle treated mice when compared to sham controls (5.91±0.03 log cfu, versus sham: 0.0±0.0 log cfu, $p<0.0001$, **Figure 3.11A**). Following treatment with Tobramycin, a dose-dependent reduction in pulmonary bacterial load was observed. However, only 300 mg/kg Tobramycin produced a significant reduction in pulmonary bacterial load when compared to vehicle controls (50 mg/kg: 6.13±0.04 log cfu, 100 mg/kg: 5.85±0.03 and 300 mg/kg: 4.62±0.16 log cfu, $p<0.0001$, versus vehicle: 5.91±0.03 log cfu, **Figure 3.11A**).

Infection with RP73 induced a significant increase in both total leukocyte ($24.13±4.26x10^5$ cells/mL, versus sham: $1.28±0.25x10^5$ cells/mL, $p<0.001$, **Figure 3.11B**) and neutrophil recruitment ($22.32±3.69x10^5$ cells/mL, versus sham: $0.02±0.02x10^5$ cells/mL, $p<0.0001$, **Figure 3.11C**) to the lungs, when compared to sham controls. No tested dose of Tobramycin had any significant effect on pulmonary total leukocyte recruitment when compared to vehicle controls (50 mg/kg: $24.58±2.43x10^5$ cells/mL, 100 mg/kg: $28.53±4.98x10^5$ cells/mL and 300

mg/kg: 24.32±0.87x10^5 cells/mL versus vehicle: 24.13±4.26x10^5 cells/mL, **Figure 3.11B**). Similarly, no significant effects of Tobramycin were observed on neutrophil (50 mg/kg: 24.06±2.45x10^5 cells/mL, 100 mg/kg: 27.04±4.41x10^5 cells/mL and 300 mg/kg: 22.77±1.04x10^5 cells/mL, versus vehicle: 22.32±3.69x10^5 cells/mL, **Figure 3.11C**), macrophage (50 mg/kg: 0.51±0.32x10^5 cells/mL, 100 mg/kg: 1.49±0.88x10^5 cells/mL and 300 mg/kg: 1.54±0.60x10^5 cells/mL, versus vehicle: 1.80±0.77x10^5 cells/mL, **Figure 3.11D**) and lymphocyte (50 mg/kg: 0.0±0.0x10^5 cells/mL, 100 mg/kg: 0.0±10.0x10^5 cells/mL and 300 mg/kg: 0.0±0.0x10^5 cells/mL, versus vehicle: 0.0±0.0x10^5 cells/mL) recruitment to the lungs, when compared to vehicle controls.

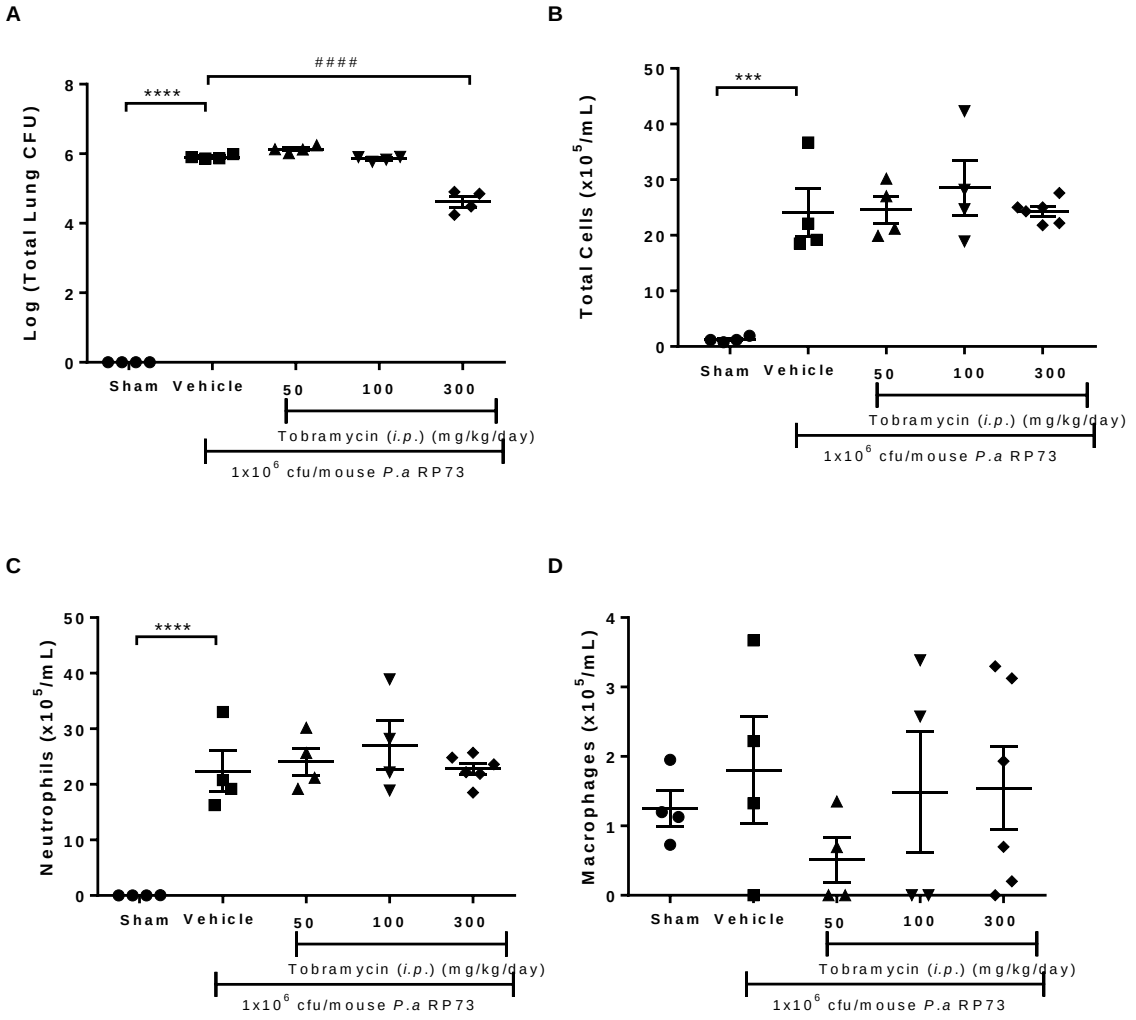

Figure 3.11 Effects of Tobramycin Following Infection with *P.aeruginosa* strain RP73

Mice were infected *(o.a)* with either sham or 1x10^6 cfu/mouse RP73 embedded agar beads. At 24 h.p.i mice were treated with a single dose of either vehicle, 50, 100, 300 mg/kg Tobramycin (200µL, *i.p*). A BAL of the lungs was performed for inflammatory cell quantification and lungs were aseptically removed, homogenised and plated for quantification of bacterial load at 48 h.p.i. (**A**) Pulmonary Bacterial Load, (**B**) Total Cells (**C**) Neutrophils and (**D**) Macrophages. One-way ANOVA and Bonferroni's multiple comparisons post hoc test, *** p< 0.0001 versus sham, #### p<0.0001 versus vehicle, n=4-6, data are presented as mean ± SEM.

3.3.2 Validation: Assessing the Ability of Tobramycin to Reduce Bacterial Load Post Infection with *P.aeruginosa* strain PAO1

Similar to RP73, experiments were performed to validate the murine model of pulmonary infection with PAO1 using Tobramycin. Mice were infected with $1x10^6$ cfu/mouse *P.aeruginosa* strain PAO1 (a Tobramycin susceptible strain), and the effects of Tobramycin (either 10, 50, or 100 mg/kg/day) on infection and inflammatory parameters were subsequently analysed.

PAO1 infection induced a significant increase in pulmonary bacterial load in vehicle treated mice, when compared to sham controls (5.91±0.17 log cfu, versus sham: 0.0±0.0 log cfu, $p<0.0001$, **Figure 3.12A**). Tobramycin treatment induced a dose-dependent reduction in pulmonary bacterial load, with a significant reduction in pulmonary bacterial load observed following treatment with 50mg/kg and 100mg/kg Tobramycin (50 mg/kg: 4.97±0.06 log cfu, $p<0.01$ and 100 mg/kg: 4.74±0.31 log cfu, $p<0.0001$, versus vehicle 5.91±0.17 log cfu, **Figure 3.12A**), when compared to vehicle controls.

Infection with $1x10^6$ cfu/mouse *P.aeruginosa* PAO1 also induced a significant increase in total leukocyte ($31.77±3.09x10^5$ cells/mL, versus sham: $1.82±0.23x10^5$ cells/mL, $p<0.0001$) and neutrophil recruitment ($29.57±3.12x10^5$ cells/mL, versus sham: $0.02±0.01x10^5$ cells/mL, $p<0.0001$) to the lungs, when compared to sham controls. Tobramycin treatment at any tested dose had no significant effect on total leukocyte recruitment when compared to vehicle controls (10 mg/kg: $33.3±4.18x10^5$ cells/mL, 50 mg/kg: $27.2±3.49x10^5$ cells/mL and 100 mg/kg: $24.93±3.43x10^5$ cells/mL versus vehicle: $31.77±3.09x10^5$ cells/mL, **Figure 3.12B**). Data suggested a trend depicting a decrease in total leukocytes and neutrophil recruitment to the lungs following Tobramycin treatment, although this data did not reach statistical

significance. Similarly, no tested Tobramycin dose had any significant effect on neutrophil (10 mg/kg: 30.52±4.83x10^5 cells/mL, 50 mg/kg: 21.93±3.68x10^5 cells/mL and 100 mg/kg: 19.22±2.07x10^5 cells/mL, versus vehicle: 22.32±3.69x10^5 cells/mL, **Figure 3.12C**) macrophage (10 mg/kg: 3.05±0.60x10^5 cells/mL, 50 mg/kg: 5.27±0.63x10^5 cells/mL and 100 mg/kg: 5.72±1.41x10^5 cells/mL, versus vehicle: 2.20±0.19x10^5 cells/mL, **Figure 3.12D**) or lymphocyte (10 mg/kg: 0.0±0.0x10^5 cells/mL, 50 mg/kg: 0.0±10.0x10^5 cells/mL and 100 mg/kg: 0.0±0.0x10^5 cells/mL, versus vehicle: 0.0±0.0x10^5 cells/mL) recruitment to the lungs, when compared to vehicle controls.

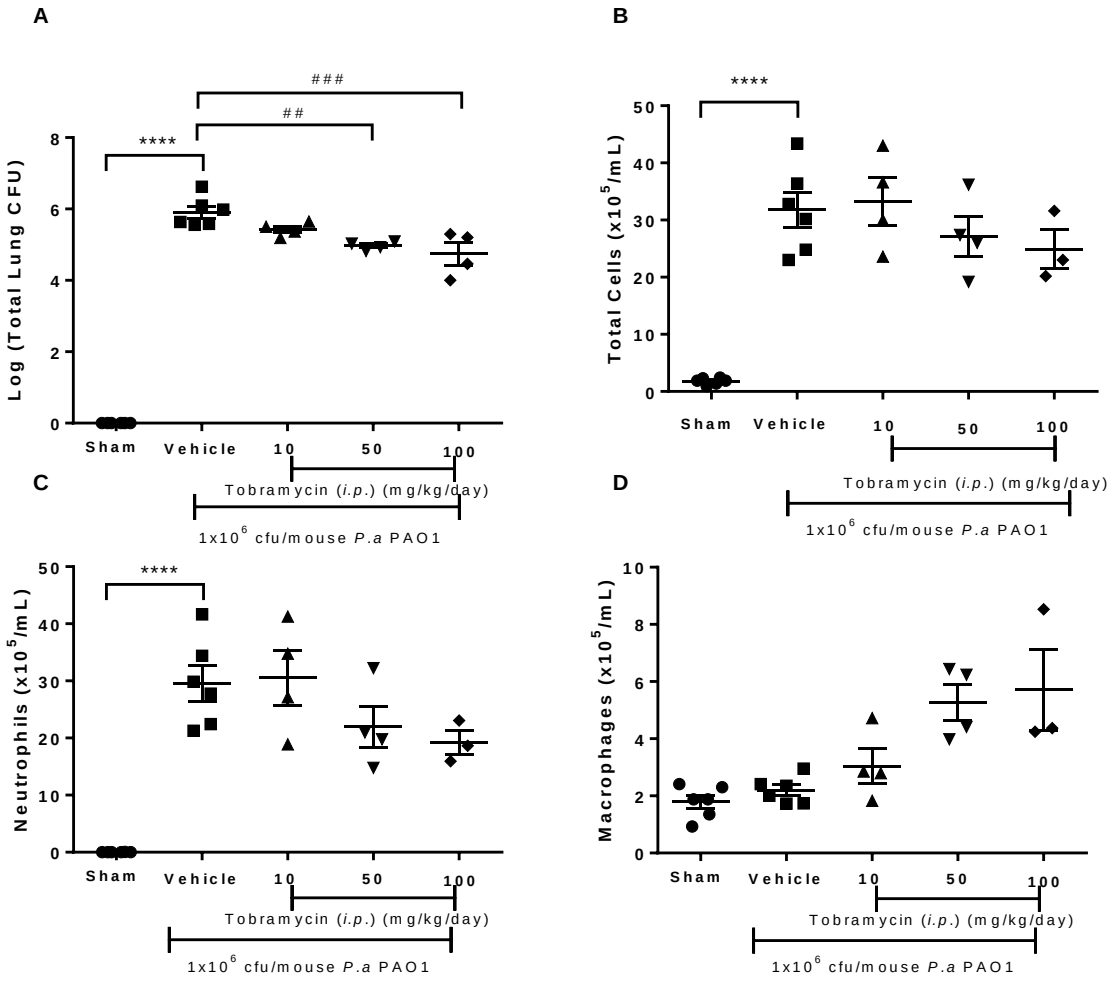

Figure 3.12 Effects of Tobramycin Following Infection with *P.aeruginosa* strain PAO1

Mice were infected *(o.a)* with either sham sterile or $1x10^6$ cfu/mouse PAO1 embedded agar beads. At 24 h.p.i mice were treated with a single dose of either vehicle, 10, 50, 100 mg/kg Tobramycin (200µL, *i.p.*). A BAL of the lungs was performed for inflammatory cell quantification and lungs were aseptically removed, homogenised and plated for quantification of bacterial load at 48 h.p.i. (**A**) Pulmonary Bacterial Load, (**B**) Total Cells (**C**) Neutrophils and (**D**) Macrophages. One-way ANOVA and Bonferroni's multiple comparisons post hoc test, **** $p<0.0001$ versus sham, ## $p<0.01$, #### $p<0.0001$ versus vehicle, n=3-4, data are presented as mean ± SEM.

3.3.3 Validation: Assessing the Ability of Tobramycin to Reduce Bacterial Load Post Infection with *P.aeruginosa* strain NN2

Experiments were performed to validate a murine model of pulmonary infection with *P.aeruginosa* strain NN2 using Tobramycin. Mice were infected with $1x10^6$ cfu/mouse *P.aeruginosa* strain NN2 (a Tobramycin resistant strain) and the effects of Tobramycin (either 50, 100 or 200 mg/kg/day) on infection and inflammatory parameters were subsequently analysed.

Infection with NN2 induced a significant increase in pulmonary bacterial load in vehicle treated mice, when compared to sham controls (6.65±0.08 log cfu, versus sham: 0.0±0.0 log cfu, $p<0.0001$, **Figure 3.13A**). Tobramycin treatment at 50 mg/kg induced a significant reduction in pulmonary bacterial load when compared to vehicle controls (6.13±0.22 log cfu, versus vehicle control: 6.65±0.08 log cfu, **Figure 3.13A**). However, no effect on pulmonary bacterial load was observed following treatment with 100 and 200 mg/kg Tobramycin when compared to vehicle controls (100 mg/kg: 6.73±0.14 log cfu and 200 mg/kg: 6.89±0.09 log cfu, versus vehicle control: 6.65±0.08 log cfu, **Figure 3.13A**).

Infection with $1x10^6$ cfu/mouse *P.aeruginosa* NN2, induced a significant increase in pulmonary total leukocytes ($49.0±10.88x10^5$ cells/mL, versus sham: $1.41±0.32x10^5$ cells/mL, $p<0.05$, **Figure 3.13B**) and neutrophil recruitment when compared to sham controls ($48.08±10.9x10^5$ cells/mL, versus sham: $0.01±0.00x10^5$ cells/mL, $p<0.01$, **Figure 3.13B**). No tested doses of Tobramycin had any significant effect on pulmonary total leukocyte recruitment (50 mg/kg: $51.38±16.14x10^5$ cells/mL, 100: $27.69±5.81x10^5$ cells/mL and 200 mg/kg: $46.93±5.34x10^5$ cells/mL, versus vehicle control: $49.00±10.88x10^5$ cells/mL, **Figure 3.13B**), or pulmonary neutrophil recruitment (50 mg/kg: $46.77±15.03x10^5$ cells/mL, 100

mg/kg: 24.43±5.07x10^5 cells/mL and 200 mg/kg: 42.23±4.81x10^5 cells/mL, versus vehicle control: 48.08±10.90x10^5 cells/mL, **Figure 3.13C**), when compared to vehicle controls. In contrast, every tested dose of Tobramycin appeared to increase macrophage recruitment to the lungs, however this was only significant at 50 and 200 mg/kg, when compared to vehicle controls (50 mg/kg: 4.61±1.12x10^5 cells/mL, $p<0.05$, 100 mg/kg: 3.14±0.81x10^5 cells/mL and 200 mg/kg: 4.69±0.55x10^5 cells/mL, $p<0.05$, versus vehicle, **Figure 3.13D**). No tested Tobramycin dose had any significant effect on lymphocyte recruitment to the lungs, when compared to vehicle controls (50 mg/kg: 0.0±0.0x10^5 cells/mL, 100 mg/kg: 0.0±10.0x10^5 cells/mL and 200 mg/kg: 0.0±0.0x10^5 cells/mL, versus vehicle: 0.0±0.0x10^5 cells/mL).

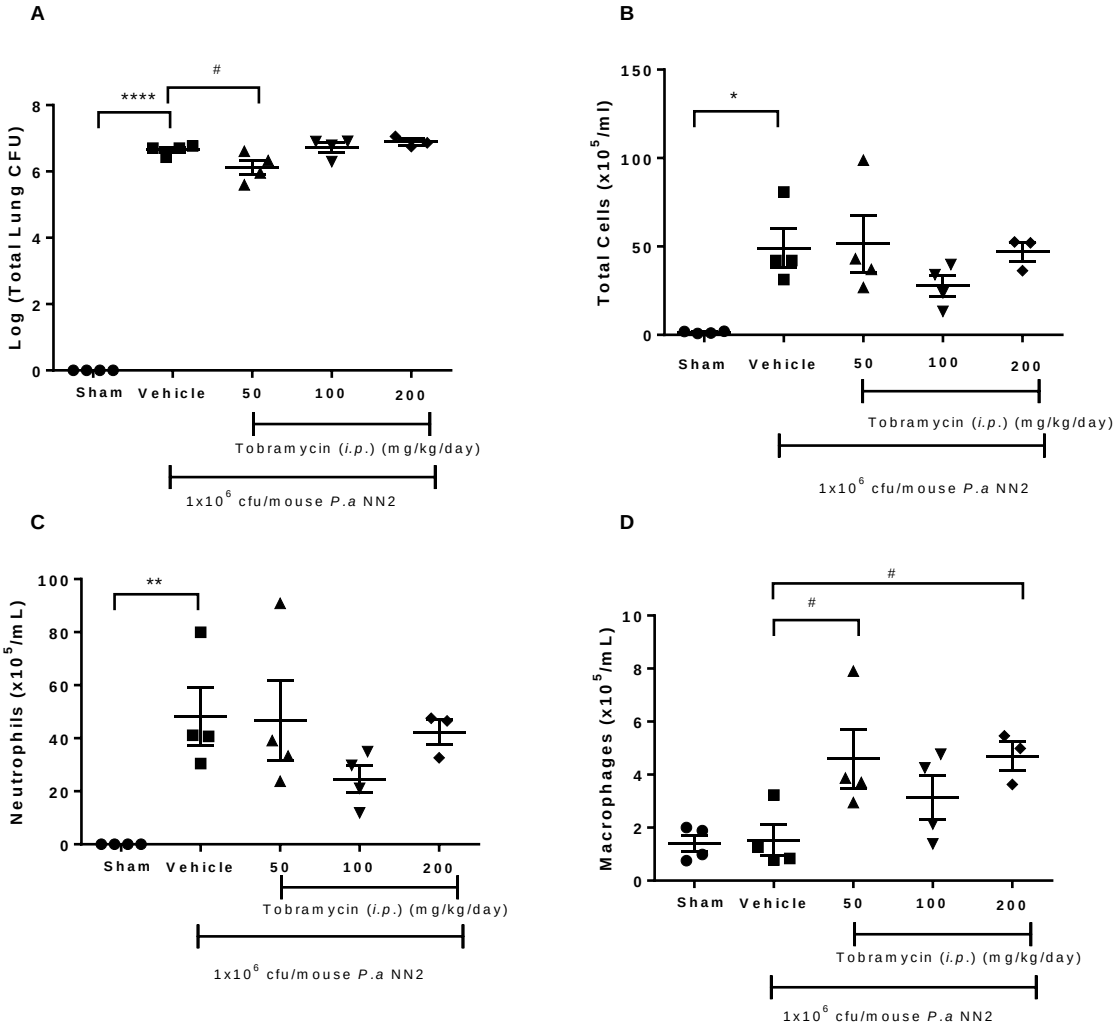

Figure 3.13 Effects of Tobramycin Following Infection with *P.aeruginosa* strain NN2

Mice were infected *(o.a)* with either sham or 1x10^6 cfu/mouse NN2 embedded agar beads. At 24 h.p.i mice were treated with a single dose of either vehicle, 50, 100, 200 mg/kg Tobramycin (200µL, *i.p.*). A BAL of the lungs was performed for inflammatory cell quantification and lungs were aseptically removed, homogenised and plated for quantification of bacterial load at 48 h.p.i. (**A**) Pulmonary Bacterial Load, (**B**) Total Cells (**C**) Neutrophils and (**D**) Macrophages. One-way ANOVA and Bonferroni's multiple comparisons post hoc test, *p<0.05, ** p<0.01, **** p<0.0001 versus sham, #p<0.01 versus vehicle, n=3-4, data are presented as mean ± SEM.

3.3.4 Validation: Assessing the Ability of Tobramycin to Reduce Bacterial Load Post Infection with MRSA strain USA300

Having validated the *P.aeruginosa* murine models of pulmonary infection with Tobramycin, additional experiments were performed to validate the murine model of pulmonary infection with MRSA strain USA300 using the conventional antibiotic Vancomycin. Mice were infected with $1x10^6$ cfu/mouse MRSA strain USA300, and the effects of Vancomycin (either 50, 100 or 200 mg/kg/day) on infection and inflammatory parameters were subsequently analysed.

Infection with MRSA induced a significant increase in pulmonary bacterial load in vehicle treated mice when compared to sham controls (4.27±0.27 log cfu, versus sham: 0.0±0.0 log cfu, $p<0.0001$, **Figure 3.14A**). Vancomycin treatment appeared to induce a dose-dependent reduction in pulmonary bacterial load when compared to vehicle controls. However, significance was only observed using 200 mg/kg Vancomycin (50 mg/kg: 3.40 ±0.11 log cfu, 100 mg/kg: 3.52±0.25 log cfu and 200 mg/kg 2.72±0.33 log cfu, $p<0.05$, versus vehicle control: 4.27±0.27 log cfu, **Figure 3.14A**).

Infection with $1x10^6$ cfu/mouse MRSA strain USA300, had no significant increase in pulmonary total leukocytes when compared to sham controls ($3.30 \times 10^5 \pm 0.29$ cells/mL, versus sham: $1.56 \times 10^5 \pm 0.33$ cells/mL, **Figure 3.14B**). However, pulmonary neutrophil recruitment was significantly increased in infected animals when compared to sham controls ($0.86±0.12x10^5$ cells/mL, versus sham: $0.00±0.00x10^5$ cells/mL, $p<0.001$, **Figure 3.14C**). No tested dose of Vancomycin had any significant effect on pulmonary total leukocyte recruitment (50 mg/kg: $3.69±0.27x10^5$ cells/mL, 100 mg/kg: $4.62±1.24x10^5$ cells/mL and 200 mg/kg: $3.27±0.07x10^5$ cells/mL, versus vehicle control: $3.30±0.07x10^5$ cells/mL, **Figure 3.14B**) or pulmonary neutrophil recruitment (50 mg/kg: $1.17±0.11x10^5$ cells/mL, 100 mg/kg:

0.75±0.21x10^5 cells/mL and 200 mg/kg: 0.49±0.15x10^5 cells/mL, versus vehicle control: 0.86±0.12x10^5 cells/mL, **Figure 3.14C**) when compared to vehicle controls. Similarly, no tested dose of Vancomycin had any significant effect on pulmonary macrophage (50 mg/kg: 2.58±0.35x10^5 cells/mL, 100 mg/kg: 2.52±0.20x10^5 cells/mL and 200 mg/kg: 2.77±0.10x10^5 cells/mL, versus vehicle: 2.48±0.35x10^5 cells/mL, **Figure 3.14D**) and lymphocyte recruitment when compared to vehicle controls (50 mg/kg: 0.0±0.0x10^5 cells/mL, 100 mg/kg: 0.0±10.0x10^5 cells/mL and 200 mg/kg: 0.0±0.0x10^5 cells/mL, versus vehicle: 0.0±0.0x10^5 cells/mL).

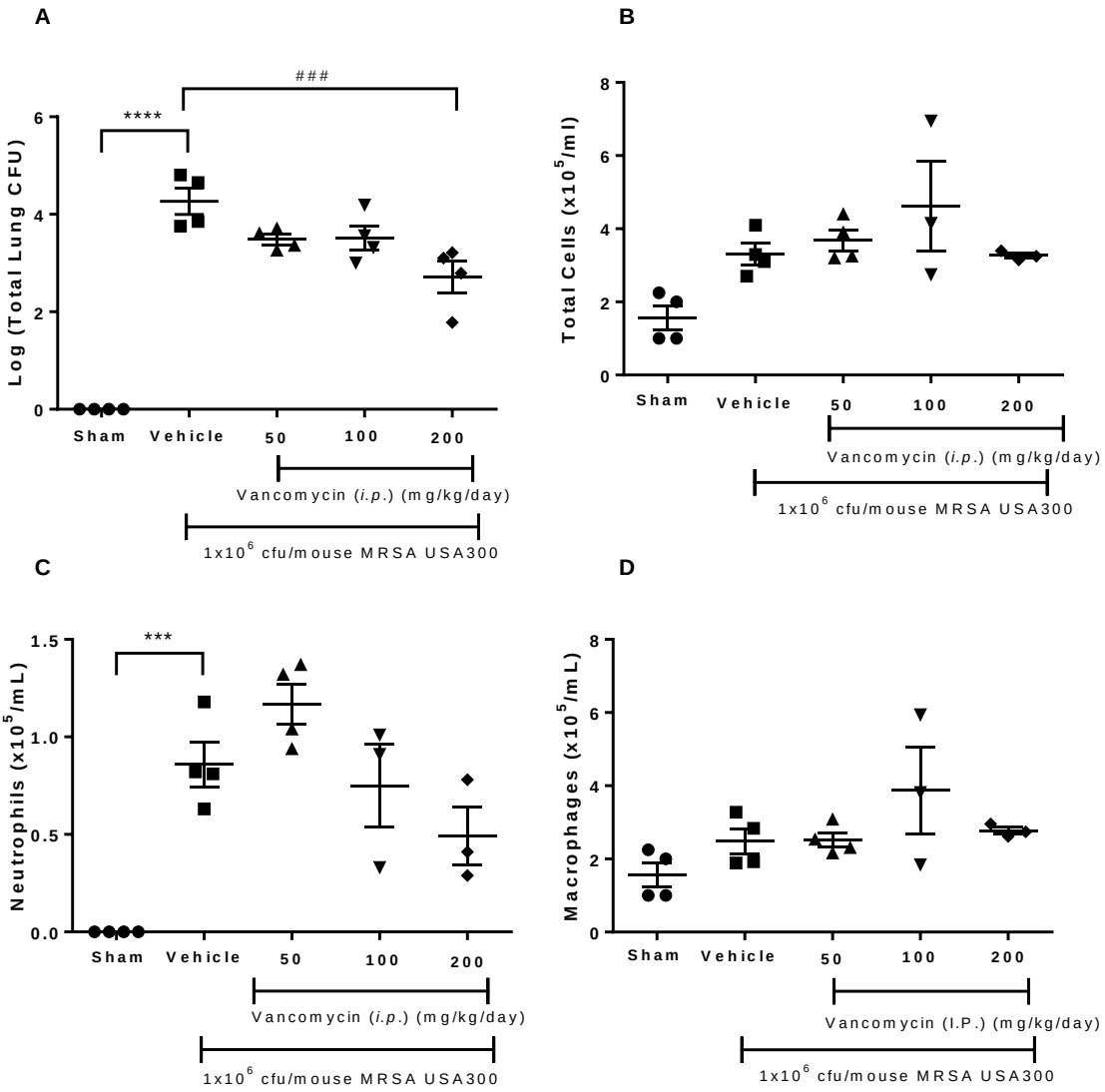

Figure 3.14 Effects of Vancomycin Following Infection with MRSA strain USA300

Mice were infected *(o.a)* with either sham or 1x10^6 cfu/mouse USA300 embedded agar beads. At 24 h.p.i mice were treated with a single dose of either vehicle, 50, 100, 200 mg/kg Vancomycin (200µL, *i.p.*). A BAL of the lungs was performed for inflammatory cell quantification and lungs were aseptically removed, homogenised and plated for quantification of bacterial load at 48 h.p.i. (**A**) Pulmonary Bacterial Load, (**B**) Total Cells (**C**) Neutrophils and (**D**) Macrophages. One-way ANOVA and Bonferroni's multiple comparisons post hoc test, ***p<0.001, **** p<0.0001 versus sham, ### p<0.001 versus vehicle, n=3-4, data are presented as mean ± SEM.

Chapter IV: Results II

The Role of Platelets in the Regulation of Pulmonary Infection

4.1 Investigating Infection Induced Thrombocytopenia

Thrombocytopenia is a common finding in patients admitted to the intensive care unit (de Stoppelaar, 2014) and patients that present to the clinic with sepsis often present with thrombocytopenia (Xiang et al., 2013). This is associated with poor prognosis and increased mortality in comparison to patients with normal circulating platelet levels (Venkata et al., 2013). Therefore, we sought to investigate the effect of infection on thrombocytopenia in a murine model of pulmonary infection with *P.aeruginosa* and MRSA.

Infection with $1x10^6$ cfu/mouse *P.aeruginosa* strain RP73 induced a significant decrease of approximately 12% in circulating platelet numbers at 48 h.p.i. when compared to sham controls (RP73: $6.11±0.21x10^8$ platelets/mL, versus sham: $6.99±0.30x10^8$ platelets/mL, 12.6% decrease, $p<0.05$, **Figure 4.1A**). Similarly, infection with $1x10^6$ cfu/mouse *P.aeruginosa* strain PAO1 (PAO1: $5.80±0.18x10^8$ platelets/mL, versus sham: $6.63±0.18x10^8$ platelets/mL, 12.7% decrease, $p<0.01$, **Figure 4.1B**) and NN2 (NN2: $6.65±0.24x10^8$ platelets/mL, versus sham: $6.65±0.24x10^8$ platelets/mL, 13.7% decrease, $p<0.05$, **Figure 4.1C**) significantly reduced circulating platelet numbers, by 12.7% and 13.7% respectively, when compared to sham controls. For the MRSA strain USA300, a significant decrease in circulating platelet numbers was observed at 48 h.p.i, with infection reducing platelet numbers by 14.7%, when compared to sham controls (MRSA: $6.36±0.28x10^8$ platelets/mL, versus sham: $7.76±0.29x10^8$ platelets/mL, 14.7% decrease, $p<0.01$, **Figure 4.1D**).

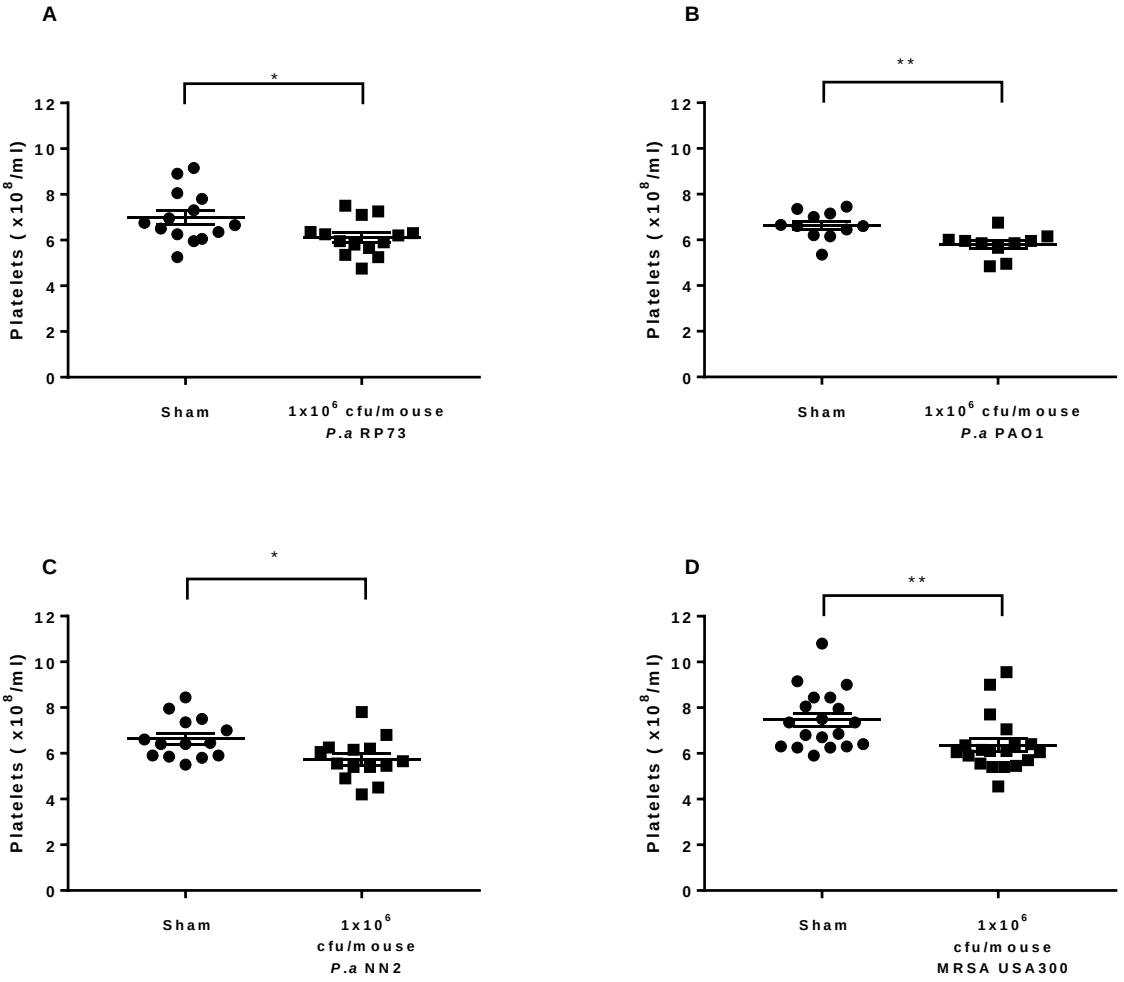

Figure 4.1 Effects of Infection with *P.aeruginosa* and MRSA on Circulating Platelet Levels

Mice were infected *(o.a)* with either sham or 1x10^6 cfu/mouse *P.aeruginosa* strain (**A**) RP73, (**B**) PAO1, (**C**) NN2 or (**D**) MRSA strain USA300 embedded agar beads. 48 h.p.i. blood was collected via cardiac puncture and platelets were quantified using an improved Neubauer haemocytometer under a x40 objective. Unpaired two-tailed t-test, * $p<0.05$, ** $p<0.01$ versus sham, n=10-19, data are presented as mean ± SEM.

4.2 Investigating *P.aeruginosa* strain RP73 Infection Induced Pulmonary Platelet Recruitment

Platelet recruitment towards bacterial products (LPS) has been demonstrated previously (Ortiz-Muñoz et al., 2014), therefore we investigated whether platelet migration to the lungs accounts for the decreased circulating platelet numbers we observed. Lung samples from sham and *P.aeruginosa* strain RP73 infected animals were collected at 48 h.p.i. and stained with a platelet-specific anti-CD42b antibody. The histological images collected showed evidence of platelet accumulation in the lung tissue following infection with RP73, when compared to sham controls (**Figure 4.2Ciii**)**.** Regions that stained positively for CD42b appeared to be present in the airways, located within close proximity to bacteria and in extravascular regions of lung tissue. Conversely, in sham controls, histological images demonstrated far fewer CD42b positively stained events (**Figure 4.2Ci**)**.** Tissue samples of both sham and infected mice were stained with only secondary antibody to rule out non-specific binding, thus acting as a negative control (**Figure 4.2Cii and iv)**.

The staining was quantified to determine whether there was a significant difference in the number of CD42b positive events per mm^2 of lung tissue or the percentage area of CD42b positive staining in sham versus RP73 infected tissue sections. Results demonstrated a significant increase in the number of CD42b positive events per mm^2 of lung tissue following infection with RP73, when compared to sham controls (RP73: 9672±1456 platelets/ mm^2, versus sham: 3809±455.1 platelets/ mm^2, $p<0.01$, **Figure 4.2A**), which represents a significant increase in the number of platelets/ mm^2 of lung tissue following infection. Furthermore, a significant increase in the percentage area of CD42b positive staining was observed following infection with RP73, when compared to sham controls (RP73: 2.80 ± 0.65%, versus sham:

1.17±0.27%, $p<0.05$, **Figure 4.2B**) which represents an increase in the total number of platelets recruited to the lung following infection.

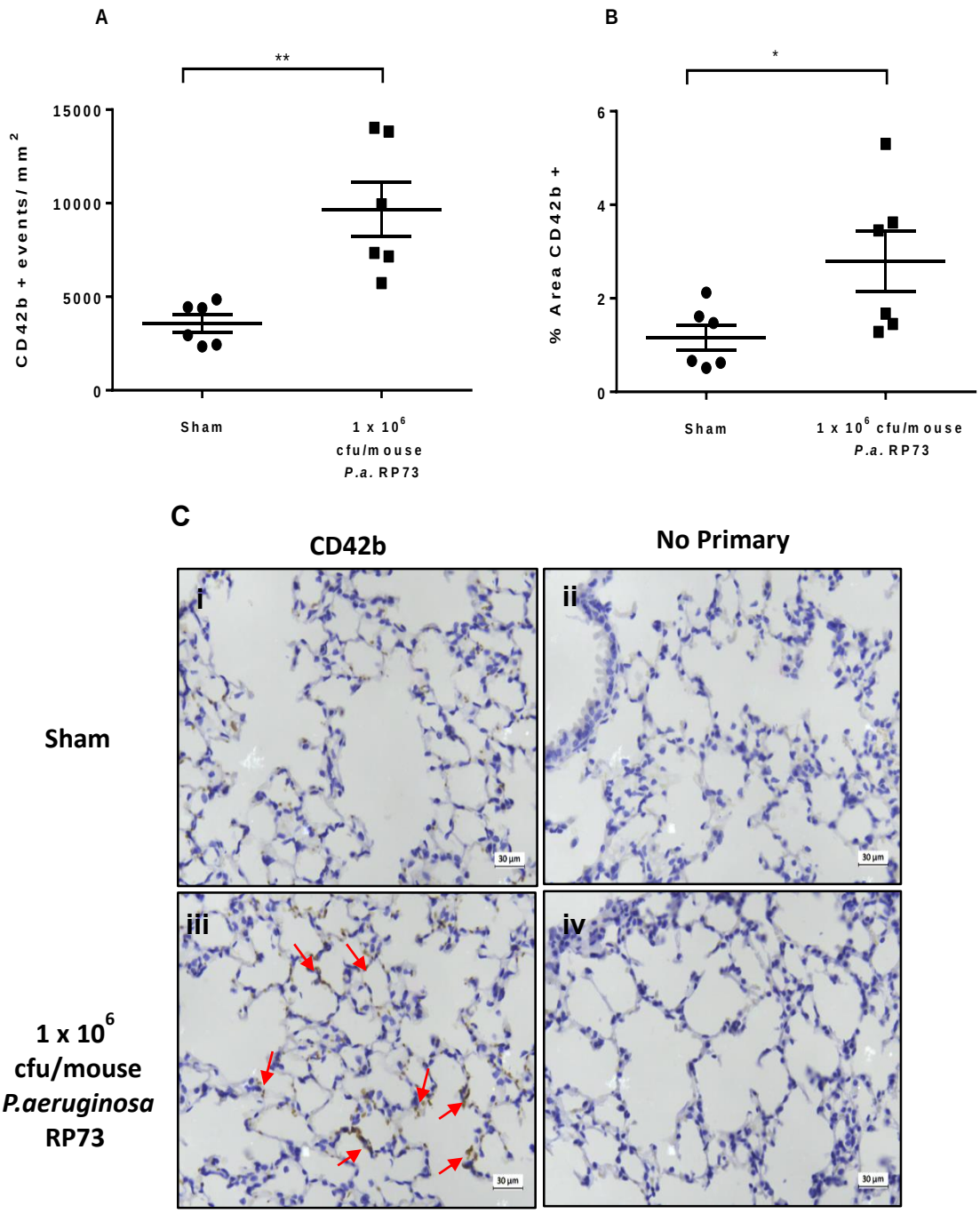

Figure 4.2 Effects of Infection with *P.aeruginosa* strain RP73 on Pulmonary Platelet Accumulation

Mice were infected *(o.a)* with either sham or $1x10^6$ cfu/mouse RP73 embedded agar beads. At 24 h.p.i, lungs were removed, fixed in 10% formaldehyde and embedded into paraffin wax blocks. Tissue sections were stained with an anti-CD42b antibody and a biotinylated anti- rabbit secondary antibody. (**A**) CD42b positive events per mm^2 of lung tissue (**B**) Percentage area of CD42b positive staining (**C**) Representative images of lung parenchyma at x40 magnification from CD42b stained lungs from (**i-ii**) sham control and (**iii-iv**) $1x10^6$ cfu/mL *P.aeruginosa* strain RP73 infected animals. Unpaired two-tailed t-test, * $p<0.05$, ** $p<0.01$ versus sham, n=6, data are presented as mean ± SEM.

4.3 Investigating the Effects of Infection on Platelet Activation Markers in BAL Fluid and Blood Plasma

Clinically, it has been demonstrated that patients admitted to the hospital with infectious diseases have an increased expression of platelet activation markers (O'Sullivan et al., 2005), as measured by increased platelet-neutrophil complexes and surface expression of adhesion molecules, such as P-selectin (Amison et al., 2018). Furthermore, a plethora of platelet microbicidal proteins and kinocidins are released upon platelet activation, including PF-4 and RANTES (Yeaman, 2010). Therefore, we sought to investigate the effect of infection induced platelet activation, by quantification of the granular secretory products PF-4 and RANTES.

4.3.1 Quantification of PF-4 Levels in BAL fluid Following Infection with *P.aeruginosa* or MRSA

48 h.p.i. with *P.aeruginosa* or MRSA, BAL fluid was collected and the platelet granular secretory product, PF-4 was quantified. Infection with RP73 did not significantly augment levels of PF-4 in BAL fluid, however a trend suggesting elevated levels was observed, when compared to sham controls (RP73: 265.10 ± 106.30 pg/mL, versus sham: 94.14 ± 19.55 pg/mL, **Figure 4.3A**). Significant increases in BAL PF-4 levels were observed following infection with PAO1 (PAO1: 246.10±63.83 pg/mL, versus sham: 85.17±18.46 pg/mL, **Figure 4.3B**, $p<0.05$) and NN2 when compared to sham controls (NN2: 298.60±89.84 pg/mL, versus sham: 20.69±5.49 pg/mL, **Figure 4.3C**, $p<0.05$). Infection with MRSA strain USA300 appeared to cause platelet activation, as indicated by increased concentrations of PF-4, however this result did not reach statistical significance (MRSA: 236.70±82.74 pg/mL, versus sham: 90.55±19.01 pg/mL, **Figure 4.3D**).

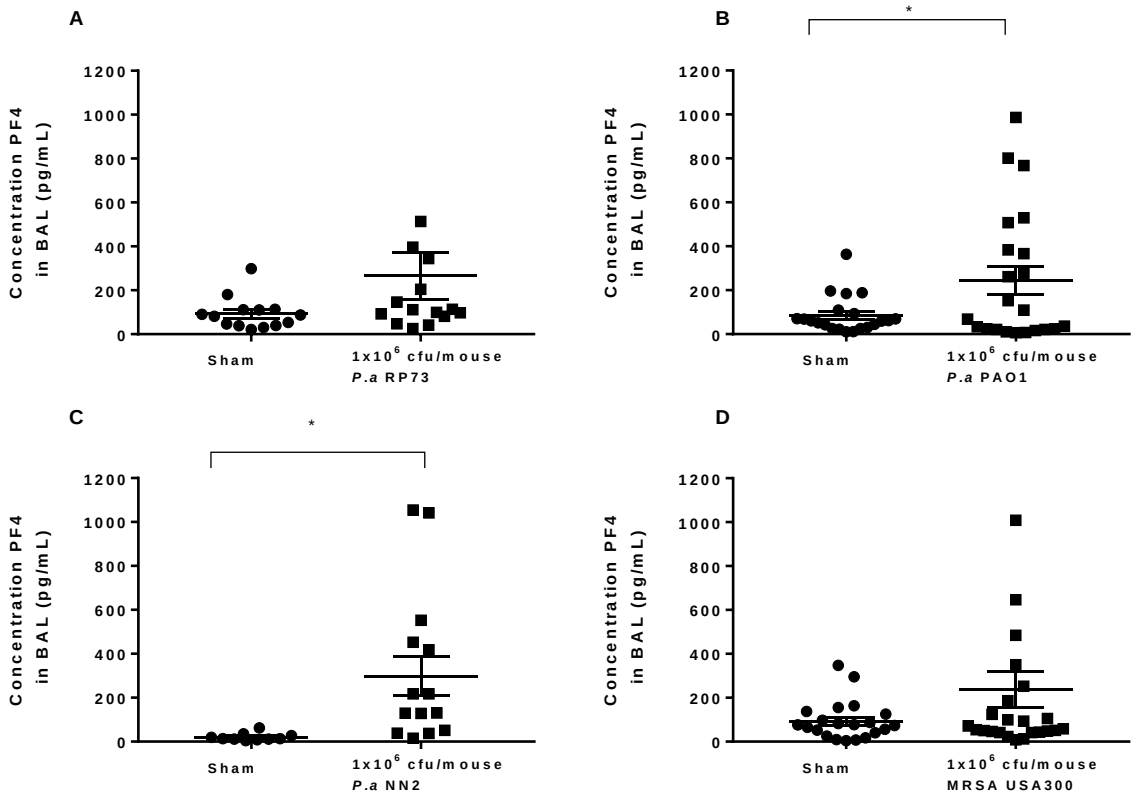

Figure 4.3 Effects of Infection with *P.aeruginosa* and MRSA on PF-4 Levels in BAL Fluid

Mice were infected *(o.a)* with either sham or 1x10^6 cfu/mouse *P.aeruginosa* strain RP73, PAO1 or NN2 or MRSA strain USA300 embedded agar beads. At 48 h.p.i, a BAL of the lungs was performed. The concentration of PF4 present in BAL fluid was measured using a murine PF4 Duoset ELISA, DY595. **(A)** RP73, **(B)** PAO1, **(C)** NN2, **(D)** USA300, unpaired two-tailed t-test, *p<0.05 versus sham, n=10-24, data are presented as mean ± SEM.

4.3.2 Quantification of RANTES Levels in BAL fluid Following Infection with *P.aeruginosa* or MRSA

48 h.p.i. with *P.aeruginosa* or MRSA, BAL fluid was collected and the platelet granular secretory product, RANTES was measured. These data suggested that infection with RP73 elevated levels of RANTES in BAL fluid when compared to sham controls, although this result did not reach statistical significance (RP73: 217.30±64.83 pg/mL, versus sham: 75.33±40.07 pg/mL, **Figure 4.4A**). A significant increase in RANTES secretion was observed in BAL fluid following infection with PAO1 (PAO1: 298.90±117.60 pg/mL, versus sham: 33.46±34.66 pg/mL, **Figure 4.4B**, $p<0.05$) and NN2 when compared to sham controls, which were below the limit of detection (NN2: 406.10±113.4 pg/mL, versus sham: -33.4±42.0 pg/mL, **Figure 4.4C**, $p<0.001$). Infection with MRSA strain USA300 induced a significant increase in BAL levels of RANTES when compared to sham controls, which were below the limit of detection (MRSA: 317.0±-55.30 pg/mL, sham: -65.94±16.24 pg/mL, **Figure 4.4D**, $p<0.0001$). Consistent with the data obtained for that of PF-4, these data suggest that platelets become activated at the site of infection, indicated by increased secretion of granular contents.

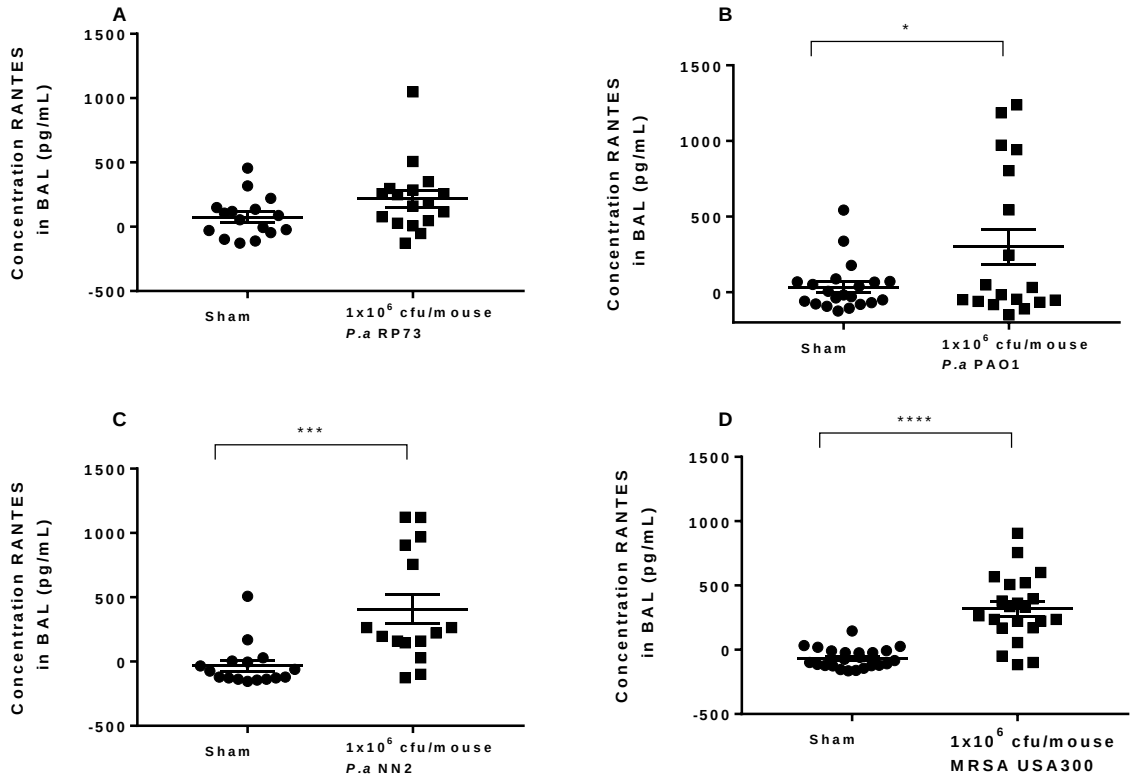

Figure 4.4 Effects of Infection with *P.aeruginosa* and MRSA on RANTES Levels in BAL Fluid

Mice were infected *(o.a)* with either sham or $1x10^6$ cfu/mouse *P.aeruginosa* strain RP73, PAO1 or NN2 or MRSA strain USA300 embedded agar beads. At 48 h.p.i, a BAL of the lungs was performed. The concentration of RANTES present in BAL fluid was measured using a murine RANTES Duoset ELISA, DY478. **(A)** RP73, **(B)** PAO1, **(C)** NN2, **(D)** USA300, unpaired two-tailed t-test, *p<0.05, ***p<0.001, ****p<0.0001 versus sham, n=15-23 data are presented as mean ± SEM.

4.3.3 Quantification of PF-4 Levels in Blood Plasma Following Infection with *P.aeruginosa* or MRSA

48 h.p.i. with *P.aeruginosa* or MRSA, plasma was isolated and the concentration of PF-4 in samples was quantified. The results collected suggested that infection with RP73 (RP73: 94.22±31.04 ng/mL, versus sham: 160.80±4.90 ng/mL, **Figure 4.5A**), PAO1 (PAO1: 359.02±134.78 ng/mL, versus sham: 248.94±52.33 ng/mL, **Figure 4.5B**) and NN2 (NN2: 461.53±112.48 ng/mL, versus sham: 399.03±56.14 ng/mL, **Figure 4.5C**) had no significant effect on the concentration of PF-4 in plasma, when compared to sham controls.

Similarly, infection with MRSA strain USA300 did not significantly increase PF-4 levels, when compared to sham controls (MRSA: 472.86±86.29 ng/mL, versus sham: 430.04±4.34 pg/mL, **Figure 4.5D**). These data suggest that PF-4 may only be released at the site of infection, since both PF4 and RANTES were significantly elevated in BAL fluid at this same time point.

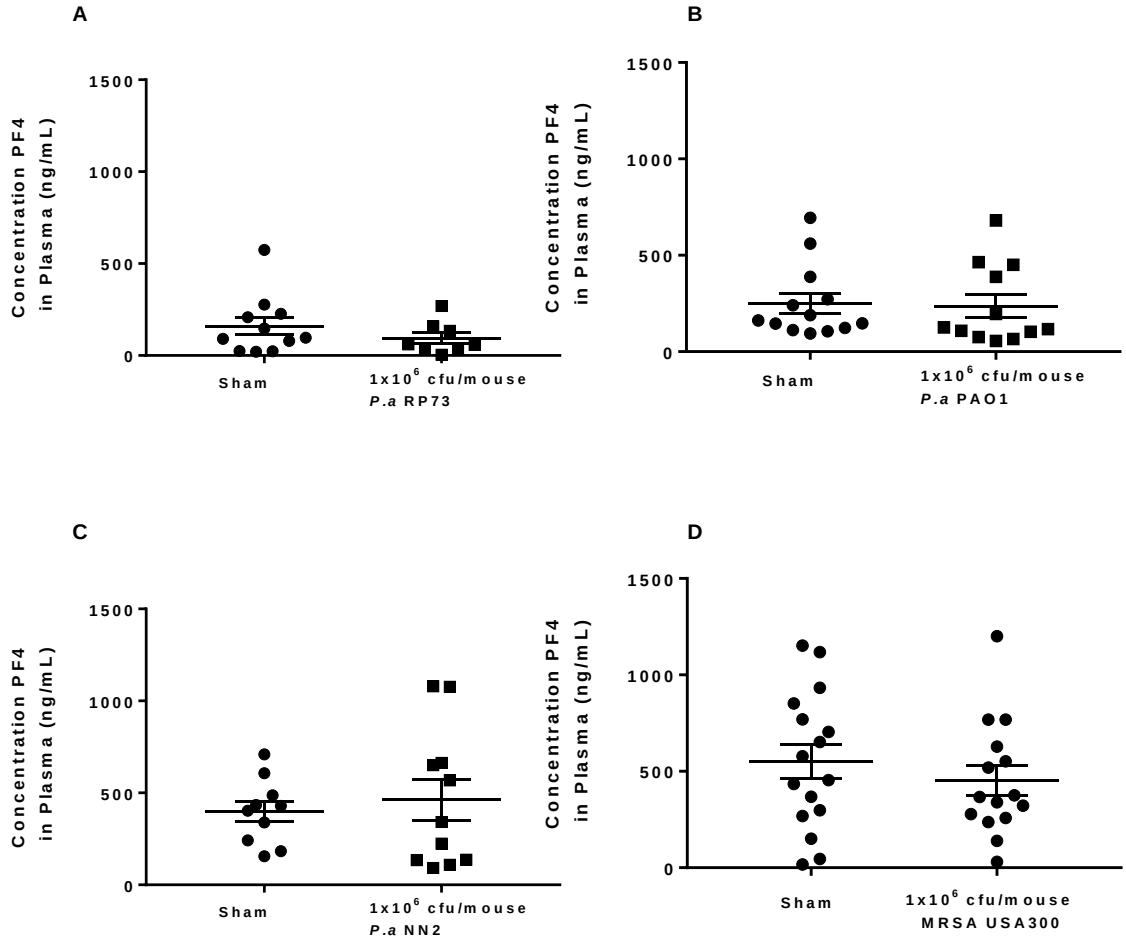

Figure 4.5 Effects of Infection with *P.aeruginosa* and MRSA on PF-4 Levels in Blood Plasma

Mice were infected *(o.a)* with either sham or $1x10^6$ cfu/mouse *P.aeruginosa* strain RP73, PAO1 or NN2 or MRSA strain USA300 embedded agar beads. At 48 h.p.i blood was taken via cardiac puncture and plasma was isolated. The concentration of PF-4 present in plasma was measured using a murine PF-4 Duoset ELISA, DY595. **(A)** RP73, **(B)** PAO1, **(C)** NN2, **(D)** USA300, unpaired two-tailed t-test, $p>0.05$ versus sham, n=8-19, data are presented as mean ± SEM.

4.4 Investigating *P.aeruginosa* strain RP73 Infection Induced Platelet-Leukocyte Complex Formation *ex vivo*

Whilst granule secretion has been used as a marker of platelet activation, the formation of platelet-leukocyte complexes has also been demonstrated as a marker of platelet activation (Pitchford et al., 2003). Therefore, we sought to investigate whether infection increases platelet activation, as measured by platelet-neutrophil complex formation in the blood, following infection with RP73.

Infection with $1x10^6$ cfu/mouse RP73 induced a ~4-fold increase in circulating platelet-neutrophil complexes when compared to sham controls (RP73: 9.24±2.45%, versus sham: 2.45±0.48%, **Figure 4.6A**, $p<0.01$), indicative of platelet activation in the blood of infected mice. Infection had no significant effect on platelet MFI on platelet-neutrophil complexes, when compared to sham controls (RP73: 10.57±0.96, versus sham: 11.35±1.09, **Figure 4.6B**), indicative of no change in the number of platelets per neutrophil.

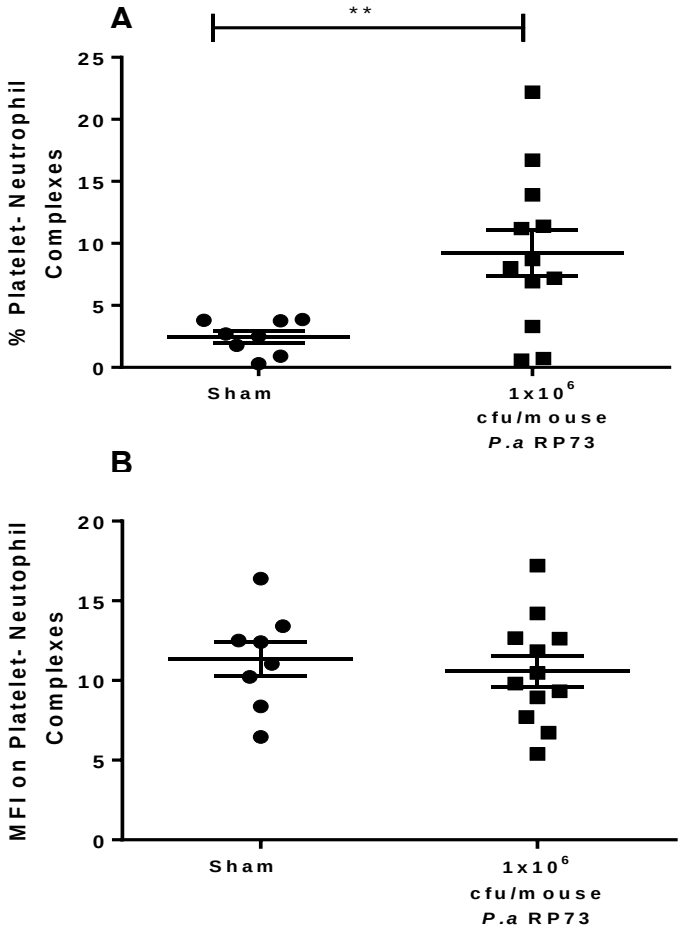

Figure 4.6 Effects of Infection with *P.aeruginosa* on Platelet-Leukocyte Complex Formation

Mice were infected *(o.a)* with either sham or $1x10^6$ cfu/mouse RP73 embedded agar beads. At 24 h.p.i blood was taken via cardiac puncture and the (**A**) percentage of platelet-neutrophil complexes and the (**B**) MFI on platelet- neutrophil complexes was measured using a FITC rat anti-mouse CD41 #553848 antibody and a PE rat anti-mouse Ly6g #551461 antibody and flow cytometry analysis, unpaired two-tailed t-test, **p<0.01 versus sham, n=8-12, data are presented as mean ± SEM.

4.5 Investigating Bacteria Induced Platelet Migration

Having previously demonstrated pulmonary platelet recruitment following infection *in vivo*, experiments were performed to determine whether bacteria induces platelet migration *in vitro*. Platelet migration towards SDF-1α was significantly elevated when compared to the RPMI negative controls (SDF-1α: 2.06±0.26, versus RPMI: 1.0±0.12, **Figure 4.7**, p<0.01). A significant increase in platelet chemotaxis towards bacteria ($1x10^7$ and $1x10^8$ cfu/mL) was observed (10^6: 1.45±0.08, 10^7: 2.05±0.18 p<0.001, 10^8: 1.74±0.27 p<0.05, CI, **Figure 4.7**), when compared to the RPMI negative controls.

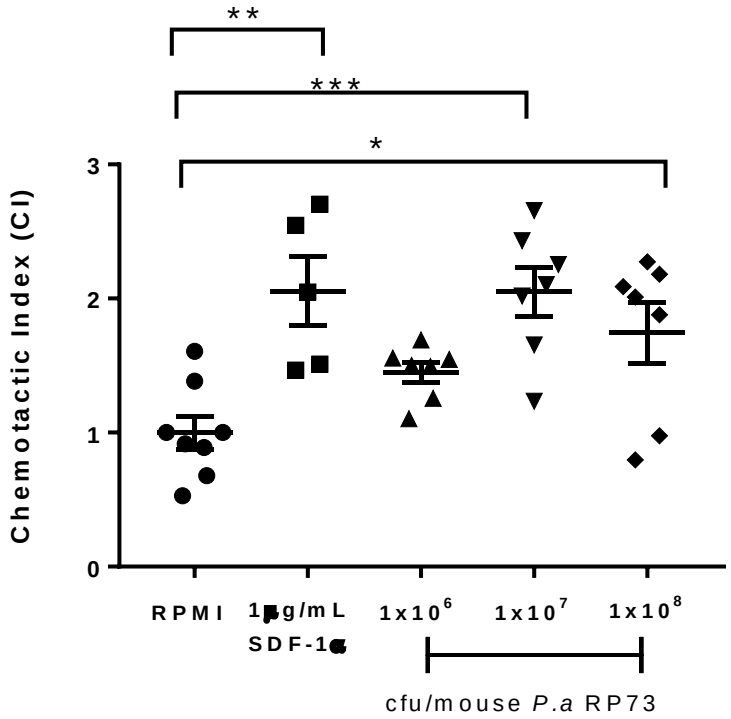

Figure 4.7 Effects of Bacteria Induced Platelet Migration

Platelets were isolated from human citrated blood and bacterial cultures of *P.aeruginosa* strain RP73 were prepared. Platelets were stimulated with 100nM ADP and added to the top well of a chemotaxis chamber. Platelet chemotaxis towards either 1µg/mL SDF-1α or RP73 was then quantified after a 90-minute incubation period and analysed as a chemotactic index. One-way ANOVA and Bonferroni's multiple comparisons post hoc test, *p<0.05, **p<0.01, ***p<0.001, versus RPMI control, n=8-12, data are presented as mean ± SEM.

4.6 Establishing a Thrombocytopenic Model of Pulmonary Infection with *P.aeruginosa* strain RP73

Experimentally induced thrombocytopenia has been associated with enhanced pulmonary bacterial load and increased systemic infection in animal models of pulmonary bacterial infection with *S.aureus* and *K.pneumonia* (Youssefian et al., 2002), (de Stoppelaar, 2014). This implicates platelets in host defence against infection in the clinic and further suggests that drugs that are being developed to target platelet participation in atherosclerosis, by interfering with normal platelet function, may be detrimental to the host's defence system (Pitchford., 2007).

The aim of this study was to investigate the effect of thrombocytopenia on bacterial induced leukocyte recruitment, bacterial growth and the systemic dissemination of bacteria, following infection with the gram-negative *P.aeruginosa,* strain RP73. In order to determine the most suitable level of infection for platelet depletion studies, mice were infected with either $1x10^6$, $1x10^5$ or $1x10^4$ cfu/mouse RP73.

4.6.1 Investigating the Effect of Pulmonary Infection on Circulating Platelet Numbers

Similarly to the results observed in Figure 4.1, a significant decrease in circulating platelet numbers was observed 24 hours following infection with *P.aeruginosa* strain RP73, at either $1x10^4$ (RP73: $5.10\pm0.16x10^8$ platelets/mL, versus sham: $6.28\pm0.23x10^8$ platelets/mL, **Figure 4.8A**, $p<0.01$), $1x10^5$ (RP73: $5.58\pm0.25x10^8$ platelets/mL, versus sham: $6.65\pm0.43x10^8$ platelets/mL, **Figure 4.8B**, $p<0.05$) or $1x10^6$ (RP73: $5.94\pm0.17x10^8$ platelets/mL, versus sham: $6.77\pm0.42x10^8$ platelets/mL, **Figure 4.8C**, $p<0.05$) cfu/mouse, when compared to sham controls.

4.6.2 Investigating the Effect of Experimentally Induced Platelet Depletion on the Circulating Platelet Numbers

In order to experimentally deplete mice of circulating platelets, mice were treated with either 1mg/kg of an anti-GPIbα platelet depleting antibody or an IgG control antibody, 24 hours prior to infection with either $1x10^4$, $1x10^5$ or $1x10^6$ cfu/mouse *P.aeruginosa* strain RP73. The anti-GPIbα platelet depleting antibody depleted circulating platelet by approximately 80% (81.56 ± 3.01%) in all 3 studies, when compared to animals treated with the IgG control (10^4 log cfu + anti-GPIbα: $1.16±0.05x10^8$ platelets/mL, versus 10^4 log cfu + IgG control: $5.10±0.16x10^8$ platelets/mL, **Figure 4.8A**, $p<0.0001$), (10^5 log cfu + anti-GPIbα: $1.12±0.09x10^8$ platelets/mL, versus 10^5 log cfu + IgG control: $5.58±0.25x10^8$ platelets/mL, **Figure 4.8B**, $p<0.001$) and (10^6 log cfu + anti-GPIbα: $0.75±0.09x10^8$ platelets/mL versus 10^6 log cfu + IgG control: $5.94±0.17x10^8$ platelets/mL, **Figure 4.8C**, $p<0.001$).

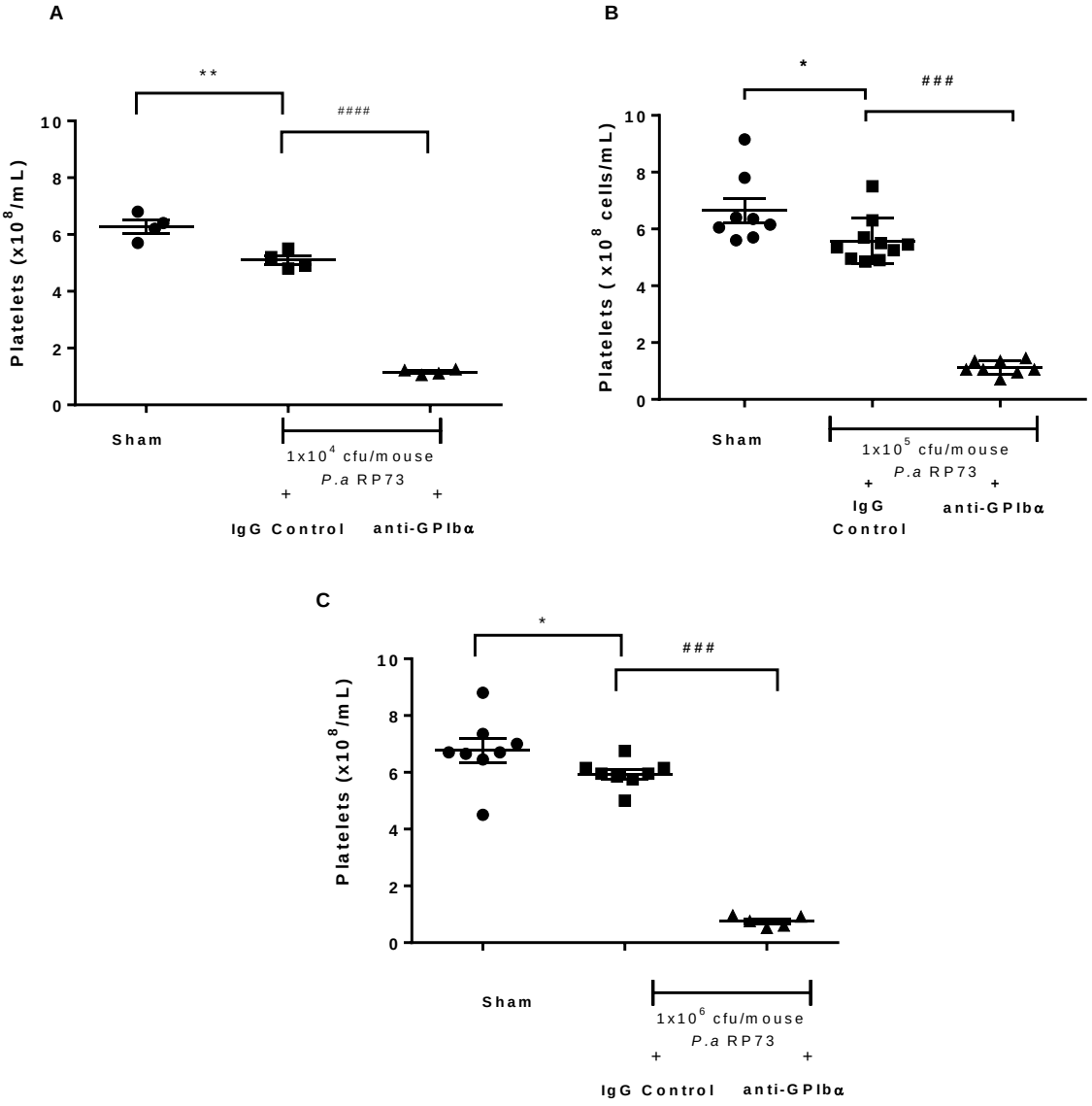

Figure 4.8 Effects of Experimentally Induced Platelet Depletion on Circulating Platelet Numbers in a Thrombocytopenic Model of Pulmonary Infection with *P.aeruginosa* strain RP73

Mice were treated with either 1mg/kg of anti-GPIbα platelet depleting antibody or IgG control antibody 24 hours prior to infection with either sham or (**A**) $1x10^4$, (**B**) $1x10^5$ or (**C**) $1x10^6$ cfu/mouse RP73 embedded agar beads. At 24 h.p.i blood was taken via cardiac puncture and the circulating platelet count was quantified using an improved neubauer haemocytometer. One-way ANOVA and Bonferroni's multiple comparisons post hoc test, *p<0.05, **p<0.01 versus sham, ### p<0.001, #### p<0.0001 versus IgG control, n=4-10, data are presented as mean ± SEM.

4.6.3 Investigating the Effect of Platelet Depletion on Pulmonary Haemorrhage

In order to investigate whether administration of the platelet depleting anti-GPIbα antibody induced pulmonary haemorrhage, haemoglobin levels present in BAL fluid were quantified following administration of either the IgG control or anti-GPIbα antibodies.

The platelet depleting anti-GPIbα antibody did not cause any significant increase in pulmonary haemorrhage in either the sham controls (10^5 log cfu + anti-GPIbα: 0.11±0.03 versus 10^5 log cfu + IgG control: 0.04±0.00, **Figure 4.9**) or RP73 infected animals (10^5 log cfu + anti-GPIbα: 0.28±0.15 versus 10^5 log cfu + IgG control: 0.04±0.00, **Figure 4.9**), when compared to mice treated with the IgG control. Although these data did not reach statistical significance, a trend was observed suggesting the platelet depleting anti-GPIbα antibody increased the optical density of the BAL fluid, suggestive of minor pulmonary haemorrhage.

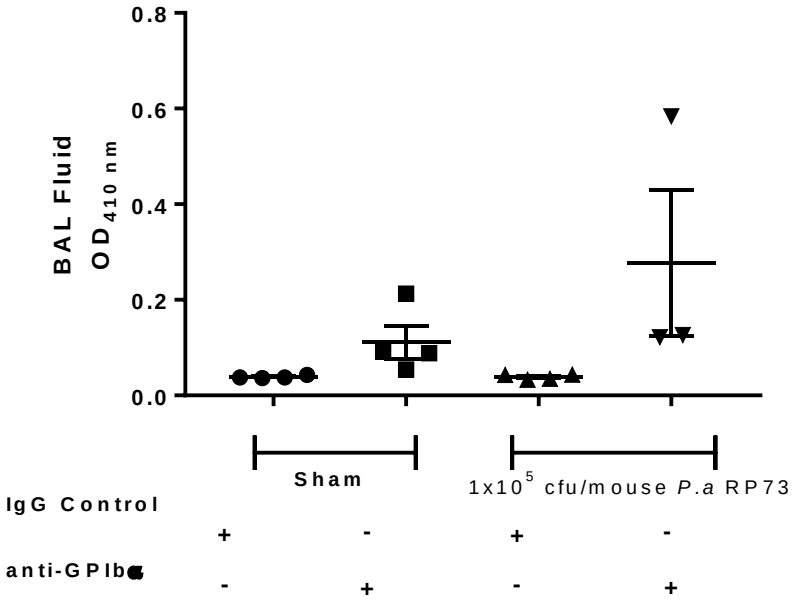

Figure 4.9 Effect of the Platelet Depleting anti-GPIbα Antibody on Pulmonary Haemorrhage in a Thrombocytopenic Model of Pulmonary Infection with *P.aeruginosa* strain RP73

Mice were treated with either 1mg/kg of anti-GPIbα platelet depleting antibody or IgG control antibody 24 hours prior to infection with either sham or $1x10^5$ cfu/mouse *P.aeruginosa* strain RP73 embedded agar beads. At 24 h.p.i, a BAL of the lungs was performed and the presence of red blood cells in the lavage was quantified, using a Spectramax 340PC microplate reader at 410nm. n=3-4, data are presented as mean ± SEM.

4.6.4 Investigating the Effect of Experimentally Induced Platelet Depletion on Weight Loss

Severity of infection is typically associated with increased weight loss, therefore the body weights of sham and infected, IgG control treated, and platelet depleted animals were recorded prior to and post infection.

The results obtained demonstrated that following infection with the lowest inoculum of $1x10^4$ cfu/mouse RP73, there was no significant difference in weight loss between any groups (sham: 0.28±0.18%, 10^4 log cfu + IgG control: 0.41±0.19%, 10^4 log cfu + anti-GPIbα: 0.23±0.09%, **Figure 4.10A**). Following infection with the intermediate inoculum of $1x10^5$ cfu/mouse, there was no significant increase in weight loss when compared to the sham controls (sham: 0.67±0.24%, 10^5 log cfu $^+$ IgG control: 2.66±1.31%, **Figure 4.10B**). However, experimentally induced platelet depletion was associated with a significant increase in weight loss when compared to mice with normal circulating platelet levels (10^5 log cfu + IgG control: 2.66±1.31%, 10^5 log cfu + anti-GPIbα: 7.01±1.45%, **Figure 4.10B**, $p<0.01$).

Following infection with the highest inoculum of $1x10^6$ cfu/mouse RP73, there was a significant increase in weight loss when compared to the sham controls (sham: 4.62±0.05%, 10^6 log cfu + IgG control: 11.31±1.39%, **Figure 4.10C**, $p<0.01$), due to the severity of the infection. As observed following infection with the $1x10^5$ cfu/mouse inoculum, experimentally induced platelet depletion resulted in a significant increase in weight loss compared to mice with normal circulating platelet levels (10^6 log cfu + IgG control: 11.31±1.39%, 10^6 log cfu + anti-GPIbα: 14.27±1.91%, **Figure 4.10C**, $p<0.01$).

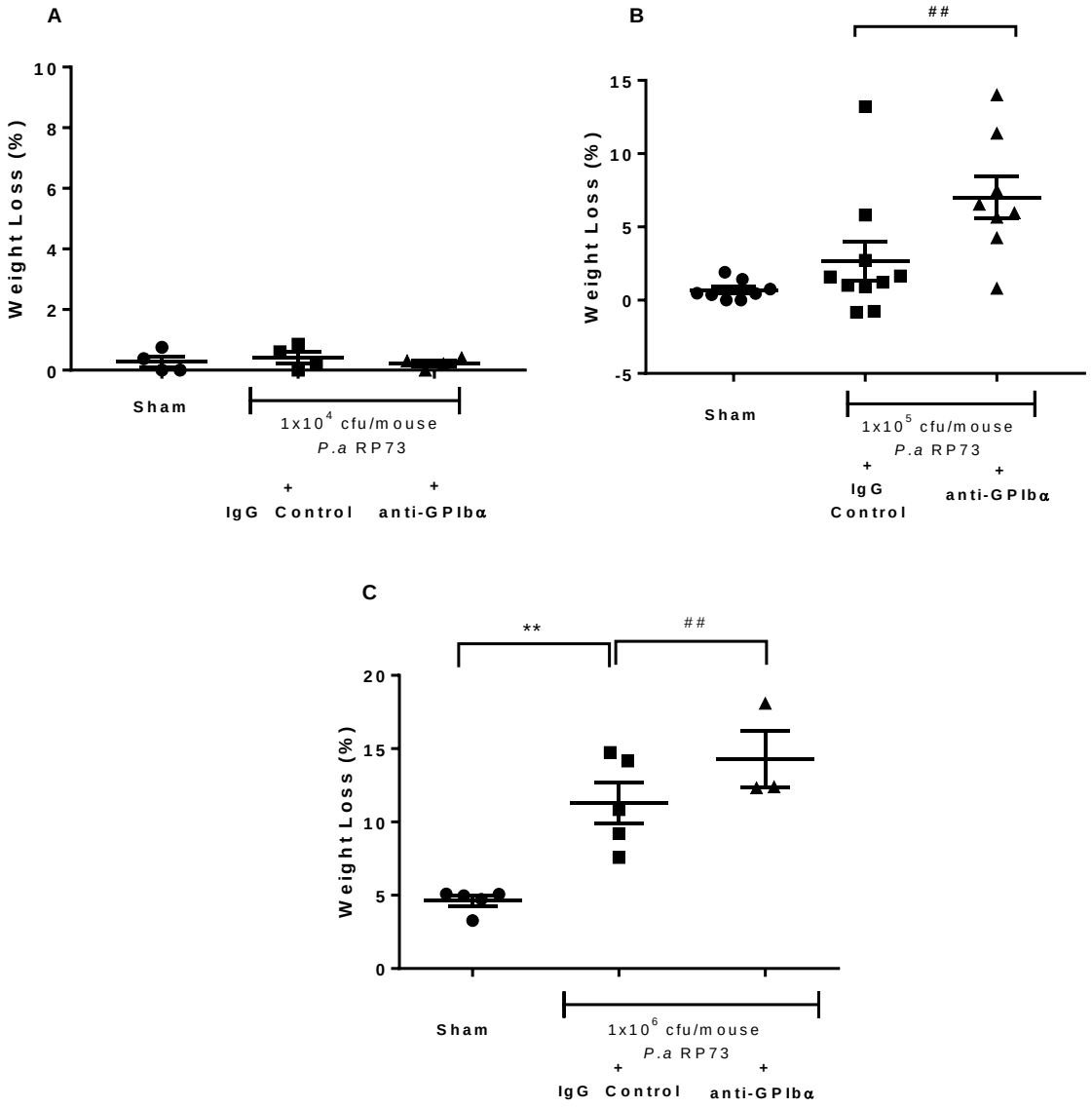

Figure 4.10 Effects of Experimentally Induced Platelet Deletion on Weight Loss in a Thrombocytopenic Model of Pulmonary Infection with *P.aeruginosa* strain RP73

Mice were treated with either 1mg/kg of anti-GPIbα platelet depleting antibody or IgG control antibody 24 hours prior to infection with either sham or (**A**) $1x10^4$, (**B**) $1x10^5$ or (**C**) $1x10^6$ cfu/mouse *P.aeruginosa* strain RP73 embedded agar beads. Body weights were recorded prior to and post infection and percentage weight loss calculated. One-way ANOVA and Bonferroni's multiple comparisons post hoc test, ** $p<0.01$ versus sham, ## $p<0.01$ versus IgG control, n=3-10, data are presented as mean ± SEM.

4.6.5 Investigating the Effect of Experimentally Induced Platelet Depletion on Pulmonary Bacterial Load

Initial titration studies were performed to determine the optimum inoculum to investigate the effect of experimentally induced platelet depletion on pulmonary bacterial load. Mice were exposed to 3 different concentrations ($1x10^4$, $1x10^5$ or $1x10^6$ cfu/mouse) of RP73 embedded agar beads and infection and inflammatory parameters were subsequently analysed.

For mice infected with the lowest inoculum of $1x10^4$ cfu/mouse RP73, 24 h.p.i, the infection was cleared from the lungs, since there was no evidence of pulmonary bacterial infection in either the sham controls or the $1x10^4$ cfu/mouse RP73 infected animals (sham: 0.0±0.0 log cfu, 10^4 log cfu + IgG: 0.0±0.0 log cfu, 10^4 log cfu + anti-GPIbα: 0.0±0.0 log cfu, **Figure 4.11A**).

For the intermediate inoculum of $1x10^5$ cfu/mouse RP73, 24 h.p.i, mice inoculated with sham agar beads demonstrated no evidence of pulmonary bacterial infection (0.0±0.0 log cfu, **Figure 4.11B**). Mice infected with $1x10^5$ cfu/mouse with normal circulating platelet levels, demonstrated a significant increase in pulmonary bacterial load when compared to sham controls (10^5 log cfu + IgG: 4.72±0.29 log cfu versus sham: 0.0±0.0 log cfu, $p<0.001$, **Figure 4.11B**). Furthermore, for mice infected with $1x10^5$ cfu/mouse and treated with the platelet depleting anti-GPIbα antibody, there was no significant increase in pulmonary bacterial load when compared to mice with normal circulating platelet levels (10^5 log cfu + anti-GPIbα: 5.21±0.39 log cfu versus 10^5 log cfu + IgG: 4.72±0.29 log cfu, **Figure 4.11B**). Although these data did not reach statistical significance, a small increase of 0.5 log cfu was observed in the platelet depleted anti-GPIbα treated animals compared to mice with normal circulating platelet levels.

For the highest inoculum of $1x10^6$ cfu/mouse RP73, 24 h.p.i, mice inoculated with sham agar beads demonstrated no evidence of pulmonary bacterial infection (0.0±0.0 log cfu, **Figure 4.11C**). In contrast, mice infected with $1x10^6$ cfu/mouse RP73 with normal circulating platelet levels, demonstrated a significant increase in pulmonary bacterial load when compared to sham controls (10^6 log cfu + IgG: 5.21±0.43 log cfu versus sham: 0.0±0.0 log cfu, $p<0.0001$, **Figure 4.11C**). In mice infected with $1x10^6$ cfu/mouse RP73 and treated with the platelet depleting anti-GPIbα antibody, pulmonary bacterial load was significantly elevated, by approximately 1.5 logs, when compared to mice with normal circulating platelet levels (10^6 log cfu + anti-GPIbα: 6.74±0.44 log cfu versus 10^6 log cfu + IgG: 5.21±0.43 log cfu, $p<0.05$, **Figure 4.11C**), demonstrating in situ bacterial growth.

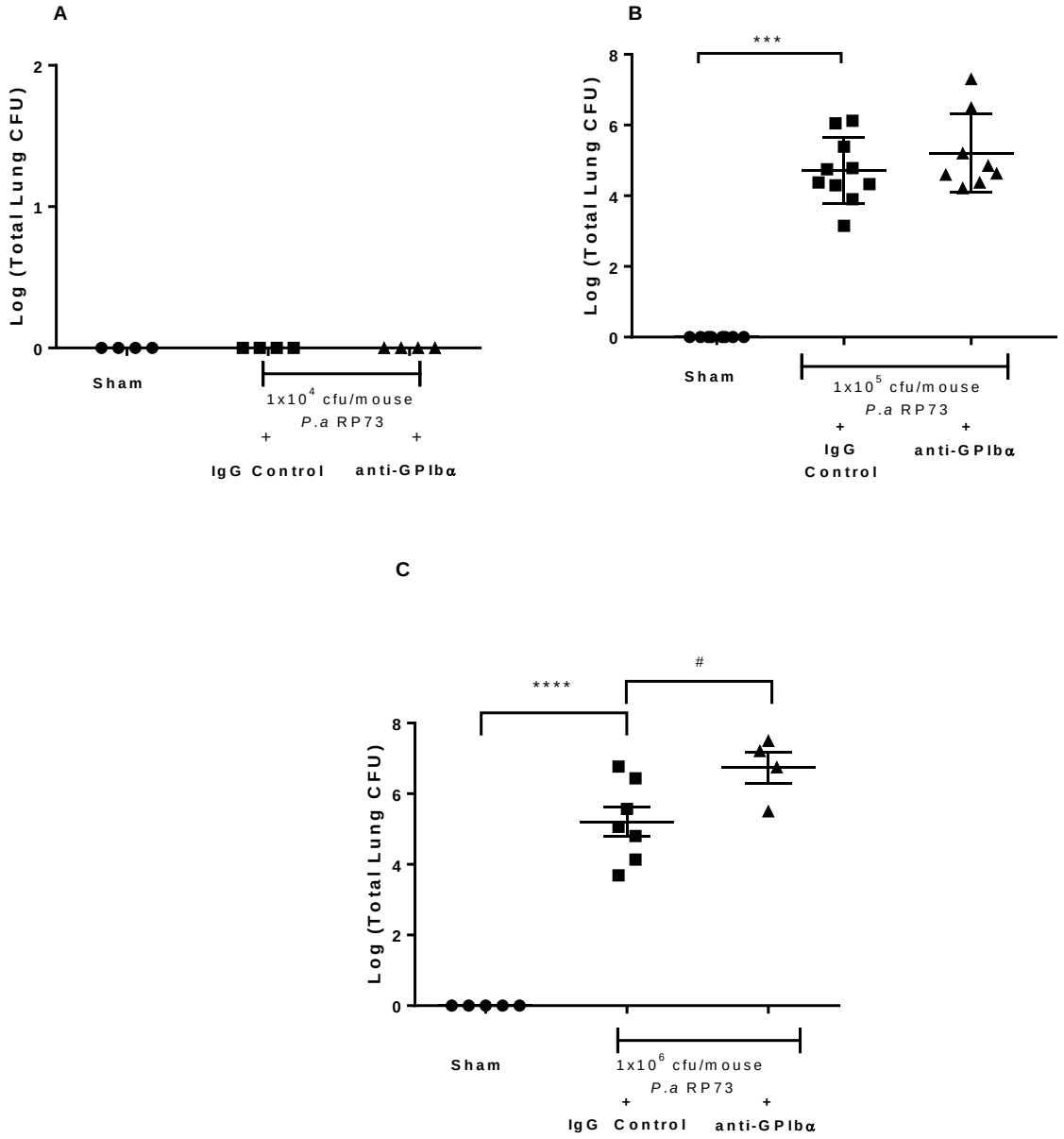

Figure 4.11 Effects of Experimentally Induced Platelet Depletion on Pulmonary Bacterial Load in a Thrombocytopenic Model of Pulmonary Infection with *P.aeruginosa* strain RP73

Mice were treated with either 1mg/kg of anti-GPIbα platelet depleting antibody or IgG control antibody 24 hours prior to infection with either sham or (**A**) $1x10^4$, (**B**) $1x10^5$ or (**C**) $1x10^6$ cfu/mouse RP73 embedded agar beads. At 24 h.p.i, lungs were aseptically removed, homogenised and plated for quantification of bacterial load. One-way ANOVA and Bonferroni's multiple comparisons post hoc test, *** $p<0.001$, **** $p<0.0001$ versus sham, # $p<0.05$ versus IgG control, n=4-10, data are presented as mean ± SEM.

4.6.6 Investigating the Effect of Experimentally Induced Platelet Depletion on Bacterial Dissemination

It has previously been demonstrated in gram-negative bacterial induced sepsis models that platelet depletion enhances bacterial dissemination (de Stoppelaar, 2014). Therefore, we sought to investigate whether experimentally induced platelet depletion has any effect on gram-negative bacterial dissemination from the lungs to other peripheral organs.

At 24 h.p.i, no evidence of bacterial dissemination to the kidney or spleen was observed in either the sham control or the lowest inoculum of $1x10^4$ cfu/mouse RP73 infected animals (Kidney: sham: 0.0±0.0 log cfu, 10^4 log cfu + IgG: 0.0±0.0 log cfu, 10^4 log cfu + anti-GPIbα: 0.0±0.0 log cfu, **Figure 4.12A,** and Spleen: sham: 0.0±0.0 log cfu, 10^4 log cfu + IgG: 0.0±0.0 log cfu, 10^4 log cfu + anti-GPIbα: 0.0±0.0 log cfu, **Figure 4.13A**).

Following infection with the intermediate inoculum of $1x10^5$ cfu/mouse RP73, at 24 h.p.i there was no evidence of bacterial dissemination to the kidney or spleen in either the sham control or the $1x10^5$ cfu/mouse RP73, IgG control treated animals (Kidney: sham: 0.0±0.0 log cfu, 10^5 log cfu + IgG: 0.0±0.0 log cfu, **Figure 4.12B** and Spleen: sham: 0.0±0.0 log cfu, 10^5 log cfu + IgG: 0.0±0.0 log cfu, **Figure 4.13B**). In contrast, there was a significant increase in the bacterial load recovered from the kidney and spleen, following infection with $1x10^5$ cfu/mouse RP73 in mice depleted of circulating platelets, when compared to mice with normal circulating platelet levels (Kidney: 10^5 log cfu + anti-GPIbα: 1.56±0.39 log cfu versus 10^5 log cfu + IgG: 0.0±0.0 log cfu, $p<0.001$, **Figure 4.12B** and Spleen: 10^5 log cfu + anti-GPIbα: 0.74±0.36 log cfu versus 10^5 log cfu + IgG: 0.0±0.0 log cfu, $p<0.05$, **Figure 4.13B**).

Following infection with the highest level of inoculum of $1x10^6$ cfu/mouse RP73, at 24 h.p.i there was no evidence of bacterial dissemination to the kidney in the sham controls (Kidney:

sham: 0.0±0.0 log cfu, **Figure 4.12C** and Spleen: sham: 0.0±0.0 log cfu, **Figure 4.13C**). Infection with $1x10^6$ cfu/mouse RP73 and treatment with the IgG control antibody induced minimal bacterial dissemination to the kidney and spleen following infection, when compared to the sham controls (Kidney: sham: 0.0±0.0 log cfu, 10^6 log cfu + IgG: 0.96±0.39 log cfu, **Figure 4.12C** and Spleen: sham: 0.0±0.0 log cfu, 10^6 log cfu + IgG: 0.59±0.31 log cfu, **Figure 4.13C**).Whilst the significant increase in pulmonary bacterial load observed following infection with $1x10^6$ cfu/mouse RP73 in mice depleted of circulating platelets (**Figure 4.11C**) was accompanied by an increase in bacterial numbers in the kidney and spleen, when compared to mice with normal circulating platelet levels, although this did not reach statistical significance (Kidney: 10^6 log cfu + anti-GPIbα: 2.64±0.43 log cfu versus 10^6 log cfu + IgG: 0.96±0.39 log cfu, **Figure 4.12C** and Spleen: 10^6 log cfu + anti-GPIbα: 2.65±0.53 log cfu versus 10^6 log cfu + IgG: 0.59±0.31 log cfu, **Figure 4.13C**).

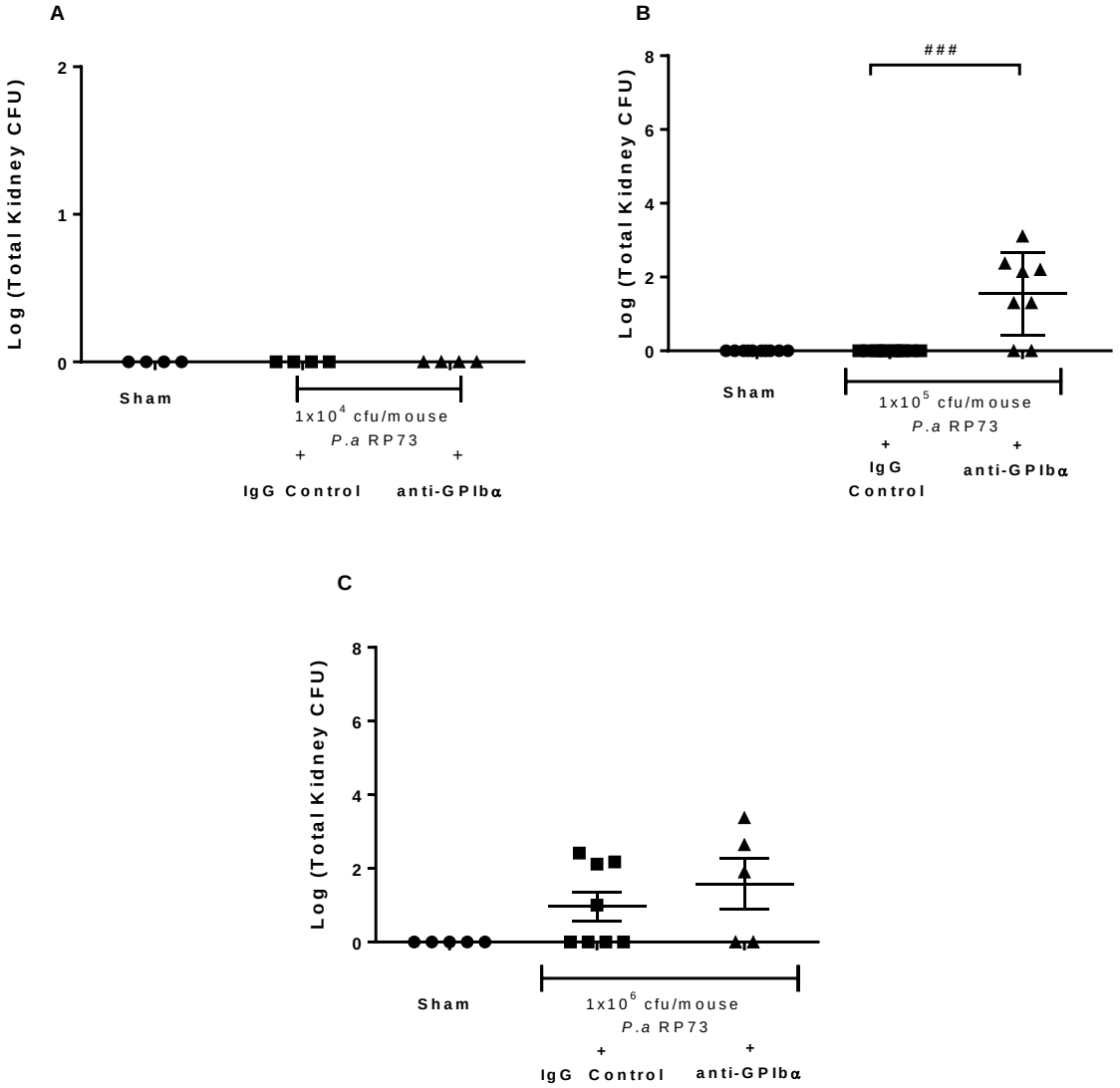

Figure 4.12 Effects of Experimentally Induced Platelet Depletion on Bacterial Dissemination to the Kidney in a Thrombocytopenic Model of Pulmonary Infection with *P.aeruginosa* strain RP73

Mice were treated with either 1mg/kg of anti-GPIbα platelet depleting antibody or IgG control antibody 24 hours prior to infection with either sham or (**A**) 1 x 10^4, (**B**) 1 x 10^5 or (**C**) 1 x 10^6 cfu/mouse *P.aeruginosa* strain RP73 embedded agar beads. At 24 h.p.i, the kidney was aseptically removed, homogenised and plated for quantification of bacterial load. One-way ANOVA and Bonferroni's multiple comparisons post hoc test, # $p<0.05$ versus IgG control, n=4-10, data are presented as mean ± SEM.

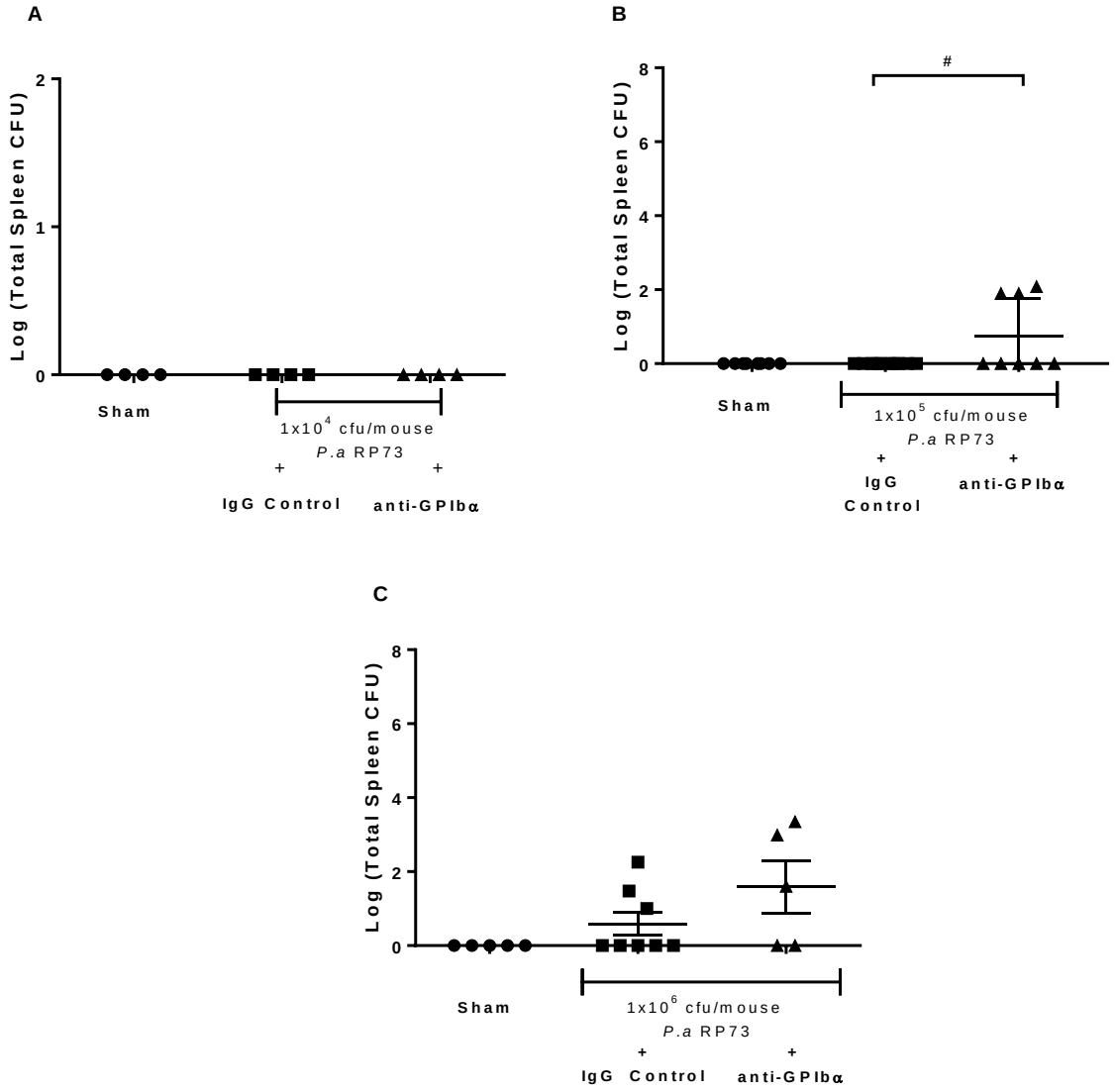

Figure 4.13 Effects of Experimentally Induced Platelet Depletion on Bacterial Dissemination to the Spleen in a Thrombocytopenic Model of Pulmonary Infection with *P.aeruginosa* strain RP73

Mice were treated with either 1mg/kg of anti-GPIbα platelet depleting antibody or IgG control antibody 24 hours prior to infection with either sham or (**A**) $1x10^4$, (**B**) $1x10^5$ or (**C**) $1x10^6$ cfu/mouse *P.aeruginosa* strain RP73 embedded agar beads. At 24 h.p.i, the spleen was aseptically removed, homogenised and plated for quantification of bacterial load. One-way ANOVA and Bonferroni's multiple comparisons post hoc test, # $p<0.05$ versus IgG control, n=4-10, data are presented as mean ± SEM.

4.6.7 Investigating the Effect of Experimentally Induced Platelet Depletion on Pulmonary Leukocyte Recruitment

It has been demonstrated previously that platelets are essential for pulmonary leukocyte recruitment in allergic inflammation (Pitchford et al., 2003), therefore we sought to investigate whether experimentally induced platelet depletion had any effect on pulmonary leukocyte recruitment following infection with *P.aeruginosa* strain RP73.

Infection with the lowest inoculum of $1x10^4$ cfu/mouse increased pulmonary total leukocyte and neutrophil recruitment when compared to sham controls, although this data did not reach statistical significance (Total leukocytes: 10^4 log cfu + IgG: $3.04\pm0.79x10^5$ cells/mL, versus sham: $1.23\pm0.29x10^5$ cells/mL, **Figure 4.14A**, and Neutrophils: 10^4 log cfu + IgG: $0.20\pm0.08x10^5$ cells/mL, versus sham: $0.00\pm 0.00x10^5$ cells/mL, **Figure 4.15A**). In mice experimentally depleted of platelets and infected with $1x10^4$ cfu/mouse RP73, no significant effect on pulmonary total leukocyte and neutrophil recruitment was observed (Total leukocytes: 10^4 log cfu + anti-GPIbα: $3.49\pm0.70x10^5$ cells/mL, versus 10^4 log cfu + IgG: $3.04\pm0.79x10^5$ cells/mL, **Figure 4.14A** and Neutrophils: 10^4 log cfu + anti-GPIbα: $0.34\pm0.09x10^5$ cells/mL, versus 10^4 log cfu + IgG: $0.20\pm0.08x10^5$ cells/mL, **Figure 4.15A**), when compared to mice with normal circulating platelet levels.

24 h.p.i with $1x10^4$ cfu/mouse RP73, no significant increase in pulmonary macrophage or lymphocyte recruitment was observed when compared to sham controls (Macrophages: 10^4 log cfu + IgG: $2.83\pm0.72x10^5$ cells/mL, versus sham: $1.22\pm0.28x10^5$ cells/mL, **Figure 4.16A** and Lymphocytes: 10^4 log cfu + IgG: $0.0\pm0.0x10^5$ cells/mL, versus sham: $0.0\pm0.0x10^5$ cells/mL). Similarly, experimentally induced platelet depletion had no significant effect on pulmonary macrophage or lymphocyte recruitment at 24 h.p.i with $1x10^4$ cfu/mouse RP73

(Macrophages: 10^4 log cfu + anti-GPIbα: 3.15±0.61x10^5 cells/mL, versus 10^4 log cfu + IgG: 2.83±0.72x10^5 cells/mL, **Figure 4.16A**, and Lymphocytes: 10^4 log cfu + anti-GPIbα: 0.0±0.0x10^5 cells/mL, versus 10^4 log cfu + IgG: 0.0±0.0x10^5 cells/mL), when compared to mice with normal circulating platelet levels.

Infection with the intermediate inoculum of 1x10^5 cfu/mouse induced a significant increase in pulmonary total leukocyte and neutrophil recruitment (Total leukocytes: 10^5 log cfu + IgG: 5.0±0.40x10^5 cells/mL, versus sham: 1.39±0.11x10^5 cells/mL, **Figure 4.14B**, $p<0.001$ and Neutrophils: 10^5 log cfu + IgG: 1.66±0.22x10^5 cells/mL, versus sham: 0.02± 0.01x10^5 cells/mL, **Figure 4.15B**, $p<0.001$), when compared to sham controls. In mice experimentally depleted of platelets and infected with 1x10^5 cfu/mouse RP73, a significant decrease in pulmonary total leukocyte and neutrophil recruitment was observed (Total leukocytes: 10^5 log cfu + anti-GPIbα: 3.03±0.51x10^5 cells/mL, versus 10^5 log cfu + IgG: 5.0±0.40x10^5 cells/mL, **Figure 4.14B**, $p<0.01$, and Neutrophils: 10^5 log cfu + anti-GPIbα: 0.91±0.26x10^5 cells/mL, versus 10^5 log cfu + IgG: 1.66±0.22x10^5 cells/mL, $p<0.05$, **Figure 4.15B**), when compared to mice with normal circulating platelet levels.

24 h.p.i with 1x10^5 cfu/mouse RP73, a significant increase in pulmonary macrophage recruitment was observed when compared to sham controls (Macrophages: 10^5 log cfu + IgG: 3.34±0.26x10^5 cells/mL, versus sham: 1.37±0.11x10^5 cells/mL, **Figure 4.16B**, $p<0.001$). Experimentally induced platelet depletion significantly decreased macrophage recruitment to the lungs (Macrophages: 10^5 log cfu + anti-GPIbα: 2.11±0.33x10^5 cells/mL, versus 10^5 log cfu + IgG: 3.34±0.26x10^5 cells/mL, **Figure 4.16A**, $p<0.05$), when compared to sham controls.

Neither infection with 1x10^5 cfu/mouse RP73 or experimentally induced platelet depletion had any significant effect on lymphocyte recruitment to the lungs (Lymphocytes: 10^5 log cfu

+ anti-GPIbα: 0.0±0.0x10^5 cells/mL, 10^5 log cfu + IgG: 0.0±0.0x10^5 cells/mL and sham: 0.0±0.0x10^5 cells/mL), when compared to sham controls and mice with normal circulating platelet levels.

Infection with the highest inoculum of 1x10^6 cfu/mouse induced a significant increase in pulmonary total leukocyte and neutrophil recruitment (Total leukocytes: 10^6 + IgG: 34.42±11.07x10^5 cells/mL, versus sham: 3.48±1.07x10^5 cells/mL, **Figure 4.14C**, $p<0.05$ and Neutrophils: 10^6 log cfu + IgG: 14.88±2.96x10^5 cells/mL, versus sham: 0.64± 0.32x10^5 cells/mL, **Figure 4.15C**, $p<0.001$), when compared to sham controls. In mice experimentally depleted of platelets and infected with 1x10^6 cfu/mouse RP73, a decrease in pulmonary total leukocyte and neutrophil recruitment was observed when compared to mice with normal circulating platelet levels, although this only reached statistical significance for the neutrophils (Total leukocytes: 10^6 log cfu + anti-GPIbα: 14.60±3.16x10^5 cells/mL, versus 10^6 log cfu + IgG: 34.42±11.07x10^5 cells/mL, **Figure 4.14C** and Neutrophils: 10^6 log cfu + anti-GPIbα: 5.41±1.96x10^5 cells/mL, versus 10^6 log cfu + IgG: 14.88±2.96x10^5 cells/mL, $p<0.05$, **Figure 4.15C**).

24 h.p.i with 1x10^6 cfu/mouse RP73, there was no significant difference in either macrophage or lymphocyte recruitment to the lungs when compared to sham controls (Macrophages: 10^6 log cfu + IgG: 3.31±0.55x10^5 cells/mL, versus sham: 2.82±0.75x10^5 cells/mL, **Figure 4.16C** and Lymphocytes: 10^6 log cfu + IgG: 0.0±0.0x10^5 cells/mL, versus sham: 0.0±0.0x10^5 cells/mL). Similarly, in mice depleted of circulating platelets there was no significant effect in either macrophage or lymphocyte recruitment to the lungs (Macrophages: 10^6 log cfu + anti-GPIbα: 2.83±0.60x10^5 cells/mL, versus 10^6 log cfu + IgG: 3.31±0.55x10^5 cells/mL, **Figure 4.16C** and

Lymphocytes: 10^6 log cfu + anti-GPIbα: 0.0±0.0x10^5 cells/mL, versus 10^6 log cfu + IgG: 0.0±0.0x10^5 cells/mL), when compared to mice with normal circulating platelet levels.

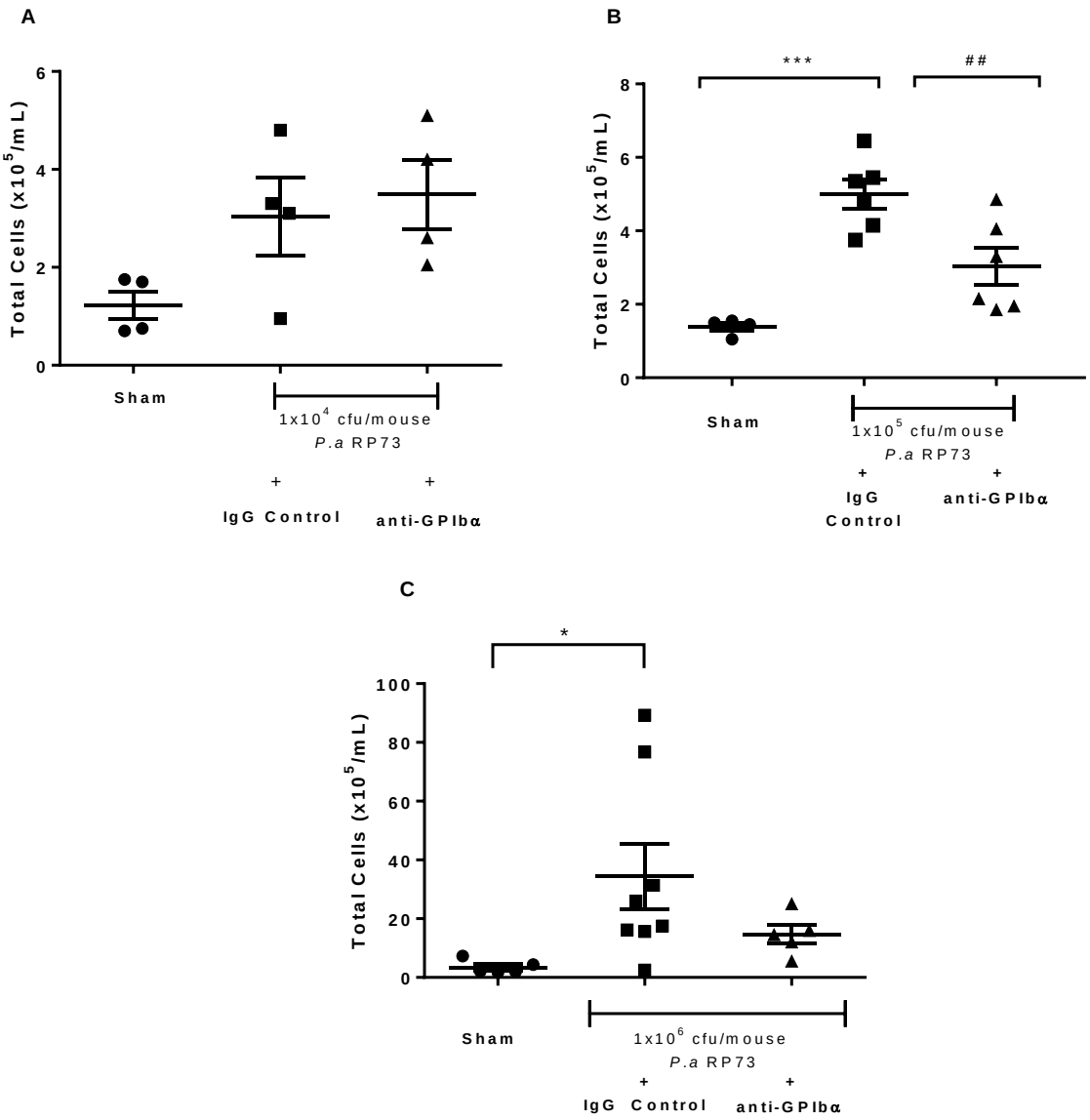

Figure 4.14 Effect of Experimentally Induced Platelet Depletion on Pulmonary Total Leukocyte Recruitment in a Thrombocytopenic Model of Pulmonary Infection with *P.aeruginosa* strain RP73

Mice were treated with either 1mg/kg of anti-GPIbα platelet depleting antibody or IgG control antibody 24 hours prior to infection with either sham or (**A**) 1x10^4, (**B**) 1x10^5 or (**C**) 1x10^6 cfu/mouse *P.aeruginosa* strain RP73 embedded agar beads. At 24 h.p.i, a BAL of the lungs was performed for inflammatory cell quantification. One-way ANOVA and Bonferroni's multiple comparisons post hoc test, * p<0.05, *** p<0.001 versus sham, ## p<0.01 versus IgG control, n=4-8, data are presented as mean ± SEM.

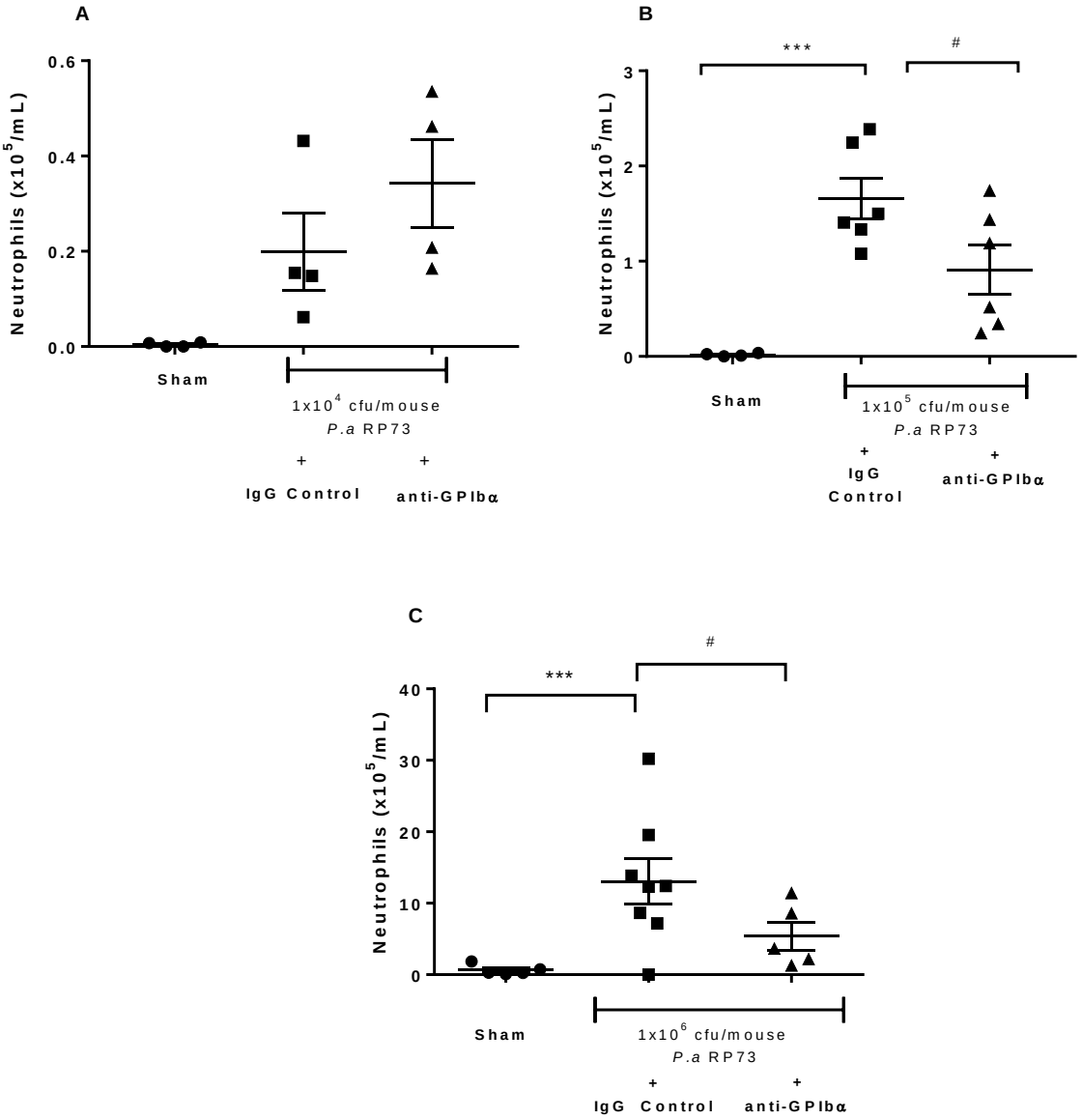

Figure 4.15 Effects of Experimentally Induced Platelet Depletion on Pulmonary Neutrophil Recruitment in a Thrombocytopenic Model of Pulmonary Infection with *P.aeruginosa* strain RP73

Mice were treated with either 1mg/kg of anti-GPIbα platelet depleting antibody or IgG control antibody 24 hours prior to infection with either sham or (**A**) $1x10^4$, (**B**) $1x10^5$ or (**C**) $1x10^6$ cfu/mouse *P.aeruginosa* strain RP73 embedded agar beads. At 24 h.p.i, a BAL of the lungs was performed for neutrophil quantification. One-way ANOVA and Bonferroni's multiple comparisons post hoc test, *** $p<0.001$ versus sham, # $p<0.05$ versus IgG control, n=4-8, data are presented as mean ± SEM.

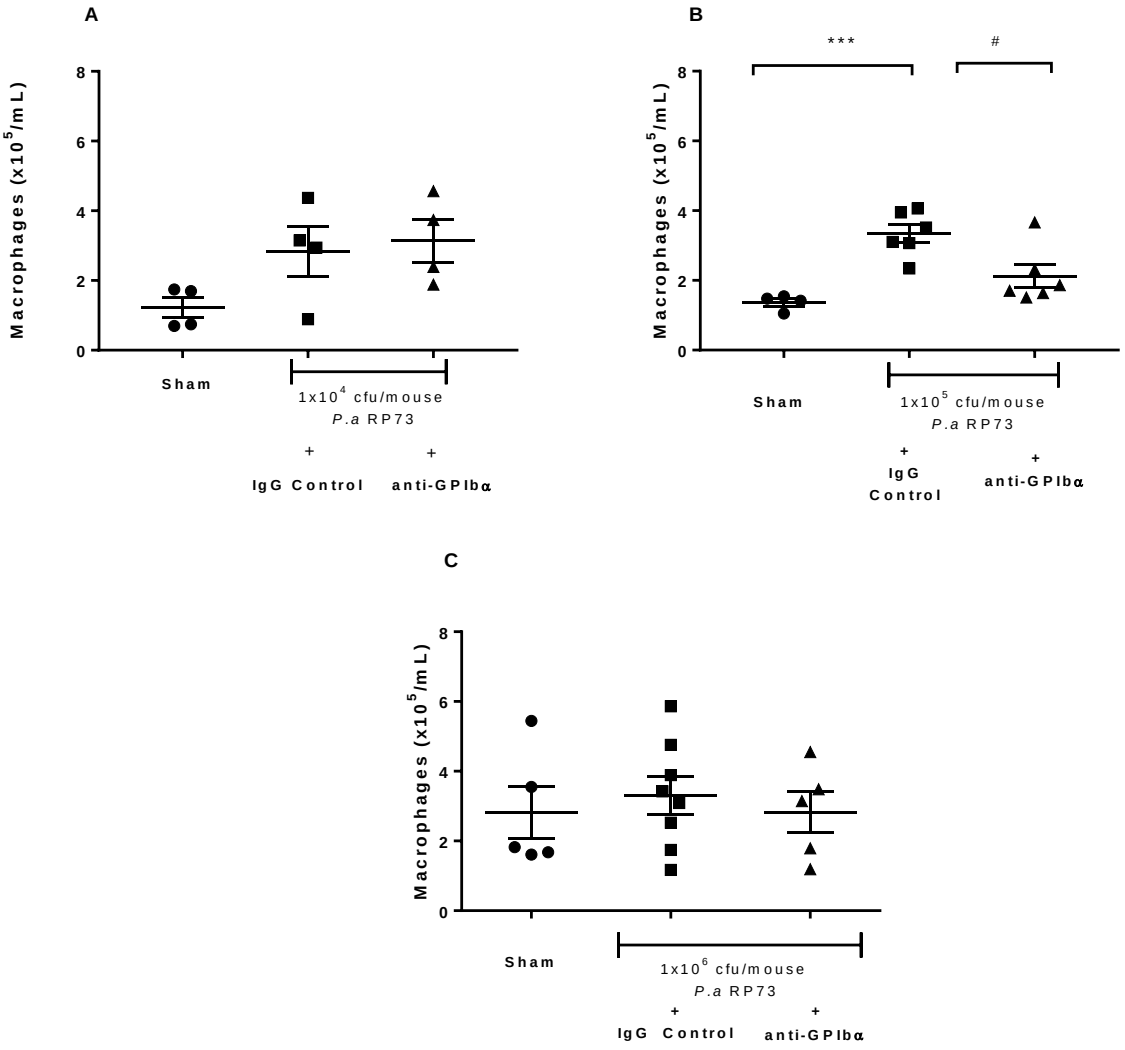

Figure 4.16 Effects of Experimentally Induced Platelet Depletion on Pulmonary Macrophage Recruitment in a Thrombocytopenic Model of Pulmonary Infection with *P.aeruginosa* strain RP73

Mice were treated with either 1mg/kg of anti-GPIbα platelet depleting antibody or IgG control antibody 24 hours prior to infection with either sham or (**A**) $1x10^4$, (**B**) $1x10^5$ or (**C**) $1x10^6$ cfu/mouse *P.aeruginosa* strain RP73 embedded agar beads. At 24 h.p.i, a BAL of the lungs was performed for macrophage quantification. One-way ANOVA and Bonferroni's multiple comparisons post hoc test, *** $p<0.001$ versus sham, # $p<0.05$ versus IgG control, n=4-8, data are presented as mean ± SEM.

4.6.8 Investigating the Effect of Experimentally Induced Platelet Depletion on Mortality

Previous studies, using experimental models of bacterial derived sepsis, have demonstrated experimentally induced platelet depletion enhances mortality (de Stoppelaar, 2014). Therefore, we investigated the effect of experimentally induced platelet depletion on mortality, following infection with *P.aeruginosa* strain RP73.

No significant differences in mortality were observed following infection with the lowest inoculum level of $1x10^4$ cfu/mouse RP73, in groups experimentally depleted of platelets and in mice with normal circulating platelet levels (10^4 log cfu + anti-GPIbα: 0%, versus 10^4 log cfu + IgG: 0%, **Figure 4.17A**).

Following infection with the intermediate inoculum level of $1x10^5$ cfu/mouse RP73, a significant increase of 20% was observed in mortality rate in mice depleted of platelets, when compared to mice with normal circulating platelet levels (10^5 log cfu + anti-GPIbα: 20%, versus 10^5 log cfu + IgG: 0%, **Figure 4.17B**, $p<0.05$).

In mice infected with the highest inoculum level of $1x10^6$ cfu/mouse RP73 and experimentally depleted of platelets, a significant increase of 40% was observed in mortality rate at 24 h.p.i, when compared to mice with normal circulating platelet levels (10^6 log cfu + anti-GPIbα: 40%, versus 10^6 log cfu + IgG: 0%, **Figure 4.17C**, $p<0.05$).

The 40% mortality rate observed following experimental depletion of platelets and infection with $1x10^6$ cfu/mouse demonstrated a more severe pulmonary infection and was associated with a worsened phenotype. Therefore, in order to refine and reduce severity of the model, the optimum level of inoculum for future experimentally induced platelet depletion studies was determined to be $1x10^5$ cfu/mouse. This level of inoculum was associated with a reduced

mortality rate when compared to that observed with the $1x10^6$ cfu/mouse inoculum level, and the pulmonary infection was well established unlike that observed with the $1x10^4$ cfu/mouse inoculum level.

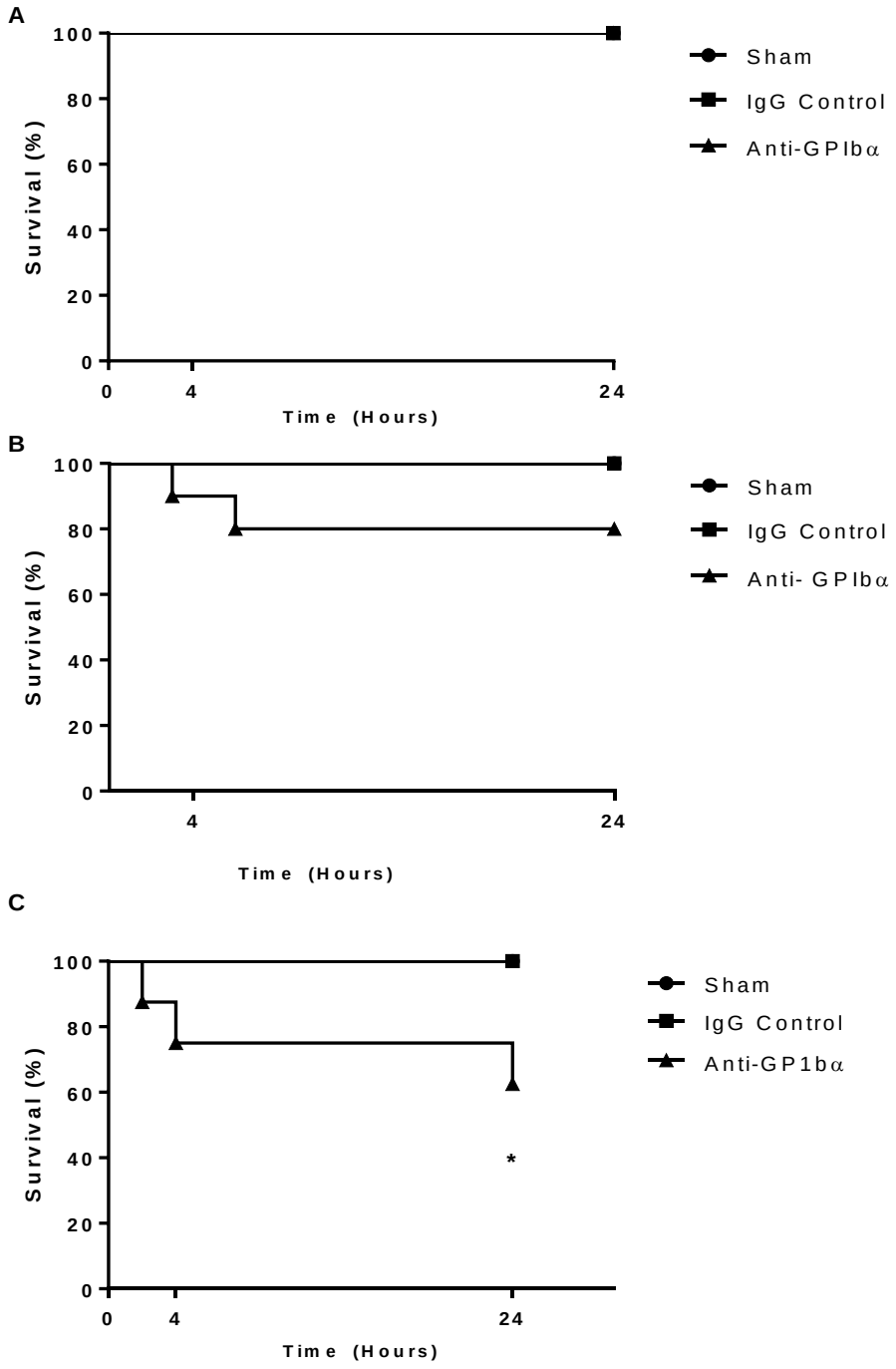

Figure 4.17 Effects of Experimentally Induced Platelet Depletion on Mortality in a Thrombocytopenic Model of Pulmonary Infection with *P.aeruginosa* strain RP73

Mice were treated with either 1mg/kg of anti-GPIbα platelet depleting antibody or IgG control antibody 24 hours prior to infection with either sham or (**A**) $1x10^4$, (**B**) $1x10^5$ or (**C**) $1x10^6$ cfu/mouse *P.aeruginosa* strain RP73 embedded agar beads. Survival numbers were collected following infection. Mantel-Cox test, * $p<0.05$ versus IgG control, n=4-10. Survival plotted as survived= 0, dead= 1.

4.6.9 Investigating the Effect of Experimentally Induced Platelet Depletion on Cause of Death

The previous findings in this study suggested that experimental induced platelet depletion coverts the non-lethal, localised infection to one with a more severe phenotype, displaying systemic infection and increased mortality. Furthermore, it has previously been demonstrated that normal circulating platelet numbers are requisite in protecting against organ damage during gram-negative sepsis (de Stoppelaar, 2014). For this reason, core body temperatures and biochemical markers of metabolic acidosis were monitored in sham controls and $1x10^5$ cfu/mouse infected, IgG control treated and platelet depleted animals, to ascertain possible causes of death in these mice.

The results obtained demonstrated that there was no significant difference in the percentage loss in body temperature between the sham controls (-0.82±0.71%), $1x10^5$ cfu/mouse RP73 infected, with normal circulating platelet levels (0.84±0.74%) and $1x10^5$ cfu/mouse RP73 infected and anti-GPIbα platelet depleted (-0.11 ± 0.76 %) groups (**Figure 4.18**).

Subtle increases in biochemical markers of metabolic acidosis were observed following infection with $1x10^5$ cfu/mouse RP73 in animals depleted of circulating platelets, when compared to the IgG control treated animals, as measured by slight changes in urea (10^5 log cfu + IgG control: 5.72±0.37 mmol/L, versus 10^5 log cfu + anti-GPIbα: 9.08±3.32 mmol/L, **Figure 4.19**), pH (10^5 log cfu + IgG control: 7.15±0.03, versus 10^5 log cfu + anti-GPIbα: 7.07±0.04, **Figure 4.19**), base excess (10^5 log cfu + IgG control: -12.88±0.91 mmol/L, versus 10^5 log cfu + anti-GPIbα: -16.61±1.49 mmol/L, **Figure 4.19**), Hydrogen Carbonate ($HCO3^-$) (10^5 log cfu + IgG control: 16.58±0.87 mmol/L, versus 10^5 log cfu + anti-GPIbα: 12.91±1.04 mmol/L, **Figure 4.19**) and partial pressure of carbon dioxide (PCO2) (10^5 log cfu + IgG control: 44.37±1.38 mmHg,

versus 10^5 log cfu + anti-GPIbα: 41.15±3.07 mmHg, **Figure 4.19**). These data suggest markers consistent with metabolic acidosis as has previously been published (Sand et al., 2015).

These data obtained for this experiment, suggest that the platelet depleting anti-GPIbα antibody caused a decrease in both Haematocrit (Hct) (Hct: Sham + IgG control: 38.0±2.0% packed cell volume (PCV), versus sham + anti-GPIbα: 19.5±3.18 %PCV and 10^5 log cfu + IgG control: 37.67±1.20 %PCV, versus 10^5 log cfu + anti-GPIbα: 19.0±1.15 %PCV, **Figure 4.19**) and Haemoglobin (Hb) (Hb: Sham + IgG control: 12.93±0.68 g/dL, versus sham + anti-GPIbα: 6.65±1.10 g/dL and 10^5 log cfu + IgG control: 12.80±0.41 g/dL, versus 10^5 log cfu + anti-GPIbα: 6.45±0.39g/dL, **Figure 4.19**) when compared to IgG control treated animals.

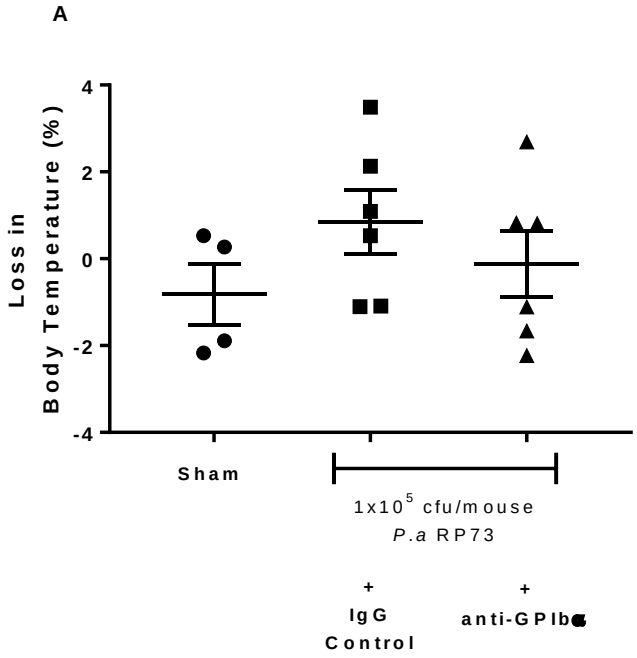

Figure 4.18 Effects of Experimentally Induced Platelet Depletion on Change in Temperature in a Thrombocytopenic Model of Pulmonary Infection with *P.aeruginosa* strain RP73

Mice were treated with either 1mg/kg of anti-GPIbα platelet depleting antibody or IgG control antibody 24 hours prior to infection with either sham or $1x10^5$ cfu/mouse *P.aeruginosa* strain RP73 embedded agar beads. Core body temperatures were recorded prior to and post infection and the percentage loss in body temperature was calculated. One-way ANOVA and Bonferroni's multiple comparisons post hoc test, $p>0.05$ versus sham, $p>0.05$ versus IgG control, n=4-6, data are presented as mean ± SEM.

	Sham IgG Control	Sham anti-GpIbα	*P.a* RP73 IgG Control	*P.a* RP73 anti-GpIbα
Urea, mmol/L	5.6 ± 0.38	5.80 ± 0.05	5.72 ± 0.37	9.08 ± 3.32
pH	7.14 ± 0.03	7.12± 0.01	7.15 ± 0.03	7.07 ± 0.04
Base Excess, mmol/L	-12.0 ± 2.35	-14.03 ± 0.58	-12.88 ± 0.91	-16.61 ± 1.49
$HCO3^-$, mmol/L	16.38 ± 1.92	14.13 ± 0.58	16.58 ± 0.87	12.91 ± 1.04
Glucose, mmol/L	12.45 ± 1.38	12.50 ± 1.01	11.27 ± 0.71	10.25 ± 0.79
Na^+, mmol/L	146.0 ± 0.41	145.67 ± 0.58	145.67 ± 0.61	141.33 ± 0.84
K^+, mmol/L	3.83 ± 0.34	4.43 ± 0.10	4.38 ± 0.30	4.93 ± 0.51
Cl^-, mmol/L	116.0 ± 1.78	119.67 ± 0.76	115.83 ± 1.08	121.67 ± 1.43
PCO2, mmHg	49.18 ± 2.71	44.37 ± 1.38	48.90 ± 2.56	41.15 ± 3.07
TCO2, mmol/L	18.50 ± 2.10	15.33 ± 0.76	18.16 ± 0.98	14.33 ± 1.24
AnGAP, mmol/L	17.25 ± 0.85	16.67 ± 0.58	17.33 ± 0.56	15.50 ± 0.72
Hct, %PCV	38.0 ± 2.0	19.5 ± 3.18 ****	37.67 ± 1.20	19.00 ± 1.15 ****
Hb, g/dL	12.93 ± 0.68	6.65 ± 1.10 ***	12.80 ± 0.41	6.45 ± 0.39 ****

Figure 4.19 Effects of Experimentally Induced Platelet Depletion on Changes in Biochemical Markers of Metabolic Acidosis in a Thrombocytopenic Model of Pulmonary Infection with *P.aeruginosa* strain RP73

Mice were treated with either 1mg/kg of anti-GPIbα platelet depleting antibody or IgG control antibody 24 hours prior to infection with either sham or $1x10^5$ cfu/mouse *P.aeruginosa* strain RP73 embedded agar beads. Blood was taken via cardiac puncture, transferred to EC8+ blood analyser cartridges and processed using a handheld i-STAT blood analyser. $HCO3^-$ (Hydrogen Carbonate), PCO2 (partial pressure carbon dioxide), TCO2 (total carbon dioxide), AnGAP (Anion Gap), Hct (Haematocrit), Hb (Haemoglobin), PCV (packed cell volume). One-way ANOVA and Bonferroni's multiple comparisons post hoc test ***p<0.001 ****p<0.0001 versus IgG control, n=4-6, data are presented as mean ± SEM.

4.6.10 Investigating the Effect of Experimentally Induced Thrombocytopenia on Pulmonary Alveolar Integrity

Experiments were performed to investigate the effect of experimentally induced thrombocytopenia on pulmonary alveolar integrity, following infection with *P.aeruginosa* strain RP73. Results demonstrated a significant increase in Evans Blue extravasated from lung tissue in RP73 infected mice depleted of circulating platelets, when compared to sham mice depleted of circulating platelets (sham + anti-GPIbα: 675.4±173.3 ng Evans Blue/ mg lung tissue, versus 10^5 RP73 + anti-GPIbα: 3737.0±742.3 ng Evans Blue/ mg lung tissue, $p<0.001$, **Figure 4.20**). Furthermore, results demonstrated a significant increase in Evans Blue extravasated from lung tissue in RP73 infected mice depleted of circulating platelets, when compared to RP73 infected mice with normal circulating platelet numbers (10^5 RP73 + anti-GPIbα: 944.5±110.6 ng Evans Blue/ mg lung tissue, versus 10^5 RP73 + anti-GPIbα: 3737.0±742.3 ng Evans Blue/ mg lung tissue, $p<0.01$, **Figure 4.20**).

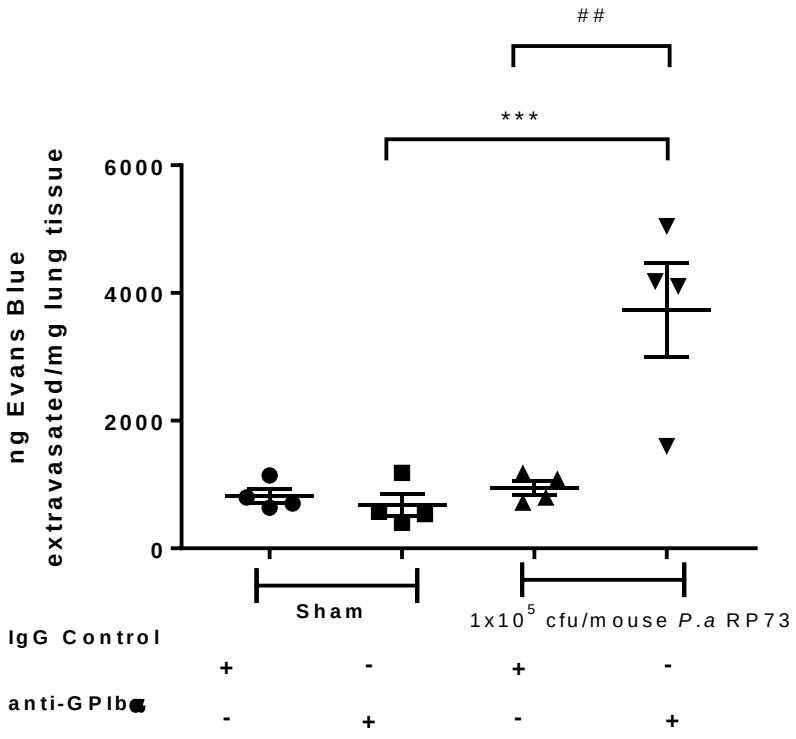

Figure 4.20 Effects of Experimentally Induced Thrombocytopenia on Pulmonary Alveolar Integrity in a Thrombocytopenic Model of Pulmonary Infection with *P.aeruginosa* strain RP73

Mice were treated with either 1mg/kg of anti-GPIbα platelet depleting antibody or IgG control antibody 24 hours prior to infection with either sham or $1x10^5$ cfu/mouse *P.aeruginosa* strain RP73 embedded agar beads. At 23 h.p.i mice were administered 0.5% Evans Blue (*i.v.)*. Lungs were removed, weighed and added to 500µL Formamide, which was subsequently incubated for 24 hours at 65^{o}C. 24 hours post incubation absorbance values were measured at 620nm and a standard curve was used to calculate nanograms (ng) Evans Blue dye per mg lung tissue. One-way ANOVA and Bonferroni's multiple comparisons post hoc test, *** $p<0.001$ versus sham + anti-GPIbα, ## $p<0.01$ versus RP73 + IgG control, n=4 data are presented as mean ± SEM.

4.7 Establishing a Thrombocytopenic Model of Pulmonary Infection with MRSA strain USA300

Having established a thrombocytopenic model of pulmonary infection with the gram-negative *P.aeruginosa* strain RP73, we aimed to establish the model with the gram-positive MRSA strain USA300, to determine whether my findings could be reproduced with a different bacterial species. The optimum level of inoculum for experimentally induced platelet depletion studies with *P.aeruginosa* strain RP73 was determined to be $1x10^5$ cfu/mouse therefore this level of inoculum was used to establish a thrombocytopenic model of pulmonary infection with the gram-positive MRSA strain USA300.

4.7.1 Investigating the Effect of Experimentally Induced Platelet Depletion on the Circulating Platelet Count

In order to experimentally induce platelet depletion, mice were treated *(i.m)* with either 1mg/kg anti-GPIbα platelet depleting antibody or IgG control antibody, 24 hours prior to infection with $1x10^5$ cfu/mouse MRSA strain USA300. Infection with $1x10^5$ cfu/mouse reduced circulating platelet count when compared to sham controls, although these data did not reach statistical significance (MRSA + IgG: $9.18\pm0.60x10^8$ platelets/mL, versus sham: $10.30\pm1.05x10^8$ platelets/mL, **Figure 4.21**).

The anti-GPIbα platelet depleting antibody significantly reduced circulating platelets by ~96%, compared to the infected IgG control treated animals (10^5 log cfu + anti-GPIbα: $0.37\pm0.03x10^8$ platelets/mL, versus IgG control: $9.18\pm0.60x10^8$ platelets/mL, **Figure 4.21**, $p<0.0001$).

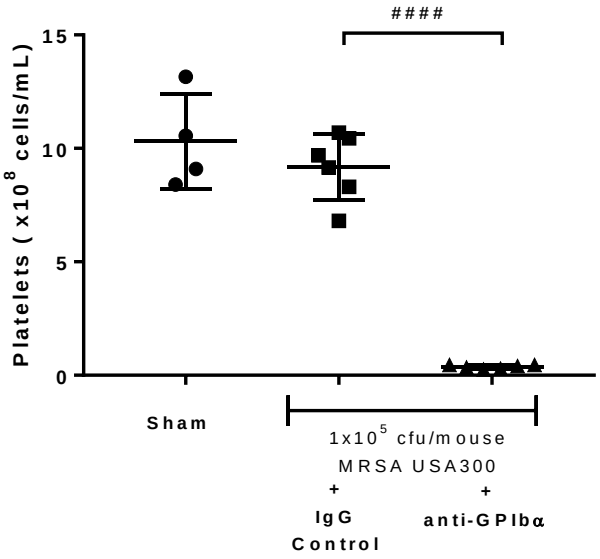

Figure 4.21 Effects of Experimentally Induced Platelet Depletion on the Circulating Platelet Count in a Thrombocytopenic Model of Pulmonary Infection with MRSA strain USA300

Mice were treated with either 1mg/kg of anti-GPIbα platelet depleting antibody or IgG control antibody 24 hours prior to infection with either sham or $1x10^5$ cfu/mouse MRSA strain USA300 embedded agar beads. At 24 h.p.i blood was taken via cardiac puncture and the circulating platelet count was quantified using an improved neubauer haemocytometer. One-way ANOVA and Bonferroni's multiple comparisons post hoc test, #### $p<0.0001$ versus IgG control, n=4-6, data are presented as mean ± SEM.

4.7.2 Investigating the Effect of Experimentally Induced Platelet Depletion on Weight Loss

The body weights of sham and infected, IgG control treated and platelet depleted animals were recorded pre and post infection. $1x10^5$ cfu/mouse USA300 infected, IgG control treated animals demonstrated a slight increase in weight loss when compared to the sham controls (sham: -0.54±0.23%, 10^5 log cfu + IgG control: 0.15±0.61 %, **Figure 4.22**), although this did not reach statistical significance. In addition, following infection with $1x10^5$ cfu/mouse USA300, animals depleted of circulating platelets showed a further increase in weight loss compared to the infected IgG control treated animals (10^5 log cfu+ IgG control: 0.15±0.61%, 10^5 log cfu

+ anti-GPIbα: 1.80±0.46%, **Figure 4.22**), although these data also did not reach statistical significance.

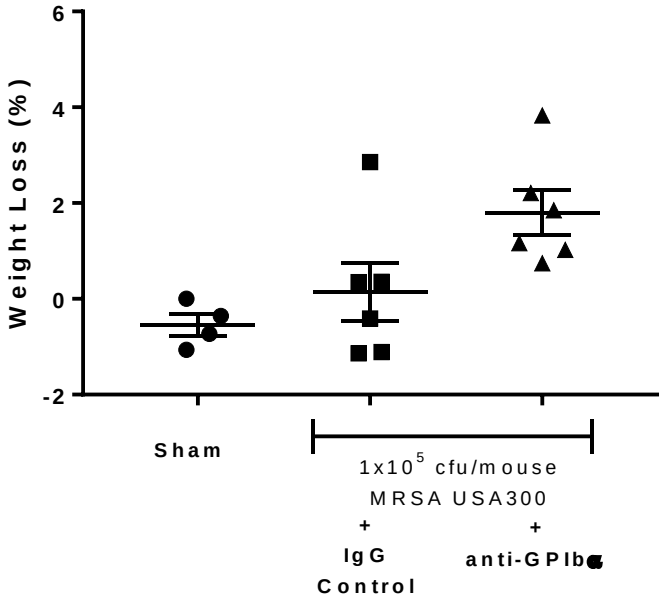

Figure 4.22 Effects of Experimentally Induced Platelet Depletion on Weight Loss in a Thrombocytopenic Model of Pulmonary Infection with MRSA strain USA300

Mice were treated with either 1mg/kg of anti-GPIbα platelet depleting antibody or IgG control antibody 24 hours prior to infection with either sham or $1x10^5$ cfu/mouse MRSA strain USA300 embedded agar beads. Body weights were recorded prior to and post infection and percentage weight loss calculated. One-way ANOVA and Bonferroni's multiple comparisons post hoc test, $p>0.05$ versus sham, $p>0.05$ versus IgG control, n=4-6, data are presented as mean ± SEM.

4.7.3 Investigating the Effect of Platelet Depletion on Pulmonary Haemorrhage

In order to investigate whether administration of the platelet depleting anti-GPIbα antibody has any effect on pulmonary haemorrhage following infection with MRSA, red blood cells present in BAL fluid were qualitatively analysed following administration of either the IgG control or anti-GPIbα antibodies.

Results indicated that the platelet depleting anti-GPIbα antibody appeared to increase pulmonary haemorrhage, as indicated by the red colouration of BAL samples in both the sham and $1x10^5$ cfu/mouse MRSA infected animals, compared to the infected IgG controls (**Figure 4.23**).

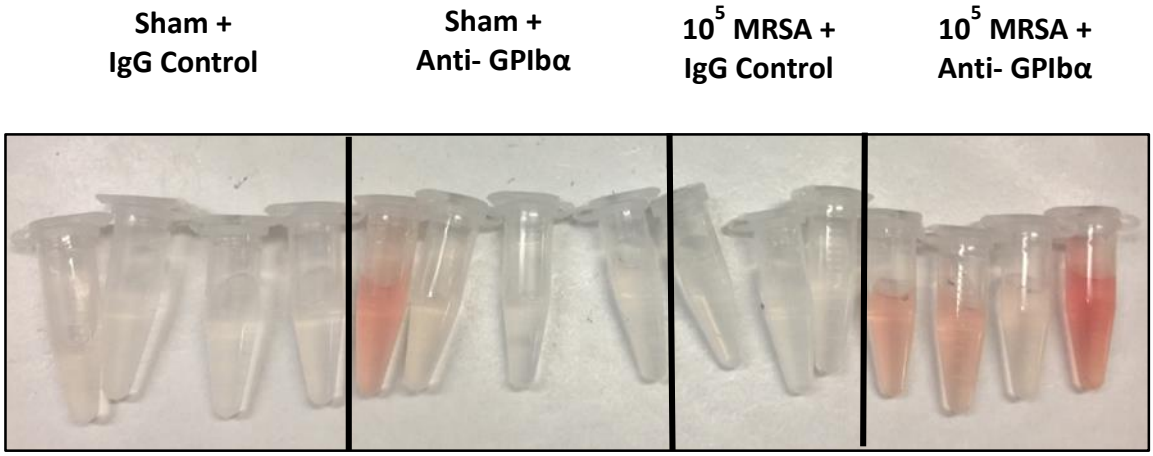

Figure 4.23 Effects of the Platelet Depleting anti-GPIbα Antibody on Pulmonary Haemorrhage in a Thrombocytopenic Model of Pulmonary Infection with MRSA strain USA300

Mice were treated with either 1mg/kg of anti-GPIbα platelet depleting antibody or IgG control antibody 24 hours prior to infection with either sham or $1x10^5$ cfu/mouse MRSA strain USA300 embedded agar beads. At 24 h.p.i, a BAL of the lungs was performed and the presence of red blood cells in the lavage was qualitatively analysed. n=3-4, data are presented as mean ± SEM.

4.7.4 Investigating the Effect of Experimentally Induced Platelet Depletion on Pulmonary Bacterial Load

Mice were treated with either IgG control antibody or the platelet depleting anti-GPIbα antibody and infected with $1x10^5$ cfu/mouse USA300 to determine the effect of platelet depletion on pulmonary bacterial load. 24 hours following infection, mice inoculated with sham agar beads demonstrated no evidence of pulmonary bacterial infection (0.0±0.0 log cfu, **Figure 4.24**). In contrast, mice infected with $1x10^5$ cfu/mouse USA300 and treated with an IgG control antibody, demonstrated a significant increase in pulmonary bacterial load when compared to sham controls (10^5 log cfu + IgG: 3.01±0.23 log cfu, versus sham: 0.0±0.0 log cfu, $p<0.0001$, **Figure 4.24**). This was further increased in mice infected with $1x10^5$ cfu/mouse USA3000 depleted of circulating platelets, with a significant increase of approximately 0.9 logs, when compared to the infected IgG controls (10^5 log cfu + anti-GPIbα: 3.92±0.29 log cfu, versus 10^5 log cfu + IgG: 3.01±0.23 log cfu, $p<0.05$, **Figure 4.24**).

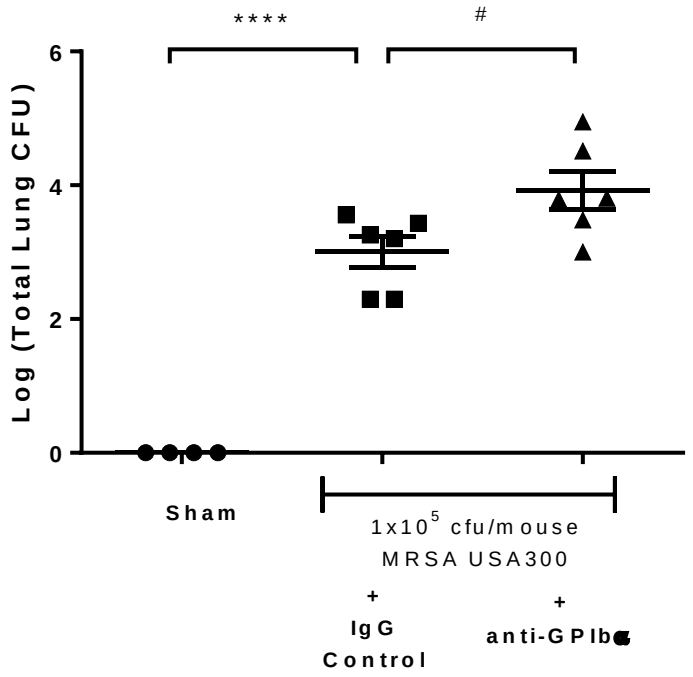

Figure 4.24 Effects of Experimentally Induced Platelet Depletion on Pulmonary Bacterial Load in a Thrombocytopenic Model of Pulmonary Infection with MRSA strain USA300

Mice were treated with either 1mg/kg of an anti-GPIbα platelet depleting antibody or IgG control antibody 24 hours prior to infection with either sham or $1x10^5$ cfu/mouse MRSA strain USA300 embedded agar beads. At 24 h.p.i, lungs were aseptically removed, homogenised and plated for quantification of bacterial load. One-way ANOVA and Bonferroni's multiple comparisons post hoc test, **** $p<0.0001$ versus sham, # $p<0.05$ versus IgG control, n=4-6, data are presented as mean ± SEM.

4.7.5 Investigating the Effect of Experimentally Induced Platelet Depletion on Bacterial Dissemination to the Kidney and Spleen

In order to investigate whether experimentally induced platelet depletion induced bacterial dissemination from the lungs to other peripheral organs, the cfu content of the kidney and spleen was quantified.

At 24 h.p.i, no evidence of bacterial dissemination to the kidney was observed in sham controls (sham: 0.0±0.0 log cfu, **Figure 4.25A**). Following infection with $1x10^5$ cfu/mouse USA300 and in mice depleted of circulating platelets, an incidence of bacterial dissemination to the kidney was observed, although these data did not reach statistical significance when compared to the infected IgG controls (10^5 log cfu + anti-GPIbα: 1.98±0.89 log cfu, versus 10^5 log cfu + IgG: 0.72±0.45 log cfu, **Figure 4.25A**).

No evidence of bacterial dissemination to the spleen was observed in shams (sham: 0.0±0.0 log cfu, **Figure 4.25B**), although there was a significant increase in bacterial dissemination to the spleen in infected animals depleted of circulating platelets (10^5 log cfu + anti-GPIbα: 3.00±0.34 log cfu, versus 10^5 log cfu + IgG: 1.40±0.63 log cfu, $p<0.05$, **Figure 4.25B**).

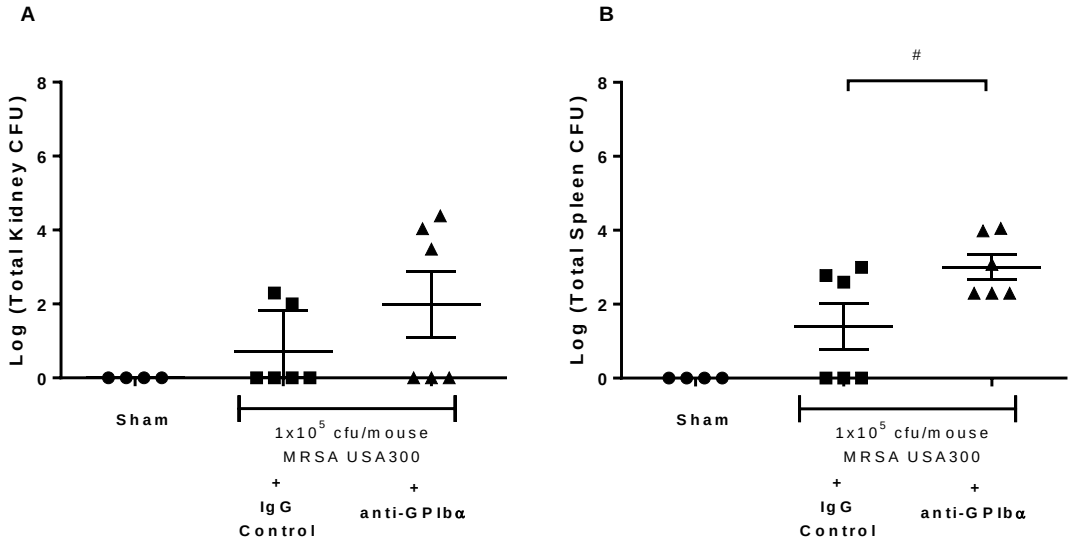

Figure 4.25 Effects of Experimentally Induced Platelet Depletion on Bacterial Dissemination to the Kidney and Spleen in a Thrombocytopenic Model of Pulmonary Infection with MRSA strain USA300

Mice were treated with either 1mg/kg of anti-GPIbα platelet depleting antibody or IgG control antibody 24 hours prior to infection with either sham or $1x10^5$ cfu/mouse MRSA strain USA300 embedded agar beads. At 24 h.p.i, the kidney and spleen were aseptically removed, homogenised and plated for quantification of bacterial load. One-way ANOVA and Bonferroni's multiple comparisons post hoc test, # $p<0.05$ versus IgG control, n=4-6, data are presented as mean ± SEM.

4.7.6 Investigating the Effect of Experimentally Induced Platelet Depletion on Pulmonary Leukocyte Recruitment

As gram-negative bacteria induced leukocyte recruitment was platelet dependent, we sought to investigate whether experimentally induced platelet depletion had any effect on pulmonary leukocyte recruitment following infection with the gram-positive MRSA strain USA300.

Infection with $1x10^5$ cfu/mouse, increased pulmonary total cell recruitment when compared to sham controls, although this data did not reach statistical significance (10^5 log cfu + IgG: $2.23\pm0.38x10^5$ cells/mL, versus sham: $1.60\pm0.40x10^5$ cells/mL, **Figure 4.26A**). For animals depleted of circulating platelets, there was no significant effect on pulmonary total cell recruitment when compared to mice with normal circulating platelet levels (10^5 log cfu + anti-GPIbα: $2.73\pm0.22x10^5$ cells/mL, versus 10^5 log cfu + IgG: $2.23\pm0.38x10^5$ cells/mL, **Figure 4.26A**).

Infection with $1x10^5$ cfu/mouse significantly elevated pulmonary neutrophil recruitment when compared to sham controls (10^5 log cfu + IgG: $0.42\pm0.04x10^5$ cells/mL, versus sham: $0.0\pm0.0x10^5$ cells/mL, **Figure 4.26B**, $p<0.001$), which was significantly attenuated in platelet depleted mice (10^5 log cfu + anti-GPIbα: $0.29\pm0.03x10^5$ cells/mL, versus 10^5 log cfu + IgG: $0.42\pm0.04x10^5$ cells/mL, $p<0.05$, **Figure 4.26B**), further highlighting the importance of platelets in pulmonary leukocyte recruitment.

No significant effects were observed in platelet depleted mice on macrophage (10^5 log cfu + IgG: $1.84\pm0.42x10^5$ cells/mL, versus 10^5 log cfu + anti-GPIbα: $2.43\pm0.19x10^5$ cells/mL, **Figure 4.26C**) and lymphocyte numbers (10^5 log cfu + IgG: $0.0\pm0.0x10^5$ cells/mL, versus 10^5 log cfu + anti-GPIbα: $0.0\pm0.0x10^5$ cells/mL, **Figure 4.26C**), when compared to IgG control treated mice.

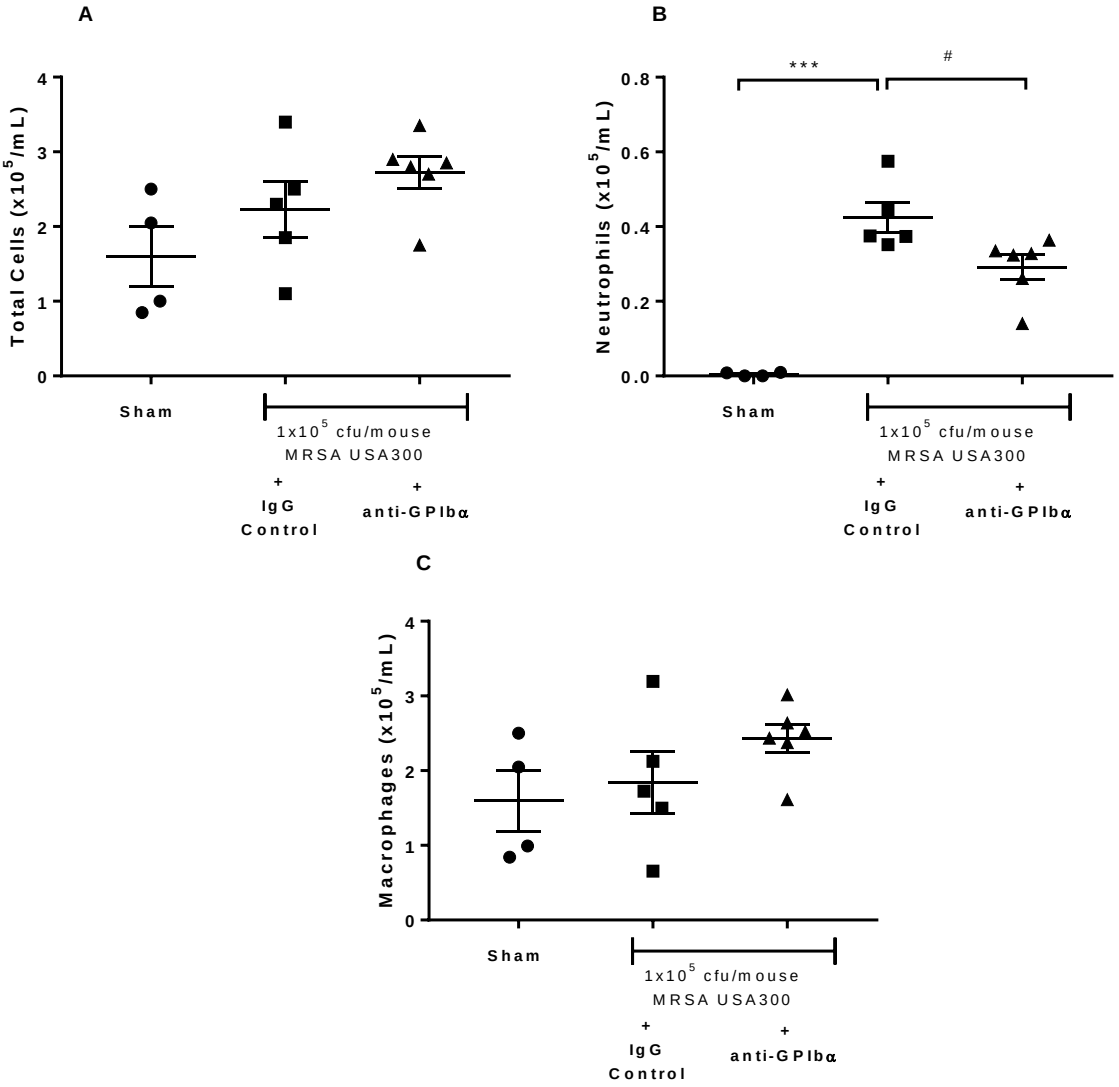

Figure 4.26 Effects of Experimentally Induced Platelet Depletion on Pulmonary Leukocyte Recruitment in a Thrombocytopenic Model of Pulmonary Infection with MRSA strain USA300

Mice were treated with either 1mg/kg of anti-GPIbα platelet depleting antibody or IgG control antibody 24 hours prior to infection with either sham or $1x10^5$ cfu/mouse MRSA strain USA300 embedded agar beads. At 24 h.p.i, a BAL of the lungs was performed for total and differential leukocyte quantification. (**A**) Total cells, (**B**) Neutrophils, (**C**) Macrophages. One-way ANOVA and Bonferroni's multiple comparisons post hoc test, *** $p<0.001$ versus sham, # $p<0.05$ versus IgG control, n=4-6, data are presented as mean ± SEM.

4.7.7 Investigating the Effect of Experimentally Induced Platelet Depletion on Mortality

Having demonstrated that depletion of circulating platelets enhances mortality following infection with *P.aeruginosa* strain RP73, we investigated whether this phenomenon was replicated following infection with MRSA strain USA300.

In mice infected with $1x10^5$ cfu/mouse USA300 and experimentally depleted of platelets, we observed no significant difference in mortality at 24 h.p.i (0%) when compared to the infected IgG controls (0%).

4.7.8 Investigating the Effect of Experimentally Induced Platelet Depletion on Changes in Biochemical Markers of Metabolic Acidosis

Results obtained in section 4.6.9 demonstrated subtle increases in biochemical markers of metabolic acidosis following infection with $1x10^5$ cfu/mouse *P.aeruginosa* RP73 in platelet depleted mice. Therefore, we measured changes in biochemical markers of metabolic acidosis following infection with MRSA strain USA300.

Results demonstrated subtle increases in biochemical markers of metabolic acidosis following infection with $1x10^5$ cfu/mouse MRSA strain USA300 in mice depleted of platelets, when compared to the IgG control treated animals, as measured by slight changes in base excess (10^5 log cfu + IgG control: -13.17±0.70 mmol/L, 10^5 log cfu + anti-GPIbα: -15.53±0.65 mmol/L, **Figure 4.27**), $HCO3^-$ (10^5 log cfu + IgG control: 16.65±0.57 mmol/L, 10^5 log cfu + anti-GPIbα: 13.62±0.59 mmol/L, **Figure 4.27**) and PCO2 (10^5 log cfu + IgG control: 55.25±3.99 mmHg, 10^5 log cfu + anti-GPIbα: 48.48±3.11 mmHg, **Figure 4.27**).

In contrast to the data obtained in section 4.6.9, which suggested that the platelet depleting anti-GPIbα antibody caused a decrease in both Hct and Hb, the results from this experiment suggested platelet depletion had no significant decrease in Hct (Hct: Sham + IgG control: 41.0±1.83 %PCV, versus sham + anti-GPIbα: 19.5±3.18 %PCV and 10^5 log cfu + IgG control: 37.67±1.20 %PCV, versus 10^5 log cfu + anti-GPIbα: 38.5±1.83 %PCV, **Figure 4.27**) and Hb (Hb: Sham + IgG control: 13.95±0.61 g/dL, versus sham + anti-GPIbα: 13.08 ± 0.69 g/dL and 10^5 log cfu + IgG control: 12.70±0.66 g/dL, 10^5 log cfu + anti-GPIbα: 10.32±1.01 g/dL, **Figure 4.27**) when compared to the IgG controls.

In order to investigate these results further, naïve mice were administered either IgG control or platelet depleting anti- GPIbα antibody and the effects of platelet depletion on Hct and Hb were determined at 24 hours post treatment. The results from this experiment further support that platelet depletion had no significant decrease in Hct (Hct: IgG control: 39.5±1.50 %PCV, versus anti-GPIbα: 40.5±3.50 %PCV) and Hb (Hb: IgG control: 13.25±0.65 g/dL, versus anti-GPIbα: 13.80±1.20 g/dL), when compared to IgG controls.

	Sham IgG Control	Sham anti-GpIbα	MRSA USA300 IgG Control	MRSA USA300 anti-GpIbα
Urea, mmol/L	8.75 ± 0.51	8.23 ± 0.25	8.92 ± 0.44	7.5 ± 0.55
pH	7.08 ± 0.02	7.08 ± 0.03	7.09 ± 0.03	7.08 ± 0.01
Base Excess, mmol/L	**-12.25 ± 0.48**	**-14.75 ± 1.32**	**-13.17 ± 0.70**	**-15.53 ± 0.65**
$HCO3^-$, mmol/L	**17.88 ± 0.49**	**15.1 ± 1.02**	**16.65 ± 0.57**	**13.62 ± 0.59**
Glucose, mmol/L	14.6 ± 1.19	13.23 ± 0.42	12.62 ± 0.82	12.12 ± 0.30
Na^+, mmol/L	141.5 ± 0.5	140.8 ± 0.48	141.7 ± 0.49	141.8 ± 0.31
K^+, mmol/L	4.62 ± 0.53	4.66 ± 0.26	5.34 ± 0.37	5.23 ± 0.46
Cl^-, mmol/L	109.5 ± 0.29	111.8 ± 1.44	111.7 ± 0.95	113.3 ± 0.74
PCO2, mmHg	**60.4 ± 3.64**	**50.75 ± 2.02**	**55.25 ± 3.99**	**48.48 ± 3.11**
TCO2, mmol/L	19.75 ± 0.48	17.0 ± 1.08	18.5 ± 0.62	15.75 ± 0.81
AnGAP, mmol/L	18.75 ± 0.48	19.0 ± 0.41	18.33 ± 0.42	19.06 ± 0.50
Hct, %PCV	41.0 ± 1.83	38.5 ± 2.02	37.33 ± 1.96	30.33 ± 2.96
Hb, g/dL	13.95 ± 0.61	13.08 ± 0.69	12.7 ± 0.66	10.32 ± 1.01

Figure 4.27 Effects of Experimentally Induced Platelet Depletion on Changes in Biochemical Markers of Metabolic Acidosis in a Thrombocytopenic Model of Pulmonary Infection with MRSA strain USA300

Mice were treated with either 1mg/kg of anti-GPIbα platelet depleting antibody or IgG control antibody 24 hours prior to infection with either sham or $1x10^5$ cfu/mouse MRSA strain USA300 embedded agar beads. Blood was taken via cardiac puncture, transferred to EC8+ blood analyser cartridges and processed using a handheld i-STAT blood analyser. $HCO3^-$ (Hydrogen Carbonate), PCO2 (partial pressure carbon dioxide), TCO2 (total carbon dioxide), AnGAP (Anion Gap), Hct (Haematocrit), Hb (Haemoglobin), PCV (packed cell volume). n=4-6, data are presented as mean ± SEM.

4.8 Investigating the Mechanisms of Platelet Involvement in Infection

4.8.1 The Role of Platelet TLR4 in the Regulation of Pulmonary Infection

Platelets express functional TLRs, which participate in platelet responsiveness to bacterial components such as LPS, and are known to be involved in LPS mediated inflammation (Hoshino et al., 1999). We investigated whether platelet TLR4 was involved in inflammatory leukocyte recruitment in response to pulmonary infection. Male C57/BI6J wild type and TLR4 knockout mice were infected with $1x10^5$ cfu/mouse with *P.aeruginosa* strain RP73 and the effects on bacteria induced leukocyte recruitment and bacterial growth were determined.

Significant increases in pulmonary bacterial load were observed at 24 h.p.i, in both C57/BI6J wild type and TLR4 knockout mice, when compared with sham controls (10^5 log cfu + C57/BI6J wild type: 4.98±0.03 log cfu, 10^5 log cfu + TLR4 knockout: 4.74±0.25 log cfu and sham: 0.0±0.0 log cfu, $p<0.0001$, **Figure 4.28A**). However, TLR4 knockout did not induce a significant increase in pulmonary bacterial load when compared to C57/BI6J wild type mice (10^5 log cfu + C57/BI6J wild type: 4.98±0.03 log cfu, 10^5 log cfu + TLR4 knockout: 4.74±0.25 log cfu and sham: 0.0±0.0 log cfu, **Figure 4.28A**).

Infection of both C57/BI6J wild type and TLR4 knockout mice with $1x10^5$ cfu/mouse RP73 induced a significant increase in pulmonary total leukocyte recruitment, when compared to sham controls (10^5 log cfu + C57/BI6J wild type: $82.0±25.42x10^5$ cells/mL, versus sham + C57/BI6J wild type: $2.53±0.41x10^5$ cells/mL, and 10^5 log cfu + TLR4 knockout: $69.67±15.92x10^5$ cells/mL, versus sham + TLR4 knockout: $3.13±0.07x10^5$ cells/mL, **Figure 4.28B**). However, no significant difference in pulmonary total leukocyte recruitment was observed between infected C57/BI6J wild type and TLR4 knockout mice (10^5 log cfu + C57/BI6J wild type:

82.0±25.42x10^5 cells/mL, versus 10^5 log cfu + TLR4 knockout: 69.67±15.92x10^5 cells/mL, **Figure 4.28B**).

This pattern was reflected in neutrophils, where infection of C57/BI6J wild type and TLR4 knockout mice with 1x10^5 cfu/mouse RP73 increased pulmonary neutrophil recruitment when compared to sham controls (10^5 log cfu + C57/BI6J wild type: 76.70±24.94x10^5 cells/mL, versus sham + C57/BI6J wild type: 0.0±0.0x10^5 cells/mL, $p<0.05$ and 10^5 log cfu + TLR4 knockout: 57.16±16.18x10^5 cells/mL, versus sham + TLR4 knockout: 0.0±0.0x10^5 cells/mL, **Figure 4.28C**). Whilst a trend suggesting a decrease in neutrophil recruitment in infected TLR4 knockout mice was observed compared to C57/BI6J mice, this did not reach statistical significance (10^5 log cfu + C57/BI6J wild type: 76.70±24.94x10^5 cells/mL, versus 10^5 log cfu + TLR4 knockout: 57.16±16.18x10^5 cells/mL, **Figure 4.28C**).

Infection of TLR4 knockout mice with 1x10^5 cfu/mouse RP73 induced a significant increase in macrophage recruitment when compared to sham TLR4 knockout controls (10^5 log cfu + TLR4 knockout: 12.7±0.39x10^5 cells/mL, versus sham + TLR4 knockout: 2.03±0.80x10^5 cells/mL, $p<0.01$, **Figure 4.28D**). In addition, there was a significant increase in pulmonary macrophage recruitment in 1x10^5 cfu/mouse infected TLR4 knockout compared to C57/BI6J wild type mice (Macrophages: 10^5 log cfu + C57/BI6J wild type: 5.35±2.54x10^5 cells/mL, versus 10^5 log cfu + TLR4 knockout: 12.75±0.39x10^5 cells/mL, $p<0.05$, **Figure 4.28D**). No significant increase in pulmonary lymphocyte recruitment was observed in either wild type or TLR4 knockout mice, when compared to sham controls (Lymphocytes: 10^5 log cfu + C57/BI6J wild type: 0.0±0.0x10^5 cells/mL, versus sham + C57/BI6J wild type: 0.0±0.0x10^5 cells/mL and 10^5 log cfu + TLR4 knockout: 0.0±0.0x10^5 cells/mL, versus sham + TLR4 knockout: 0.0±0.0x10^5 cells/mL).

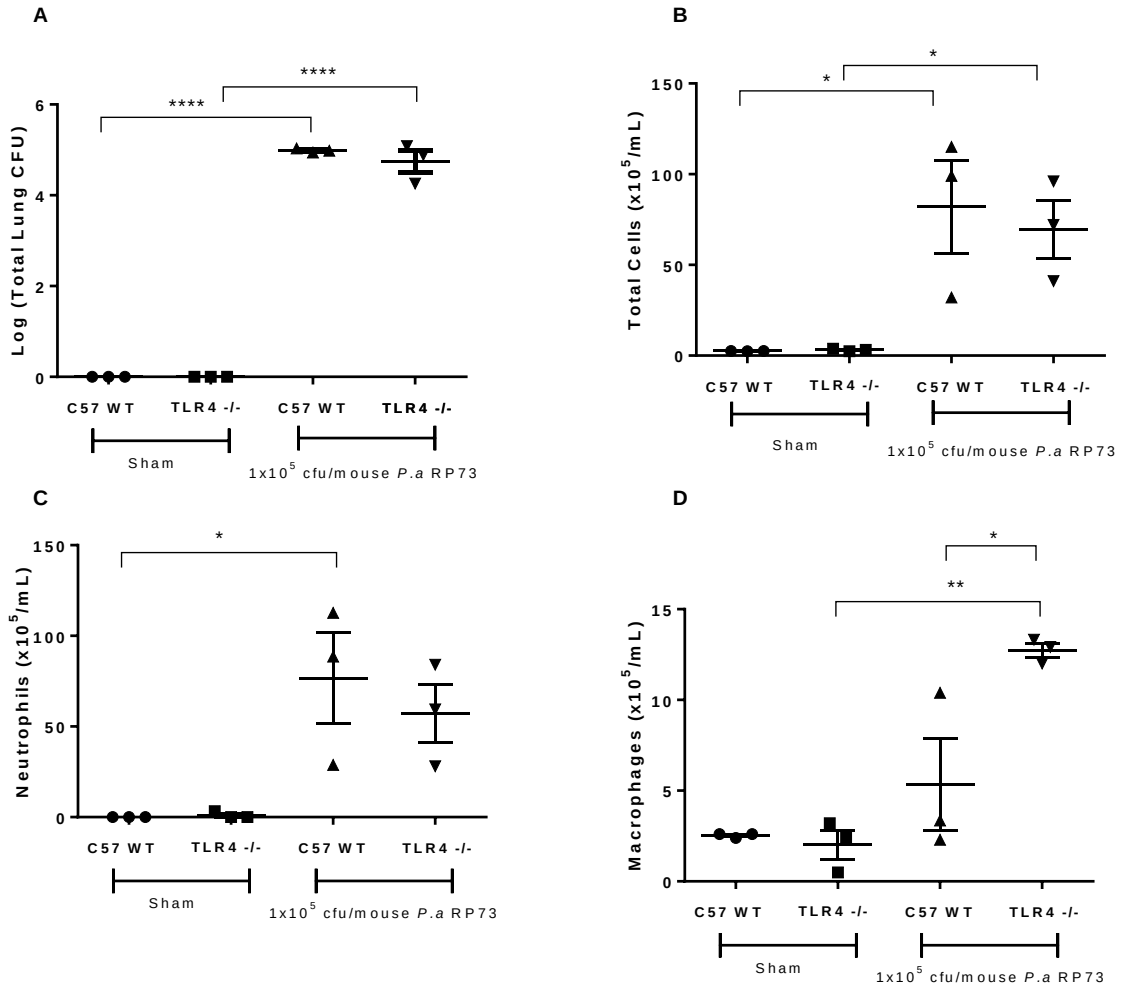

Figure 4.28 The Role of Platelet TLR4 in the Regulation of Pulmonary Infection with *P.aeruginosa* strain RP73

C57/BI6J wild type and TLR4 knockout mice were infected *(o.a)* with either sham or $1x10^5$ cfu/mouse *P.aeruginosa* strain RP73 embedded agar beads. A BAL of the lungs was performed for inflammatory cell quantification and lungs were aseptically removed, homogenised and plated for quantification of bacterial load at 24 h.p.i. Pulmonary Bacterial Load (**A**), Total Cells (**B**), Neutrophils (**C**) and Macrophages (**D**). One-way ANOVA and Bonferroni's multiple comparisons post hoc test, *p<0.05, ** p<0.01, **** p<0.0001 versus sham/wild type, n=3, data are presented as mean ± SEM.

4.8.1.1 PCR Analysis of Murine TLR4 cDNA

In order to confirm that the TLR4 knockout mice used in section 4.8.1 were indeed knockout mice, DNA was extracted from murine tails and PCR analysis was performed. The results obtained demonstrated that the DNA extracted from TLR4 knockout mice showed a band at >1000Kb (**Figure 4.29**), indicating that the gene knockout is present in these mice, whilst no band was present in the DNA extracted from C57/BI6J wild type mice, suggesting that these control mice did not contain the gene knockout.

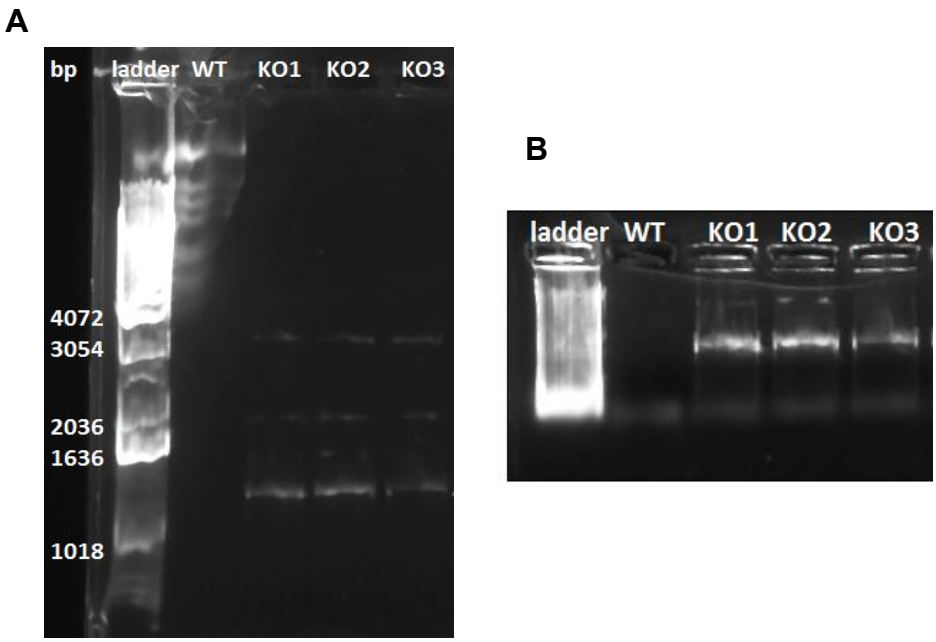

Figure 4.29 PCR Analysis of TLR4 Knockout and C57/BI6J Wild Type DNA

DNA was extracted from tail clips of TLR4 knockout and C57/BI6J wild type mice. PCR was performed on the samples using a PCR Reaction Kit (Sigma Aldrich R2648 20RXN) according to manufacturer's instructions. (**A**) Agarose gel for TLR4 knockout primers (**B**) Agarose gel for TLR4 knockout and C57/BI6J wild type mice.

4.8.2 The Role of Platelet Purinergic Receptors in the Regulation of Pulmonary Infection

As the worsened phenotype observed in platelet depleted mice was not reproduced in the TLR4 knockout mice, other potential platelet receptors involved in the regulation of pulmonary infection were investigated.

Previous work has demonstrated that allergen induced pulmonary leukocyte recruitment is dependent upon the purinergic receptor $P2Y_1$ (Amison et al., 2017). Furthermore, a protective role for the $P2Y_1$ receptor has been suggested following infection with *P.aeruginosa* (Geary et al., 2005). Therefore, the role of purines and purinergic receptors in the regulation of pulmonary infection was investigated.

4.8.2.1 Investigating the Effect of Apyrase Treatment on Circulating Platelet Count

Apyrase is a purine hydrolysing enzyme, which converts ATP and ADP into inactive AMP, thus preventing activation of the platelet purinergic receptors.

100 units/mL Apyrase was administered to mice 30 minutes prior to infection with $1x10^5$ cfu/mouse RP73 and the effect on the circulating platelet count was determined. Infection with $1x10^5$ cfu/mouse reduced circulating platelet count when compared to sham controls, although these data did not reach statistical significance (10^5 log cfu + vehicle: $6.19\pm0.28x10^8$ platelets/mL, versus sham: $7.00\pm0.28x10^8$ platelets/mL, **Figure 4.30**). Animals Infected and treated with Apyrase showed slightly increased circulating platelet counts when compared to vehicle controls, although these data also did not reach statistical significance (10^5 log cfu + vehicle: $6.19\pm0.28x10^8$ platelets/mL, versus 10^5 log cfu + Apyrase: $6.77\pm0.28x10^8$ platelets/mL, **Figure 4.30**).

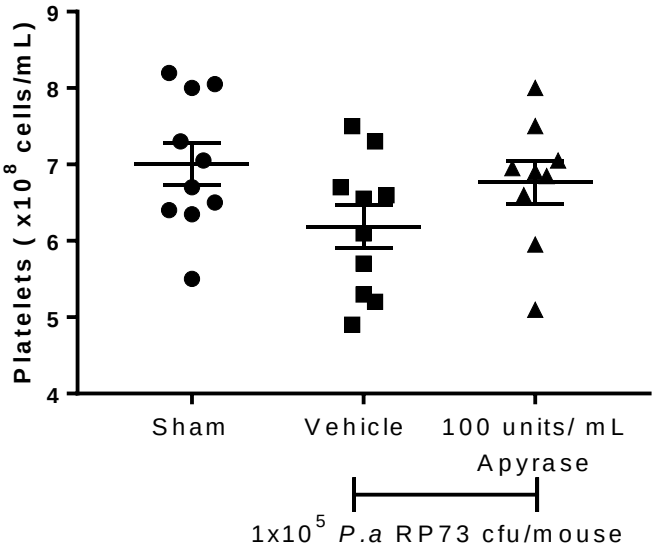

Figure 4.30 Effects of Apyrase on Circulating Platelet Count in a Murine Model of Pulmonary Infection with *P.aeruginosa* strain RP73

Mice were infected (*o.a)* with either sham or $1x10^5$ cfu/mouse *P.aeruginosa* strain RP73 embedded agar beads. 30 minutes prior to infection, mice were treated with either 100 units/mL Apyrase or vehicle control. At 24 h.p.i blood was taken via cardiac puncture and the circulating platelet count was quantified using an improved neubauer haemocytometer. One-way ANOVA and Bonferroni's multiple comparisons post hoc test, $p>0.05$ versus vehicle, n=9-10, data are presented as mean ± SEM.

4.8.2.2 Investigating the Effect of Apyrase Treatment on Weight Loss

$1x10^5$ cfu/mouse RP73 infected, vehicle control treated animals showed a slight increase in weight loss when compared to sham controls (sham: 0.89±0.37%, 10^5 log cfu + vehicle control: 3.13±0.61%, **Figure 4.31**). In addition, following infection with $1x10^5$ cfu/mouse RP73, Apyrase treatment was associated with a further increase in weight loss when compared to sham controls (sham: 0.89±0.37%, 10^5 log cfu + Apyrase: 4.76±0.76%, $p<0.001$, **Figure 4.31**).

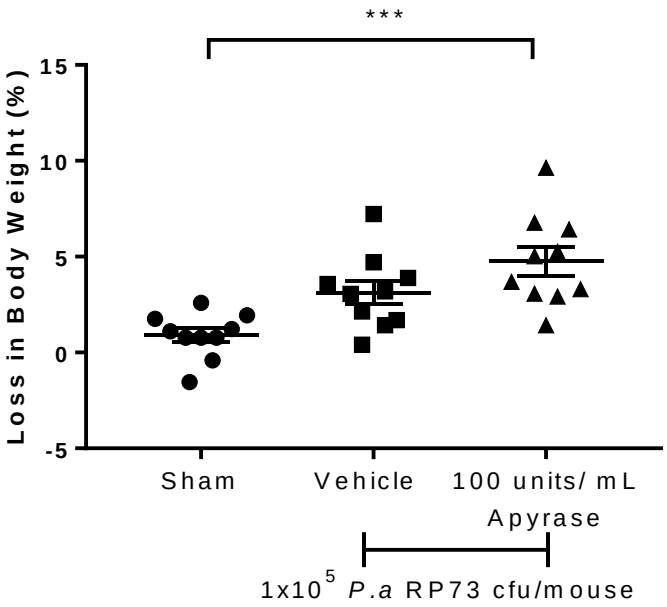

Figure 4.31 Effects of Apyrase on Weight Loss in a Murine Model of Pulmonary Infection with *P.aeruginosa* strain RP73

Mice were infected (*o.a)* with either sham or $1x10^5$ cfu/mouse *P.aeruginosa* strain RP73 embedded agar beads. 30 minutes prior to infection, mice were treated with either 100 units/mL Apyrase or vehicle control. Body weights were recorded prior to and 24 h.p.i and percentage weight loss calculated. One-way ANOVA and Bonferroni's multiple comparisons post hoc test, ***$p<0.001$ versus sham, n=10, data are presented as mean ± SEM.

4.8.2.3 Investigating the Effect of Apyrase Treatment on Pulmonary Bacterial Load and Leukocyte Recruitment

A significant increase in pulmonary bacterial load was observed at 24 h.p.i when compared to sham controls (10^5 log cfu + vehicle control: 4.83±0.10 log cfu, versus sham: 0.0 ± 0.0 log cfu, p<0.0001, **Figure 4.32A**)**.** 100 units/mL Apyrase significantly increased pulmonary bacterial load when compared to vehicle control treated animals (10^5 log cfu + vehicle control: 4.83±0.10 log cfu, versus 10^5 log cfu + Apyrase: 5.28±0.12 log cfu, p<0.01, **Figure 4.32A**), indicating in situ bacterial growth, similar to that observed in animals depleted of circulating platelets.

Infection with RP73 induced a significant increase in pulmonary total leukocyte recruitment, when compared to sham controls (10^5 log cfu + vehicle control: 10.55±1.49x10^5 cells/mL, versus sham: 1.43±0.11x10^5 cells/mL, p<0.001, **Figure 4.32B**). 100 units/mL Apyrase significantly reduced infection induced pulmonary total leukocyte recruitment compared to vehicle control treated animals (10^5 log cfu + vehicle control: 10.55±1.49x10^5 cells/mL, versus 10^5 log cfu + Apyrase: 5.39±0.57x10^5 cells/mL, p<0.001, **Figure 4.32B**).

This was reflected in neutrophil numbers, where a significant increase in pulmonary neutrophil recruitment was observed following infection with 1x10^5 cfu/mouse compared to sham controls (10^5 log cfu + vehicle control: 9.14±1.47x10^5 cells/mL, versus sham: 0.01±0.01x10^5 cells/mL, p<0.0001, **Figure 4.32C**). This was significantly reduced in animals pre-treated with 100 units/mL Apyrase (10^5 log cfu + vehicle control: 9.14±1.47x10^5 cells/mL versus 10^5 log cfu + Apyrase: 3.94±0.64x10^5 cells/mL, p<0.001, **Figure 4.32C**). No significant changes in macrophages (Macrophages: 10^5 log cfu + vehicle control: 0.95±0.35x10^5 cells/mL, 10^5 log cfu + Apyrase: 0.65±0.26x10^5cells/mL, versus sham: 0.98±0.27x10^5 cells/mL, **Figure**

4.32D) or lymphocytes (Lymphocytes: 10^5 log cfu + vehicle control: 0.0±0.0x10^5 cells/mL, 10^5 log cfu + Apyrase: 0.0±0.0x10^5cells/mL, versus sham: 0.0±0.0x10^5 cells/mL, **Figure 4.32D**) were observed in any groups.

These data suggest a potential role of platelet purinergic receptors in the regulation of the host response to infection in the mouse.

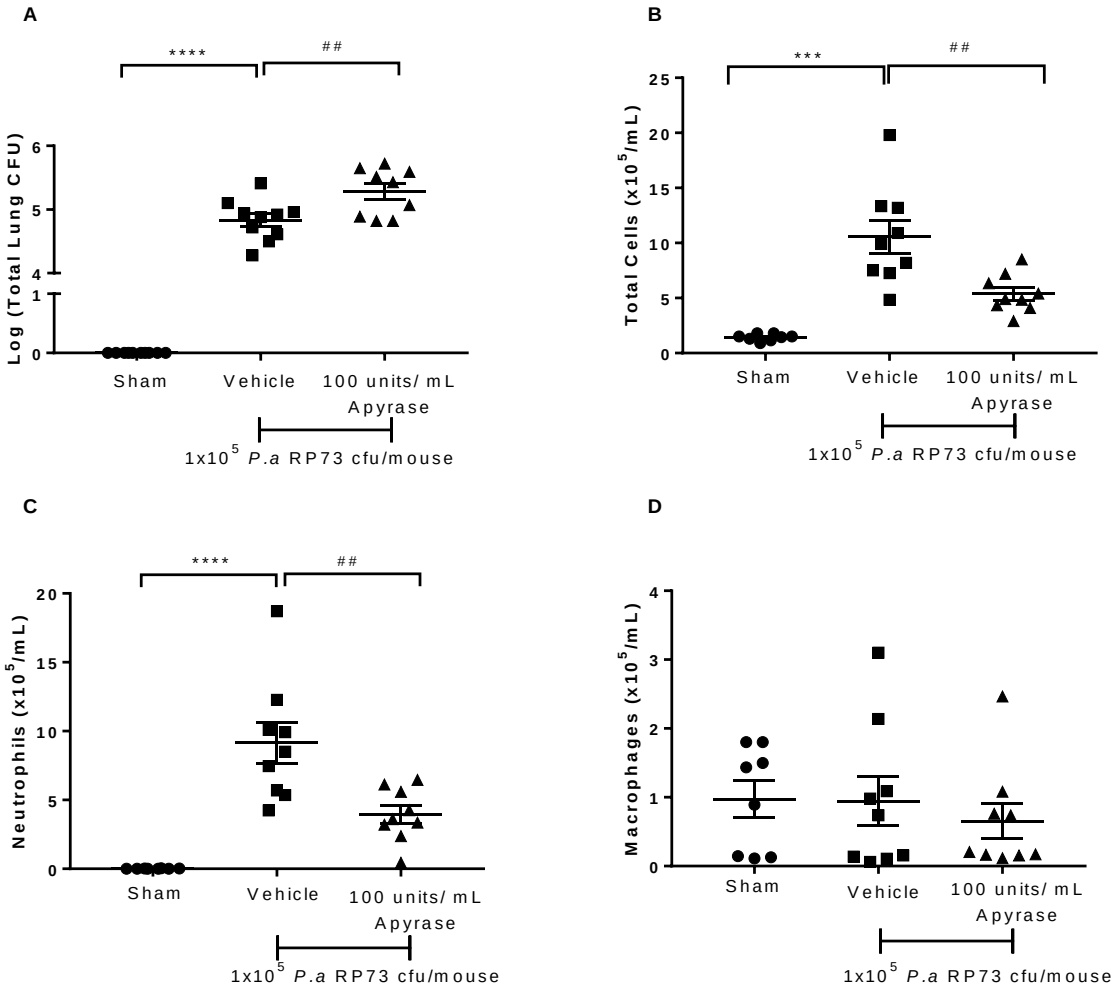

Figure 4.32 Effects of Apyrase on Pulmonary Bacterial Load and Leukocyte Recruitment in a Murine Model of Pulmonary Infection with *P.aeruginosa* strain RP73

Mice were infected (*o.a*) with either sham or $1x10^5$ cfu/mouse *P.aeruginosa* strain RP73 embedded agar beads. 30 minutes prior to infection, mice were treated with either 100 units/mL Apyrase or vehicle control. A BAL of the lungs was performed for inflammatory cell quantification and lungs were aseptically removed, homogenised and plated for quantification of bacterial load at 24 h.p.i. Pulmonary Bacterial Load (**A**), Total Cells (**B**), Neutrophils (**C**) and Macrophages (**D**). One-way ANOVA and Bonferroni's multiple comparisons post hoc test, *** $p<0.001$, **** $p<0.0001$ versus sham, ## $p<0.01$ versus vehicle control, n=8-10, data are presented as mean ± SEM.

4.8.2.4 Investigating the Effect of Apyrase Treatment on Bacterial Dissemination to the Kidney and Spleen

As Apyrase treatment reflected the phenomena of platelet depletion observed on bacterial load and inflammatory leukocyte recruitment, we assessed whether this was also reflected on the systemic dissemination of bacteria.

At 24 h.p.i, no evidence of bacterial dissemination to the kidney or spleen was observed in sham or vehicle control animals (sham: 0.0±0.0 log cfu, and 10^5 log cfu + vehicle: 0.0±0.0 log cfu, **Figure 4.33A** and **Figure 4.33B**). However, treatment with Apyrase induced a significant increase in bacterial dissemination to both the kidney and spleen, when compared to vehicle control treated animals (Kidney: 10^5 + Apyrase: 1.07 ± 0.45 log cfu, versus 10^5 + vehicle: 0.0 ± 0.0 log cfu, $p<0.01$, **Figure 4.33A** and Spleen: 10^5 log cfu + Apyrase: 0.52±0.26 log cfu, versus 10^5 log cfu + vehicle: 0.0±0.0 log cfu, $p<0.05$, **Figure 4.33B**).

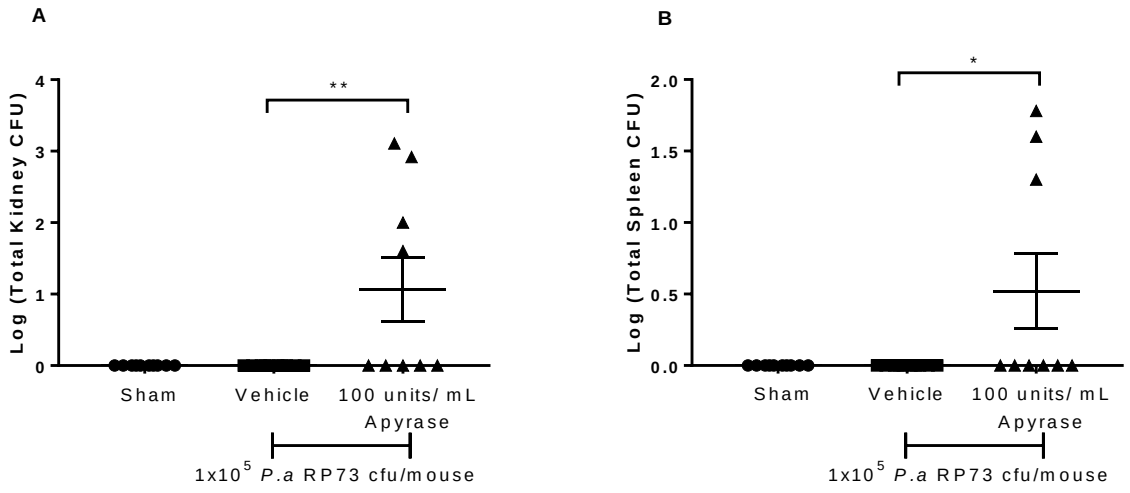

Figure 4.33 Effects of Apyrase on Bacterial Dissemination to the Kidney and Spleen in a Murine Model of Pulmonary Infection with *P.aeruginosa* strain RP73

Mice were infected *(o.a)* with either sham or $1x10^5$ cfu/mouse *P.aeruginosa* strain RP73 embedded agar beads. 30 minutes prior to infection, mice were treated with either 100 units/mL Apyrase or vehicle control. At 24 h.p.i, the kidney and spleen were aseptically removed, homogenised and plated for quantification of bacterial load. One-way ANOVA and Bonferroni's multiple comparisons post hoc test, * $p<0.05$, ** $p<0.01$ versus vehicle control, n=9-10, data are presented as mean ± SEM.

4.8.2.5 Investigating the Effect of Purinergic Receptor Antagonists on Pulmonary Bacterial Load and Leukocyte Recruitment

To further investigate the role of specific platelet purinergic receptors, mice were treated with either a $P2Y_1$ antagonist, MRS2500, a $P2Y_{12}$ antagonist, AR-C66096, a $P2X_1$ antagonist, NF-279 or a $P2Y_{14}$ antagonist, PPTN, and the effects on pulmonary bacterial load and leukocyte recruitment were observed.

A significant increase in pulmonary bacterial load was observed at 24 h.p.i when compared to sham controls (10^5 log cfu + vehicle control: 4.69±0.11 log cfu, versus sham: 0.0 ± 0.0 log cfu, $p<0.0001$, **Figure 4.34A**). Treatment with the $P2Y_{14}$ receptor antagonist, PPTN, significantly increased pulmonary bacterial load when compared to the vehicle controls (10^5 log cfu + PPTN: 5.30±0.15 log cfu, $p<0.05$, 10^5 log cfu + MRS2500: 4.57±0.18 log cfu, 10^5 log cfu + AR-C66096: 4.79±0.16 log cfu, 10^5 log cfu + NF-279: 4.99±0.25 log cfu, versus vehicle: 4.69±0.11 log cfu, **Figure 4.34A**).

Infection with $1x10^5$ cfu/mouse RP73 significantly increased total leukocyte recruitment to the lungs compared to sham controls (10^5 log cfu + vehicle control: $12.04±1.33x10^5$ cells/mL, versus sham: $1.75±0.36x10^5$ cells/mL, $p<0.05$, **Figure 4.34B**). This was significantly reduced following treatment with MRS2500, AR-C66096 and PPTN (10^5 log cfu + MRS2500: $3.74±1.36x10^5$ cells/mL, $p<0.01$, 10^5 log cfu + AR-C66096: $7.13±1.41x10^5$ cells/mL, $p<0.05$, 10^5 log cfu + NF-279: $7.44±1.82x10^5$ cells/mL, 10^5 log cfu + PPTN: $6.39±0.52x10^5$ cells/mL, $p<0.05$, versus 10^5 log cfu + vehicle: $12.04±1.33x10^5$ cells/mL, **Figure 4.34B**) when compared to vehicle controls. This pattern was reflected in neutrophils, where treatment with MRS2500 and PPTN significantly reduced neutrophil recruitment to the lungs, when compared to vehicle controls (10^5 log cfu + MRS2500: $3.59±1.12x10^5$ cells/mL, $p<0.001$, 10^5 log cfu + AR-C66096:

6.25±1.26x10^5 cells/mL, 10^5 log cfu + NF-279: 6.31±1.57x10^5 cells/mL, 10^5 log cfu + PPTN: 4.96±0.37x10^5 cells/mL, $p<0.05$, versus 10^5 log cfu + vehicle: 10.28±1.20x10^5 cells/mL, **Figure 4.34C**)**.** No significant difference in pulmonary macrophage (10^5 log cfu + MRS2500: 2.13±0.59x10^5 cells/mL, 10^5 log cfu + AR-C66096: 0.88±0.16x10^5 cells/mL, 10^5 log cfu + NF-279: 1.12±0.31x10^5 cells/mL, 10^5 log cfu + PPTN: 1.44±0.22x10^5 cells/mL, versus 10^5 log cfu + vehicle: 1.76±0.24x10^5 cells/mL, **Figure 4.34D**) or lymphocyte (10^5 log cfu + MRS2500: 0.0±0.0x10^5 cells/mL, 10^5 log cfu + AR-C66096: 0.0±0.0x10^5 cells/mL, 10^5 log cfu + NF-279: 0.0±0.0x10^5 cells/mL, 10^5 log cfu + PPTN: 0.0±0.0x10^5 cells/mL, versus 10^5 log cfu + vehicle: 0.0±0.0x10^5 cells/mL) recruitment was observed between any groups.

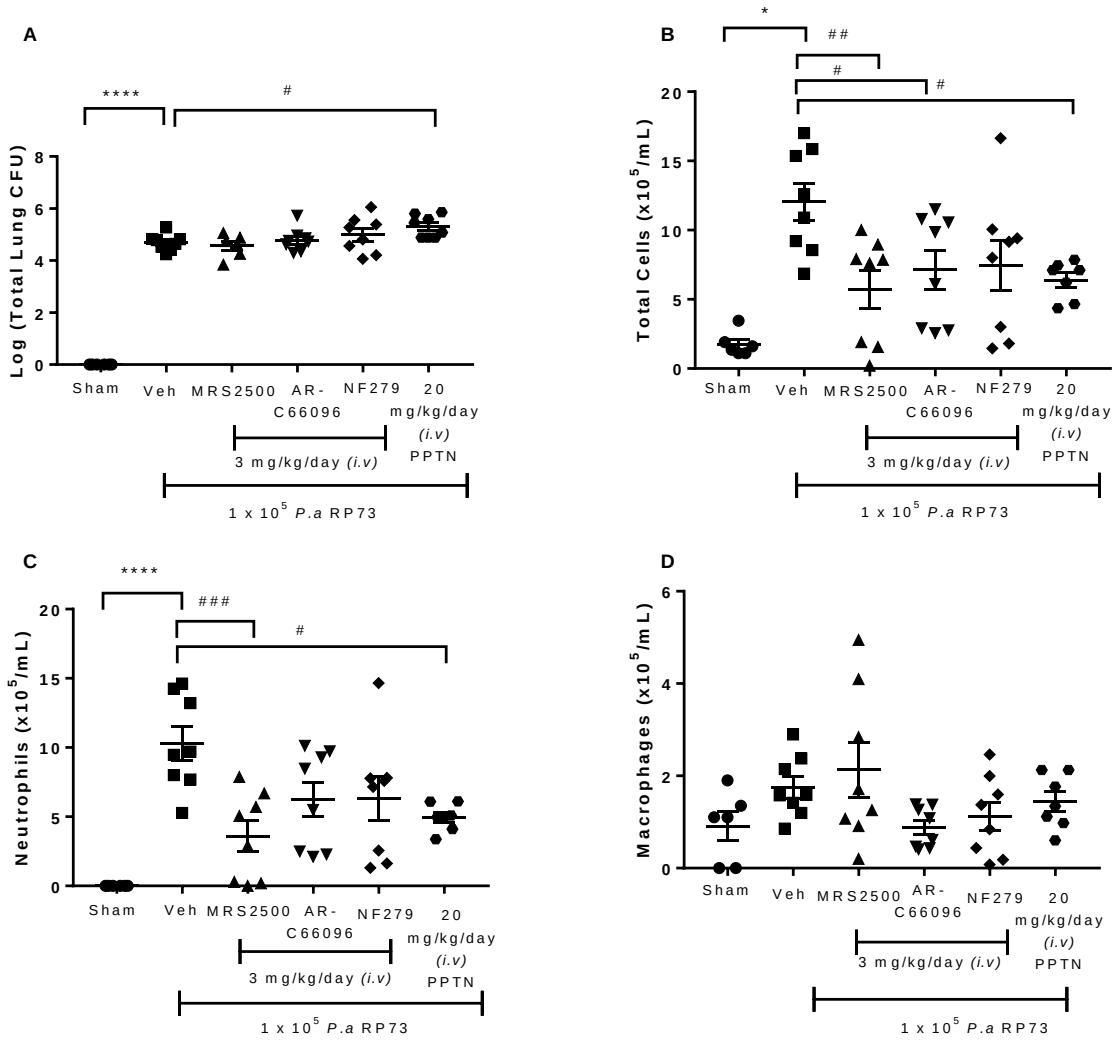

Figure 4.34 Effects of Purinergic Receptor Antagonists on Pulmonary Bacterial Load and Leukocyte Recruitment in a Murine Model of Pulmonary Infection with *P.aeruginosa* strain RP73

Mice were infected *(o.a)* with either sham or 1x10^5 cfu/mouse *P.aeruginosa* strain RP73 embedded agar beads. 30 minutes prior to infection, mice were administered a single dose of either vehicle, a $P2Y_1$ antagonist, MRS2500 (3mg/kg), a $P2Y_{12}$ antagonist, AR-C66096 (3mg/kg), a $P2X_1$ antagonist, NF-279 (3mg/kg) or a $P2Y_{14}$ antagonist, PPTN Mesylate (10mg/kg) (*i.v)*. A second dose of PPTN was administered at 6 h.p.i. A BAL of the lungs was performed for inflammatory cell quantification and lungs were aseptically removed, homogenised and plated for quantification of bacterial load at 24 h.p.i. Pulmonary Bacterial Load (**A**), Total Cells (**B**), Neutrophils (**C**) and Macrophages (**D**). One-way ANOVA and Bonferroni's multiple comparisons post hoc test, * p<0.05, **** p<0.0001 versus sham, #p<0.05, ## p<0.01, ### p<0.001 versus vehicle control, n=6-8, data are presented as mean ± SEM.

4.8.2.6 Investigating the Effect of Purinergic Receptor Antagonists on Bacterial Dissemination to the Kidney and Spleen

As inhibition of the platelet purinergic $P2Y_{14}$ receptor reflected the phenomena of platelet depletion observed on bacterial load and inflammatory leukocyte recruitment, we assessed whether this was also reflected on the systemic dissemination of bacteria.

At 24 h.p.i, no evidence of bacterial dissemination to the kidney or spleen was observed in sham animals, or in mice treated with vehicle control or MRS2500 (sham: 0.0±0.0 log cfu, 10^5 log cfu + vehicle: 0.0±0.0 log cfu, 10^5 log cfu + MRS2500: 0.0±0.0 log cfu, **Figure 4.35A** and **Figure 4.35B**). However, treatment with PPTN induced an increase in bacterial dissemination to the kidney and spleen, although these data reached statistical significance only for the kidney (Kidney: 10^5 log cfu + AR-C66096: 0.16±0.16 log cfu, 10^5 log cfu + NF-279: 0.36±0.24 log cfu, 10^5 log cfu + PPTN: 1.00±0.40 log cfu, $p<0.01$ and Spleen: 10^5 log cfu + AR-C66096: 0.32±0.21 log cfu, 10^5 log cfu + NF-279: 0.25±0.25 log cfu, 10^5 log cfu + PPTN: 0.55±0.37 log cfu, **Figure 4.35A** and **Figure 4.35B**) when compared to vehicle controls.

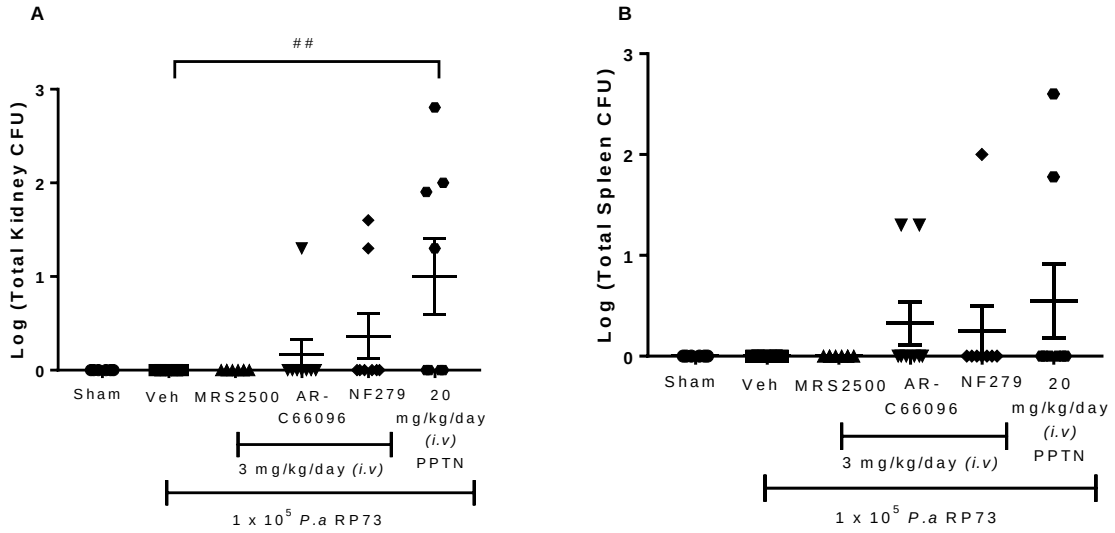

Figure 4.35 Effects of Purinergic Receptor Antagonists on Bacterial Dissemination to the Kidney and Spleen in a Murine Model of Pulmonary Infection with *P.aeruginosa* strain RP73

Mice were infected *(o.a)* with either sham or $1x10^5$ cfu/mouse *P.aeruginosa* strain RP73 embedded agar beads. 30 minutes prior to infection, mice were administered a single dose of either vehicle, a $P2Y_1$ antagonist, MRS2500 (3mg/kg), a $P2Y_{12}$ antagonist, AR-C66096 (3mg/kg), a $P2X_1$ antagonist, NF-279 (3mg/kg) or a $P2Y_{14}$ antagonist, PPTN Mesylate (10mg/kg) (*i.v)*. A second dose of PPTN was administered at 6 h.p.i. At 24 h.p.i, the kidney and spleen were aseptically removed, homogenised and plated for quantification of bacterial load. One-way ANOVA and Bonferroni's multiple comparisons post hoc test, ## $p<0.01$ versus vehicle control, n=6-8, data are presented as mean ± SEM.

4.8.3 Investigating the Effect of Platelets on Growth of *P.aeruginosa* strain RP73 *in vitro*

From the *in vivo* experiments performed, experimentally induced platelet depletion was associated with an increase in pulmonary bacterial load. Animals infected with the higher inoculum of $1x10^6$ cfu/mL RP73 demonstrated a significant 1.5 log increase when compared to the IgG control treated animals. (**Figure 4.11C**). Interestingly, this particular strain of *P.aeruginosa* has previously demonstrated a similar log cfu increase over the same time period in *in vitro* cultures (Bragonzi et al., 2012).

For this reason, platelet-bacteria co-culture experiments were performed to determine whether platelets modulate bacterial growth kinetics *in vitro.* $1x10^6$ cfu/mL RP73 was incubated both in the presence and absence of $1x10^6$ platelets/mL and aliquots of the co-culture were taken periodically over an 8-hour time period.

My results demonstrated that bacteria cultured in the presence of $1x10^6$/mL platelets demonstrated a significant decrease in bacterial growth at both 6 (Bacteria alone: log 8.49±0.22 cfu/mL, versus bacteria + platelets: log 7.74±0.42 cfu/mL, $p<0.05$, **Figure 4.36**) and 8 hours (Bacteria alone: log 8.91±0.19 cfu/mL, versus bacteria + platelets: log 7.80±0.28 cfu/mL, $p<0.001$, **Figure 4.36**), when compared to bacterial cultures in the absence of platelets.

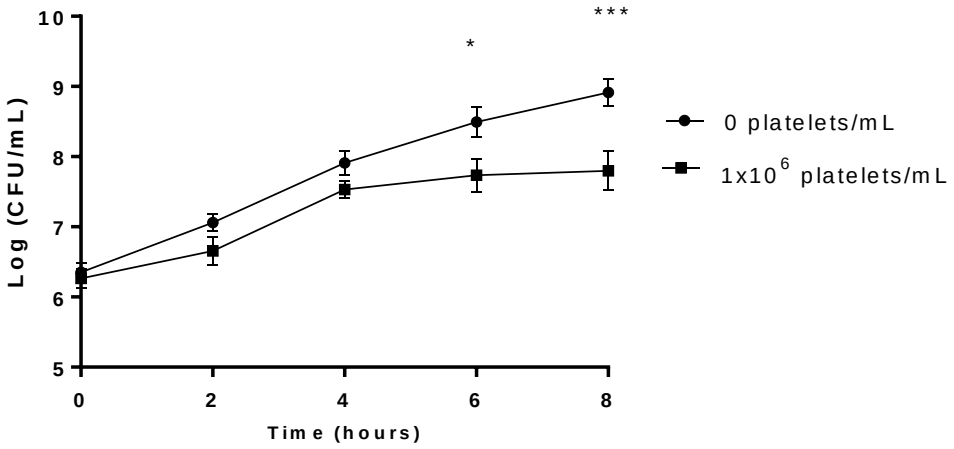

Figure 4.36 Effect of Platelets on Growth of *P.aeruginosa* strain RP73 *in vitro*

In vitro cultures of $1x10^6$ cfu/mL *P.aeruginosa* strain RP73 were prepared alone or in the presence of $1x10^6$ platelets/mL at a 1:1 ratio. Aliquots were taken at 0, 2, 4, 6 and 8 hours and viable colony forming units were quantified on TSA plates. Unpaired two-tailed t-test, * $p<0.05$, *** $p<0.001$ versus bacterial control cultures, n=6, data are presented as mean ± SEM.

4.8.4 Investigating the Effect of Platelets on Death of *P.aeruginosa* strain RP73 *in vitro*

As my previous experiments highlighted the ability of platelets to modulate bacterial growth kinetics *in vitro*, we performed additional experiments to determine whether this was via increased bacterial death *in vitro*. A LIVE/DEAD *Bac*Light bacterial viability kit was therefore used to monitor the viability of bacteria as a function of membrane integrity of the cell. For these experiments, $1x10^6$ cfu/mL RP73 was incubated with and without platelets at either $1x10^6$, $1x10^7$ or $1x10^8$ platelets/mL. Aliquots were taken periodically over an 8-hour time period and bacteria with a compromised cell membrane were considered dead and stained red with the DNA stain PI.

My findings suggested that incubation of $1x10^7$ platelets/mL significantly enhanced bacterial death of *P.aeruginosa* strain RP73 at 6 hours when compared to bacterial cultures in the absence of platelets (Bacteria alone: 724.1±35.5 RFU PI, versus bacteria + 10^7 platelets: 880.30±24.17 RFU PI, $p<0.05$, **Figure 4.37A**). Similarly, incubation of $1x10^7$ platelets/mL enhanced bacterial death of *P.aeruginosa* strain RP73 at 8 hours compared to bacterial cultures in the absence of platelets, although these data did not reach statistical significance. (Bacteria alone: 639.0±54.37 RFU PI, versus bacteria + 10^7 platelets: 827.50±24.54 RFU PI, **Figure 4.37A**).

The RFU of PI decreased between 6 and 8 hours. Therefore, to assess whether the platelets remained viable after prolonged culture with bacteria, aliquots of the 10^7 co-culture were taken periodically between 0 and 8 hours and stimulated with either vehicle, 100µM ADP or 10µM TRAP and the percentage of CD62P positive events was quantified, as a functional marker of platelet viability. Platelets remained viable at 8 hours, since the percentage of CD62P positive events continued to increase. Furthermore, there appeared to be no difference between vehicle control, ADP and TRAP stimulated platelets, perhaps suggesting that the platelets have already reached their maximum activated state in the presence of bacteria (vehicle: 52.79%, ADP: 51.88% and TRAP 54.75%, **Figure 4.37B**).

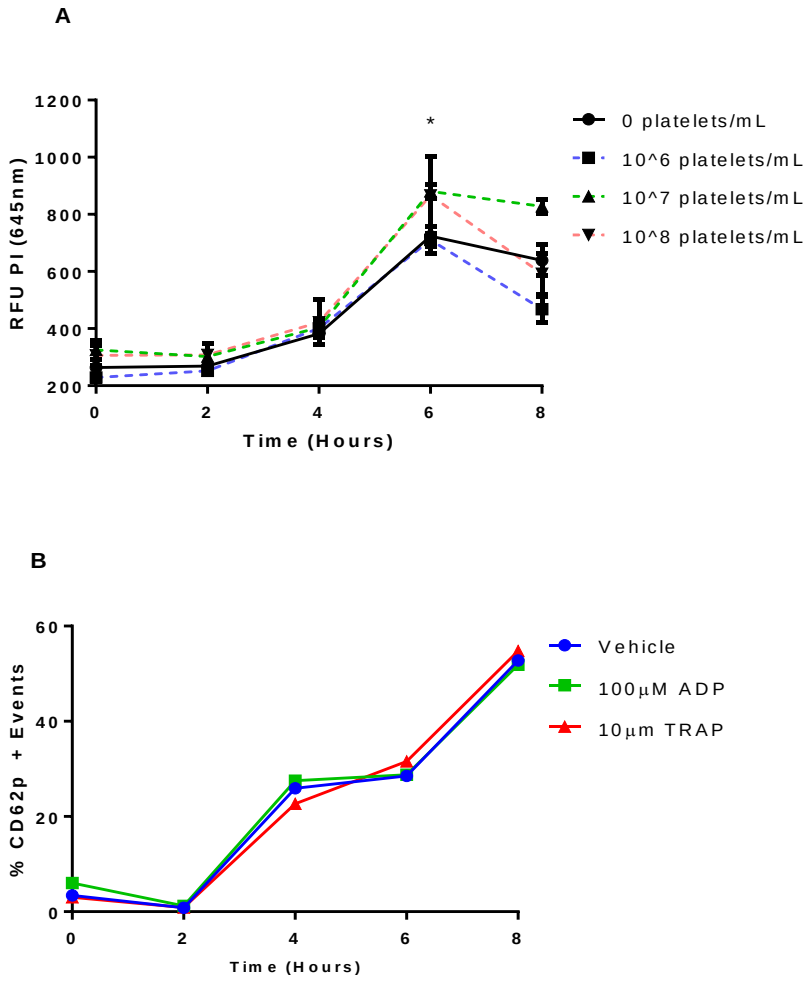

Figure 4.37 Effect of Platelets on Death of *P.aeruginosa* strain RP73 *in vitro*

Cultures of 1x10^6 cfu/mL *P.aeruginosa* strain RP73 were prepared alone or in the presence of either 1x10^6,10^7 or 10^8 platelets/mL. Aliquots were taken at 0, 2, 4, 6 and 8 hours and stained with 2.5uM SYTO9 and 15uM Propidium Iodide. Samples were read on a fluorescent plate reader at 488/20nm excitation and either 528/20nm or 645/20nm emission. (**A**) Relative fluorescent units of PI. Platelets were stimulated with either 100µM ADP, 10µM TRAP or vehicle to determine the percentage CD62P positive events (**B**), using a Beckman Coulter Cytomics FC 500 flow cytometer. One-way ANOVA and Bonferroni's multiple comparisons post hoc test, *$p<0.05$, 10^7 platelets versus bacterial control cultures

Chapter V: Results III

The Use of a Murine Model of Pulmonary Infection for Therapeutic Analysis

5.1 Investigating the Effect of HT61 in Model of Pulmonary Infection with the Gram-Negative *P.aeruginosa*

One approach to provide improved treatments for infectious diseases is the use of enhancer compounds, which act by restoring sensitivity of resistant bacteria to currently available antibiotics. Hu and colleagues (Hu et al., 2010) have developed such a drug, the antibiotic enhancer, HT61, a small quinolone derived compound as an exemplar of this novel approach. HT61 has previously been reported to show efficacy against gram-positive bacteria, particularly MRSA and MSSA, *in vitro* (Hu et al., 2010). Therefore, the aim of this work was to determine the effect of HT61, as a singular treatment, *in vivo,* using a murine model of pulmonary infection with the gram-negative bacterial species, *P.aeruginosa*

5.1.1 Investigating the Effect of HT61 in a Model of Pulmonary Infection with *P.aeruginosa* strain RP73

Mice were inoculated with either sham or $1x10^6$ cfu/mouse RP73 embedded agar beads and treated with a singular dose of HT61 at either 0.1, 1 or 5 mg/kg HT61 to determine the efficacy of HT61 as a singular treatment. The effect on pulmonary leukocyte recruitment and pulmonary bacterial load was determined.

Data from these experiments indicated that infection with $1x10^6$ cfu/mouse *P.aeruginosa* strain RP73 induced a significant increase in pulmonary bacterial load when compared to sham controls (6.16±0.22 log cfu, versus sham: 0.0±0.0 log cfu, $p<0.0001$, **Figure 5.1A**). Furthermore, HT61 treatment demonstrated no significant attenuation of bacterial load at any tested dose when compared to vehicle controls (0.1 mg/kg: 5.91±0.12 log cfu, 1 mg/kg:

6.45±0.12 log cfu and 5 mg/kg: 6.64±0.41 log cfu, versus vehicle: 6.16 ± 0.22 log cfu, **Figure 5.1A**).

Infection with $1x10^6$ cfu/mouse RP73 induced a significant increase in total leukocyte ($28.7±2.63x10^5$ cells/mL, versus sham: $1.98±0.01x10^5$ cells/mL, $p<0.01$, **Figure 5.1B**). and neutrophil ($26.96±3.11x10^5$ cells/mL, versus sham: $0.06±0.01x10^5$ cells/mL, $p<0.01$, **Figure 5.1C**) recruitment to the lungs when compared to sham controls. HT61 treatment at any tested dose had no significant reduction in total leukocyte recruitment (0.1 mg/kg: $25.33±2.14x10^5$ cells/mL, 1 mg/kg: $33.0±1.0x10^5$ cells/mL, 5 mg/kg: $25.97±2.84$ $x10^5$ cells/mL, versus vehicle: $28.7±2.63x10^5$ cells/mL, **Figure 5.1B**) or neutrophil recruitment to the lungs (0.1 mg/kg: $23.79±2.13x10^5$ cells/mL, 1 mg/kg: $31.61±1.21x10^5$ cells/mL, 5 mg/kg: $24.13±2.88x10^5$ cells/mL, versus vehicle: $26.96±3.11x10^5$ cells/mL, **Figure 5.1C**) compared to vehicle controls. Data from this study indicated that infection with RP73 had no significant effect on macrophage (vehicle: $1.74±0.48x10^5$ cells/mL, versus sham: $1.40±0.26x10^5$ cells/mL, **Figure 5.1D**) or lymphocyte (vehicle: $0.0±0.0x10^5$ cells/mL, versus sham: $0.0±0.0x10^5$ cells/mL) recruitment to the lungs compared to sham controls. This was consistent with macrophage recruitment following HT61 treatment, whereby HT61 treatment had no significant effect on macrophages at any dose tested (0.1 mg/kg: $1.54±0.12x10^5$ cells/mL, 1 mg/kg: $1.40±0.21x10^5$ cells/mL, 5 mg/kg: $1.84±0.16x10^5$ cells/mL, versus vehicle: $1.74±0.48x10^5$ cells/mL, **Figure 5.1D**) or lymphocyte (0.1 mg/kg: $0.0±0.0x10^5$ cells/mL, 1 mg/kg: $0.0±0.0x10^5$ cells/mL, 5 mg/kg: $0.0±0.0x10^5$ cells/mL, versus vehicle: $0.0±0.0x10^5$ cells/mL) recruitment to the lungs when compared to vehicle controls.

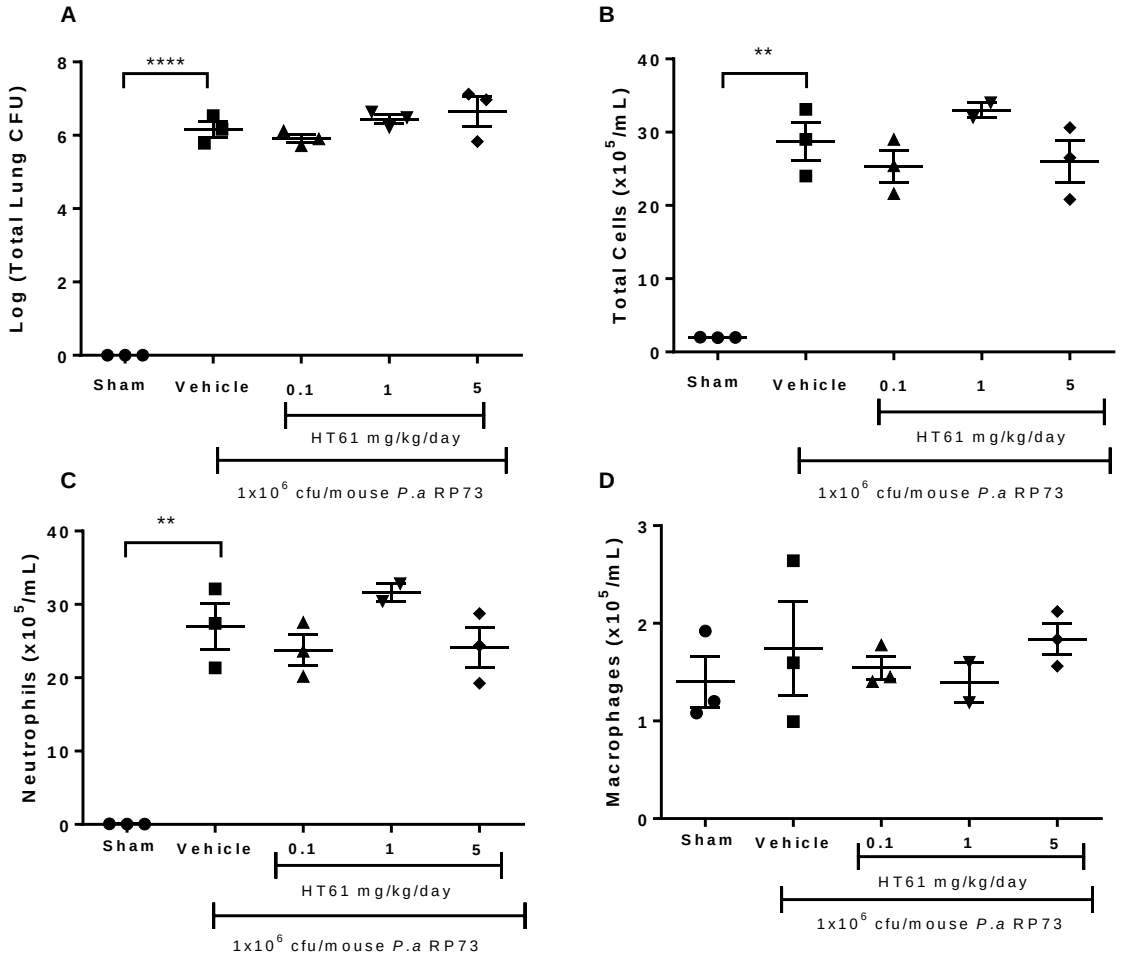

Figure 5.1 Effects of HT61 as a Singular Treatment on Infection with *P.aeruginosa* strain RP73

Mice were infected *(o.a)* with either sham or 1x10^6 cfu/mouse *P.aeruginosa* strain RP73 embedded agar beads. 24 hours post infection, mice were administered with either 0.1, 1 or 5 mg/kg HT61 or vehicle, via *i.p* injection. A BAL of the lungs was performed for inflammatory cell quantification and lungs were aseptically removed, homogenised and plated for quantification of bacterial load at 48 h.p.i. Pulmonary Bacterial Load (**A**), Total Cells (**B**), Neutrophils (**C**) and Macrophages (**D**). One-way ANOVA and Bonferroni's multiple comparisons post hoc test, ** $p<0.01$, **** $p<0.0001$ versus sham, n=2-4, data are presented as mean ± SEM.

5.1.2 Investigating the Effect of HT61 in a Model of Pulmonary Infection with *P.aeruginosa* strain PAO1

Having determined the effect of HT61, as a singular treatment, against infection with a multidrug resistant *P.aeruginosa* strain, RP73, HT61 was tested against a Tobramycin susceptible strain, *P.aeruginosa,* strain PAO1. The effect of HT61 on pulmonary leukocyte recruitment and pulmonary bacterial load was determined.

Infection with $1x10^6$ cfu/mouse PAO1 induced a significant increase in pulmonary bacterial load when compared to sham controls (5.56±0.31 log cfu, versus sham: 0.0±0.0 log cfu, $p<0.0001$, **Figure 5.2A**). HT61 treatment demonstrated no significant attenuation of bacterial load at any tested dose when compared to vehicle controls (0.1 mg/kg: 6.98±0.17 log cfu, 1 mg/kg: 5.74±0.14 log cfu and 5 mg/kg: 5.74±0.33 log cfu, versus vehicle: 5.56±0.31 log cfu, **Figure 5.2A**).

Infection with $1x10^6$ cfu/mouse PAO1 induced a significant increase in total leukocyte ($26.93±0.52x10^5$ cells/mL, versus sham: $1.98±0.01x10^5$ cells/mL, $p<0.001$, **Figure 5.2B**) and neutrophil ($23.60±1.11x10^5$ cells/mL, versus sham: $0.01±0.01x10^5$ cells/mL, $p<0.001$, **Figure 5.2C**) recruitment to the lungs when compared to sham controls. HT61 treatment had no significant effect on total leukocyte number at any dose tested (0.1 mg/kg: $31.15±3.63x10^5$ cells/mL, 1 mg/kg: $23.5±1.78x10^5$ cells/mL, 5 mg/kg: $22.80±6.03x10^5$ cells/mL, versus vehicle: $26.9±0.52x10^5$ cells/mL, **Figure 5.2B**) or neutrophil recruitment to the lungs (0.1 mg/kg: $27.72±2.85x10^5$ cells/mL, 1 mg/kg: $20.57±1.89x10^5$ cells/mL, 5 mg/kg: $19.44±5.14x10^5$ cells/mL, versus vehicle: $23.60±1.11x10^5$ cells/mL, **Figure 5.2C**) when compared to vehicle controls. Additionally, infection with PAO1 had no significant effect on macrophage (vehicle: $3.43±1.29x10^5$ cells/mL, versus sham: $1.70±0.20x10^5$ cells/mL, **Figure 5.2D**) or lymphocyte

(vehicle: 0.0±0.0x10^5 cells/mL, versus sham: 0.0±0.0x10^5 cells/mL) recruitment to the lungs when compared to sham controls. This was consistent with HT61 treatment, whereby no tested doses of HT61 had a significant effect on macrophage (0.1 mg/kg: 3.43±0.80x10^5 cells/mL, 1 mg/kg: 3.58±0.26x10^5 cells/mL, 5 mg/kg: 3.40±0.88x10^5 cells/mL, versus vehicle: 3.43±1.29x10^5 cells/mL, **Figure 5.2D**) or lymphocyte (0.1 mg/kg: 0.0±0.0x10^5 cells/mL, 1 mg/kg: 0.0±0.0x10^5 cells/mL, 5 mg/kg: 0.0±0.0x10^5 cells/mL, versus vehicle: 0.0±0.0x10^5 cells/mL) recruitment to the lungs when compared to vehicle controls.

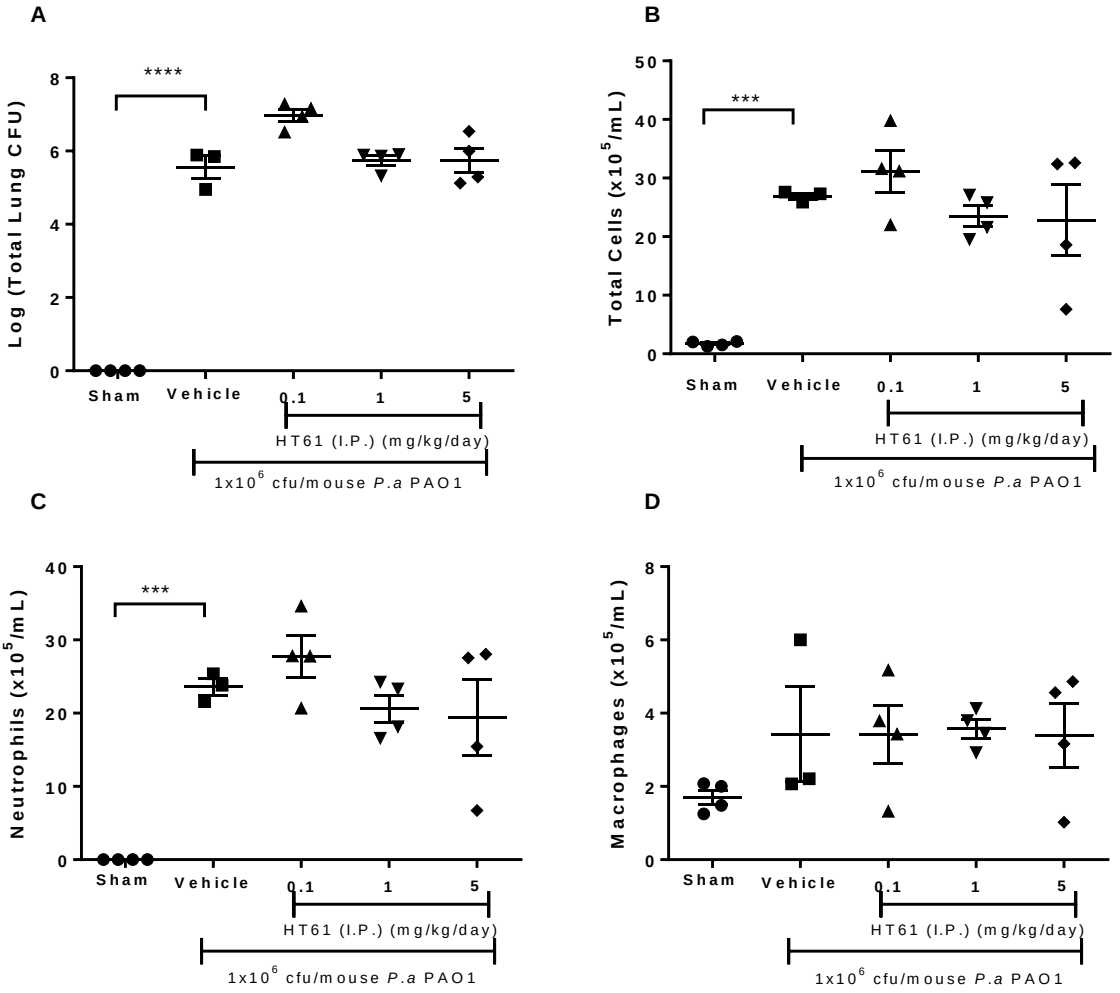

Figure 5.2 Effects of HT61 as a Singular Treatment on Infection with *P.aeruginosa* strain PAO1

Mice were infected *(o.a)* with either sham or 1x10^6 cfu/mouse *P.aeruginosa* strain PAO1 embedded agar beads. 24 hours post infection, mice were administered with either 0.1, 1 or 5 mg/kg HT61 or vehicle, via *i.p* injection. A BAL of the lungs was performed for inflammatory cell quantification and lungs were aseptically removed, homogenised and plated for quantification of bacterial load at 48 h.p.i. Pulmonary Bacterial Load (**A**), Total Cells (**B**), Neutrophils (**C**) and Macrophages (**D**). One-way ANOVA and Bonferroni's multiple comparisons post hoc test, *** p<0.001, **** p<0.0001 versus sham, n=3-4, data are presented as mean ± SEM.

5.1.3 Investigating the Effect of HT61 in a Model of Pulmonary Infection with *P.aeruginosa* strain NN2

Having determined the efficacy of HT61 against infection with a multidrug resistant *P.aeruginosa* strain, RP73 and a Tobramycin susceptible strain of *P.aeruginosa*, PAO1, HT61 was tested against a Tobramycin resistant strain of *P.aeruginosa*, NN2. The effect of HT61 on pulmonary leukocyte recruitment and pulmonary bacterial load was determined.

Infection with $1x10^6$ cfu/mouse NN2 induced a significant increase in pulmonary bacterial load when compared to sham controls (4.85±0.18 log cfu, versus sham: 0.0±0.0 log cfu, $p<0.0001$, **Figure 5.3A**). HT61 treatment demonstrated no significant attenuation of bacterial load at any tested dose when compared to vehicle controls (0.1 mg/kg: 5.34±0.32 log cfu, 1 mg/kg: 5.12±0.43 log cfu and 5 mg/kg: 5.8±0.69 log cfu, versus vehicle: 4.85±0.18 log cfu, **Figure 5.3A**).

Infection with $1x10^6$ cfu/mouse NN2 induced a significant increase in total leukocyte ($13.13±1.86x10^5$ cells/mL, versus sham: $1.93±0.18x10^5$ cells/mL, $p<0.01$, **Figure 5.3B**) and neutrophil ($10.45±1.53x10^5$ cells/mL, versus sham: $0.0±0.0x10^5$ cells/mL, $p<0.01$, **Figure 5.3C**) recruitment to the lungs when compared to sham controls. HT61 treatment at any tested dose had no significant reduction in either total leukocyte (0.1 mg/kg: $12.30±2.60x10^5$ cells/mL, 1 mg/kg: $11.58±1.51x10^5$ cells/mL, 5 mg/kg: $11.73±2.89x10^5$ cells/mL, versus vehicle: $13.13±1.86x10^5$ cells/mL, **Figure 5.3B**) or neutrophil recruitment to the lungs (0.1 mg/kg: $10.63±2.49x10^5$ cells/mL, 1 mg/kg: $9.70±1.19x10^5$ cells/mL, 5 mg/kg: $9.70±2.91x10^5$ cells/mL, versus vehicle: $10.45±1.53x10^5$ cells/mL, **Figure 5.3C**) when compared to vehicle controls. Additionally, infection with NN2 had no significant effect on macrophage or (vehicle: $2.40±0.24x10^5$ cells/mL, versus sham: $1.93±0.18x10^5$ cells/mL, **Figure 5.3D**) lymphocyte

(vehicle: 0.0±0.0x10^5 cells/mL, versus sham: 0.0±0.0x10^5 cells/mL) recruitment to the lungs when compared to sham controls. The data obtained suggested HT61 treatment at any tested dose had no significant effect on macrophage (0.1 mg/kg: 1.71±0.50x10^5 cells/mL, 1 mg/kg: 1.88±0.43x10^5 cells/mL, 5 mg/kg: 2.02±0.42x10^5 cells/mL, versus vehicle: 2.40±0.24x10^5 cells/mL, **Figure 5.3D**) or lymphocyte (0.1 mg/kg: 0.0±0.0x10^5 cells/mL, 1 mg/kg: 0.0±0.0x10^5 cells/mL, 5 mg/kg: 0.0±0.0x10^5 cells/mL, versus vehicle: 0.0±0.0x10^5 cells/mL) recruitment to the lungs when compared to vehicle controls.

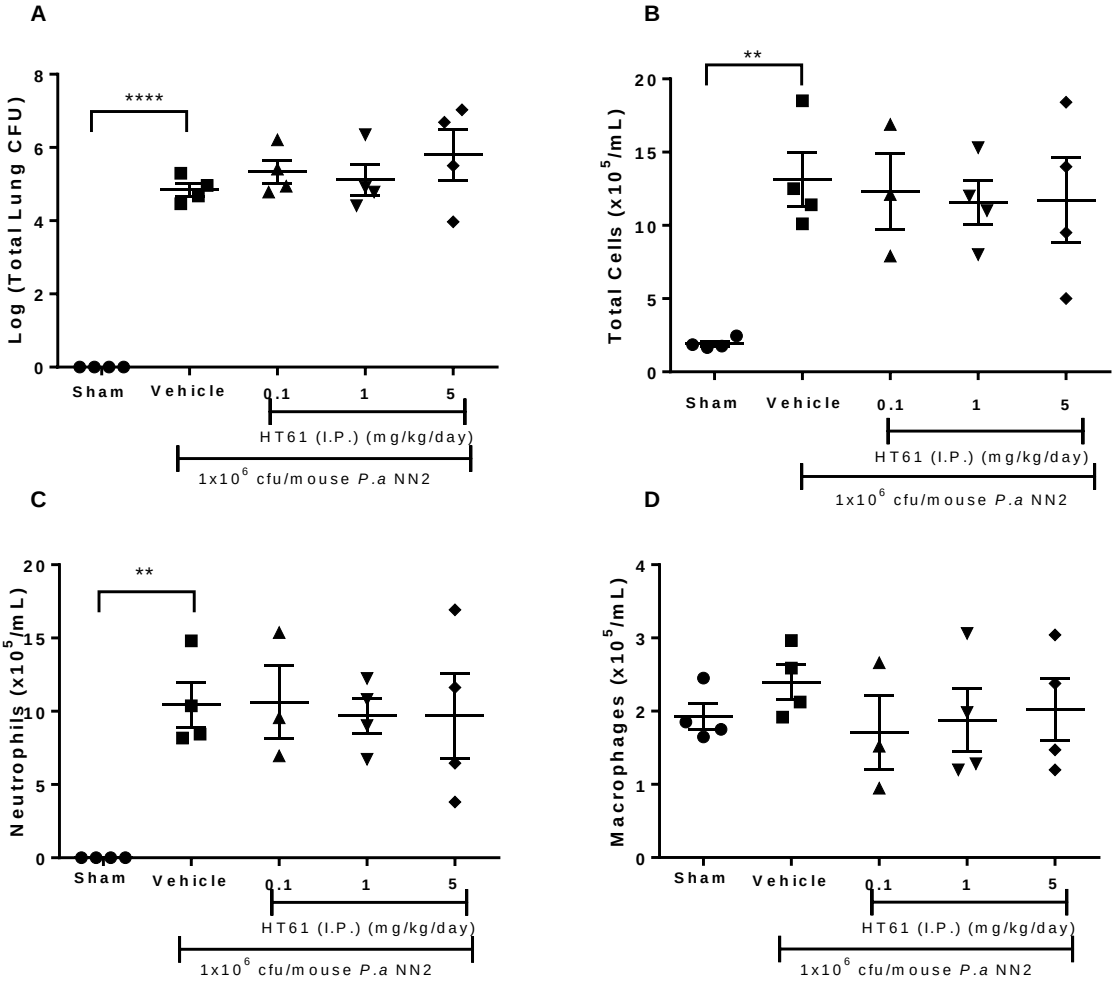

Figure 5.3 Effects of HT61 as a Singular Treatment on Infection with *P.aeruginosa* strain NN2

Mice were infected *(o.a)* with either sham or 1x10^6 cfu/mouse *P.aeruginosa* strain NN2 embedded agar beads. 24 hours post infection, mice were administered with either 0.1, 1 or 5 mg/kg HT61 or vehicle, via *i.p* injection. A BAL of the lungs was performed for inflammatory cell quantification and lungs were aseptically removed, homogenised and plated for quantification of bacterial load at 48 h.p.i. Pulmonary Bacterial Load (**A**), Total Cells (**B**), Neutrophils (**C**) and Macrophages (**D**). One-way ANOVA and Bonferroni's multiple comparisons post hoc test, ** $p<0.01$, **** $p<0.0001$ versus sham, n=3-4, data are presented as mean ± SEM.

5.2 Investigating the Effect of HT61 in a Model of Pulmonary Infection with the Gram-Positive MRSA

5.2.1 Investigating the Effect of HT61 in a Model of Pulmonary Infection with MRSA strain USA300

The data suggested HT61, as a singular treatment, had no significant effect on infection with gram-negative *P.aeruginosa,* although HT61 has previously been reported to show efficacy against gram-positive bacteria, particularly MRSA and MSSA, *in vitro* (Hu et al., 2010). Therefore, we sought to investigate the effect of this compound on the gram-positive bacterial species, MRSA, strain USA300, *in vivo.*

Infection with $1x10^6$ cfu/mouse USA300, induced a significant increase in pulmonary bacterial load when compared to sham controls (4.62±0.31 log cfu, versus sham: 0.0±0.0 log cfu, $p<0.0001$, **Figure 5.4A**). HT61 treatment demonstrated no significant attenuation of bacterial load at any tested dose when compared to vehicle controls (0.1 mg/kg: 4.36±0.19 log cfu, 1 mg/kg: 4.27±0.19 log cfu and 10 mg/kg: 3.92±0.22 log cfu, versus vehicle: 4.62±0.31 log cfu, **Figure 5.4A**). Although no significant effect was observed, these data indicated a trend towards a dose dependent reduction in pulmonary bacterial load with increasing doses of HT61.

Furthermore, infection with $1x10^6$ cfu/mouse USA300 induced a significant increase in total leukocyte ($4.99±0.73x10^5$ cells/mL, versus sham: $2.01±0.32x10^5$ cells/mL, $p<0.001$, **Figure 5.4B**) and neutrophil recruitment to the lungs ($2.78±0.61x10^5$ cells/mL, versus sham: $0.0±0.0x10^5$ cells/mL, $p<0.0001$, **Figure 5.4C**) when compared to sham controls. HT61 treatment at any tested dose had no significant reduction in total leukocyte recruitment (0.1 mg/kg: $4.04±0.28x10^5$ cells/mL, 1 mg/kg: $5.29±0.39x10^5$ cells/mL, 10 mg/kg: $4.17±0.48x10^5$

cells/mL, versus vehicle: 4.99±0.73x10^5 cells/mL, **Figure 5.4B**) to the lungs when compared to vehicle controls. At the highest tested dose of 10mg/kg, HT61 significantly reduced neutrophil recruitment to the lungs when compared to vehicle controls (0.1 mg/kg: 1.84±0.26x10^5 cells/mL, 1 mg/kg: 1.79±0.37x10^5 cells/mL and 10 mg/kg: 0.69±0.12x10^5 cells/mL $p<0.001$, versus vehicle: 2.78±0.61x10^5 cells/mL, **Figure 5.4C**).

Infection with MRSA strain USA300 had no significant effect on either macrophage (vehicle: 2.33±0.39x10^5 cells/mL, versus sham: 2.01±0.32x10^5) or lymphocyte (vehicle: 0.0±0.0x10^5 cells/mL, versus sham: 0.0±0.0x10^5) recruitment to the lungs when compared to vehicle controls. This was consistent with HT61 treatment, whereby no tested dose had a significant effect on either macrophage (0.1 mg/kg: 2.20±0.30x10^5 cells/mL, 1 mg/kg: 3.34±0.18x10^5 cells/mL, 10 mg/kg: 3.47±0.41x10^5 cells/mL, versus vehicle: 2.33±0.39x10^5 cells/mL, **Figure 5.4D**) or lymphocyte (0.1 mg/kg: 0.0±0.0x10^5 cells/mL, 1 mg/kg: 0.0±0.0x10^5 cells/mL, 10 mg/kg: 0.0±0.0x10^5 cells/mL, versus vehicle: 0.0±0.0x10^5 cells/mL) recruitment to the lungs when compared to vehicle controls.

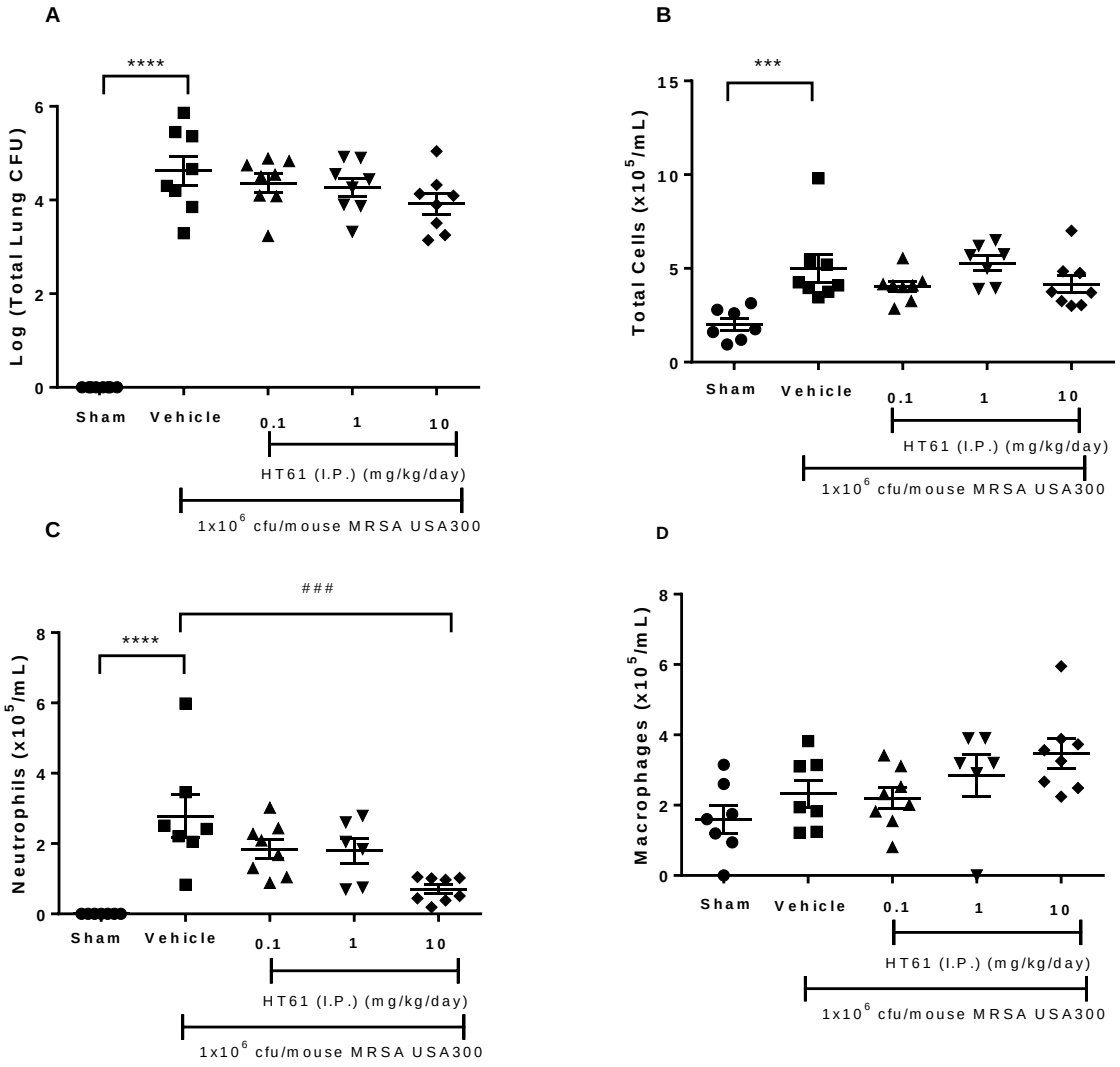

Figure 5.4 Effects of HT61 as a Singular Treatment on Infection with MRSA strain USA300

Mice were infected *(o.a)* with either sham or $1x10^6$ cfu/mouse MRSA strain USA300 embedded agar beads. 24 hours post infection, mice were administered with either 0.1, 1 or 10 mg/kg HT61 or vehicle, via *i.p* injection. A BAL of the lungs was performed for inflammatory cell quantification and lungs were aseptically removed, homogenised and plated for quantification of bacterial load at 48 h.p.i. Pulmonary Bacterial Load (**A**), Total Cells (**B**), Neutrophils (**C**) and Macrophages (**D**). One-way ANOVA and Bonferroni's multiple comparisons post hoc test, *** $p<0.001$, **** $p<0.0001$ versus sham, ### $p<0.001$ versus vehicle, n=6-8, data are presented as mean ± SEM.

5.3 Investigating the Effect of HT61 and Tobramycin Combination Therapy in a Model of Pulmonary Infection with Gram- Negative *P.aeruginosa*

The data in this chapter suggests that HT61 has no significant anti-microbial effect, when administered as a singular treatment. *In vitro* studies however have demonstrated an enhancement of the activity of older generation antibiotics (gentamicin, neomycin and chlorhexidine) when used in combination with HT61 (Hu, 2013) (Hu, 2010) against MRSA. The aim of this work was to determine whether the novel enhancer compound HT61 is able to potentiate the effect of low doses of Tobramycin or Vancomycin on attenuating the pulmonary bacterial load induced by the gram-negative *P.aeruginosa* and the gram-positive MRSA.

5.3.1 Investigating the Effect of HT61 and Tobramycin in a Model of Pulmonary Infection with *P.aeruginosa* RP73

Initial experiments were performed to determine whether combination treatment with HT61 and Tobramycin significantly attenuates pulmonary bacterial infection with a multidrug resistant strain of *P.aeruginosa*, RP73, compared to singular treatment alone.

Infection with $1x10^6$ cfu/mouse RP73 induced a significant increase in pulmonary bacterial load when compared to sham control animals (5.54±0.01 log cfu, versus sham: 0.0±0.0 log cfu, $p<0.0001$, **Figure 5.5A**). Singular treatments of 100 mg/kg Tobramycin (5.56±0.01 log cfu) or 1 mg/kg HT61 (5.65±0.02 log cfu) had no significant reduction in bacterial load when compared to vehicle controls (5.54±0.01 log cfu, **Figure 5.5A**). However, following combination treatment with 100 mg/kg Tobramycin and 1 mg/kg HT61, bacterial load was significantly reduced (4.51±0.12 log cfu, $p<0.0001$, **Figure 5.5A**) when compared to vehicle

controls (5.54±0.01 log cfu). A similar significant reduction in bacterial load was observed following treatment with 300 mg/kg Tobramycin (4.36±0.07 log cfu, p<0.0001, **Figure 5.5A**).

Infection with $1x10^6$ cfu/mouse RP73 induced a significant increase in total leukocyte ($6.35±0.72x10^5$ cells/mL, versus sham: $3.40±0.06x10^5$ cells/mL, p<0.05, **Figure 5.5B**) and neutrophil recruitment to the lungs ($5.34±0.40x10^5$ cells/mL, versus sham: $0.10±0.02x10^5$ cells/mL, p<0.0001, **Figure 5.5C**) when compared to sham controls.

These data demonstrated that singular treatments of 100 or 300 mg/kg Tobramycin or 1 mg/kg HT61 had no significant reduction in total leukocyte recruitment to the lungs when compared to vehicle controls (100 mg/kg Tobramycin: $4.23±1.05x10^5$ cells/mL, 300 mg/kg Tobramycin: $6.45±0.46x10^5$ cells/mL, 1 mg/kg HT61: $7.37±0.58x10^5$ cells/mL versus vehicle: $6.35±0.72x10^5$ cells/mL, **Figure 5.5B**). Similarly, combination therapy of Tobramycin and HT61 caused no significant reduction in total leukocyte recruitment to the lungs ($5.88 \times 10^5 \pm 0.26$ cells/mL, versus vehicle: $6.35 \times 10^5 \pm 0.72$ cells/mL, **Figure 5.5B**) when compared to vehicle controls.

Furthermore, both singular and combination therapies had no significant reduction in neutrophil recruitment to the lungs compared to vehicle controls (100 mg/kg Tobramycin: $3.16±1.03x10^5$ cells/mL, 300 mg/kg Tobramycin: $4.76±0.29x10^5$ cells/mL, 1 mg/kg HT61: $6.62±0.51x10^5$ cells/mL, combination therapy: $4.38±0.20x10^5$ cells/mL, versus vehicle: $5.34±0.40x10^5$ cells/mL, **Figure 5.5C**).

Infection with $1x10^6$ cfu/mouse RP73 induced a significant decrease in macrophage recruitment ($1.01±0.32x10^5$ cells/mL, versus sham: $3.30±0.08x10^5$ cells/mL, p<0.0001, **Figure 5.5D**) to the lungs, when compared to sham controls. Both singular and combination

therapies had no significant reduction in macrophage (100 mg/kg Tobramycin: 1.10±0.05x10^5 cells/mL, 300 mg/kg Tobramycin: 1.69±0.18x10^5 cells/mL, 1 mg/kg HT61: 0.76±0.08x10^5 cells/mL, combination therapy: 1.68±0.10x10^5 cells/mL, versus vehicle: 1.01±0.32x10^5 cells/mL, **Figure 5.5D**) or lymphocyte (100 mg/kg Tobramycin: 0.0±0.0x10^5 cells/mL, 300 mg/kg Tobramycin: 0.0±0.0x10^5 cells/mL, 1 mg/kg HT61: 0.0±0.0x10^5 cells/mL, combination therapy: 0.0±0.0x10^5 cells/mL, versus vehicle: 0.0±0.0x10^5 cells/mL) recruitment to the lungs when compared to vehicle controls.

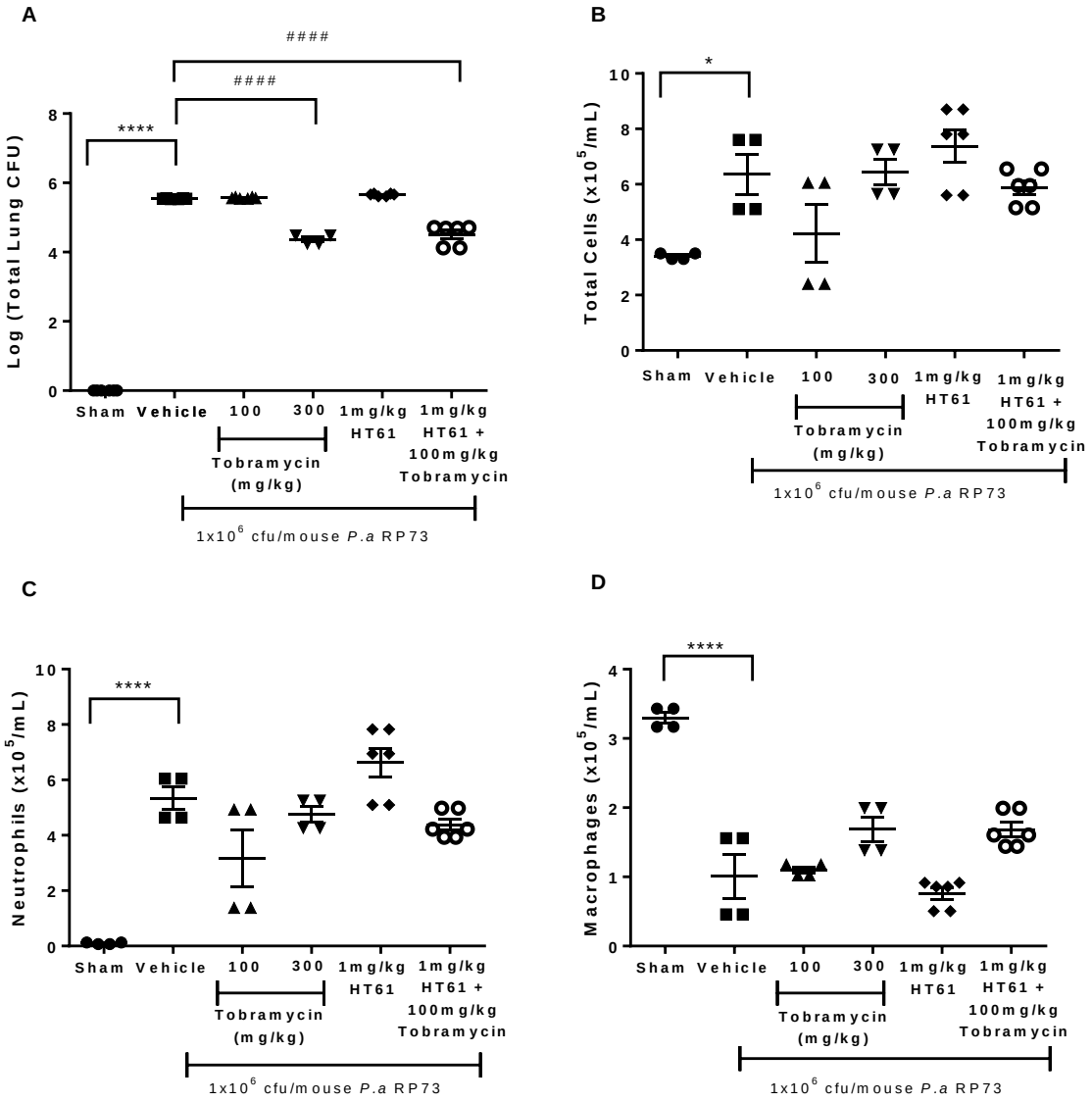

Figure 5.5 Effects of Combination Therapy of HT61 and Tobramycin on Infection with *P.aeruginosa* strain RP73

Mice were infected *(o.a)* with either sham or 1x10^6 cfu/mouse *P.aeruginosa* strain RP73 embedded agar beads. 24 hours post infection, mice were administered with singular treatments of either 100 or 300 mg/kg Tobramycin or 1 mg/kg HT61, combination therapy of 1 mg/kg HT61 and 100 mg/kg Tobramycin or vehicle, via *i.p* injection. A BAL of the lungs was performed for inflammatory cell quantification and lungs were aseptically removed, homogenised and plated for quantification of bacterial load at 48 h.p.i. Pulmonary Bacterial Load (**A**), Total Cells (**B**), Neutrophils (**C**) and Macrophages (**D**). One-way ANOVA and Bonferroni's multiple comparisons post hoc test, * $p<0.05$, **** $p<0.0001$ versus sham, #### $p<0.0001$ versus vehicle, n=4-6, data are presented as mean ± SEM.

5.3.2 Investigating the Effect of HT61 and Tobramycin in a Model of Pulmonary Infection with *P.aeruginosa* PAO1

Combination therapy with HT61 and Tobramycin significantly attenuated infection with RP73. We therefore performed additional experiments to determine whether combination therapy with HT61 and Tobramycin also significantly attenuates pulmonary bacterial infection with *P.aeruginosa* strain PAO1, a Tobramycin susceptible strain.

Infection with $1x10^6$ cfu/mouse PAO1 induced a significant increase in pulmonary bacterial load when compared to sham controls (4.70±0.13 log cfu, versus sham: 0.0±0.0 log cfu, $p<0.0001$, **Figure 5.6A**). Singular treatments of 50 mg/kg Tobramycin (5.06±0.11 log cfu) or 1 mg/kg HT61 (4.97±0.06 log cfu) had no significant reduction in bacterial load compared to vehicle controls (4.70±0.13 log cfu, **Figure 5.6A**). Similarly, combination therapy with 50 mg/kg Tobramycin and 1 mg/kg HT61, had no significant reduction in pulmonary bacterial load (5.0±0.06 log cfu, **Figure 5.6A**) when compared to vehicle controls (4.70±0.13 log cfu).

These data suggested that infection with $1x10^6$ cfu/mouse PAO1 induced a significant increase in total leukocyte ($9.70±1.06x10^5$ cells/mL, versus sham: $1.40±0.22x10^5$ cells/mL, $p<0.0001$, **Figure 5.6B**) and neutrophil recruitment to the lungs ($6.65±0.94x10^5$ cells/mL, versus sham: $0.0±0.00x10^5$ cells/mL, $p<0.0001$, **Figure 5.6C**) when compared to sham controls.

Singular treatments with 50 mg/kg Tobramycin or 1 mg/kg HT61 and combination therapy had no significant reduction in total leukocyte (50 mg/kg Tobramycin: $8.96±0.37x10^5$ cells/mL, 1 mg/kg HT61: $8.10±0.39x10^5$ cells/mL, combination therapy: $7.19±0.49x10^5$ cells/mL, versus vehicle: $9.70±1.06x10^5$ cells/mL, **Figure 5.6B**) or neutrophil recruitment to the lungs when compared to vehicle controls (50 mg/kg Tobramycin: $6.16±0.65x10^5$ cells/mL,

1 mg/kg HT61: 4.77±0.74x10^5 cells/mL, combination therapy: 4.06±0.67x10^5 cells/mL, versus vehicle: 6.65±0.94x10^5 cells/mL, **Figure 5.6C**).

Infection with 1x10^6 cfu/mouse PAO1 had no significant effect on macrophage (3.07±0.44x10^5 cells/mL, versus sham: 1.39±0.22x10^5 cells/mL, **Figure 5.6D**) or lymphocyte (0.0±0.0x10^5 cells/mL, versus sham: 0.0±0.0x10^5 cells/mL) recruitment to the lungs, when compared to sham controls. Furthermore, both singular and combination therapies had no significant effect on macrophage (50 mg/kg Tobramycin: 2.69±0.33x10^5 cells/mL, 1 mg/kg HT61: 3.55±0.33x10^5 cells/mL, combination therapy: 3.62±0.52x10^5 cells/mL, versus vehicle: 3.07±0.44x10^5 cells/mL, **Figure 5.6D**) or lymphocyte (50 mg/kg Tobramycin: 0.0±0.0x10^5 cells/mL, 1 mg/kg HT61: 0.0±0.0x10^5 cells/mL, combination therapy: 0.0±0.0x10^5 cells/mL, versus vehicle: 0.0±0.0x10^5 cells/mL) recruitment to the lungs when compared to vehicle controls.

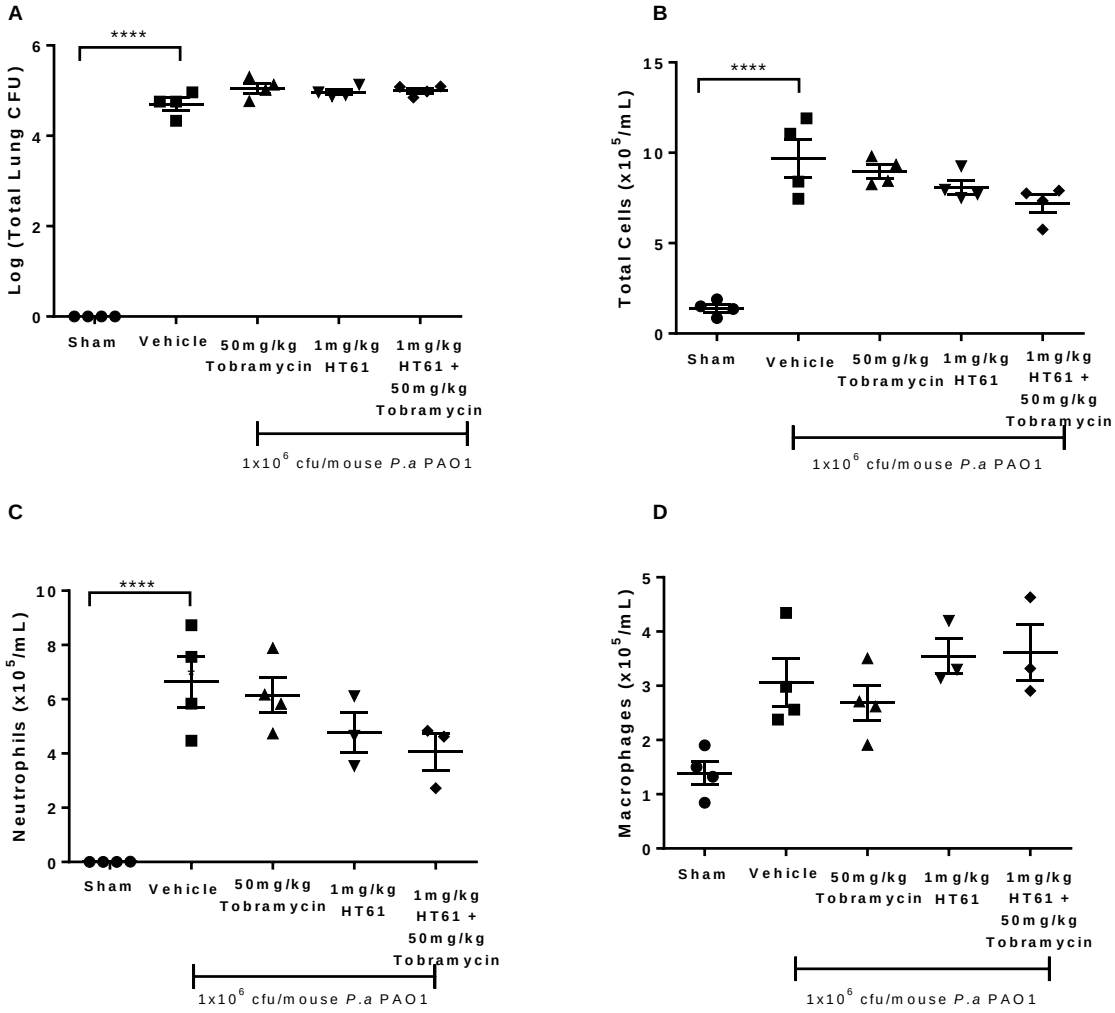

Figure 5.6 Effects of Combination Therapy of HT61 and Tobramycin on Infection with *P.aeruginosa* strain PAO1

Mice were infected *(o.a)* with either sham or 1x10^6 cfu/mouse *P.aeruginosa* strain PAO1 embedded agar beads. 24 hours post infection, mice were administered with singular treatments of either 50 mg/kg Tobramycin or 1 mg/kg HT61, combination therapy of 1 mg/kg HT61 and 50 mg/kg Tobramycin or vehicle, via *i.p* injection. A BAL of the lungs was performed for inflammatory cell quantification and lungs were aseptically removed, homogenised and plated for quantification of bacterial load at 48 h.p.i. Pulmonary Bacterial Load (**A**), Total Cells (**B**), Neutrophils (**C**) and Macrophages (**D**). One-way ANOVA and Bonferroni's multiple comparisons post hoc test, **** $p<0.0001$ versus sham, n=3-4, data are presented as mean ± SEM.

5.3.3 Investigating the Effect of HT61 and Tobramycin in a Model of Pulmonary Infection with *P.aeruginosa* NN2

Experiments were performed to determine whether combination therapy with HT61 and Tobramycin significantly attenuates pulmonary bacterial infection with a Tobramycin resistant strain of *P.aeruginosa*, compared to singular treatment alone.

Infection with $1x10^6$ cfu/mouse NN2 induced a significant increase in pulmonary bacterial load when compared to sham controls (6.64±0.28 log cfu, versus sham: 0.0±0.0 log cfu, $p<0.0001$, **Figure 5.7A**). Singular treatments of 100 mg/kg Tobramycin (6.02±0.13 log cfu), 200 mg/kg Tobramycin (6.63±0.32 log cfu), or 1 mg/kg HT61 (6.61±0.26 log cfu) had no significant reduction in bacterial load when compared to vehicle controls (6.64±0.28 log cfu, **Figure 5.7A**). However, following combination therapy of 100 mg/kg Tobramycin and 1 mg/kg HT61, a significant synergistic reduction in bacterial load was observed (5.49±0.33 log cfu, $p<0.05$, **Figure 5.7A**) when compared to vehicle controls (6.64±0.28 log cfu).

Infection with $1x10^6$ cfu/mouse NN2 induced a significant increase in total leukocyte ($4.53±0.21x10^5$ cells/mL, versus sham: $0.17±0.0x10^5$ cells/mL, $p<0.01$, **Figure 5.7B**) and neutrophil recruitment to the lungs ($4.46±0.19x10^5$ cells/mL, versus sham: $0.0±0.0x10^5$ cells/mL, $p<0.01$, **Figure 5.7C**) when compared to sham controls.

Singular treatments of 100 and 200 mg/kg Tobramycin and 1 mg/kg HT61 and combination therapy of 100 mg Tobramycin and 1 mg/kg HT61 had no significant reduction in total leukocyte (100 mg/kg Tobramycin: $2.37±0.31x10^5$ cells/mL, 200 mg/kg Tobramycin: $3.76±0.46x10^5$ cells/mL, 1 mg/kg HT61: $4.07±0.99x10^5$ cells/mL, combination therapy: $2.84±1.24x10^5$ cells/mL, versus vehicle: $4.53±0.21x10^5$ cells/mL, **Figure 5.7B**) and neutrophil recruitment (100 mg/kg Tobramycin: $2.07±0.29x10^5$ cells/mL, 200 mg/kg Tobramycin:

3.73±0.43x10^5 cells/mL, 1 mg/kg HT61: 3.69±0.91x10^5 cells/mL, combination therapy: 2.25±1.13x10^5 cells/mL, versus vehicle: 4.46±0.19x10^5 cells/mL, **Figure 5.7C**) to the lungs when compared with vehicle controls.

Infection with 1x10^6 cfu/mouse NN2 had no significant effect on macrophage (0.07±0.02x10^5 cells/mL, versus sham: 0.17±0.00x10^5 cells/mL, **Figure 5.7D**) or lymphocyte (0.0±0.0x10^5 cells/mL, versus sham: 0.0±0.00x10^5 cells/mL) recruitment to the lungs, when compared to sham controls. Singular treatment of 100 mg/kg Tobramycin had no significant effect on macrophage recruitment to the lungs when compared to vehicle controls (100 mg/kg Tobramycin: 0.30±0.03x10^5 cells/mL, **Figure 5.7D**). However, singular treatments of 200 mg/kg Tobramycin or 1 mg/kg HT61 and combination therapy of 100 mg/kg Tobramycin and 1 mg/kg HT61 had a significant increase in macrophage recruitment to the lungs when compared to vehicle controls (200 mg/kg Tobramycin: 0.39±0.02x10^5 cells/mL, 1 mg/kg HT61: 0.38±0.08x10^5 cells/mL, combination therapy: 0.60±0.12x10^5 cells/mL, versus vehicle: 0.07±0.02x10^5 cells/mL, **Figure 5.7D**). Both singular and combination therapies had no significant effect on lymphocyte recruitment to the lungs when compared to vehicle controls (100 mg/kg Tobramycin: 0.0±0.0x10^5 cells/mL, 200 mg/kg Tobramycin: 0.0±0.0x10^5 cells/mL, 1 mg/kg HT61: 0.0±0.0x10^5 cells/mL, combination therapy: 0.0±0.0x10^5 cells/mL, versus vehicle: 0.0±0.0x10^5 cells/mL).

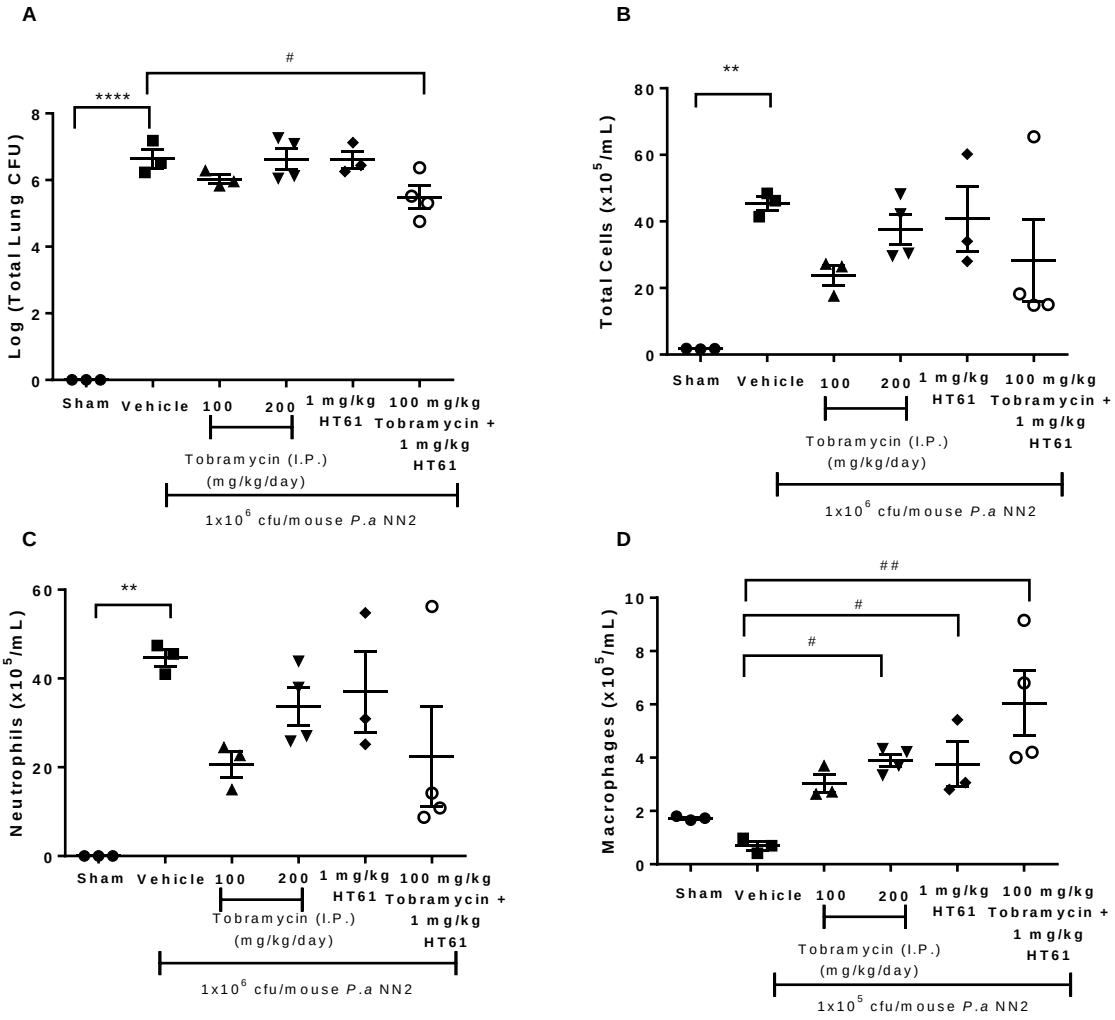

Figure 5.7 Effects of Combination Therapy of HT61 and Tobramycin on Infection with *P.aeruginosa* strain NN2

Mice were infected *(o.a)* with either sham or 1x10^6 cfu/mouse *P.aeruginosa* strain NN2 embedded agar beads. 24 hours post infection, mice were administered with singular treatments of either 100 or 200 mg/kg Tobramycin or 1 mg/kg HT61, combination therapies of 1 mg/kg HT61 and 100 mg/kg Tobramycin or vehicle, via *i.p* injection. A BAL of the lungs was performed for inflammatory cell quantification and lungs were aseptically removed, homogenised and plated for quantification of bacterial load at 48 h.p.i. Pulmonary Bacterial Load (**A**), Total Cells (**B**), Neutrophils (**C**) and Macrophages (**D**). One-way ANOVA and Bonferroni's multiple comparisons post hoc test, ** p<0.01, **** p<0.0001 versus sham, # p<0.05, ## p<0.01 versus vehicle, n=3-4, data are presented as mean ± SEM.

5.4 Investigating the Effect of HT61 and Vancomycin Combination Therapy in a Model of Pulmonary Infection with Gram- Positive MRSA

5.4.1 Investigating the Effect of HT61 and Vancomycin in a Model of Pulmonary Infection with MRSA strain USA300

A synergistic effect and a significant attenuation of pulmonary bacterial load was observed following combination therapy of HT61 and Tobramycin against two out of the three tested *P.aeruginosa* strains. Therefore, additional experiments were performed to determine whether this effect could be replicated against a gram-positive species of bacteria, MRSA, strain USA300.

Infection with $1x10^6$ cfu/mouse USA300 induced a significant increase in pulmonary bacterial load when compared to sham controls (5.57±0.11 log cfu, versus sham: 0.0±0.0 log cfu, $p<0.0001$, **Figure 5.8A**). Single treatments of 100 mg/kg Vancomycin (5.81±0.30 log cfu) or 1 mg/kg HT61 (6.03±0.36 log cfu) had no significant reduction in bacterial load when compared to vehicle controls (5.57±0.11 log cfu, **Figure 5.8A**). Furthermore, combination therapy of 100 mg/kg Vancomycin and 1 mg/kg HT61, had no significant reduction in pulmonary bacterial load (5.92±0.13 log cfu, **Figure 5.8A**) when compared to vehicle controls (5.57±0.11 log cfu).

Infection with $1x10^6$ cfu/mouse USA300 induced a significant increase in total leukocyte ($27.90±7.92x10^5$ cells/mL, versus sham: $2.01±0.30x10^5$ cells/mL, $p<0.01$, **Figure 5.7B**) and neutrophil recruitment to the lungs ($24.31±6.73x10^5$ cells/mL, versus sham: $0.04±0.03x10^5$ cells/mL, $p<0.01$, **Figure 5.8C**) when compared to sham controls.

Both singular treatments of 100 mg/kg Vancomycin and 1 mg/kg HT61 and combination therapy produced no significant reduction in total leukocyte recruitment to the lungs, when

compared to vehicle controls (100 mg/kg Vancomycin: 19.93±5.84x10^5 cells/mL, 1 mg/kg HT61: 20.18±1.98x10^5 cells/mL, combination therapy: 17.30±4.14x10^5 cells/mL, versus vehicle: 27.90±7.92x10^5 cells/mL, **Figure 5.8B**).

This was also reflected by the neutrophil quantification, whereby both singular treatments and combination therapy had no significant reduction on neutrophil recruitment to the lungs when compared to vehicle controls (100 mg/kg Vancomycin: 16.82±6.12x10^5 cells/mL, 1 mg/kg HT61: 17.82±1.61x10^5 cells/mL, combination therapy: 15.0±3.74x10^5 cells/mL, versus vehicle: 24.31±6.73x10^5 cells/mL, **Figure 5.8C**).

Infection with 1x10^6 cfu/mouse USA300 had no significant effect on macrophage (3.59±1.21x10^5 cells/mL, versus sham: 1.98±0.32x10^5cells/mL, **Figure 5.8D**) or lymphocyte (0.0±0.0x10^5 cells/mL, versus sham: 0.0±0.0x10^5cells/mL) recruitment to the lungs when compared to sham controls. Furthermore, both singular and combination therapy had no significant effect on macrophage (100 mg/kg Vancomycin: 3.11±0.41x10^5 cells/mL, 1 mg/kg HT61: 2.46±0.56x10^5 cells/mL, combination therapy: 2.31±0.42x10^5 cells/mL, versus vehicle: 3.59±1.21x10^5 cells/mL, **Figure 5.8D**) or lymphocyte recruitment (100 mg/kg Vancomycin: 0.0±0.0x10^5 cells/mL, 1 mg/kg HT61: 0.0±0.0x10^5 cells/mL, combination therapy: 0.0±0.0x10^5 cells/mL, versus vehicle: 0.0±0.0x10^5 cells/mL) to the lungs, when compared to vehicle controls.

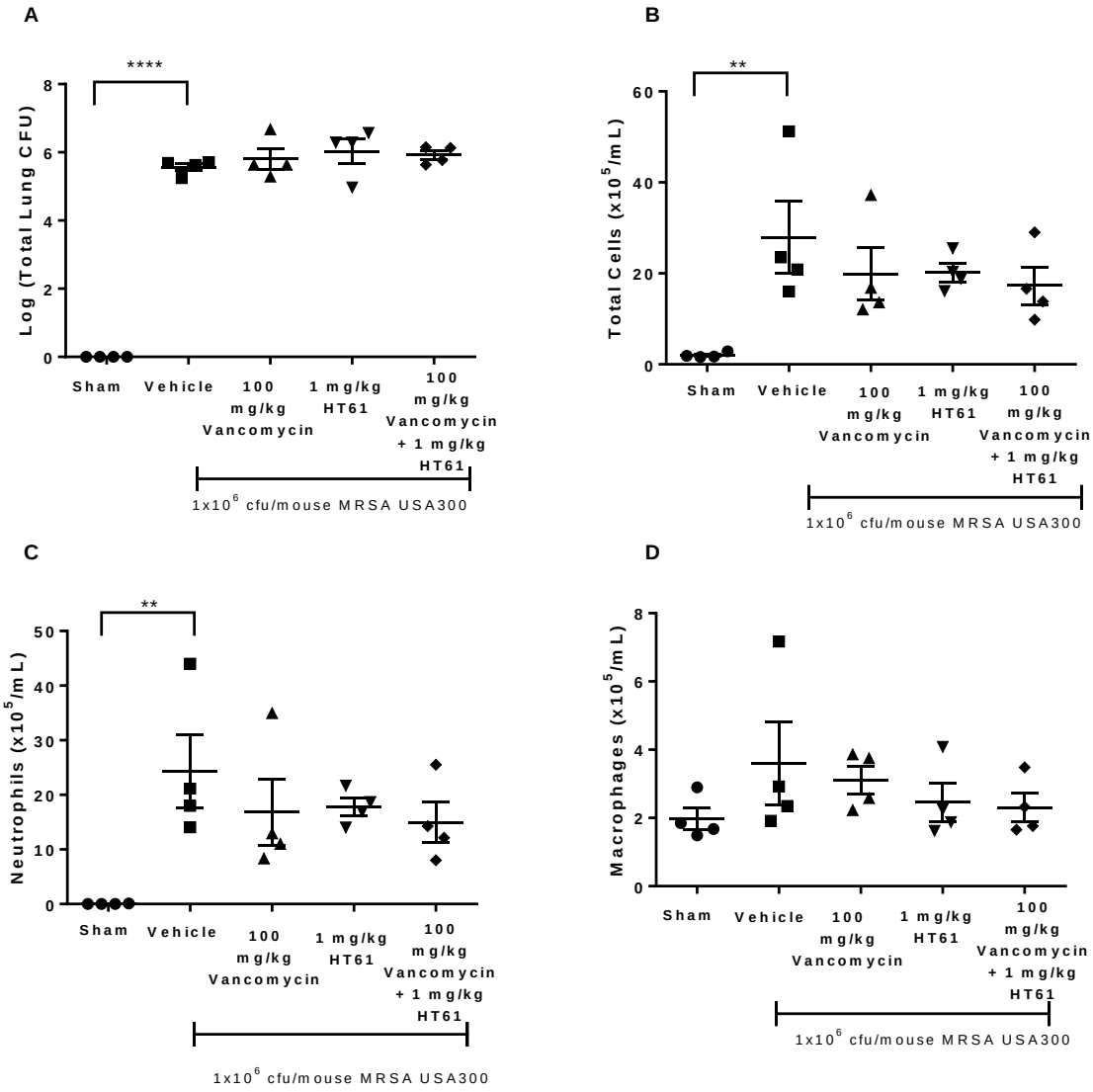

Figure 5.8 Effects of Combination Therapy of HT61 and Vancomycin on Infection with MRSA strain USA300

Mice were infected *(o.a)* with either sham or $1x10^6$ cfu/mouse MRSA strain USA300 embedded agar beads. 24 hours post infection, mice were administered with singular treatments of either 100 mg/kg Vancomycin or 1 mg/kg HT61, combination therapy of 1 mg/kg HT61 and 100 mg/kg Vancomycin or vehicle, via *i.p* injection. A BAL of the lungs was performed for inflammatory cell quantification and lungs were aseptically removed, homogenised and plated for quantification of bacterial load at 48 h.p.i. Pulmonary Bacterial Load (**A**), Total Cells (**B**), Neutrophils (**C**) and Macrophages (**D**). One-way ANOVA and Bonferroni's multiple comparisons post hoc test, ** $p<0.01$, **** $p<0.0001$ versus sham, n=4, data are presented as mean ± SEM.

Chapter VI

Discussion

6.1 Establishment and Validation of a Murine Model of Pulmonary Infection

Initial experiments were required to establish a murine model of pulmonary infection using three strains of *P.aeruginosa* and one strain of MRSA, to produce an infection and inflammatory profile representative of a chronic pulmonary infection observed in the clinic.

Experimental models may be established in order to investigate infection and inflammatory parameters, and the underlying signalling pathways associated with chronic pulmonary infections. *P.aeruginosa* is an opportunistic pathogen that exploits immunocompromised hosts. *P.aeruginosa* is frequently associated with the CF lung and the establishment of chronic infection, and is also a common cause of acute lower-respiratory tract infections in critically ill patients. Intrapulmonary infection with *P.aeruginosa* was initially profiled *in vivo* as it is plays a critical role in the development and progression of multiple pulmonary diseases (Van Heeckeren et al., 1997) (Growcott et al., 2011) (Bragonzi et al., 2012). My findings demonstrated that pulmonary instillation of $1x10^6$ cfu/mouse *P.aeruginosa* embedded into agar beads resulted in the establishment of a non-lethal localised infection. The establishment of infection is one of the major challenges in experimental models of pulmonary infection, with previous studies demonstrating that both aerosol and direct tracheal instillation have resulted in the establishment of a transient pulmonary infection (Cash et al., 1979). Literature has suggested that the establishment of a chronic pulmonary infection can be achieved only if mice are inoculated with bacteria embedded in an immobilising agent such as agar, agarose, or seaweed alginate (Facchini et al., 2014) (Bragonzi, 2010). Therefore, bacteria were embedded into agar beads for the induction of an infection in my studies. $1x10^6$ cfu/mouse was chosen as the optimum inoculum for pulmonary infection studies with *P.aeruginosa* strains RP73, PAO1 and NN2 producing the desired infection profile. Similar studies

performed by (Facchini et al., 2014), demonstrated that infection with $1x10^6$ cfu/mouse *P.aeruginosa* RP73 resulted in a bacterial burden of $1.3x10^6$ cfu/lung recovered from the lungs, however this data represented the sum of the bacterial burden present in both BAL fluid and the lungs and was determined at 3 d.p.i. Other dose-dependent infection studies using PAO1 embedded into agar beads have indicated that a dose in the range of $10^{6-}10^7$ cfu/mouse established an infection associated with low mortality, thus showing consistency with my findings (Bragonzi, 2010).

The emergence of community acquired MRSA, as distinct from hospital strains, has been reported in Australasia, Europe, and North America (Durrington and Summers, 2008). MRSA strain USA300 is a major source of community acquired infections and has been implicated in epidemiologically outbreaks of skin and soft tissue infections in healthy individuals (Diep et al., 2006) (Klevens et al., 2007). I therefore investigated the infection and inflammatory parameters associated with intrapulmonary infection with MRSA strain USA300. Similar to the results obtained for *P.aeruginosa*, intrapulmonary infection with MRSA induced a non-lethal, localised infection, associated with a neutrophilic infiltrate. Studies performed by others (Cigana et al., 2018) have demonstrated that infection with $1x10^6$ cfu/mouse USA300 produced a similar inflammatory profile, although infection in this model was associated with a high mortality occurring within 4 days. Mortality was not directly quantified in my model however, at 48 h.p.i no mortality was observed.

Pulmonary bacterial infections are typically characterised by an inflammatory response dominated by a neutrophilic infiltrate in the airways (Courtney et al., 2004) (Houston et al., 2013). Consistent with clinical observations, the findings shown in this study highlighted a clear pro-inflammatory effect of both *P.aeruginosa* and MRSA infection as measured by a

significant increase in both neutrophils and cytokines in the BAL fluid and lung tissue of infected mice when compared to sham controls. An inflammatory infiltrate primarily neutrophilic in nature in response to infection is consistent with published literature in a rat model of chronic respiratory infection with *P.aeruginosa* (Cash et al., 1979) and in murine models of pulmonary infection with *P.aeruginosa* (Bayes et al., 2016) (Tam et al., 1999) (Van Heeckeren et al., 2002) (Van Heeckeren et al., 2006) (Bragonzi, 2010), compared to the presence of alveolar macrophages in sham controls. These findings are further supported following infection with RP73, whereby the inflammatory infiltrate in the airway lumen and alveolar spaces is predominantly composed of neutrophils (80%), (Facchini et al., 2014), although the inflammatory profile in this case was characterised at 7 days post infection. Moreover, the histological features and the increase in neutrophils observed in BAL fluid are consistent with data published by others (Boyer et al., 2005) (Growcott et al., 2011) (Liu et al., 2013) (Gregory et al., 2007) at the same time point following infection with PAO1 in mice and rats.

Inflammatory markers, including IL-6 and IL-8, are significantly elevated in chronic neutrophilic inflammation (Carpagnano et al., 2003) and infection (Takahashi et al., 2016). IL-6 contributes to host defence through stimulation of the acute phase response and haematopoiesis (Tanaka et al., 2014) and IL-8 is involved in neutrophil activation and recruitment (Sawant et al., 2016). The findings shown in this study suggested that pulmonary infection with *P.aeruginosa* and MRSA is associated with significant increases in the pro-inflammatory cytokines IL-6 and KC (the murine analogue of human IL-8). These data are consistent with studies performed by others (Van Heeckeren et al., 2000), whereby *P.aeruginosa* infected mice had a rapid, transient rise in IL-6, KC and absolute neutrophil counts in BAL fluid. Similarly, others (Cigana et al., 2018) have demonstrated a significant

increases in BAL levels of IL-6 following infection with clinical isolates of *S.aureus.* Interestingly, the significant rise in the neutrophil chemoattractant KC correlated with the rise in neutrophils observed in this model, perhaps suggesting a mechanism underlying neutrophil recruitment, although this requires further investigation.

The standard of care therapy for patients with pulmonary infections with *P.aeruginosa*, such as CF, involves the use of aminoglycoside and β-lactam antibiotics (Marier et al., 2003). Aggressive treatment regimens using aerosolised Tobramycin have been shown to improve the quality of life of patients, reducing symptoms of acute pulmonary exacerbations (Marier et al., 2003) (Scheinberg and Shore, 2005). Following establishment of the murine model of pulmonary infection, I aimed to validate the model using drugs used clinically to treat pulmonary infections with *P.aeruginosa* and MRSA.

For mice infected with the multidrug resistant strain of *P.aeruginosa*, RP73, high doses of Tobramycin (~300 mg/kg) were required to significantly attenuate pulmonary bacterial load at 48 h.p.i. Additionally, for the remaining strains of *P.aeruginosa* complete eradication of *P.aeruginosa* was not achieved, although, this may be due to the dosing regimen used in my studies as only a single treatment was administered. In comparison, single intratracheal treatments with conventional formulations of Tobramycin had no significant effect against *P.aeruginosa* infection in rats, although multiple doses of Tobramycin have previously shown efficacy (Marier et al., 2003). Similarly, previous studies using a murine model of *P.aeruginosa* PAO1 pneumonia have indicated a 4 log reduction in pulmonary bacterial load following *i.p* treatment of 150 mg/kg/day of Tobramycin (Louie et al., 2013). Although in this instance, Tobramycin was administered on a humanised dosing scheme administered every 4 hours over a 24-hour time period. This suggests that altering the dosing regimen in my model may

improve the efficacy of Tobramycin in this model, whereby multiple doses may increase penetration of the antibiotic, improve pulmonary function and eradicate the colonisation of *P.aeruginosa.* Other research suggests that the combination of Tobramycin with additional antibiotics, such as Meropenem may also enhance the reduction in bacterial burden (Louie et al., 2013).

Tobramycin treatment appeared to reduce the inflammatory infiltrate in response to infection with PAO1, although these data did not reach statistical significance. This result may be an indirect effect on inflammation as a result of Tobramycin reducing the pulmonary bacterial burden. These findings are supported by a clinical study, which demonstrated that inhaled Tobramycin therapy eradicated *P.aeruginosa* infection from the lower airways in 74% of patients and significantly reduced airway neutrophilic inflammation (Chuchalin et al., 2009).

Moreover, other literature has suggested through both clinical studies and experimental models that Tobramycin treatment failed to reduce bacterial numbers yet significantly reduced *P.aeruginosa* exoenzyme activity (Grimwood et al., 1993), which contributes to lung injury frequently observed during pulmonary infection. These results suggest that Tobramycin may improve pulmonary function by decreasing *P.aeruginosa* exoenzyme expression, regardless of any other antimicrobial effect. Whilst research has demonstrated that Tobramycin reduces pro-inflammatory cytokines, including IL-8, IL-6 and TNF-α, in *P.aeruginosa* infected CF patients (Husson et al., 2005), this was not quantified in my model.

Vancomycin has been considered to be the reference standard of therapy for the treatment of infections with MRSA (Tang et al., 2015), hence I validated the murine model of pulmonary infection with MRSA using this antibiotic. My results demonstrated that Vancomycin

treatment at 200 mg/kg significantly attenuated pulmonary infection with MRSA at 48 h.p.i, in agreement with results obtained in the literature using a murine model of pulmonary infection with MRSA embedded into agar beads (Harada et al., 2013). In these experiments a 2.5 log reduction in pulmonary bacterial load was obtained at 3 days post infection, although Vancomycin treatment was administered at 50 mg/kg *i.p.* every 12 hours (Harada et al., 2013), perhaps explaining the more dramatic decrease in pulmonary bacterial burden when compared to those observed in these studies. This study further highlights that the optimum dosing regimen and formulation of antibiotic are essential in order to achieve the greatest possible reduction in bacterial load.

After validation of these models, subsequent research was performed to investigate the role of platelets in the regulation of pulmonary infection and host defence, as described in the next section.

6.2 The Role of Platelets in the Regulation of Pulmonary Infection and Host Defence

The role of platelets in haemostatic and thrombotic processes has been extensively documented in response to vascular injury (Brass, 2010) (Kuijpers et al., 2004) (Li et al., 2010) (Rivera et al., 2009) (Andrews and Berndt, 2004). More recently however, platelets have received increasing attention for their role in the pathophysiology of inflammation, infection and immunity (Pitchford et al., 2003) (Bunescu et al, 2004) (Gresele et al., 1993) (Ortiz-Muñoz et al., 2014) (Van den Boogaard et al., 2015) (de Stoppelaar, 2014) (Wuescher et al., 2015) (Amison et al., 2015) (Amison et al., 2018).

Thrombocytopenia is a common finding in patients with sepsis (de Stoppelaar, 2014) (Hurley et al,. 2016), and is a well-known biomarker for disease severity (Gafter-Gvili et al., 2011) (Claushuis et al., 2016) (Goto et al., 2018). A low platelet count is associated with an adverse outcome and strongly impaired host defence system, significantly enhancing morality in critically ill patients (Xiang et al., 2013) (Claushuis et al., 2016) (Goto et al., 2018). Initial experiments were therefore performed to determine whether systemic thrombocytopenia occurs during pulmonary infection with *P.aeruginosa* or MRSA. Here, I demonstrated that intrapulmonary infection with both *P.aeruginosa* and MRSA induced a mild peripheral thrombocytopenia, demonstrated by a significant decrease in circulating platelet numbers. In comparison, other experimental models have verified platelet consumption in a mouse model of invasive *S.pyogenes* infection. At 12 and 18 h.p.i, mice exhibited significantly decreased circulating platelet numbers (Hurley et al., 2016) when compared to the initial time of infection. Collectively, these data provide evidence that platelets rapidly respond to infection and support the clinical observation that patients with sepsis display thrombocytopenia.

There are several proposed mechanisms to explain the occurrence of infection induced thrombocytopenia, including platelet sequestration (Aster, 1966) and direct platelet activation during acute inflammation, resulting in a shortened platelet lifespan (Taytard et al., 1986). Previous research has stated that platelets are recruited to sites of inflammation (Pitchford et al., 2003)(Lax et al., 2017) (Boilard et al., 2010), and there is now compelling evidence to suggest that individual platelets can migrate towards bacterial products (Ortiz-Muñoz et al., 2014) (Czapiga et al., 2005) and act as cellular scavengers, migrating towards and collecting deposited bacteria (Gaertner et al., 2017).

It was therefore hypothesized that the occurrence of peripheral thrombocytopenia in response to infection may occur as a consequence of platelet activation and accumulation of activated platelets in lung tissue. It has been demonstrated that platelets are the first and most abundant inflammatory cell type recruited in response to infection (Kerrigan, 2015). Therefore, experiments were performed to investigate whether platelet activation and accumulation occurred in lung tissue at 24 h.p.i. A significant increase in extravascular pulmonary platelet accumulation was observed following infection with $1x10^6$ cfu/mouse *P.aeruginosa*, providing a plausible mechanism to explain the observed systemic thrombocytopenia. This is in agreement with published literature demonstrating pulmonary platelet accumulation following exposure to *E.coli* endotoxin (Itoha et al., 1996) and platelet accumulation in the liver sinusoids and hepatic circulation in response to infection with *S.pyogenes* (Hurley et al., 2016) and *E.coli* (Gaertner et al., 2017). Moreover, an *in vitro* chemotaxis model was developed to determine whether platelets are able to directly migrate towards bacterial stimuli. Further supporting my *in vivo* findings, the chemotaxis assay validated platelet migration across a membrane towards bacteria, further describing the potential for platelet accumulation at sites of infection.

Numerous reports have indicated that platelets possess direct antimicrobial functions, acting as a source of an array of antimicrobial peptides (Yang et al., 2015) (Yeaman, 2010) (Krijgsveld et al., 2000) (Tang et al., 2002) (Kraemer et al., 2011) (Dewitte et al., 2017) (Ali et al., 2017), which are released from internal granules upon platelet activation. Furthermore, experimental models of pulmonary infection have demonstrated platelet activation in response to bacterial infection, with an array of bacterial species including *S.aureus, S.pyogenes* and *K.pneumoniae* (Youssefian et al., 2002) (Hurley et al., 2016) (Shannon, 2015) (de Stoppelaar, 2014) (de Stoppelaar et al., 2015). Platelet activation induced by bacteria has

resulted in marked increases in P-selectin surface expression (Youssefian et al., 2002), platelet-neutrophil complexes (Hurley et al., 2016) and PF-4 secretion from platelet granules (de Stoppelaar, 2014). Consistent with bacterial induced platelet activation observed in the literature (Youssefian et al., 2002) (Hurley et al., 2016) (Shannon, 2015) (de Stoppelaar, 2014) (de Stoppelaar et al., 2015) (Kahn et al., 2013), my results demonstrated enhanced platelet activation in response to infection with $1x10^6$ cfu/mouse *P.aeruginosa*, as measured by significant increases in platelet-neutrophil complexes and BAL levels of RANTES and PF-4 released in infected mice. Intriguingly, plasma levels of PF-4 were not significantly elevated, perhaps indicating PF-4 is only released at the site of the infection. This is consistent with other findings (Amison et al., 2018), whereby it was demonstrated that PF-4 is only significantly elevated at the site of infection. It is worth noting that platelet-neutrophil complexes have been reported to increase during early sepsis but decreased significantly during late sepsis (Hurley et al., 2016). This perhaps suggests that platelets have reached their maximum activation state and become exhausted in response to infection, although this requires further investigation. As platelet-neutrophil complexes were only quantified at 24 h.p.i in my model, it would therefore be interesting to monitor this at a later time point.

Platelets express an array of cell surface receptors allowing both direct and indirect interactions with bacteria (Dewitte et al., 2017) (Deppermann and Kubes, 2016). Platelets express functional Toll-like receptors (TLR2, TLR4), which recognise bacterial peptidoglycans and LPS in gram-positive and gram-negative pathogens respectively (Andonegui et al., 2005) (Aslam et al., 2016). In addition, platelets variably express GPIbα, FcγRIIa, $\alpha_{IIb}\beta_3$ receptors (Bennett, 2005) (Karas et al., 1982) (Lopez, 1994), which facilitate direct and indirect interactions with bacteria. This provides a plausible mechanism that may contribute to bacterial induced platelet activation in numerous infectious diseases, including sepsis, CF and

multiple organ dysfunction syndrome (MODS) (Russwurm et al., 2002) (Ogura et al., 2001) (O'Sullivan et al., 2005) (Gawaz et al., 1997), which has been suggested to precede platelet recruitment (Hurley et al., 2016).

To further investigate the role of platelets in infection and host defence, I established an experimentally induced platelet depletion model with pulmonary infection using *P.aeruginosa* and MRSA, adapted from a well-documented model originally described by (Cash et al., 1979), and used regularly to date (Facchini et al., 2014) (Bayes et al., 2016) (Van Heeckeren et al., 2000). In order to produce profound platelet depletion, an anti-GPIbα platelet depleting antibody was utilised to deplete mice of circulating platelets. This method of platelet depletion significantly reduced circulating platelet numbers and has been used previously in the literature in both models of infection (de Stoppelaar, 2014) (Asaduzzaman et al., 2009) and inflammation (Amison et al., 2018). In addition, peripheral blood leukocyte populations remained unaltered by this method of platelet depletion, although these data were not shown. Alternative methods of platelet depletion have also been utilised in order to render animals thrombocytopenic in the literature, including an anti-mouse CD42b antibody (Kahn et al., 2013), anti-platelet anti-serum and bulsulfan (Pitchford et al., 2003)(Amison et al., 2015). Other methods of platelet depletion have been associated with inherent problems regarding long-term infection and chronic disease, including $a_{IIb}\beta_3$ inducing anaphylactic shock in mice (Wuescher et al., 2015). My rationale for choosing the anti- GPIbα platelet depleting antibody was due to reports in the literature that mice receiving this antibody do not display pulmonary oedema, haemorrhage or weight loss beyond 10% (Amison et al., 2018) (Xiang et al., 2013). However, the results were suggestive of minor pulmonary haemorrhage in response to administration of the anti-GPIbα platelet depleting antibody in both sham and infected groups. Indeed, other groups have reported that thrombocytopenia results in lung

haemorrhage following exposure to both inflammatory (Goerge et al., 2008) and infectious stimuli (de Stoppelaar, 2014), consistent with my findings. In these studies, very low platelet count mice demonstrated severe haemorrhaging in the lungs following infection with *K.pneumonaie*, whereas infected low platelet count mice revealed sites of haemorrhage albeit to a much lesser extent than in very low platelet count mice (de Stoppelaar, 2014). Similarly, other published research has reported that *i.v* administration of the anti-GPIbα platelet depleting antibody, which lowered platelet count to less than 2.5%, induced severe lung haemorrhage, however 10-15% of normal platelet counts was sufficient to prevent inflammatory bleeding (Goerge et al., 2008). This suggests that the level of platelet depletion in my studies may account for the observed haemorrhaging in the lungs in platelet depleted groups.

Consistent with my preliminary pulmonary infection studies (discussed in section 6.1), mice experimentally depleted of circulating platelets were initially infected with $1x10^6$ cfu/mouse *P.aeruginosa*. Here I provided compelling evidence to suggest that platelet depletion in mice enhances the pathogenicity of pulmonary infection with *P.aeruginosa,* with an increased weight loss, increased mortality and higher pulmonary bacterial burden observed. Compared to non-thrombocytopenic mice, pulmonary bacterial load significantly increased by 1.5 logs over the course of 24 hours, whilst the mortality rate observed in these mice was greatly elevated (40%). In order to refine and reduce severity of the model, thrombocytopenic mice were infected with the lower inocula of $1x10^4$ and $1x10^5$ cfu/mouse *P.aeruginosa.* Intriguingly, the $1x10^4$ cfu/mouse level of inoculum was completely cleared by 24 hours, whilst $1x10^5$ cfu/mouse was associated with an increased pulmonary bacterial load (0.5 logs) and mortality rate (20%) when compared to non-thrombocytopenic mice, albeit to a lesser extent than that of the $1x10^6$ cfu/mouse inoculum. Having established a thrombocytopenic infection model

with *P.aeruginosa*, thrombocytopenic mice were infected with $1x10^5$ cfu/mouse MRSA. Similarly, platelet depletion in this model resulted in a higher bacterial burden and increased weight loss, suggesting that platelets protect against both gram-negative and gram-positive bacterial species.

Similar studies using experimentally induced thrombocytopenic infection models have demonstrated an enhanced total bacterial burden per mouse following infection with *S.aureus*, strain USA300 (Wuescher et al., 2015). However, a novel experimental model of conditional platelet depletion based on the Cre-recombinase cell ablation system was used to obtain these data (Wuescher et al., 2015), therefore a direct comparison with my data which used a different method of platelet depletion cannot be performed. Consistent with my findings, experimentally induced thrombocytopenia has been shown to dramatically impair host defence during infection, increasing mortality and enhancing bacterial growth during both *Klebsiella* and *Streptococcus*-induced pneumonia (de Stoppelaar, 2014) (van den Boogaard et al., 2015) and also in LPS-induced endotoxemia (Xiang et al., 2013). In contrast, it has been reported that weight loss in response to infection with *S.pyogenes* is less aggressive and less bacteria were recovered from the lungs of platelet depleted animals (Kahn et al., 2013). In these studies, an anti-CD42b antibody (*i.p)* was used to render mice thrombocytopenic to 15% of their normal circulating platelet levels and infection was induced using a bacterial culture of $1.5\text{-}3x10^7$ cfu *S.pyogenes (i.p)* (Kahn et al., 2013), perhaps suggesting that different bacterial provocations and different methods of platelet depletion may elicit a different response. Moreover, I demonstrated that the removal of circulating platelets from the $1x10^5$ and $1x10^6$ infection models converts the infection from non-lethal and non-systemic, to one displaying the presence of systemic infection in both the kidneys and spleen. Similarly in the literature, mice experimentally depleted of circulating platelets

are associated with higher systemic bacterial loads in the blood and distal organs in *pneumococcal* pneumonia (van den Boogaard et al., 2015), *Klebsiella*-derived pneumonia (de Stoppelaar, 2014) and *S.aureus* bacteraemia (Wuescher et al., 2015). In addition, research has stated that bacterial sepsis and organ failure is exacerbated in mice experimentally depleted of circulating platelets. Significant increases in the inflammatory cytokines IL-10, IL-6, IFN-γ and TNF-α were observed in mice experimentally depleted of circulating platelets, cytokines which are frequently associated with sepsis lethality and play important roles in the development of ARDS (Wuescher et al., 2015) (de Stoppelaar, 2014) (Xiang et al., 2013). These studies provide compelling evidence to suggest that thrombocytopenic mice succumbed to infection much more rapidly than non-thrombocytopenic mice.

Metabolic acidosis is a common finding in patients with sepsis and is indicative of MODS (Kellum, 2004). Having observed an increase in mortality in platelet depleted animals, I investigated the potential cause of death in these animals by assessing biochemical markers of metabolic acidosis present in the blood following infection with *P.aeruginosa* $1x10^5$ cfu/mouse. Consistent with my previous findings, the data suggested the conversion of a phenotype associated with localised infection to one displaying systemic infection, as demonstrated by subtle increases in key biochemical markers of metabolic acidosis, including pCO_2, base excess and $HCO3^-$. Whilst these data did not show any significant differences, the absolute values observed were comparable with previously published murine models of septic infection (Sand et al., 2015), which have been known to correlate with MODS (Kellum, 2004), providing a potential cause of mortality in these mice. The degree of change observed in biochemical markers of metabolic acidosis may have been more pronounced in mice that failed to reach the 24-hour end point, although further work is required to determine whether this is the primary cause of death.

Previous studies have suggested that thrombocytopenia leads to increased permeability of pulmonary vessels in several models, and platelets are important regulators of pulmonary endothelial barrier function and integrity (Middleton et al., 2016) (Ho-Tin-Noé et al., 2011) (Weyrich and Zimmerman, 2013). My observations suggested that pulmonary vascular permeability was enhanced in infected mice depleted of circulating platelets. However, pulmonary oedema was not a consequence of the anti-GPIbα antibody, consistent with findings published by (Amison et al., 2018). Indeed, this has been demonstrated in other experimental models; in mice with LPS-induced ALI, severe thrombocytopenia was associated with alveolar haemorrhage whereas animals with the same degree of thrombocytopenia without LPS-induced lung inflammation did not spontaneously bleed into the lungs (Goerge et al., 2008). This is consistent with my findings whereby haemorrhaging was observed in infected mice depleted of circulating platelets. This suggests that platelets are required for maintenance of the endothelial barrier and this may be mediated by platelet and endothelial selectins, since studies have demonstrated P-selectin deficient mice displayed enhanced bacterial outgrowth in their lungs and distant organs (de Stoppelaar, 2014). That said, the intrapulmonary administration of Evan's Blue dye could have been used as a more representative measure of pulmonary alveolar integrity, since bacteria are disseminating from the lungs to the distal organs in my model. These data suggest that platelets may play a requisite role in maintaining the integrity of the pulmonary vasculature under basal conditions, preventing bacterial dissemination from the lung to the distal organs.

Platelets have previously been reported to contribute towards pulmonary neutrophil recruitment in response to infection in animal models of sepsis (Asaduzzaman et al., 2009), in addition to leukocyte recruitment induced by allergic and non-allergic insults (Pitchford et al., 2003) (Kornerup et al., 2010) (Amison et al., 2015) (Amison et al., 2017). This was consistent

with my findings, whereby I observed a significant decrease in pulmonary neutrophil recruitment in platelet depleted mice. Although, other studies have reported that thrombocytopenia did not influence lung inflammation or neutrophil recruitment in response to infection (Kahn et al., 2013) (de Stoppelaar, 2014), whereby there was no significant difference in pulmonary neutrophil accumulation between thrombocytopenic and non-thrombocytopenic mice. This suggests a platelet-independent recruitment of neutrophils to the lung and perhaps explains why I observed partial neutrophil recruitment in response to infection in my studies. However, another explanation could also be through the increased haemorrhaging of the lungs observed in infected mice depleted of circulating platelets, resulting in vascular leakage into the lung tissue distorting the cellular infiltrate response to infection.

Neutrophils are the first line of innate defence against infection, directly engulfing and killing bacteria in blood and tissues during infection (Clark et al., 2007), whilst they can also release dense web-like structures of DNA, called NETs, which possess proteolytic activity (Yost et al., 2015) (Clark et al., 2007). These NETs have been shown to exhibit antimicrobial activity by trapping and killing bacteria during infection (McDonald et al., 2012) (Clark et al., 2007) (Caudrillier et al., 2012). This observed reduction in pulmonary neutrophil recruitment may therefore account for the worsened phenotype observed in platelet depleted mice, through decreased NETosis. However, the role of platelets in inducing NET formation from neutrophils was not assessed in this model and requires further evaluation.

Numerous studies have stated that platelets and platelet signalling factors, including PAF, can induce NET formation (Kraemer et al., 2011) (Yost et al., 2015) (McDonald et al., 2012) following platelet activation via platelet TLR4 in response to a bacterial trigger, such as LPS

(Clark et al., 2007). For example, in sepsis, activation of platelet TLR4 is a potent stimulus for neutrophil activation and NETosis (Caudrillier et al., 2012). Intriguingly (Clark et al., 2007) have demonstrated that platelets are requisite for LPS-induced neutrophil NET formation, since high concentrations of LPS were unable to induce NET formation from neutrophils directly. In comparison, depletion of circulating platelets was shown to prevent the release of NETs and enhance bacterial dissemination in an *E.coli* infection model (McDonald et al., 2012), highlighting that the release of intravascular NETs is dependent on contact dependent platelet-neutrophil interactions . Similarly, studies (Kraemer et al., 2011) have shown that human platelets express and release type 1 beta-defensins in response to infection, which are responsible for NET formation (Kraemer et al., 2011). These data may provide a possible additional mechanism by which platelets may be involved in indirect killing of bacteria.

Interestingly, the in situ bacterial growth rate observed in the *P.aeruginosa* RP73 model (1.5 logs per 24 hours) is comparable to that reported for the same strain in *in vitro* cultures over the same time period (Bragonzi et al., 2012). This led to the hypothesis that platelets may act independent of neutrophils to limit bacterial growth and serve an additional function of direct host defence against infection, given that platelets have previously been shown to interact directly with bacteria independent of neutrophils (Kraemer et al., 2011) (Ali et al., 2017). To this end, bacterial growth curves were performed both in the presence and absence of platelets *in vitro*. Here a significant reduction in pulmonary bacteria load was observed at both 6 and 8 hours in the presence of platelets when compared to bacteria alone, suggestive of a direct mechanism by which platelets can limit bacterial growth *in vitro*. Indeed, other published literature has suggested a direct mechanism of platelet modulation on bacterial growth. (Ali et al., 2017) indicated that platelets kill *S.aureus* directly in an activation-dependent manner, whilst (Kraemer et al., 2011) have demonstrated that platelets can limit

the growth rate of *S.aureus in vitro*. These findings supported by the fact that the platelet is the first and most abundant cell type present, indicate the possibility that platelets serve as an early and independent function of direct host defence against bacterial pathogens. Furthermore, previous published work has suggested that platelets possess the capacity to directly internalise and phagocytose pathogens (Youssefian et al., 2002); and indeed, platelets contain many mediators with antimicrobial activity that are secreted from their granules upon platelet activation (Yeaman, 2014). However, the relative contribution of platelet microbicidal activity to host defence against infection remains unclear and further work is required to fully determine the mechanisms by which platelets independently modulate bacterial growth/ survival.

In order to elucidate the mechanism by which platelets defend against infection and to determine whether there were specific components of platelets that mediate protection against infection, additional studies were performed to investigate potential mechanisms. Literature published by (Clark et al., 2007) and (Caudrillier et al., 2012) indicated that platelet TLR4 induces NET formation from activated neutrophils, therefore I speculated that a worsened phenotype would be observed using TLR4 knockout mice. As expected pulmonary neutrophil recruitment was reduced, however the severity of infection was not enhanced in TLR4 knockout mice when compared to wild type mice, suggesting a more direct mechanism for platelets. In contrast, studies performed by (Oliveira et al., 2010) demonstrated a higher mortality in TLR4 deficient mice following parasitic infection with Trypanosoma cruzi. However, these studies highlighted that older (>7 weeks) TLR4 deficient mice did not elicit enhanced susceptibility to infection, which perhaps helps to explain the data observed in the current study.

Recent studies have also postulated that the purinergic receptors exert a protective role against infection, whereby it was reported that $P2Y_1$ and $P2Y_2$ single and double knockout mice displayed increased susceptibility and increased morality to pulmonary infection with *P.aeruginosa* (Geary et al., 2005). Therefore, the purine (ATP/ ADP) hydrolysing enzyme, Apyrase, was used to investigate the role of ATP/ADP and purinergic receptors in the regulation of pulmonary infection. My results provided compelling evidence to suggest that activation of the purinergic receptors exerts a protective effect against infection, since the inhibition of these receptors enhanced the pathogenicity of *P.aeruginosa* infection, with enhanced pulmonary bacterial load, bacterial dissemination and increased weight loss. Administration of Apyrase also induced a significant reduction in both pulmonary total cell and neutrophil recruitment induced by *P.aeruginosa* infection. This is consistent with findings published by (Kukulski et al., 2010), whereby Apyrase was seen to abrogate LPS-induced neutrophil migration.

The contribution of the purinergic receptors to host defence remains unclear, however (Trier et al., 2008) suggests an association between purinergic receptor inhibition ($P2X_1$/ $P2Y_{12}$) and decreased production of PMPs and kinocidins from platelets. To this end, I sought to identify specific purinergic receptors implicated in host defence through the use of purinergic receptor antagonists. Consistent with previous findings (Amison et al., 2017), results demonstrated that inhibition of the $P2Y_1$ and $P2Y_{14}$ receptors significantly attenuated infection induced pulmonary neutrophil recruitment by 2-3 fold. It is therefore plausible to suggest that these receptors are involved in pulmonary neutrophil recruitment in this model, comparable to that observed in the literature (Amison et al., 2017) (Amison et al., 2015). Intriguingly, inhibition of the $P2Y_{14}$ receptor with PPTN demonstrated evidence of enhanced pulmonary bacterial load and bacterial dissemination to the kidney. The increase in

pulmonary bacterial load observed following $P2Y_{14}$ receptor inhibition was equivalent to the increase observed following depletion of circulating platelets in mice. This is perhaps suggestive of an involvement of the purinergic receptors in host defence against infection with *P.aeruginosa*, although further work is required to investigate this further. It is also possible to postulate that the worsened phenotype may be as a result of a diminished neutrophil population at the site of infection and reduced NETosis, in addition to a direct function of platelets.

(Trier et al., 2008) have reported the platelet anti-*staphylococcal* responses occur through the $P2X_1$ and $P2Y_{12}$ purinergic receptors, since Apyrase, Suramin (a general P2 receptor antagonist), Pyridoxal (a $P2X_1$ receptor antagonist) and Cangrelor (a $P2Y_{12}$ receptor antagonist) reduced levels of PMP present in reaction supernatant. These studies suggest that bacteria induced platelet activation results in the release of ATP and ADP (**Figure 6.1**), which subsequently activates resting platelets within close proximity to augment platelet activation. This response is inhibited using the ATP/ADP hydrolysing agent, Apyrase (**Figure 6.1**). In addition, (Trier et al., 2008) highlight that activated platelets release PMPs to target bacteria and this response can be inhibited using both $P2X_1$ and $P2Y_{12}$ purinergic receptors (**Figure 6.1**).

It is thought that $P2Y_{14}$ is coupled to the same G-protein as $P2Y_{12}$ (G_i) (Dovlatova et al., 2008), however the exact signalling mechanism associated with $P2Y_{14}$ remains controversial. In the current study no effects were observed following administration of $P2X_1$ and $P2Y_{12}$ receptor antagonists, demonstrating conflicting results and highlighting the requirement for further research to deduce the signalling pathways associated with $P2Y_{14}$. To this end, I propose that inhibition of the $P2Y_{14}$ receptor using PPTN was associated with a worsened phenotype due to the inhibition of the release of PMPs from platelets, thereby reducing the direct killing

effect of platelets (**Figure 6.1**), although this requires further investigation. It is worthy to note that (Trier et al., 2008) did not investigate the effect of $P2Y_{14}$ receptor antagonism on the platelet anti-*staphylococcal* response and indeed, different platelet signalling pathways and receptors may be utilised by species of bacteria, which may help explain the results obtained here.

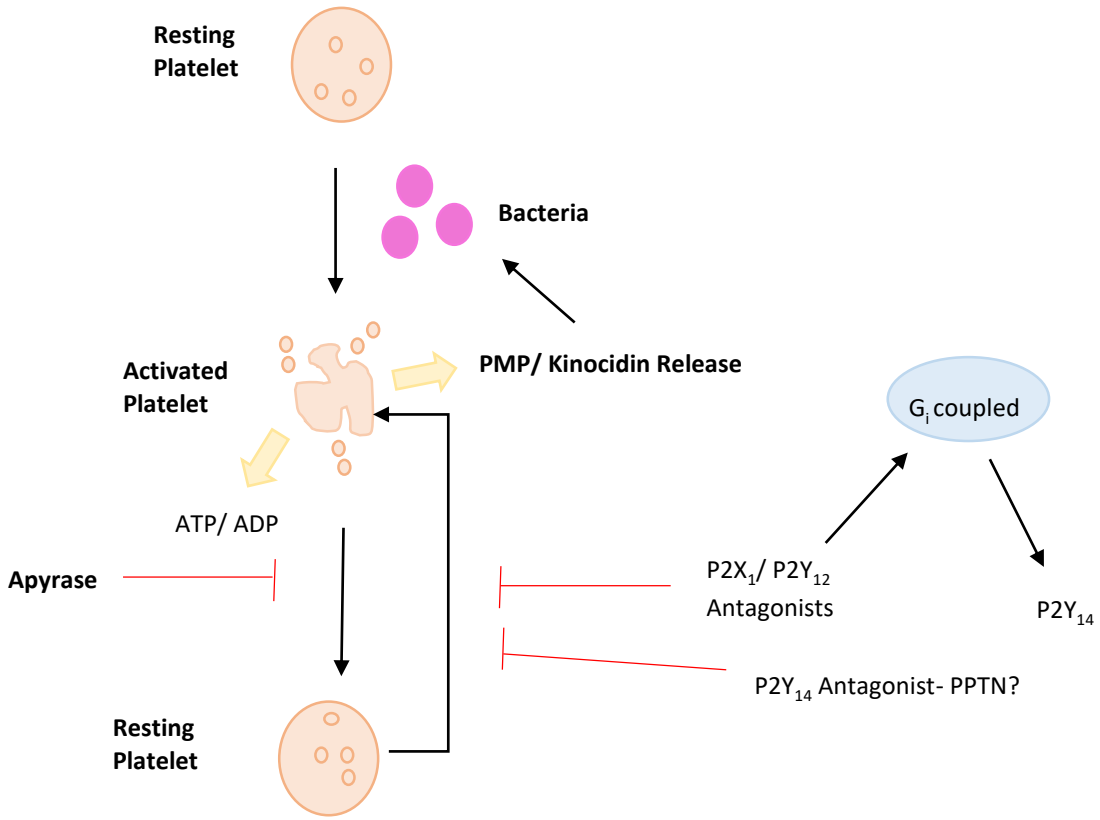

Figure 6. 1 A Proposed Mechanism of Action of the Platelet Antimicrobial Response

Adapted from (Trier et al., 2008)

What's more, these receptor antagonists do not specifically target platelet purinergic receptors and indeed the use of P2 receptor knockout mice may be a useful tool for investigating purinergic receptor function in host defence against infection, although this was beyond the scope of the project.

A role for purinergic receptors in response to infection has been detailed elsewhere in the literature (Coutinho-Silva and Ojcius, 2012) (Miller et al., 2011), whereby a loss of function in the human $P2X_7$ receptor led to increased susceptibility to infection, bolstering claims of purinergic involvement in infection, however this receptor subtype is not expressed by platelets suggesting that its effects are attributed to different cell types. It is reported that different pathogens use different strategies to manipulate purinergic signalling, therefore further identification of these may clarify platelet involvement in infection and host defence in my model.

6.3 The Use of a Murine Model of Pulmonary Infection for Therapeutic Analysis

Having established and validated a murine model of pulmonary infection with *P.aeruginosa* and MRSA, another part of this project was aimed at demonstrating the use of the model for therapeutic analysis with novel compounds.

The rapid era of antibiotic discovery led to overconfidence that infectious diseases could be eradicated (Coates et al., 2002). However, the overuse and misuse of antibiotics has led to a crisis where many antibiotics are no longer effective against even the simplest infections (Laxminarayan, 2014). The emergence of antibiotic resistance has led to an urgent need for

novel approaches for treating infectious diseases. One such approach is the development of enhancer compounds, which act by restoring sensitivity of resistant bacteria to currently available antibiotics. (Hu, 2013) and colleagues have developed such a drug, the antibiotic enhancer, HT61, a small quinolone derived compound as an exemplar of this novel approach.

Prior to testing this novel enhancer compound *in vivo*, *in vitro* studies were performed by collaborators to compare HT61 to commercially available antibiotics, including Amoxicillin and Levofloxacin, and to test its activity against different strains of bacteria (Hu et al., 2010). This research demonstrated that HT61 as a singular treatment produced a 7 log CFU/ml reduction against MSSA, although no activity was observed against gram-negative bacteria, including *P.aeruginosa* (Hu et al., 2010). Subsequent *in vitro* experiments were performed using HT61 in combination with commercially available antibiotics, with the aim of restoring sensitivity to drug resistant bacteria (Hu, 2013). These studies reported an enhancement of the activity of older generation antibiotics (gentamicin, neomycin and chlorhexidine) when used in combination with HT61 (Hu, 2013) *in vitro* against MRSA and MSSA, eradicating the total bacterial population by 2-8 hours.

To this end, we sought to investigate whether the effects of HT61 observed *in vitro* could be reproduced in this *in vivo* model of pulmonary infection. Here I demonstrated for the first time that the novel enhancer compound HT61 is able to potentiate the effect of low doses of Tobramycin on attenuating the pulmonary bacterial load induced by two drug resistant clinical isolate strains of the gram-negative *P.aeruginosa*, RP73 and NN2, whilst having no direct anti-microbial effect itself. Furthermore, this combination approach may lead to the use of lower doses of antibiotics, particularly aminoglycosides, which have significant toxic side-effects.

It has previously been reported that combination treatments using different antibiotic classes induced synergistic antimicrobial effects against Tobramycin resistant strains of *P.aeruginosa* (Chan and Zabransky, 1987). In comparison to my work, this research detailed the synergistic effect following co-treatment of Tobramycin and Ceftazidime *in vitro* using the checkerboard technique. In addition, the combination treatment of Colistin and Ceftazidime had an additive effect against Tobramycin resistant *P.aeruginosa*, demonstrated using the time kill curve technique (Chan and Zabransky, 1987). Such observations highlight the potential beneficial effects of utilising combination treatments and enhancer compounds to optimally kill bacteria. These observations have been supported by other studies (Pieri et al., 2014), which have demonstrated an enhancement of the activity of Doxycycline with ianthelliformisamine derivatives against resistant Gram-negative bacteria. These studies, consistent with my work, highlight the importance of combining treatments in order to slow the emergence of resistance and reduce the concentrations of single treatment antibiotics. However, these previous studies have been largely *in vitro* and I have now demonstrated that it is possible to enhance the effect of Tobramycin *in vivo* against lung infections with *P.aeruginosa,* by restoring the sensitivity of resistant strains to this antibiotic.

However, despite the enhancing effect of HT61 I observed against the two Tobramycin resistant strains of *P.aeruginosa*, I saw no significant reduction in pulmonary bacterial load following co-treatment of Tobramycin and HT61 against the Tobramycin susceptible strain of *P.aeruginosa* PAO1. This observation contrasts with other findings (Chan and Zabransky, 1987), that have demonstrated a synergistic effect of Tobramycin in combination with azlocillin, piperacillin, ceftazidime and imipenem against the Tobramycin susceptible strain of *P.aeruginosa* PAO1. Other investigators (Pieri et al., 2014) have demonstrated that

ianthelliformisamine derivatives, as enhancer compounds, restore the activity of Doxycycline against *P.aeruginosa* PAO1 *in vitro*. Comparable results were observed in work carried out by (Borselli et al., 2017), whereby polyamine derivatives were used as antibiotic enhancers to restore sensitivity to Doxycycline against *P.aeruginosa* strain PAO1. My results suggest that HT61 may be best utilised in combination with Tobramycin against resistant organisms, rather than with Tobramycin in the treatment of sensitive strains.

HT61 was initially developed as a topical agent for the decolonisation of nasal *S.aureus* and mini pig skin was used to test HT61 for potential dermal toxicity, which demonstrated 14 days of administration to 10% of the body surface had no related adverse effects (irritation, inflammation, itching) (Hu et al., 2010) (Hu, 2013). Consequently prior to initiating *in vivo* studies, little information was known regarding the pharmacokinetics/ pharmacodynamics and the bioavailability of HT61. Similarly, no prior experiments were performed to deduce the safety profile of HT61, therefore the optimum concentrations, dosing regimens and route of administration of HT61 may not have been adequately identified for these experiments. The synergistic effect observed against RP73 and NN2 may in fact be augmented if additional experiments were performed to deduce further information about HT61, including drug toxicology and bioavailability, and similarly, an effect may be observed against PAO1 and MRSA following administration of HT61 at an optimum concentration, dosing regimens and route.

No significant reduction in pulmonary bacterial load was observed with HT61 and Vancomycin against the *MRSA* strain USA300 *in vivo*, which was surprising as other work has demonstrated a significant augmentation of the bactericidal efficacy of older generation antibiotics *in vitro* (Gentamycin, Neomycin, Chlorhexidine) in the presence of HT61 by (Hu, 2013) (Hu et al.,

2010). However, as this is the first study to investigate HT61 in the lung *in vivo,* it is plausible that the optimal dosing regimen has not yet been identified and as discussed previously, further work is required to optimise the *in vivo* therapeutic regimen of HT61 to enhance the reduction in pulmonary bacterial load when administered with different antibiotics.

Using membrane potential and ATP release assays, it has been reported that HT61 acts on the bacterial cell membrane, causing cell depolarisation and the release of the intracellular contents of the cell (Hubbard et al., 2017), leading to bacterial destruction. Furthermore, HT61 at high concentrations (40 µg/mL) has been shown to nick the bacterial cell wall structure following 10 minutes of treatment (Hu et al., 2010). This has been suggested as a possible mechanism of action of HT61 as this would increase the permeability of the bacterial membrane allowing greater cellular access to the antibiotic (Hu et al., 2010). It is also thought that when HT61 exerts its action on the bacterial cell membrane, the membrane-embedded enzymes that are involved in anaerobic metabolism and disrupted (Hu, 2013). As a result, non-multiplying bacteria are required to activate their anaerobic metabolic pathways when they are oxygen deprived and consequently become susceptible to killing by compounds that poison the respiratory chain (Hu, 2013). This provides a plausible explanation for my *in vivo* findings, although the mechanisms of action of this compound requires further research and is beyond the scope of this project.

Future Work

In chapter IV it was demonstrated that the depletion of circulating platelets results in enhanced pathogenicity of infection with *P.aeruginosa* and MRSA, as measured by enhanced

weight loss, a higher bacterial burden and evidence of systemic infection. Platelets were also seen to decrease pulmonary neutrophil recruitment in response to infection. This research has raised several key questions, including what is the nature of the interaction between platelets and *P.aeruginosa* and MRSA and can activated platelets directly engulf bacteria in this model? This would provide a plausible mechanism for the worsened phenotype observed following experimentally induced platelet depletion. What's more, this work has highlighted the points of whether bacteria can trigger the destruction of host tissue in a manner that necessitates the protective effect of platelets and whether platelet derived PMPs and kinocidins can potentially exert a direct bacterial killing effect both *in vitro* and *in vivo.*

Whilst modulation of the purinergic pathways appeared to be associated with a worsened phenotype comparable to that observed following depletion of circulating platelets, it remains unclear as to why activation of $P2Y_{14}$ exerts a protective effect against infection. Future work is therefore required to investigate in more detail how purinergic signalling is affected during infection, and whether this effect is replicated in experimental models of both gram-negative and gram-positive infection.

I have demonstrated that platelets can directly modulate bacterial growth kinetics, however future work is required to elucidate the relative contribution of platelet microbicidal activity to host defence against infection. It has previously been demonstrated that platelet reinfusion reduces mortality in LPS- induced endotoxemia and a bacterial infusion sepsis model (Xiang et al., 2013) and the protective role of platelets in this context has highlighted the potential beneficial effect of platelet transfusions in infection and sepsis (Yeaman, 2010). Future experiments could therefore be performed to determine whether the protective role of

platelets could be reinstated in conditions such as sepsis and CF, where platelets dysfunction or thrombocytopenia is observed.

The murine model of pulmonary infection that was established during the course of this project could be extended to 14-28 days post infection to be more representative of the processes occurring in chronic diseases, including CF and COPD. Heparan Sulfate competitors have been shown to attenuate *P.aeruginosa* lung infection and decrease *P.aeruginosa* biofilm formation upon treatment (Lorè et al., 2018), however most studies that investigate the effect of certain compounds on biofilm formation are performed *in vitro.* In the future, this model could be adapted and used to investigate the effect of certain antimicrobials on biofilm formation *in vivo*, or even to examine platelet involvement in biofilm formation and tissue remodelling in the context of infection.

Concerning the use of the model for therapeutic analysis, further experiments could be performed to determine the mechanism of action of HT61, in addition to toxicity, bioavailability and pharmacokinetics studies. These results may highlight the most effective dose regime, route of administration and concentration of HT61 to ensure total bacterial eradication. Several chronic respiratory diseases are characterized by incessant cycles of chronic airway inflammation, tissue remodelling and persistent infections (Lorè et al., 2018). Aggressive treatment regimens, using high, sometimes toxic doses of antibiotics are used and therefore a better understanding of the pathophysiological mechanisms underlying infection may improve future treatments. Different isolates of *P.aeruginosa* display considerable variation in both their phenotypic and genotypic characteristics, including swimming and twitching motility, expression of virulence factors and protease secretion (Cigana et al., 2018) and this consequently affects their susceptibility to antimicrobials.

Final Remarks

Here I provide compelling evidence to suggest that platelets are implicated in infection and host defence. I have demonstrated that intrapulmonary administration of bacteria induces platelet activation, as measured by the production of PF-4, RANTES and platelet-neutrophil complexes. Furthermore, I have revealed that infection induces peripheral thrombocytopenia with accumulation of activated platelets in lung tissue. The experimental depletion of circulating platelets in a murine model of pulmonary infection was associated with a worsened phenotype in both gram-negative and gram-positive infection, enhancing mortality, increasing pulmonary bacterial load and bacterial dissemination to the distal organs. This clearly highlights a critical role for platelets in host defence. I have suggested that signalling at the platelet purinergic receptors is implicated in infection, however further work is required to elucidate the mechanism by which platelets defence against infection

References

Abi-Younes, S., Sauty, A., Mach, F., Sukhova, G. K., Libby, P., & Luster, A. D. (2000). The Stromal Cell The Stromal Cell–Derived Factor-1 Chemokine Is a Potent Platelet Agonist Highly Expressed in Atherosclerotic Plaques. *Circ Res*, *86*, 131–138. https://doi.org/10.1161/01.RES.86.2.131

Abi-Younes, S., Si-Tahar, M., & Luster, A. D. (2001). The CC chemokines MDC and TARC induce platelet activation via CCR4. *Thrombosis Research*, *101*(4), 279–289. https://doi.org/10.1016/S0049-3848(00)00402-3

Ali, R. A., Wuescher, L. M., Dona, K. R., & Worth, R. G. (2017). Platelets Mediate Host Defense against *Staphylococcus aureus* through Direct Bactericidal Activity and by Enhancing Macrophage Activities. *The Journal of Immunology*, *198*(1), 344–351. https://doi.org/10.4049/jimmunol.1601178

Alon, R., Fuhlbrigge, R. C., Finger, E. B., & Springer, T. A. (1996). Interactions through L-selectin between leukocytes and adherent leukocytes nucleate rolling adhesions on selectins and VCAM-1 in shear flow. *Journal of Cell Biology*, *135*(3), 849–865. https://doi.org/10.1083/jcb.135.3.849

Amison, R., Pitchford, S., & Page, C. (2012). Pharmalogical Modulation of the Inflammatory Actions of Platelets. *Handbook of Experimental Pharmacology*, 447–468. https://doi.org/10.1007/978-3-642-29423-5

Amison, R. T., Arnold, S., O'Shaughnessy, B. G., Cleary, S. J., Ofoedu, J., Idzko, M., … Pitchford, S. C. (2017). Lipopolysaccharide (LPS) induced pulmonary neutrophil recruitment and platelet activation is mediated via the P2Y1and P2Y14receptors in mice. *Pulmonary Pharmacology and Therapeutics*, *45*, 62–68. https://doi.org/10.1016/j.pupt.2017.05.005

Amison, R. T., Cleary, S., Riffo-Vasquez, Y., Bajwa, M., Page, C. P., & Pitchford, S. C. (2018). Platelets Play a Central Role in Sensitization to Allergen. *American Journal of Respiratory Cell and Molecular Biology*, *59*(C), 1–32. https://doi.org/10.1165/rcmb.2017-0401OC

Amison, R. T., Jamshidi, S., Rahman, K. M., Page, C. P., & Pitchford, S. C. (2018). Diverse signalling of the platelet P2Y1receptor leads to a dichotomy in platelet function. *European Journal of Pharmacology*, *827*, 58–70. https://doi.org/10.1016/j.ejphar.2018.03.014

Amison, R. T., Momi, S., Morris, A., Manni, G., Keir, S., Gresele, P., … Pitchford, S. C. (2015). RhoA signaling through platelet P2Y1 receptor controls leukocyte recruitment in allergic mice. *Journal of Allergy and Clinical Immunology*, *135*(2), 528–538. https://doi.org/10.1016/j.jaci.2014.09.032

Amison, R. T., O'Shaughnessy, B. G., Arnold, S., Cleary, S. J., Nandi, M., Pitchford, S. C., … Page, C. P. (2018). Platelet Depletion Impairs Host Defence to Pulmonary Infection with Pseudomonas aeruginosa in Mice. *American Journal of Respiratory Cell and Molecular Biology*, *58*(3), 331–340. https://doi.org/10.1165/rcmb.2017-0083OC

Andonegui, G., Kerfoot, S., McNagny, K., Ebbert, K., Patel, K., & Kubes, P. (2005). Platelets express functional toll-like receptor-4. *Blood*, *106*(7), 2417–2423. https://doi.org/10.1182/blood-2005-03-0916.Supported

Andrews, R. K., & Berndt, M. C. (2004). Platelet physiology and thrombosis. *Thrombosis Research*, *114*, 447–453. https://doi.org/10.1016/j.thromres.2004.07.020

Anwar, H., Strap, J. L., Chen, K., & Costerton, J. W. (1992). Dynamic interactions of biofilms of mucoid *Pseudomonas aeruginosa* with tobramycin and piperacillin. *Antimicrob Agents Chemother*, *36*(6), 1208–1214. https://doi.org/10.1128/AAC.36.6.1208

Archer, N. K., Mazaitis, M. J., Costerton, J. W., Leid, J. G., Powers, M. E., & Shirtliff, M. E. (2011). Properties , regulation and roles in human disease Staphylococcus aureus biofilms. *Virulence*, *2*(5), 445–459.

Arman, M., Krauel, K., Tilley, D. O., Weber, C., Cox, D., Greinacher, A., … Watson, S. P. (2014). Amplification of bacteria-induced platelet activation is triggered by FcgRIIA , integrin aIIbb3, and platelet factor 4. *Blood*, *123*(20), 3166–3175. https://doi.org/10.1182/blood-2013-11-540526.S.W.K.

Asaduzzaman, M., Lavasani, S., Rahman, M., Zhang, S., Braun, O. Ö., Jeppsson, B., & Thorlacius, H. (2009). Platelets support pulmonary recruitment of neutrophils in abdominal sepsis. *Critical Care Medicine*, *37*(4), 1389–1396. https://doi.org/10.1097/CCM.0b013e31819ceb71

Asensi, V., & Fierer, J. (1991). Synergistic effect of human lysozyme plus ampicillin or beta-lysin on the killing of Listeria monocytogenes. *The Journal of Infectious Diseases*, *163*(3), 574–8. Retrieved from http://www.ncbi.nlm.nih.gov/pubmed/1899873

Aslam, R., Speck, E. R., Kim, M., Crow, A. R., Bang, K. W. A., Nestel, F. P., … Semple, J. W. (2016). Platelet Toll-like receptor expression modulates lipopolysaccharide-induced thrombocytopenia and tumor necrosis factor- a production in vivo. *Blood*, *107*(2), 637–642. https://doi.org/10.1182/blood-2005-06-2202.Supported

Aslan, J. E., & McCarty, O. J. T. (2013). Rho GTPases in platelet function. *Journal of Thrombosis and Haemostasis : JTH*, *11*(1), 35–46. https://doi.org/10.1111/jth.12051

Aster, R. (1966). Pooling of Platelets in the Spleen : Role in the Pathogenesis of "Hypersplenic " Thrombocytopenia. *Journal of Clinical Investigation*, *45*(5), 645–657.

Bajaj, H., Acosta Gutierrez, S., Bodrenko, I., Malloci, G., Scorciapino, M. A., Winterhalter, M., & Ceccarelli, M. (2017). Bacterial Outer Membrane Porins as Electrostatic Nanosieves: Exploring Transport Rules of Small Polar Molecules. *ACS Nano*, *11*(6), 5465–5473. https://doi.org/10.1021/acsnano.6b08613

Batoni, G., Maisetta, G., & Esin, S. (2016). Antimicrobial peptides and their interaction with biofilms of medically relevant bacteria. *Biochimica et Biophysica Acta - Biomembranes*, *1858*(5), 1044–1060. https://doi.org/10.1016/j.bbamem.2015.10.013

Bayer, a S., Sullam, P. M., Ramos, M., Li, C., Cheung, a L., & Yeaman, M. R. (1995). Staphylococcus aureus induces platelet aggregation via a fibrinogen-dependent mechanism which is independent of principal platelet glycoprotein IIb/IIIa fibrinogen-binding domains. *Infection and Immunity*, *63*(9), 3634–41. Retrieved from http://www.pubmedcentral.nih.gov/articlerender.fcgi?artid=173504&tool=pmcentrez&rendertype=abstract

Bayes, H. K., Ritchie, N., Irvine, S., & Evans, T. J. (2016). A murine model of early Pseudomonas aeruginosa lung disease with transition to chronic infection. *Scientific Reports*, *6*(35838), 1–10. https://doi.org/10.1038/srep35838

Bearer, E. L. (1991). Direct observation of actin filament severing by gelsolin and binding by gCap39 and CapZ. *Journal of Cell Biology*, *115*(6), 1629–1638. https://doi.org/10.1083/jcb.115.6.1629

Bearer, E. L., Prakash, J. M., & Li, Z. (2002). Actin dynamics in platelets. *International Review of Cytology*, *217*, 137–182. https://doi.org/10.1016/S0074-7696(02)17014-8

Belley, A., Neesham-Grenon, E., McKay, G., Arhin, F. F., Harris, R., Beveridge, T., … Moeck, G. (2009). Oritavancin kills stationary-phase and biofilm Staphylococcus aureus cells in vitro. *Antimicrobial Agents and Chemotherapy*, *53*(3), 918–925. https://doi.org/10.1128/AAC.00766-08

Bennett, J. S. (2005). Structure and function of the platelet integrin α. *The Journal of Clinical Investigation*, *115*(12), 3363–3369. https://doi.org/10.1172/JCI26989.ligand-binding

Berman, M. E., & Muller, W. A. (1995). Ligation of platelet/endothelial cell adhesion molecule 1 (PECAM-1/CD31) on monocytes and neutrophils increases binding capacity of leukocyte CR3 (CD11b/CD18). *Journal of Immunology (Baltimore, Md. : 1950)*, *154*(1), 299–307. Retrieved from http://www.ncbi.nlm.nih.gov/pubmed/7995949

Bhakdi, S., Klonisch, T., Nuber, P., & Fischer, W. (1991). Stimulation of monokine production by lipoteichoic acids. *Infection and Immunity*, *59*(12), 4614–4620. https://doi.org/papers3://publication/uuid/9EB2E3DA-3333-4096-B59A-EFBAF49F3016

Bjarnsholt, T. (2013). The role of bacterial biofilms in chronic infections. *APMIS. Supplementum*, *121*(136), 1–51. https://doi.org/10.1111/apm.12099

Boilard, E., Nigrovic, P. A., Larabee, K., Watts, G. F. M., Coblyn, J. S., Weinblatt, M. E., … Lee, D. M. (2010). Platelets amplify inflammation in arthritis via collagen-dependent microparticle production. *Science*, *327*(5965), 580–583. https://doi.org/10.1126/science.1181928

Bozza, F. A., Shah, A. M., Weyrich, A. S., & Zimmerman, G. A. (2009). Amicus or adversary platelets in lung biology, acute injury, and inflammation. *American Journal of Respiratory Cell and Molecular Biology*, *40*(2), 123–134. https://doi.org/10.1165/rcmb.2008-0241TR

Bragonzi, A. (2010). Murine models of acute and chronic lung infection with cystic fibrosis pathogens. *International Journal of Medical Microbiology*, *300*(8), 584–593. https://doi.org/10.1016/j.ijmm.2010.08.012

Bragonzi, A., Farulla, I., Paroni, M., Twomey, K. B., Pirone, L., Lorè, N. I., … Bevivino, A. (2012). Modelling Co-Infection of the Cystic Fibrosis Lung by Pseudomonas aeruginosa and Burkholderia cenocepacia Reveals Influences on Biofilm Formation and Host Response. *PLoS ONE*, *7*(12). https://doi.org/10.1371/journal.pone.0052330

Bragonzi, A., Paroni, M., Nonis, A., Cramer, N., Montanari, S., Rejman, J., … Tümmler, B. (2009). Pseudomonas aeruginosa microevolution during cystic fibrosis lung infection establishes clones with adapted virulence. *American Journal of Respiratory and Critical Care Medicine*, *180*(2), 138–145. https://doi.org/10.1164/rccm.200812-1943OC

Bragonzi, A., Wiehlmann, L., Klockgether, J., Cramer, N., Worlitzsch, D., Döning, G., & Tümmler, B. (2006). Sequence diversity of the mucABD locus in Pseudomonas aeruginosa isolates from patients with cystic fibrosis. *Microbiology*, *152*(11), 3261–3269. https://doi.org/10.1099/mic.0.29175-0

Brass, L. (2010). Understanding and evaluating platelet function. *Hematology*, *2010*(1), 387–396. https://doi.org/10.1182/asheducation-2010.1.387

Bray, M. A., Ford-Hutchinson, A. W., & Smith, M. J. H. (1981). Leukotriene B 4 : an Inflammatory Mediator in Vivo. *Prostaglandins*, *22*(2), 213–222. https://doi.org/10.1017/CBO9781107415324.004

Broug-Holub, E., Toews, G. B., Van Iwaarden, J. F., Strieter, R. M., Kunkel, S. L., Paine, R., & Standiford, T. J. (1997). Alveolar macrophages are required for protective pulmonary defenses in murine Klebsiella pneumonia: Elimination of alveolar macrophages increases neutrophil recruitment but decreases bacterial clearance and survival. *Infection and Immunity*, *65*(4),

1139–1146.

Brown, G., Narayanan, P., Li, W., Silverstein, R., & McIntyre, T. (2013). Lipopolysaccharide stimulates platelets through an IL-1β autocrine loop. *J Immunol*, *191*(10), 1–16. https://doi.org/10.4049/jimmunol.1300354.

Bunescu, A., Seideman, P., Lenkei, R., Levin, K., & Egberg, N. (2004). Enhanced Fc- gamma receptor αMβ2 integrin receptor expression by monocytes and neutrophils in rheumatoid arthritis: Interaction with platelets. *J Rheumatol*, (31), 2347–55.

Byrne, M. F., Kerrigan, S. W., Corcoran, P. A., Atherton, J. C., Murray, F. E., Fitzgerald, D. J., & Cox, D. M. (2003). Helicobacter pylori binds von Willebrand factor and interacts with GPIb to induce platelet aggregation. *Gastroenterology*, *124*(7), 1846–1854. https://doi.org/10.1016/S0016-5085(03)00397-4

Cabot, G., Zamorano, L., Moyà, B., Juan, C., Navas, A., Blázquez, J., & Oliver, A. (2016). Evolution of Pseudomonas aeruginosa antimicrobial resistance and fitness under low and high mutation supply rates. *Antimicrobial Agents and Chemotherapy*, *60*(3), 1767–1778. https://doi.org/10.1128/AAC.02676-15

Campbell, J. I., Ciofu, O., & Hoiby, N. (1997). Pseudomonas aeruginosa isolates from patients with cystic fibrosis have different beta-lactamase expression phenotypes but are homogeneous in the ampC-ampR genetic region. *Antimicrobial Agents and Chemotherapy*, *41*(6), 1380–1384. Retrieved from http://www.ncbi.nlm.nih.gov/pubmed/9174204%5Cnhttp://www.pubmedcentral.nih.gov/articlerender.fcgi?artid=PMC163920%5Cnhttp://www.ncbi.nlm.nih.gov/pubmed/9174204%5Cnhttp://www.pubmedcentral.nih.gov/articlerender.fcgi?artid=PMC163920%5Cnhttp://www.ncbi.nlm.n

Camussi, G., & Tetta, C. (1989). Tumor necrosis factor stimulates human neutrophils to release leukotriene B4 and platelet-activating factor. *Eur J Biochem*, *182*(3), 661–6. Retrieved from http://onlinelibrary.wiley.com/doi/10.1111/j.1432-1033.1989.tb14876.x/full

Carpagnano, G. E., Barnes, P. J., Geddes, D. M., Hodson, M. E., & Kharitonov, S. A. (2003). Increased leukotriene B4 and interleukin-6 in exhaled breath condensate in cystic fibrosis. *American Journal of Respiratory and Critical Care Medicine*, *167*(8), 1109–1112. https://doi.org/10.1164/rccm.200203-179OC

Cash, H. A., Woods, D. E., McCullough, B., Johanson, W. G., & Bass, J. A. (1979). A rat model of chronic respiratory infection with Pseudomonas aeruginosa. *American Review of Respiratory Disease*, *119*(3), 453–459. Retrieved from http://www.scopus.com/inward/record.url?eid=2-s2.0-0018344638&partnerID=tZOtx3y1

Cattaneo, M. (2015). The platelet P2 receptors in inflammation. *Hamostaseologie*, *35*(3), 262–266. https://doi.org/10.5482/HAMO-14-09-0044

Cattaneo, M., Lecchi, A., Ohno, M., Joshi, B. V., Besada, P., Tchilibon, S., … Jacobson, K. A. (2004). Antiaggregatory activity in human platelets of potent antagonists of the P2Y1receptor. *Biochemical Pharmacology*, *68*(10), 1995–2002. https://doi.org/10.1016/j.bcp.2004.06.026

Caudrillier, A., Kessenbrock, K., Gilliss, B. M., Nguyen, J. X., Marques, M. B., Monestier, M., … Looney, M. R. (2012). Platelets induce neutrophil extracellular traps in transfusion-related acute lung injury. *J. Clin. Invest.*, *122*(7), 2661–2671. https://doi.org/10.1172/JCI61303.ALI

Chambers, H. F. (2001). The changing epidemiology of Staphylococcus aureus? *Emerging Infectious Diseases*, *7*(2), 178–182. https://doi.org/10.3201/eid0702.700178

Chambers, J. K., Macdonald, L. E., Sarau, H. M., Ames, R. S., Freeman, K., Foley, J. J., … Livi, G. P. (2000). A G Protein-coupled Receptor for UDP-glucose. *Journal of Biological Chemistry*, *275*(15), 10767–10771.

Chan, E. L., & Zabransky, R. J. (1987). Determination of synergy by two methods with eight antimicrobial combinations against tobramycin-susceptible and tobramycin-resistant strains of pseudomonas. *Diagnostic Microbiology and Infectious Disease*, *6*(2), 157–164. https://doi.org/10.1016/0732-8893(87)90101-5

Chatham, W., & Blackburn, W. (1993). Fixation of C3 to IgG attenuates neutrophil HOCl generation and collagenase activation. *J Immunol 1993*, (151), 949–958.

Chavakis, T., Keiper, T., Matz-Westphal, R., Hersemeyer, K., Sachs, U. J., Nawroth, P. P., … Santoso, S. (2004). The junctional adhesion molecule-C promotes neutrophil transendothelial migration in vitro and in vivo. *Journal of Biological Chemistry*, *279*(53), 55602–55608. https://doi.org/10.1074/jbc.M404676200

Chuchalin, A., Amelina, E., & Bianco, F. (2009). Tobramycin for inhalation in cystic fibrosis: Beyond respiratory improvements. *Pulmonary Pharmacology and Therapeutics*, *22*(6), 526–532. https://doi.org/10.1016/j.pupt.2009.06.001

Cigana, C., Bianconi, I., Baldan, R., De Simone, M., Riva, C., Sipione, B., … Bragonzi, A. (2018). Staphylococcus aureus Impacts Pseudomonas aeruginosa Chronic Respiratory Disease in Murine Models. *The Journal of Infectious Diseases*, *217*(6), 933–942. https://doi.org/10.1093/infdis/jix621

Clark, S. R., Ma, A. C., Tavener, S. A., Mcdonald, B., Goodarzi, Z., Kelly, M. M., … Kubes, P. (2007). Platelet TLR4 activates neutrophil extracellular traps to ensnare bacteria in septic blood, *13*(4), 463–469. https://doi.org/10.1038/nm1565

Claushuis, T. A. M., Van Vught, L. A., Scicluna, B. P., Wiewel, M. A., Klein Klouwenberg, P. M. C., Hoogendijk, A. J., … Van Der Poll, T. (2016). Thrombocytopenia is associated with a dysregulated host response in critically ill sepsis patients. *Blood*, *127*(24), 3062–3072. https://doi.org/10.1182/blood-2015-11-680744

Clawson, C. C., & White, J. G. (1971a). Platelet interaction with bacteria. I. Reaction phases and effects of inhibitors. *The American Journal of Pathology*, *65*(2), 367–380.

Clawson, C. C., & White, J. G. (1971b). Platelet interaction with bacteria. II. Fate of the bacteria. *The American Journal of Pathology*, *65*(2), 381–397.

Coates, A. R. M., & Hu, Y. (2008). Targeting non-multiplying organisms as a way to develop novel antimicrobials. *Trends in Pharmacological Sciences*, *29*(3), 143–150. https://doi.org/10.1016/j.tips.2007.12.001

Cognasse, F., Hamzeh-Cognasse, H., Lafarge, S., Delezay, O., Pozzetto, B., McNicol, A., & Garraud, O. (2008). Toll-like receptor 4 ligand can differentially modulate the release of cytokines by human platelets. *British Journal of Haematology*, *141*(1), 84–91. https://doi.org/10.1111/j.1365-2141.2008.06999.x

Cognasse, F., Hamzeh, H., Chavarin, P., Acquart, S., Genin, C., & Garraud, O. (2005). Evidence of Toll-like receptor molecules on human platelets. *Immunology and Cell Biology*, *83*(2), 196–198. https://doi.org/10.1111/j.1440-1711.2005.01314.x

Colom, K., Fdz-Aranguiz, A., Suinaga, E., & Cisterna, R. (1995). Emergence of resistance to beta-lactam agents in Pseudomonas aeruginosa with group I beta-lactamases in Spain. *European Journal of Clinical Microbiology and Infectious Diseases*, *14*(11), 964–971.

https://doi.org/10.1007/BF01691378

Cooper, A. M., Roberts, A. D., Rhoades, E. R., Callahan, J. E., Getzy, D. M., & Orme, I. M. (1995). The role of interleukin-12 in acquired immunity to Mycobacterium tuberculosis infection. *Immunology*, *84*(3), 423–32. Retrieved from http://www.pubmedcentral.nih.gov/articlerender.fcgi?artid=1415123&tool=pmcentrez&rendertype=abstract%5Cnhttp://www.ncbi.nlm.nih.gov/pubmed/7751026%5Cnhttp://www.pubmedcentral.nih.gov/articlerender.fcgi?artid=PMC1415123

Costerton, A. J. W., Stewart, P. S., & Greenberg, E. P. (1999). Bacterial Biofilms: A Common Cause of Persistent Infections. *Science*, *284*(5418), 1318–1322.

Coutinho-Silva, R., & Ojcius, D. M. (2012). Role of extracellular nucleotides in the immune response against intracellular bacteria and protozoan parasites. *Microbes and Infection*, *14*(14), 1271–1277. https://doi.org/10.1016/j.micinf.2012.05.009

Coyle, A., Page, C., Atkinson, L., Flanagan, R., & Metzger, W. (1990). The Requirement for Platelets in Allergen-induced Late Asthmatic Airway Obstruction: Eosinophil Infiltration and Heightened Airway Responsiveness in Allergic Rabbits. *Am Rev Respir Dis*, *142*(3), 587–93.

Cramer, E. M., Norol, F., Guichard, J., Breton-Gorius, J., Vainchenker, W., Massé, J.-M., & Debili, N. (1997). Ultrastructure of Platelet Formation by Human Megakaryocytes Cultured With the Mpl Ligand. *Blood*, *89*(7), 2336–2346. https://doi.org/10.1182/blood.v97.1.154

Czapiga, M., Gao, J. L., Kirk, A., & Lekstrom-Himes, J. (2005). Human platelets exhibit chemotaxis using functional N-formyl peptide receptors. *Experimental Hematology*, *33*(1), 73–84. https://doi.org/10.1016/j.exphem.2004.09.010

Danese, S., de la Motte, C., Reyes, B. M. R., Sans, M., Levine, A. D., & Fiocchi, C. (2004). T Cells Trigger CD40-Dependent Platelet Activation and Granular RANTES Release: A Novel Pathway for Immune Response Amplification. *The Journal of Immunology*, *172*(4), 2011–2015. https://doi.org/10.4049/jimmunol.172.4.2011

de Stoppelaar, S. F. (2014). Thrombocytopenia impairs host defense in gram-negative pneumonia-derived sepsis in mice. *Blood*, *124*(25), 3781–3790. https://doi.org/10.1182/blood-2014-05-573915.The

de Stoppelaar, S. F., van't Veer, C., Roelofs, J. J. T. H., Claushuis, T. A. M., de Boer, O. J., Tanck, M. W. T., … van der Poll, T. (2015). Platelet and endothelial cell P-selectin are required for host defense against Klebsiella pneumoniae-induced pneumosepsis. *Journal of Thrombosis and Haemostasis*, (March), 1128–1138. https://doi.org/10.1111/jth.12893

Defres, S., Marwick, C., & Nathwani, D. (2009). MRSA as a cause of lung infection including airway infection, community-acquired pneumonia and hospital-acquired pneumonia. *European Respiratory Journal*, *34*(6), 1470–1476. https://doi.org/10.1183/09031936.00122309

Deppermann, C., & Kubes, P. (2016). Platelets and infection. *Seminars in Immunology*, (28), 536–545.

Dewitte, A., Lepreux, S., Villeneuve, J., Rigothier, C., Combe, C., Ouattara, A., & Ripoche, J. (2017). Blood platelets and sepsis pathophysiology: A new therapeutic prospect in critical ill patients? *Annals of Intensive Care*, *7*(1). https://doi.org/10.1186/s13613-017-0337-7

Dhooghe, B., Noël, S., Huaux, F., & Leal, T. (2014). Lung inflammation in cystic fibrosis: Pathogenesis and novel therapies. *Clinical Biochemistry*, *47*(7–8), 539–546. https://doi.org/10.1016/j.clinbiochem.2013.12.020

Di Lorenzo, F., Silipo, A., Bianconi, I., Lore', N. I., Scamporrino, A., Sturiale, L., … Molinaro, A. (2015).

Persistent cystic fibrosis isolate Pseudomonas aeruginosa strain RP73 exhibits an under-acylated LPS structure responsible of its low inflammatory activity. *Molecular Immunology*, *63*(2), 166–175. https://doi.org/10.1016/j.molimm.2014.04.004

Diacovo, T. G., DeFougerolles, A. R., Bainton, D. F., & Springer, T. A. (1994). A functional integrin ligand on the surface of platelets: Intercellular adhesion molecule-2. *Journal of Clinical Investigation*, *94*(3), 1243–1251. https://doi.org/10.1172/JCI117442

Diep, B. A., Gill, S. R., Chang, R. F., Phan, T. H. Van, Chen, J. H., Davidson, M. G., … Perdreau-Remington, F. (2006). Complete genome sequence of USA300, an epidemic clone of community-acquired meticillin-resistant Staphylococcus aureus. *Lancet*, *367*(9512), 731–739. https://doi.org/10.1016/S0140-6736(06)68231-7

Dötsch, A., Eckweiler, D., Schniederjans, M., Zimmermann, A., Jensen, V., Scharfe, M., … Häussler, S. (2012). The pseudomonas aeruginosa transcriptome in planktonic cultures and static biofilms using rna sequencing. *PLoS ONE*, *7*(2). https://doi.org/10.1371/journal.pone.0031092

Dovlatova, N., Wijeyeratne, Y. D., Fox, S. C., Manolopoulos, P., Johnson, A. J., White, A. E., … Heptinstall, S. (2008). Detection of P2Y14 protein in platelets and investigation of the role of P2Y14 in platelet function in comparison with the EP3 receptor. *Thrombosis and Haemostasis*, *100*(2). https://doi.org/10.1160/TH07-10-0601

Drago, L., Bortolin, M., Vassena, C., Taschieri, S., & Del Fabbro, M. (2013). Antimicrobial activity of pure platelet-rich plasma against microorganisms isolated from oral cavity. *BMC Microbiology*, *13*(1), 47. https://doi.org/10.1186/1471-2180-13-47

Duerschmied, D., Suidan, G. L., Demers, M., Herr, N., Carbo, C., Brill, A., … Wagner, D. D. (2013). Platelet serotonin promotes the recruitment of neutrophils to sites of acute inflammation in mice. *Blood*, *121*(6), 1008–1015. https://doi.org/10.1182/blood-2012-06-437392

Durrington, H. J., & Summers, C. (2008). Recent changes in the management of community acquired pneumonia in adults. *Bmj*, *336*(7658), 1429–1433. https://doi.org/10.1136/bmj.a285

Elson, G., & Daubeuf, B. (2007). Contribution of Toll-like receptors to the innate immune response to Gram-negative and Gram-positive bacteria. *The American Society of Hematology*, *109*(4), 1574–1583. https://doi.org/10.1182/blood-2006-06-032961.The

Enright, M. C., Robinson, D. A., Randle, G., Feil, E. J., Grundmann, H., & Spratt, B. G. (2002). The evolutionary history of methicillin-resistant *Staphylococcus aureus* (MRSA). *Proceedings of the National Academy of Sciences of the United States of America*, *99*(11), 7687–92. https://doi.org/10.1073/pnas.122108599

Fabre, J. E., Nguyen, M., Latour, A., Keifer, J. A., Audoly, L. P., Coffman, T. M., & Koller, B. H. (1999). Decreased platelet aggregation, increased bleeding time and resistance to thromboembolism in P2Y1-deficient mice. *Nature Medicine*, *5*(10), 1199–1202. https://doi.org/10.1038/13522

Facchini, M., De Fino, I., Riva, C., & Bragonzi, A. (2014). Long term chronic Pseudomonas aeruginosa airway infection in mice. *Journal of Visualized Experiments : JoVE*, (85), e51019. https://doi.org/10.3791/51019

Ferroni, P., Basili, S., Martini, F., Vieri, M., Labbadia, G., & Cordova, C. (2000). Soluble P-Selectin as a Marker of Platelet Hyperactivity in Patients with Chronic Obstructive Pulmonary Disease. *J Investig Med*, (48), 21–7.

Flamm, R. K., Weaver, M. K., Thornsberry, C., Jones, M. E., Karlowsky, J. a., & Sahm, D. F. (2004). Factors Associated with Relative Rates of Antibiotic Resistance in Pseudomonas aeruginosa Isolates Tested in Clinical Laboratories in the United States from 1999 to 2002. *Antimicrobial*

Agents and Chemotherapy, *48*(7), 2431. https://doi.org/10.1128/AAC.48.7.2431

Frank, M. M., & Fries, L. F. (1991). The role of complement in inflammation and phagocytosis. *Immunology Today*, *12*(9), 322–326. https://doi.org/10.1016/0167-5699(91)90009-I

Frenette, P. S., Denis, C. V., Weiss, L., Jurk, K., Subbarao, S., Kehrel, B., … Wagner, D. D. (2000). P-Selectin Glycoprotein Ligand 1 (Psgl-1) Is Expressed on Platelets and Can Mediate Platelet–Endothelial Interactions in Vivo. *The Journal of Experimental Medicine*, *191*(8), 1413–1422. https://doi.org/10.1084/jem.191.8.1413

Friedl, P., König, B., & König, W. (1992). Effects of mucoid and non-mucoid Pseudomonas aeruginosa isolates from cystic fibrosis patients on inflammatory mediator release from human polymorphonuclear granulocytes and rat mast cells. *Immunology*, *76*(1), 86–94. Retrieved from http://www.pubmedcentral.nih.gov/articlerender.fcgi?artid=1421756&tool=pmcentrez&rendertype=abstract

Gaboriaud, C., Juanhuix, J., Gruez, A., Lacroix, M., Darnault, C., Pignol, D., … Arlaud, G. J. (2003). The Crystal Structure of the Globular Head of Complement Protein C1q Provides a Basis for Its Versatile Recognition Properties. *Journal of Biological Chemistry*, *278*(47), 46974–46982. https://doi.org/10.1074/jbc.M307764200

Gachet, C. (2006). Regulation of Platelet Functions By P2 Receptors. *Annual Review of Pharmacology and Toxicology*, *46*(1), 277–300. https://doi.org/10.1146/annurev.pharmtox.46.120604.141207

Gachet, C. (2012). P2Y12 receptors in platelets and other hematopoietic and non-hematopoietic cells. *Purinergic Signalling*, *8*(3), 609–619. https://doi.org/10.1007/s11302-012-9303-x

Gaertner, F., Ahmad, Z., Rosenberger, G., Fan, S., Nicolai, L., Busch, B., … Massberg, S. (2017). Migrating Platelets Are Mechano-scavengers that Collect and Bundle Bacteria. *Cell*, *171*(6), 1368–1382.e23. https://doi.org/10.1016/j.cell.2017.11.001

Gafter-Gvili, A., Mansur, N., Bivas, A., Zemer-Wassercug, N., Bishara, J., Leibovici, L., & Paul, M. (2011). Thrombocytopenia in Staphylococcus aureus bacteremia: Risk factors and prognostic importance. *Mayo Clinic Proceedings*, *86*(5), 389–396. https://doi.org/10.4065/mcp.2010.0705

García-Álvarez, L., Holden, M. T. G., Lindsay, H., Webb, C. R., Brown, D. F. J., Curran, M. D., … Holmes, M. A. (2011). Meticillin-resistant Staphylococcus aureus with a novel mecA homologue in human and bovine populations in the UK and Denmark: A descriptive study. *The Lancet Infectious Diseases*, *11*(8), 595–603. https://doi.org/10.1016/S1473-3099(11)70126-8

Garcia, A. E., Mada, S. R., Rico, M. C., DelaCadena, R. A., & Kunapuli, S. P. (2011). Clopidogrel, a P2Y12 receptor antagonist, potentiates the inflammatory response in a rat model of peptidoglycan polysaccharide-induced arthritis. *PLoS ONE*, *6*(10). https://doi.org/10.1371/journal.pone.0026035

Gawaz, M., Dickfeld, T., Bogner, C., Fateh-Moghadam, S., Neumann, F. J., & Bogner, · C. (1997). Platelet function in septic multiple organ dysfunction syndrome. *Intensive Care Med*, *23*, 379–385. https://doi.org/10.1007/s001340050344

Gawaz, M., Fateh-moghadam, S., Pilz, J., Gurland, H., & Werdan, K. (1995). Platelet activation and interaction with leucocytes in patients with sepsis or multiple organ failure. *European Journal of Clinical Investigation*, *25*(11), 843–851.

Geary, C., Akinbi, H., Korfhagen, T., Fabre, J., Boucher, R., Rice, W., … Rice, W. (2005). Increased susceptibility of purinergic receptor-deficient mice to lung infection with Pseudomonas aeruginosa. *Am J Physiol Lung Cell Mol Physiol*, *289*, 890–895. https://doi.org/10.1152/ajplung.00428.2004.

Gellatly, S. L., & Hancock, R. E. W. (2013). Pseudomonas aeruginosa: New insights into pathogenesis and host defenses. *Pathogens and Disease*, *67*(3), 159–173. https://doi.org/10.1111/2049-632X.12033

Georgopapadakou, N. H., & Liu, F. Y. (1980). Binding of beta-lactam antibiotics to penicillin-binding proteins of Staphylococcus aureus and Streptococcus faecalis: relation to antibacterial activity. *Antimicrobial Agents and Chemotherapy*, *18*(5), 834–6. https://doi.org/10.1128/AAC.18.5.834

Giani, T., Arena, F., Vaggelli, G., Conte, V., Chiarelli, A., De Angelis, L. H., … Rossolini, G. M. (2015). Large nosocomial outbreak of colistin-resistant, carbapenemase-producing klebsiella pneumoniae traced to clonal expansion of an mgrb deletion mutant. *Journal of Clinical Microbiology*, *53*(10), 3341–3344. https://doi.org/10.1128/JCM.01017-15

Gibson, R. L., Burns, J. L., & Ramsey, B. W. (2003). Pathophysiology and Management of Pulmonary Infections in Cystic Fibrosis. *American Journal of Respiratory and Critical Care Medicine*, *168*(8), 918–951. https://doi.org/10.1164/rccm.200304-505SO

Goerge, T., Ho-Tin-Noe, B., Carbo, C., Benarafa, C., Remold-O'Donnell, E., Zhao, B. Q., … Wagner, D. D. (2008). Inflammation induces hemorrhage in thrombocytopenia. *Blood*, *111*(10), 4958–4964. https://doi.org/10.1182/blood-2007-11-123620

Goto, H., Horita, N., Tashiro, K., Nagai, K., Yamamoto, M., Sato, T., … Kaneko, T. (2018). The Platelet Count can Predict In-hospital Death in HIV-negative Smear-positive Pulmonary Tuberculosis Inpatients. *Internal Medicine*, 1391–1397. https://doi.org/10.2169/internalmedicine.0138-17

Greco, E., Lupia, E., Bosco, O., Vizio, B., & Montrucchio, G. (2017). Platelets and Multi-Organ Failure in Sepsis. *International Journal of Molecular Sciences*, (10), 2200. https://doi.org/10.3390/ijms18102200

Green, B. N., Johnson, C. D., Egan, J. T., Rosenthal, M., Griffith, E. A., & Evans, M. W. (2012). Methicillin-resistant Staphylococcus aureus: An overview for manual therapists. *Journal of Chiropractic Medicine*, *11*(1), 64–76. https://doi.org/10.1016/j.jcm.2011.12.001

Gregory, A. D., Hogue, L. A., Ferkol, T. W., & Link, D. C. (2007). Regulation of systemic and local neutrophil responses by G-CSF during pulmonary Pseudomonas aeruginosa infection. *Blood*, *109*(8), 3235–3243. https://doi.org/10.1182/blood-2005-01-015081

Gresele, P., Dottorini, M., Selli, M. L., lannacci, L., Canino, S., Todisco, T., … Nenci, G. G. (1993). Altered platelet function associated with the bronchial hyperresponsiveness accompanying nocturnal asthma. *The Journal of Allergy and Clinical Immunology*, *91*(4), 894–902. https://doi.org/10.1016/0091-6749(93)90347-I

Grimwood, K., To, M., Semple, R. A., Sokol, P. A., & Woods, D. E. (1993). Elevated exoenzyme expression by Pseudomonas aeruginosa is correlated with exacerbations of lung disease in cystic fibrosis. *Pediatric Pulmonology*, *15*(3), 135–139. https://doi.org/10.1002/ppul.1950150302

Growcott, E. J., Coulthard, A., Amison, R., Hardaker, E. L., Saxena, V., Malt, L., … Banner, K. H. (2011). Characterisation of a refined rat model of respiratory infection with Pseudomonas aeruginosa and the effect of ciprofloxacin. *Journal of Cystic Fibrosis*, *10*(3), 166–174. https://doi.org/10.1016/j.jcf.2010.12.007

Guo, Y. L., Liu, D. Q., Bian, Z., Zhang, C. Y., & Zen, K. (2009). Down-regulation of platelet surface CD47 expression in Escherichia coli O157:H7 infection-induced thrombocytopenia. *PLoS ONE*, *4*(9), 4–9. https://doi.org/10.1371/journal.pone.0007131

Hamada, K., Takuwa, N., Yokoyama, K., & Takuwa, Y. (1998). Stretch activates Jun N-terminal

kinase/stress-activated protein kinase in vascular smooth muscle cells through mechanisms involving autocrine ATP stimulation of purinoceptors. *Journal of Biological Chemistry*, *273*(11), 6334–6340. https://doi.org/10.1074/jbc.273.11.6334

Hamzeh-Cognasse, H., Damien, P., Chabert, A., Pozzetto, B., Cognasse, F., & Garraud, O. (2015). Platelets and infections - Complex interactions with bacteria. *Frontiers in Immunology*, *6*(82), 1–18. https://doi.org/10.3389/fimmu.2015.00082

Harada, Y., Yanagihara, K., Yamada, K., Migiyama, Y., Nagaoka, K., Morinaga, Y., … Kohnob, S. (2013). In vivo efficacy of daptomycin against methicillin-resistant staphylococcus aureus in a mouse model of hematogenous pulmonary infection. *Antimicrobial Agents and Chemotherapy*, *57*(6), 2841–2844. https://doi.org/10.1128/AAC.02331-12

Hartwig, J. H. (1992). Mechanisms of actin rearrangements mediating platelet activation. *Journal of Cell Biology*, *118*(6), 1421–1441. https://doi.org/10.1083/jcb.118.6.1421

Hartwig, J. H. (2013). *The Platelet Cytoskeleton*. *Platelets* (Third Edit). Elsevier Inc. https://doi.org/10.1016/B978-0-12-387837-3.00008-0

Hartwig, J., Italiano, J., Thompson, C., Love, D. G., Quinn, P. G., & Valeri, C. R. (2003). The Birth of the Platelet. *Blood*, *62*, 1580–1586. https://doi.org/10.1016/j.healthplace.2014.04.003

Hechler, B., & Gachet, C. (2015). Purinergic Receptors in Thrombosis and Inflammation. *Arteriosclerosis, Thrombosis, and Vascular Biology*, *35*(11), 2307–2315. https://doi.org/10.1161/ATVBAHA.115.303395

Hechler, B., Lenain, N., Marchese, P., Vial, C., Heim, V., Freund, M., … Gachet, C. (2003). A Role of the Fast ATP-gated P2X $_1$ Cation Channel in Thrombosis of Small Arteries In Vivo. *The Journal of Experimental Medicine*, *198*(4), 661–667. https://doi.org/10.1084/jem.20030144

Hidekazu Itoha, Carla Cicalab, Garry J Douglas, C. P. P. (1996). Platelet Accumulation Induced by Bacterial Endotoxin in Rats. *Science*, *83*(6).

Ho-Tin-Noé, B., Demers, M., & Wagner, D. D. (2011). How platelets safeguard vascular integrity. *Journal of Thrombosis and Haemostasis*, *9*(1), 56–65. https://doi.org/10.1111/j.1538-7836.2011.04317.x

Homolya, L., Steinberg, T. H., & Boucher, R. C. (2000). Cell to Cell Communication in Response to Mechanical Stress via Bilateral Release of ATP and UTP in Polarized Epithelia. *The Journal of Cell Biology*, *150*(6), 1349–1359.

Hoshino, K., Takeuchi, O., Kawai, T., Sanjo, H., Ogawa, T., Takeda, Y., … Akira, S. (1999). Cutting edge: Toll-like receptor 4 (TLR4)-deficient mice are hyporesponsive to lipopolysaccharide: evidence for TLR4 as the Lps gene product. *Journal of Immunology*, *162*(7), 3749–52. https://doi.org/10.1038/nri2275

Houston, N., Stewart, N., Smith, D. S., Bell, S. C., Champion, A. C., & Reid, D. W. (2013). Sputum neutrophils in cystic fibrosis patients display a reduced respiratory burst. *Journal of Cystic Fibrosis*, *12*(4), 352–362. https://doi.org/10.1016/j.jcf.2012.11.004

Hu, Y. (2013). Enhancement by novel anti-MRSA compound HT61 of the activity of other antibiotics. *J Antimicrob Chemother*, *68*, 374–384.

Hu, Y., Shamaei-Tousi, A., Liu, Y., & Coates, A. (2010). A new approach for the discovery of antibiotics by targeting non-multiplying bacteria: A novel topical antibiotic for Staphylococcal infections. *PLoS ONE*, *5*(7). https://doi.org/10.1371/journal.pone.0011818

Huang, H. C., Shieh, C. C., Yu, W. L., Cheng, K. C., Chen, C. C., Chang, S. T., & Chuang, Y. C. (2008).

Comparing the protective effects of ciprofloxacin, moxifloxacin and levofloxacin in mice with lipopolysaccharide-induced acute lung injuries. *Respirology*, *13*(1), 47–52. https://doi.org/10.1111/j.1440-1843.2007.01192.x

Hubbard, A. T. M., Barker, R., Rehal, R., Vandera, K. K. A., Harvey, R. D., & Coates, A. R. M. (2017). Mechanism of Action of a Membrane-Active Quinoline-Based Antimicrobial on Natural and Model Bacterial Membranes. *Biochemistry*, *56*(8), 1163–1174. https://doi.org/10.1021/acs.biochem.6b01135

Hui, P., Cook, D. J., Lim, W., Fraser, G. A., & Arnold, D. M. (2011). The frequency and clinical significance of thrombocytopenia complicating critical illness: A systematic review. *Chest*, *139*(2), 271–278. https://doi.org/10.1378/chest.10-2243

Hurley, S. M., Lutay, N., Holmqvist, B., & Shannon, O. (2016). The dynamics of platelet activation during the progression of streptococcal sepsis. *PLoS ONE*, *11*(9), 1–14. https://doi.org/10.1371/journal.pone.0163531

Idzko, M., Pitchford, S., & Page, C. (2015). Role of platelets in allergic airway inflammation. *Journal of Allergy and Clinical Immunology*, *135*(6), 1416–1423. https://doi.org/10.1016/j.jaci.2015.04.028

Jawien, J., Chlopicki, S., & Gryglewski, R. J. (2002). Interactions between human platelets and eosinophils are mediated by selectin-P. *Pol.J.Pharmacol.*, *54*(1230–6002 (Print)), 157–160.

Jenne, C. N., Urrutia, R., & Kubes, P. (2013). Platelets: Bridging hemostasis, inflammation, and immunity. *International Journal of Laboratory Hematology*, *35*(3), 254–261. https://doi.org/10.1111/ijlh.12084

Johansson, D., Shannon, O., & Rasmussen, M. (2011). Platelet and neutrophil responses to Gram positive pathogens in patients with bacteremic infection. *PLoS ONE*, *6*(11). https://doi.org/10.1371/journal.pone.0026928

Johansson, M. W., & Mosher, D. F. (2013). Integrin activation states and eosinophil recruitment in asthma. *Frontiers in Pharmacology*, *4*(33), 1–9. https://doi.org/10.3389/fphar.2013.00033

Joseph, J. E., Harrison, P., Mackie, I. J., Isenberg, D. a, & Machin, S. J. (2001). Increased circulating platelet-leucocyte complexes and platelet activation in patients with antiphospholipid syndrome, systemic lupus erythematosus and rheumatoid arthritis. *British Journal of Haematology*, *115*(2), 451–459. https://doi.org/10.1046/j.1365-2141.2001.03101.x

Kahn, F., Hurley, S., & Shannon, O. (2013). Platelets promote bacterial dissemination in a mouse model of streptococcal sepsis. *Microbes and Infection*, *15*(10–11), 669–676. https://doi.org/10.1016/j.micinf.2013.05.003

Kaplan, J. B. (2010). Biofilm Dispersal : Mechanisms , Clinical Implications , and Potential Therapeutic Uses. *Journal of Dental Research*, *89*(3), 205–218. https://doi.org/10.1177/0022034509359403

Kaplan, M. H., Schindler, U., Smiley, S. T., & Grusby, M. J. (1996). Stat6 is required for mediating responses to IL-4 and for the development of Th2 cells. *Immunity*, *4*(3), 313–319. https://doi.org/10.1016/S1074-7613(00)80439-2

Karas, S., Rosse, W., & Kurlander, R. (1982). Characterization of the IgG-Fc receptor on human platelets. *Blood*, *60*, 1277–1282.

Kasper, B., Brandt, E., Brandau, S., & Petersen, F. (2007). Platelet factor 4 (CXC chemokine ligand 4) differentially regulates respiratory burst, survival, and cytokine expression of human monocytes by using distinct signaling pathways. *Journal of Immunology (Baltimore, Md. :*

1950), *179*(4), 2584–91. https://doi.org/10.4049/jimmunol.179.4.2584

Kauffenstein, G., Bergmeier, W., Eckly, A., Ohlmann, P., Léon, C., Cazenave, J. P., … Gachet, C. (2001). The P2Y $_{12}$ receptor induces platelet aggregation through weak activation of the $\alpha_{IIb}\beta_3$ integrin - a phosphoinositide 3-kinase-dependent mechanism. *FEBS Letters*, *505*(2), 281–290. https://doi.org/10.1016/S0014-5793(01)02824-1

Kawakami, M., Pekala, P. H., Lane, M. D., Lane, D., Knight, D. M., Ringold, G. M., … Liu, L. (1983). Passive Immunization Against Cachectin/Tumor Necrosis Factor Protects Mice from Lethal Effect of Endotoxin. *Science*, (13), 869–871.

Keane, C., Tilley, D., Cunningham, A., Smolenski, A., Kadioglu, A., Cox, D., … Kerrigan, S. W. (2010). Invasive Streptococcus pneumoniae trigger platelet activation via Toll-like receptor 2. *Journal of Thrombosis and Haemostasis*, *8*(12), 2757–2765. https://doi.org/10.1111/j.1538-7836.2010.04093.x

Kellum, J. A. (2004). Metabolic acidosis in patients with sepsis: epiphenomenon or part of the pathophysiology? *Critical Care and Resuscitation : Journal of the Australasian Academy of Critical Care Medicine*, *6*(3), 197–203. https://doi.org/AACCM-JSeptember04.9 [pii]

Kerrigan, S. W. (2015). The expanding field of platelet-bacterial interconnections. *Platelets*, *26*(4), 293–301. https://doi.org/10.3109/09537104.2014.997690

Kerrigan, S. W., & Cox, D. (2010). Platelet-bacterial interactions. *Cellular and Molecular Life Sciences*, *67*(4), 513–523. https://doi.org/10.1007/s00018-009-0207-z

Kerrigan, S. W., Douglas, I., Wray, A., Heath, J., Byrne, M. F., Fitzgerald, D., & Cox, D. (2002). A role for glycoprotein Ib in Streptococcus sanguis -induced platelet aggregation. *Blood*, *100*(2), 509–516. https://doi.org/10.1182/blood.V100.2.509

Kerrigan, S. W., Jakubovics, N. S., Keane, C., Maguire, P., Wynne, K., Jenkinson, H. F., & Cox, D. (2007). Role of Streptococcus gordonii surface proteins SspA/SspB and Hsa in platelet function. *Infection and Immunity*, *75*(12), 5740–5747. https://doi.org/10.1128/IAI.00909-07

King, S., & Reed, G. (2002). Development of platelet secretory granules. *Seminars in Cell & Developmental Biology*, *13*(6), 293–302. https://doi.org/10.1016/S1084–9521(02)00059-9

Klausen, M., Heydorn, A., Ragas, P., Lambertsen, L., Aaes-jørgensen, A., Molin, S., & Tolker-nielsen, T. (2003). Biofilm formation by Pseudomonas aeruginosa wild type , flagella and type IV pili mutants, *48*, 1511–1524. https://doi.org/10.1046/j.1365-2958.2003.03525.x

Klevens, R. M., Morrison, M. A., Nadle, J., Petit, S., Gershman, K., Ray, S., … Fridkin, S. K. (2007). Invasive Methicillin-Resistant Staphylococcus aureus Infections in the United States. *JAMA*, *298*(15), 1763–1771.

Klinkhardt, U., Graff, J., & Harder, S. (2002). Clopidogrel, but not abciximab, reduces platelet leukocyte conjugates and P-selectin expression in a human ex vivo in vitro model. *Clinical Pharmacology and Therapeutics*, *71*(3), 176–185. https://doi.org/10.1067/mcp.2002.122018

Kornerup, K. N., Salmon, G. P., Pitchford, S. C., Liu, W. L., & Page, C. P. (2010). Circulating platelet-neutrophil complexes are important for subsequent neutrophil activation and migration. *Journal of Applied Physiology*, *109*(3), 758–767. https://doi.org/10.1152/japplphysiol.01086.2009

Kosaki, G. (2005). In Vivo Platelet Production from Mature Megakaryocytes: Does Platelet Release Occur via Proplatelets? *International Journal of Hematology*, *81*(3), 208–219. https://doi.org/10.1532/IJH97.04177

Kowal, K., Pampuch, a, Kowal-Bielecka, O., DuBuske, L. M., & Bodzenta-Łukaszyk, a. (2006). Platelet activation in allergic asthma patients during allergen challenge with Dermatophagoides pteronyssinus. *Clinical and Experimental Allergy : Journal of the British Society for Allergy and Clinical Immunology*, *36*(4), 426–432. https://doi.org/10.1111/j.1365-2222.2006.02446.x

Kowalska, M. a, Ratajczak, M. Z., Majka, M., Jin, J., Kunapuli, S., Brass, L., & Poncz, M. (2000). Stromal cell-derived factor-1 and macrophage-derived chemokine: 2 chemokines that activate platelets. *Blood*, *96*(1), 50–57.

Kraemer, B. F., Borst, O., Gehring, E. M., Schoenberger, T., Urban, B., Ninci, E., … Lindemann, S. (2010). PI3 kinase-dependent stimulation of platelet migration by stromal cell-derived factor 1 (SDF-1). *Journal of Molecular Medicine*, *88*(12), 1277–1288. https://doi.org/10.1007/s00109-010-0680-8

Kraemer, B. F., Campbell, R. A., Schwertz, H., Cody, M. J., Franks, Z., Tolley, N. D., … Weyrich, A. S. (2011). Novel anti-bacterial activities of β-defensin 1 in human platelets: Suppression of pathogen growth and signaling of neutrophil extracellular trap formation. *PLoS Pathogens*, *7*(11). https://doi.org/10.1371/journal.ppat.1002355

Kraemer, B. F., Campbell, R. A., Schwertz, H., Franks, Z. G., De Abreu, A. V., Grundler, K., … Weyrich, A. S. (2012). Bacteria differentially induce degradation of Bcl-xL, a survival protein, by human platelets. *Blood*, *120*(25), 5014–5020. https://doi.org/10.1182/blood-2012-04-420661

Krijgsveld, J., Zaat, S. a, Meeldijk, J., van Veelen, P. a, Fang, G., Poolman, B., … Dankert, J. (2000). Thrombocidins, microbicidal proteins from human blood platelets, are C-terminal deletion products of CXC chemokines. *The Journal of Biological Chemistry*, *275*(27), 20374–20381. https://doi.org/10.1074/jbc.275.27.20374

Kuijper, P., Gallardo Tores, H., Lammers, J., Sixma, J., Koenderman, L., & Zwaginga, J. (1998). Platelet associated fibrinogen and ICAM-2 induce firm adhesion of neutrophils under flow conditions. *Thromb Haemost.*, *80*(3), 443–448.

Kuijpers, M. J. E., Schulte, V., Oury, C., Lindhout, T., Broers, J., Hoylaerts, M. F., … Heemskerk, J. W. M. (2004). Facilitating roles of murine platelet glycoprotein Ib and α IIbβ3 in phosphatidylserine exposure during vWF-collagen-induced thrombus formation. *Journal of Physiology*, *558*(2), 403–415. https://doi.org/10.1113/jphysiol.2004.062414

Kukulski, F., Yebdri, F. Ben, Bahrami, F., Lévesque, S. A., Martín-Satué, M., & Sévigny, J. (2010). The P2 receptor antagonist PPADS abrogates LPS-induced neutrophil migration in the murine air pouch via inhibition of MIP-2 and KC production. *Molecular Immunology*, *47*(4), 833–839. https://doi.org/10.1016/j.molimm.2009.09.037

Kurup, S. P., & Tarleton, R. L. (2013). Perpetual expression of PAMPs necessary for optimal immune control and clearance of a persistent pathogen. *Nature Communications*, *4*, 1–10. https://doi.org/10.1038/ncomms3616

Langer, H. F., & Chavakis, T. (2009). Leukocyte - Endothelial interactions in inflammation. *Journal of Cellular and Molecular Medicine*, *13*(7), 1211–1220. https://doi.org/10.1111/j.1582-4934.2009.00811.x

Lapetina, E. G., & Siegel, F. L. (1983). Shape Change Induced in Human Platelets. *The Journal of Biological Chemistry*, *285*(12), 7241–7244.

Lax, S., Rayes, J., Wichaiyo, S., Haining, E. J., Lowe, K., Grygielska, B., … Watson, S. P. (2017). Platelet CLEC-2 protects against lung injury via effects of its ligand podoplanin on inflammatory alveolar macrophages in the mouse. *American Journal of Physiology - Lung Cellular and Molecular*

Physiology, *313*(6), l1016-1029. https://doi.org/10.1152/ajplung.00023.2017

Lecut, C., Frederix, K., Johnson, D. M., Deroanne, C., Thiry, M., Faccinetto, C., … Oury, C. (2009). P2X1 Ion Channels Promote Neutrophil Chemotaxis through Rho Kinase Activation. *The Journal of Immunology*, *183*(4), 2801–2809. https://doi.org/10.4049/jimmunol.0804007

Lee, B. C., Cheng, T., Adams, G. B., Attar, E. C., Miura, N., Lee, S. B., … Scadden, D. T. (2003). P2Y-like receptor, GPR105 (P2Y14), identifies and mediates chemotaxis of bone-marrow hematopoietic stem cells. *Genes and Development*, *17*(13), 1592–1604. https://doi.org/10.1101/gad.1071503

Leon, C., Alex, M., Klocke, A., Morgenstern, E., Moosbauer, C., Eckly, A., … Engelmann, B. (2008). Platelet ADP receptors contribute to the initiation of intravascular coagulation Platelet ADP receptors contribute to the initiation of intravascular coagulation, *103*(2), 594–600. https://doi.org/10.1182/blood-2003-05-1385

Léon, C., Ravanat, C., Freund, M., Cazenave, J. P., & Gachet, C. (2003). Differential involvement of the P2Y1 and P2Y12 receptors in platelet procoagulant activity. *Arteriosclerosis, Thrombosis, and Vascular Biology*, *23*(10), 1941–1947. https://doi.org/10.1161/01.ATV.0000092127.16125.E6

Levaditi, C. (1901). Et des organisms vaccines contre le vibron cholerique. *Ann Inst Pasteur*, (15), 894–924.

Leven, R., & Yee, M. (1987). Megakaryocyte morphogenesis stimulated in vitro by whole and partially fractionated thrombocytopenic plasma: a model system for the study of platelet formation. *Blood*, *69*(4), 1046–1052.

Li, Z., Delaney, M., O'Brien, K., & Du, K. (2010). Signaling during platelet adhesion and activation. *Arterioscler Thromb Vasc Biol*, *30*(12), 2341–2349. https://doi.org/10.1161/ATVBAHA

Li, Z., Kim, E. S., & Bearer, E. L. (2002). Arp2/3 complex is required for actin polymerization during platelet shape change. *Blood*, *99*(12), 4466–4474.

Lian, L., Wang, Y., Draznin, J., Eslin, D., Bennett, J. S., Poncz, M., … Abrams, C. S. (2005). The relative role of PLCbeta and PI3K gamma in platelet activation. *Blood*, *106*(1), 110–117. https://doi.org/10.1182/blood-2004-05-2005

Liu, Y., Di, M., Chu, H., Liu, X., Wang, L., Wenzel, S., & Di, P. (2013). Increased susceptibility to pulmonary Pseudomonas infection in Splunc1 knockout mice. *J Immunol*, *191*(8), 1–24. https://doi.org/10.1016/j.steroids.2010.09.006.Membrane

Liverani, E., Rico, M. C., Tsygankov, A. Y., Kilpatrick, L. E., & Kunapuli, S. P. (2016). P2Y12 Receptor Modulates Sepsis-Induced Inflammation. *Arteriosclerosis, Thrombosis, and Vascular Biology*, *36*(5), 961–71. https://doi.org/10.1161/ATVBAHA.116.307401

Liverani, E., Rico, M. C., Yaratha, L., Tsygankov, A. Y., Kilpatrick, L. E., & Kunapuli, S. P. (2014). LPS-induced systemic inflammation is more severe in P2Y12 null mice. *Journal of Leukocyte Biology*, *95*(2), 313–323. https://doi.org/10.1189/jlb.1012518

Lopez, J. (1994). The platelet glycoprotein Ib-IX complex. *Blood Coagul Fibrinolysis*, *5*(1), 97–119.

Lorè, N. I., Veraldi, N., Riva, C., Sipione, B., Spagnuolo, L., De Fino, I., … Cigana, C. (2018). Synthesized heparan sulfate competitors attenuate Pseudomonas aeruginosa lung infection. *International Journal of Molecular Sciences*, *19*(1), 1–16. https://doi.org/10.3390/ijms19010207

Lorenz, R., & Brauer, M. (1988). Platelet Factor 4 (PF4) in septicaemia. *Infection*, *16*(5), 273–276.

Loughman, A., Fitzgerald, J. R., Brennan, M. P., Higgins, J., Downer, R., Cox, D., & Foster, T. J. (2005). Roles for fibrinogen, immunoglobulin and complement in platelet activation promoted by

Staphylococcus aureus clumping factor A. *Molecular Microbiology*, *57*(3), 804–818. https://doi.org/10.1111/j.1365-2958.2005.04731.x

Lourbakos, A., Yuan, Y. P., Jenkins, A. L., Travis, J., Andrade-Gordon, P., Santulli, R., … Pike, R. N. (2001). Activation of protease-activated receptors by gingipains from Porphyromonas gingivalis leads to platelet aggregation: A new trait in microbial pathogenicity. *Blood*, *97*(12), 3790–3797. https://doi.org/10.1182/blood.V97.12.3790

Lukacs, N. W., John, A., Berlin, A., Bullard, D. C., Knibbs, R., & Stoolman, L. M. (2002). E- and P-Selectins Are Essential for the Development of Cockroach Allergen-Induced Airway Responses. *The Journal of Immunology*, *169*(4), 2120–2125. https://doi.org/10.4049/jimmunol.169.4.2120

Lyczak, J. B., Cannon, C. L., & Pier, G. B. (2002). Lung infections associated with cystic fibrosis. *Clinical Microbiology Reviews*. https://doi.org/10.1128/CMR.15.2.194-222.2002

Maccia, C. A., Gallagher, J. S., Ataman, G., Glueck, H. I., Brooks, S. M., & Bernstein, I. L. (1977). Platelet thrombopathy in asthmatic patients with elevated immunoglobulin E. *The Journal of Allergy and Clinical Immunology*, *59*(2), 101–108. https://doi.org/10.1016/0091-6749(77)90210-X

Machlus, K. R., & Italiano, J. E. (2013). The incredible journey: From megakaryocyte development to platelet formation. *Journal of Cell Biology*, *201*(6), 785–796. https://doi.org/10.1083/jcb.201304054

Mahaut-Smith, M. P., Jones, S., & Evans, R. J. (2011). The P2X1 receptor and platelet function. *Purinergic Signalling*, *7*(3), 341–356. https://doi.org/10.1007/s11302-011-9224-0

Mandal, R. V., Mark, E. J., & Kradin, R. L. (2007). Megakaryocytes and platelet homeostasis in diffuse alveolar damage. *Experimental and Molecular Pathology*, *83*(3), 327–331. https://doi.org/10.1016/j.yexmp.2007.08.005

Mangin, P., Ohlmann, P., Eckly, A., Cazenave, J. P., Lanza, F., & Gachet, C. (2004). The P2Y1 receptor plays an essential role in the platelet shape change induced by collagen when TxA2 formation is prevented. *Journal of Thrombosis and Haemostasis*, *2*(6), 969–977. https://doi.org/10.1111/j.1538-7836.2004.00722.x

Marier, J. F., Brazier, J. L., Lavigne, J., & Ducharme, M. P. (2003). Liposomal tobramycin against pulmonary infections of Pseudomonas aeruginosa: A pharmacokinetic and efficacy study following single and multiple intratracheal administrations in rats. *Journal of Antimicrobial Chemotherapy*, *52*(2), 247–252. https://doi.org/10.1093/jac/dkg317

Martens, E., & Demain, A. L. (2017). The antibiotic resistance crisis , with a focus on the United States, *70*(5), 520–526. https://doi.org/10.1038/ja.2017.30

Martin, J. F., Slater, D. N., Bridge, & Trowbridge, E. A. (1983). Abnormal Intrapulmonary Platelet Production: a Possible Cause of Vascular and Lung Disease. *The Lancet*, *321*(8328), 793–796. https://doi.org/10.1016/S0140-6736(83)91851-2

Mauler, M., Seyfert, J., Haenel, D., Seeba, H., Guenther, J., Stallmann, D., … Duerschmied, D. (2016). Platelet-neutrophil complex formation-a detailed in vitro analysis of murine and human blood samples. *Journal of Leukocyte Biology*, *99*(5), 781–789. https://doi.org/10.1189/jlb.3TA0315-082R

McDonald, B., Urrutia, R., Yipp, B. G., Jenne, C. N., & Kubes, P. (2012). Intravascular neutrophil extracellular traps capture bacteria from the bloodstream during sepsis. *Cell Host and Microbe*, *12*(3), 324–333. https://doi.org/10.1016/j.chom.2012.06.011

Mezzano, S., Burgos, M. E., Ardiles, L., Olavarria, F., Concha, M., Caorsi, I., … Mezzano, D. (1992). Glomerular localization of platelet factor 4 in streptococcal nephritis. *Nephron*, *61*(1), 58–63. Retrieved from http://www.ncbi.nlm.nih.gov/pubmed/1528342

Miajlovic, H., Loughman, A., Brennan, M., Cox, D., & Foster, T. J. (2007). Both complement- and fibrinogen-dependent mechanisms contribute to platelet aggregation mediated by Staphylococcus aureus clumping factor B. *Infection and Immunity*, *75*(7), 3335–3343. https://doi.org/10.1128/IAI.01993-06

Miajlovic, H., Zapotoczna, M., Geoghegan, J. A., Kerrigan, S. W., Speziale, P., & Foster, T. J. (2010). Direct interaction of iron-regulated surface determinant IsdB of Staphylococcus aureus with the GPIIb/IIIa receptor on platelets. *Microbiology*, *156*(3), 920–928. https://doi.org/10.1099/mic.0.036673-0

Middleton, E. A., Weyrich, A. S., & Zimmerman, G. A. (2016). Platelets in Pulmonary Immune Responses and Inflammatory Lung Diseases. *Physiological Reviews*, *96*(4), 1211–1259. https://doi.org/10.1152/physrev.00038.2015

Middleton, E., MT, R., Schwertz, H., & GA, Z. (2018). Amicus or Adversary Revisited: Platelets in Acute Lung Injury & Acute Respiratory Distress Syndrome. *American Journal of Respiratory Cell and Molecular Biology*, (35824), 1–59. https://doi.org/10.1165/rcmb.2017-0420TR

Miller, C. M., Boulter, N. R., Fuller, S. J., Zakrzewski, A. M., Lees, M. P., Saunders, B. M., … Smith, N. C. (2011). The role of the P2X7 receptor in infectious diseases. *PLoS Pathogens*, *7*(11). https://doi.org/10.1371/journal.ppat.1002212

Moore, D. J., Murdock, P. R., Watson, J. M., Faull, R. L. M., Waldvogel, H. J., Szekeres, P. G., … Emson, P. C. (2003). GPR105, a novel Gi/o-coupled UDP-glucose receptor expressed on brain glia and peripheral immune cells, is regulated by immunologic challenge: Possible role in neuroimmune function. *Molecular Brain Research*, *118*(1–2), 10–23. https://doi.org/10.1016/S0169-328X(03)00330-9

Murugappan, S., & Kunapuli, S. (2006). The role of ADP receptors in platelet function. *Frontiers in Bioscience*, *11*, 1977–1986.

Nachman, R., & Weksler, B. (1972). The platelet as an inflammatory cell. *Ann NY Acad Sci*, *201*(1), 131–137.

Naito, M., Sakai, E., Shi, Y., Ideguchi, H., Shoji, M., Ohara, N., … Nakayama, K. (2006). Porphyromonas gingivalis-induced platelet aggregation in plasma depends on Hgp44 adhesin but not Rgp proteinase. *Molecular Microbiology*, *59*(1), 152–167. https://doi.org/10.1111/j.1365-2958.2005.04942.x

Nanvazadeh, F., Khosravi, A. D., Zolfaghari, M. R., & Parhizgari, N. (2013). Genotyping of Pseudomonas aeruginosa strains isolated from burn patients by RAPD-PCR. *Burns*, *39*(7), 1409–1413. https://doi.org/10.1016/j.burns.2013.03.008

Nguyen, T., Ghebrehiwet, B., & Ellinor, I. B. (2000). Staphylococcus aureus Protein A Recognizes Platelet gC1qR / p33 : a Novel Mechanism for Staphylococcal Interactions with Platelets Staphylococcus aureus Protein A Recognizes Platelet gC1qR / p33 : a Novel Mechanism for Staphylococcal Interactions with Pla. *Infection and Immunity*, *68*(4), 2061–2068. https://doi.org/10.1128/IAI.68.4.2061-2068.2000.Updated

O'Seaghdha, M., Van Schooten, C. J., Kerrigan, S. W., Emsley, J., Silverman, G. J., Cox, D., … Foster, T. J. (2006). Staphylococcus aureus protein A binding to von Willebrand factor A1 domain is mediated by conserved IgG binding regions. *FEBS Journal*, *273*(21), 4831–4841.

https://doi.org/10.1111/j.1742-4658.2006.05482.x

O'Sullivan, B. P. O., Linden, M. D., Iii, A. L. F., Barnard, M. R., Spencer-manzon, M., Morris, J. E., … Michelson, A. D. (2005). Platelet activation in cystic fibrosis. *Blood*, *105*(12), 4635–4641. https://doi.org/10.1182/blood-2004-06-2098.)

O'Sullivan, S. T., Lederer, J. a, Horgan, a F., Chin, D. H., Mannick, J. a, & Rodrick, M. L. (1995). Major injury leads to predominance of the T helper-2 lymphocyte phenotype and diminished interleukin-12 production associated with decreased resistance to infection. *Annals of Surgery*, *222*(4), 482–492. https://doi.org/10.1097/00000658-199522240-00006

Ochs, M. M., McCusker, M. P., Bains, M., & Hancock, R. E. W. (1999). Negative regulation of the Pseudomonas aeruginosa outer membrane porin OprD selective for imipenem and basic amino acids. *Antimicrobial Agents and Chemotherapy*, *43*(5), 1085–1090.

Ogura, H., Kawasaki, T., Tanaka, H., Koh, T., Tanaka, R., Ozeki, Y., … Sugimoto, H. (2001). Activated platelets enhance microparticle formation and platelet-leukocyte interaction in severe trauma and sepsis. *Journal of Trauma - Injury, Infection and Critical Care*, *50*(5), 801–809. https://doi.org/10.1097/00005373-200105000-00005

Oliveira, A.-C., de Alencar, B. C., Tzelepis, F., Klezewsky, W., da Silva, R. N., Neves, F. S., … Bellio, M. (2010). Impaired Innate Immunity in Tlr4−/− Mice but Preserved CD8+ T Cell Responses against Trypanosoma cruzi in Tlr4-, Tlr2-, Tlr9- or Myd88-Deficient Mice. *PLoS Pathogens*, *6*(4), e1000870. https://doi.org/10.1371/journal.ppat.1000870

Ortiz-Muñoz, G., Mallavia, B., Bins, A., Headley, M., Krummel, M. F., & Looney, M. R. (2014). Aspirin-triggered 15-epi-lipoxin A4 regulates neutrophil-platelet aggregation and attenuates acute lung injury in mice. *Blood*, *124*(17), 2625–34. https://doi.org/10.1182/blood-2014-03-562876

Page, C., & Pitchford, S. (2013). Neutrophil and platelet complexes and their relevance to neutrophil recruitment and activation. *International Immunopharmacology*, *17*(4), 1176–1184. https://doi.org/10.1016/j.intimp.2013.06.004

Pan, D., Amison, R. T., Riffo-Vasquez, Y., Spina, D., Cleary, S. J., Wakelam, M. J., … Welch, H. C. E. (2015). P-Rex and Vav Rac-GEFs in platelets control leukocyte recruitment to sites of inflammation. *Blood*, *125*(7), 1146–1158. https://doi.org/10.1182/blood-2014-07-591040

Papapanagiotou, D., Nicu, E. A., Bizzarro, S., Gerdes, V. E. A., Meijers, J. C., Nieuwland, R., … Loos, B. G. (2009). Periodontitis is associated with platelet activation. *Atherosclerosis*, *202*(2), 605–611. https://doi.org/10.1016/j.atherosclerosis.2008.05.035

Patrauchan, M. A., Sarkisova, S. A., & Franklin, M. J. (2007). Strain-specific proteome responses of Pseudomonas aeruginosa to biofilm-associated growth and to calcium. *Microbiology*, *153*(11), 3838–3851. https://doi.org/10.1099/mic.0.2007/010371-0

Paul, B. Z. S., Daniel, J. L., & Kunapuli, S. P. (1999). Platelet Shape Change Is Mediated by both Calcium-dependent and -independent Signaling Pathways. *Journal of Biological Chemistry*, *274*(40), 28293–28300.

Peerschke, E., Murphy, T., & Ghebrehiwet, B. (2003). Activation-dependent surface expression of gClqR/p33 on human blood platelets. *Thrombosis and Haemostasis*, *89*(2), 331–339.

Pereira, S. F. F., Henriques, A. O., Pinho, M. G., De Lencastre, H., & Tomasz, A. (2007). Role of PBP1 in cell division of Staphylococcus aureus. *Journal of Bacteriology*, *189*(9), 3525–3531. https://doi.org/10.1128/JB.00044-07

Peters, M. J., Heyderman, R. S., Faust, S., Dixon, G. L. J., Inwald, D. P., & Klein, N. J. (2003). Severe

meningococcal disease is characterized by early neutrophil but not platelet activation and increased formation and consumption of platelet-neutrophil complexes. *Journal of Leukocyte Biology*, *73*(6), 722–730. https://doi.org/10.1189/jlb.1002509

Pieri, C., Borselli, D., Di Giorgio, C., De Méo, M., Bolla, J. M., Vidal, N., … Brunel, J. M. (2014). New ianthelliformisamine derivatives as antibiotic enhancers against resistant gram-negative bacteria. *Journal of Medicinal Chemistry*, *57*(10), 4263–4272. https://doi.org/10.1021/jm500194e

Pillarisetti, N., Williamson, E., Linnane, B., Skoric, B., Robertson, C. F., Robinson, P., … Ranganathan, S. (2011). Infection, inflammation,and lung function decline in infants with cystic fibrosis. *American Journal of Respiratory and Critical Care Medicine*, *184*(1), 75–81. https://doi.org/10.1164/rccm.201011-1892OC

Pitchford, S. C. (2007). Defining a role for platelets in allergic inflammation. *Biochemical Society Transactions*, *35*(5), 1104–8. https://doi.org/10.1042/BST0351104

Pitchford, S. C. (2007). Novel uses for anti-platelet agents as anti-inflammatory drugs. *British Journal of Pharmacology*, *152*(7), 987–1002. https://doi.org/10.1038/sj.bjp.0707364

Pitchford, S. C., Momi, S., Baglioni, S., Casali, L., Giannini, S., Rossi, R., … Gresele, P. (2008). Allergen induces the migration of platelets to lung tissue in allergic asthma. *American Journal of Respiratory and Critical Care Medicine*, *177*(6), 604–612. https://doi.org/10.1164/rccm.200702-214OC

Pitchford, S. C., Momi, S., Giannini, S., Casali, L., Spina, D., Page, C. P., & Gresele, P. (2005). Platelet P-selectin is required for pulmonary eosinophil and lymphocyte recruitment in a murine model of allergic inflammation. *Blood*, *105*(5), 2074–2081. https://doi.org/10.1182/blood-2004-06-2282

Pitchford, S. C., Riffo-Vasquez, Y., Sousa, A., Momi, S., Gresele, P., Spina, D., & Page, C. P. (2004). Platelets are necessary for airway wall remodeling in a murine model of chronic allergic inflammation. *Blood*, *103*(2), 639–647. https://doi.org/10.1182/blood-2003-05-1707

Pitchford, S. C., Yano, H., Lever, R., Riffo-Vasquez, Y., Ciferri, S., Rose, M. J., … Page, C. P. (2003). Platelets are essential for leukocyte recruitment in allergic inflammation. *Journal of Allergy and Clinical Immunology*, *112*(1), 109–118. https://doi.org/10.1067/mai.2003.1514

Pitchford, S., Pan, D., & Welch, H. C. E. (2017). Platelets in neutrophil recruitment to sites of inflammation. *Current Opinion in Hematology*, *24*(1), 23–31. https://doi.org/10.1097/MOH.0000000000000297

Plummer, C., Wu, H., Kerrigan, S. W., Meade, G., Cox, D., & Douglas, C. W. I. (2005). A serine-rich glycoprotein of Streptococcus sanguis mediates adhesion to platelets via GPIb. *British Journal of Haematology*, *129*(1), 101–109. https://doi.org/10.1111/j.1365-2141.2005.05421.x

Polley, M., & Nachman, R. (1983). Human platelet activation by C3a and C3a des-arg. *Journal of Experimental Medicine*, *158*(2), 603–615.

Polley, M., Nachman, R., & Weksler, B. (1981). Human complement in the arachidonic acid transformation pathway in platelets. *J Exp Med*, *153*(2), 257–268.

Qian, F., Le Breton, G. C., Chen, J., Deng, J., Christman, J. W., Wu, D., & Ye, R. D. (2012). Role for the guanine nucleotide exchange factor phosphatidylinositol-3,4,5- trisphosphate-dependent rac exchanger 1 in platelet secretion and aggregation. *Arteriosclerosis, Thrombosis, and Vascular Biology*, *32*(3), 768–777. https://doi.org/10.1161/ATVBAHA.111.243675

Radley, J. M., & Haller, C. J. (1983). Fate of senescent megakaryocytes in the bone marrow. *British*

Journal of Haematology, *53*(2), 277–287. https://doi.org/10.1111/j.1365-2141.1983.tb02022.x

Radley, J., & Scurfield, G. (1980). The Mechanism of Platelet Release. *Blood*, *56*(6), 996–999. https://doi.org/10.1038/nature13314.A

Rainger, G., Chimen, M., Harrison, M. J., Yates, C. M., Harrison, P., Watson, S. P., … Nash, G. B. (2015). The role of platelets in the recruitment of leukocytes during vascular disease. *Platelets*, *26*(6), 507–520. https://doi.org/10.3109/09537104.2015.1064881

Rice, W. R., Burton, F. M., & Fiedeldey, D. T. (1995). Cloning and expression of the alveolar type II cell P2u-purinergic receptor. *Am J Respir Cell Mol Biol*, *12*(1), 27–32. https://doi.org/10.1165/ajrcmb.12.1.7811468

Richardson, J. L., Shivdasani, R. A., Boers, C., Hartwig, J. H., & Italiano, J. E. (2005). Mechanisms of organelle transport and capture along proplatelets during platelet production. *Blood*, *106*(13), 4066–4075. https://doi.org/10.1182/blood-2005-06-2206

Riffo-Vasquez, Y., Coates, A. R. M., Page, C. P., & Spina, D. (2012). Mycobacterium tuberculosis chaperonin 60.1 inhibits leukocyte diapedesis in a murine model of allergic lung inflammation. *American Journal of Respiratory Cell and Molecular Biology*, *47*(2), 245–252. https://doi.org/10.1165/rcmb.2011-0412OC

Riffo-Vasquez, Y., Somani, A., Man, F., Amison, R., Pitchford, S., & Page, C. P. (2016). A non-anticoagulant fraction of heparin inhibits leukocyte diapedesis into the lung by an effect on platelets. *American Journal of Respiratory Cell and Molecular Biology*, *55*(4), 554–563. https://doi.org/10.1165/rcmb.2015-0172OC

Rivera, J., Lozano, M. L., Navarro-Núñez, L., & Vicente, V. (2009). Platelet receptors and signaling in the dynamics of thrombus formation. *Haematologica*, *94*(5), 700–711. https://doi.org/10.3324/haematol.2008.003178

Russwurm, S., Vickers, J., Meier-Hellmann, A., Spangenberg, P., Bredle, D., Reinhart, K., & Lö, W. (2002). Platelet and Leukocyte Activation Correlate With the Severity of Septic Organ Dysfunction. *Shock*, *17*(4), 263–268.

Sand, C. A., Starr, A., Wilder, C. D. E., Rudyk, O., Spina, D., Thiemermann, C., … Nandi, M. (2015). Quantification of microcirculatory blood flow: a sensitive and clinically relevant prognostic marker in murine models of sepsis. *Journal of Applied Physiology*, *118*(3), 344–354. https://doi.org/10.1152/japplphysiol.00793.2014

Sarma, J., & Ward, P. (2011). The Compliment System. *Cell Tissue Res*, *343*(1), 227–235. https://doi.org/10.1007/s00441-010-1034-0.The

Sawant, K. V., Poluri, K. M., Dutta, A. K., Sepuru, K. M., Troshkina, A., Garofalo, R. P., & Rajarathnam, K. (2016). Chemokine CXCL1 mediated neutrophil recruitment: Role of glycosaminoglycan interactions. *Scientific Reports*, *6*, 4–11. https://doi.org/10.1038/srep33123

Schiffmann, E., Corcoran, B. A., & Wahl, S. M. (1975). N-formylmethionyl peptides as chemoattractants for leucocytes. *Proceedings of the National Academy of Sciences*, *72*(3), 1059–1062. https://doi.org/10.1073/pnas.72.3.1059

Scott, T., & Owens, M. D. (2008). Thrombocytes respond to lipopolysaccharide through Toll-like receptor-4, and MAP kinase and NF-κB pathways leading to expression of interleukin-6 and cyclooxygenase-2 with production of prostaglandin E2. *Molecular Immunology*, *45*(4), 1001–1008. https://doi.org/10.1016/j.molimm.2007.07.035

Scrivens, M., & Dickenson, J. M. (2005). Functional expression of the P2Y 14 receptor in murine T-

lymphocytes. *British Journal of Pharmacology*, *146*(3), 435–444. https://doi.org/10.1038/sj.bjp.0706322

Scrivens, M., & Dickenson, J. M. (2006). Functional expression of the P2Y14 receptor in human neutrophils. *European Journal of Pharmacology*, *543*(1–3), 166–173. https://doi.org/10.1016/j.ejphar.2006.05.037

Semple, J. W., & Freedman, J. (2010). Platelets and innate immunity. *Cellular and Molecular Life Sciences*, *67*(4), 499–511. https://doi.org/10.1007/s00018-009-0205-1

Shafer, W. M., Martin, L. E., & Spitznagel, J. K. (1986). Late intraphagosomal hydrogen ion concentration favors the in vitro antimicrobial capacity of a 37-kilodalton cationic granule protein of human neutrophil granulocytes. *Infection and Immunity*, *53*(3), 651–655.

Shannon, O. (2015). Platelet interaction with bacterial toxins and secreted products. *Platelets*, *26*(4), 302–308. https://doi.org/10.3109/09537104.2015.1014471

Shannon, O., Hertzén, E., Norrby-Teglund, A., Mörgelin, M., Sjöbring, U., & Björck, L. (2007). Severe streptococcal infection is associated with M protein-induced platelet activation and thrombus formation. *Molecular Microbiology*, *65*(5), 1147–1157. https://doi.org/10.1111/j.1365-2958.2007.05841.x

Sherwood, E. R., & Toliver-Kinsky, T. (2004). Mechanisms of the inflammatory response. *Best Practice and Research: Clinical Anaesthesiology*, *18*(3), 385–405. https://doi.org/10.1016/j.bpa.2003.12.002

Shin, E. K., Park, H., Noh, J. Y., Lim, K. M., & Chung, J. H. (2017). Platelet shape changes and cytoskeleton dynamics as novel therapeutic targets for anti-thrombotic drugs. *Biomolecules and Therapeutics*, *25*(3), 223–230. https://doi.org/10.4062/biomolther.2016.138

Siauw, C., Kobsar, A., Dornieden, C., Beyrich, C., Schinke, B., Schubert-Unkmeir, A., … Eigenthaler, M. (2006). Group B streptococcus isolates from septic patients and healthy carriers differentially activate platelet signaling cascades. *Thrombosis and Haemostasis*, *95*(5), 836–849. https://doi.org/10.1160/TH05–08–0534

Siboo, I., Chambers, H., & Sullam, P. M. (2005). Role of SraP, a serine-rich surface protein of Staphylococcus aureus, in binding to human platelets. *Infection and Immunity*, *73*(4), 2273–2280. https://doi.org/10.1128/IAI.73.4.2273

Signas, C., Rauccit, G., Jonsson, K., Lindgren, P.-E., Anantharamaiaht, G. M., Hooks, M., & Lindberg, M. (1989). Nucleotide sequence of the gene for a fibronectin-binding protein from Staphylococcus aureus: Use of this peptide sequence in the synthesis of biologically active peptides. *Proceedings of the National Academy of Sciences USA*, *86*(2), 699–703. https://doi.org/10.1073/pnas.86.2.699

Smyth, S., McEver, R., AS, W., Morrell, C., Hoffman, M., Arepally, G., … Becker, R. (2009). Platelet functions beyond hemostasis. *Journal of Thrombosis and Haemostasis*, *7*, 1759–1766. https://doi.org/10.1007/978-3-319-39562-3_10

Ståhl, A. L., Svensson, M., Mörgelin, M., Svanborg, C., Tarr, P. I., Mooney, J. C., … Karpman, D. (2006). Lipopolysaccharide from enterohemorrhagic Escherichia coli binds to platelets through TLR4 and CD62 and is detected on circulating platelets in patients with hemolytic uremic syndrome. *Blood*, *108*(1), 167–176. https://doi.org/10.1182/blood-2005-08-3219

Stapleton, P. D., & Taylor, P. W. (2007). Methicillin resistance in Staphylococcus aureus: mechanisms and modulation. *Sci Prog*, *85*(1), 1–14.

Steinhubl, S. R., Badimon, J. J., Bhatt, D. L., Herbert, J. M., & Lüscher, T. (2007). Clinical evidence for anti-inflammatory effects of antiplatelet therapy in patients with atherothrombotic disease. *Vascular Medicine*, *12*(2), 113–122. https://doi.org/10.1177/1358863X07077462

Stenberg, P. E., Shuman, M. A., Levine, S. P., & Bainton, D. F. (1984). Redistribution of alpha-granules and their contents in thrombin-stimulated platelets. *Journal of Cell Biology*, *98*(2), 748–760. https://doi.org/10.1083/jcb.98.2.748

Stewart, P. S. (2002). Mechanisms of antibiotic resistance in bacterial biofilms. *International Journal of Medical Microbiology*, *292*(2), 107–113. https://doi.org/10.1078/1438-4221-00196

Storey, R. F., Judge, H. M., Wilcox, R. G., & Heptinstall, S. (2002). Inhibition of ADP-induced P-selectin expression and platelet-leukocyte conjugate formation by clopidogrel and the P2Y12 receptor antagonist AR-C69931MX but not aspirin. *Thrombosis and Haemostasis*, *88*(3), 488–494. https://doi.org/10.1267/THRO88030488

Storey, R. F., Sanderson, H. M., White, A. E., May, J. A., Cameron, K. E., & Heptinstall, S. (2000). The central role of the P(2T) receptor in amplification of human platelet activation, aggregation, secretion and procoagulant activity. *British Journal of Haematology*, *110*(4), 925–934. https://doi.org/10.1046/j.1365-2141.2000.02208.x

Stover, C. K., Pham, X. Q., Erwin, A. L., Mizoguchi, S. D., Warrener, P., Hickey, M. J., … Olson, M. V. (2000). Complete genome sequence of Pseudomonas aeruginosa PAO1, an opportunistic pathogen. *Nature*, *406*(6799), 959–964. https://doi.org/10.1038/35023079

Sullam, P. M., Frank, U., Yeaman, M. R., Täuber, M. G., Bayer, A. S., & Chambers, H. F. (1993). Effect of thrombocytopenia on the early course of streptococcal endocarditis. *The Journal of Infectious Diseases*, *168*(4), 910–4.

Sun, B., Li, J., Okahara, K., & Kambayashi, J. (1998). P2X 1 Purinoceptor in Human Platelets. *The Journal of Biological Chemistry*, *273*(19), 11544–11547.

Swartz, T. H., Dubyak, G. R., & Chen, B. K. (2015). Purinergic receptors: Key mediators of HIV-1 infection and inflammation. *Frontiers in Immunology*, *6*(585), 1–9. https://doi.org/10.3389/fimmu.2015.00585

Tablin, F., Castro, M., & Leven, R. M. (1990). Blood platelet formation in vitro. The role of the cytoskeleton in megakaryocyte fragmentation. *Journal of Cell Science*, *97*, 59–70.

Takahashi, W., Nakada, T. A., Yazaki, M., & Oda, S. (2016). Interleukin-6 Levels Act as a Diagnostic Marker for Infection and a Prognostic Marker in Patients with Organ Dysfunction in Intensive Care Units. *Shock*, *46*(3), 254–260. https://doi.org/10.1097/SHK.0000000000000616

Takeuchi, O., Hoshino, K., & Kawai, T. (1999). Differential roles of TLR2 and TLR4 in recognition of gram-negative and gram-positive bacterial cell wall components. *Immunity*, *11*, 443–451.

Tam, M., Snipes, G., & Stevenson, M. (1999). Characterization of chronic bronchopulmonary pseudomonas aeruginosa infection in resistant and susceptible inbred mouse strains. *American Journal of Respiratory Cell and Molecular Biology*, *20*(4), 710–719. https://doi.org/10.1165/ajrcmb.20.4.3223

Tamagawa-Mineoka, R., Katoh, N., & Kishimoto, S. (2009). Platelets play important roles in the late phase of the immediate hypersensitivity reaction. *Journal of Allergy and Clinical Immunology*, *123*(3), 581–587.e9. https://doi.org/10.1016/j.jaci.2008.12.1114

Tanaka, T., Narazaki, M., & Kishimoto, T. (2014). IL-6 in Inflammation, Immunity, and Disease. *Cold Spring Harb Perspect Biol*, *6*(10), 1–16. https://doi.org/10.1101/cshperspect.a016295

Tang, J., Hu, J., Kang, L., Deng, Z., Wu, J., & Pan, J. (2015). The use of vancomycin in the treatment of adult patients with methicillin-resistant staphylococcus aureus (MRSA) infection: A survey in a tertiary hospital in China. *International Journal of Clinical and Experimental Medicine*, *8*(10), 19436–19441.

Tang, Y., Yeaman, M., & Selsted, M. (2002). Antimicrobial peptides from human platelets. *Journal of Infectious Immunology*.

Taytard, A., Guenard, H., Vuillemin, L., Bouvot, J., Vergeret, J., & Ducassou, D. (1986). Platelet Kinetics in Stable Atopic Asthma. *Am Rev Respir Dis*, *134*(5), 983–985.

Thompson, C., Jakubowski, J., Quinn, P., Deykin, D., & Valeri, C. (1984). Platelet Size and Age Determine Platelet Function Independently. *Blood*, *63*(6), 1372–1375.

Thon, J. N., & Italiano, J. E. (2012). Platelets : Production , Morphology and Ultrastructure. *Handbook of Experimental Pharmacology*, (210), 3–22. https://doi.org/10.1007/978-3-642-29423-5

Tilley, D. O., Arman, M., Smolenski, A., Cox, D., O'Donnell, J. S., Douglas, C. W. I., … Kerrigan, S. W. (2013). Glycoprotein Ibα and FcγRIIa play key roles in platelet activation by the colonizing bacterium, Streptococcus oralis. *Journal of Thrombosis and Haemostasis*, *11*(5), 941–950. https://doi.org/10.1111/jth.12175

Tobias Junt, Harald Schulze, Zhao Chen, Steffen Massberg, T. G., Krueger, A., Wagner, D. D., Graf, T., Jr., J. E. I., Shivdasani, R. A., & Andrian, U. H. von. (2007). Dynamic Visualization of Thrombopoiesis Within Bone Marrow. *Science*, *317*(5845), 1767–1770. https://doi.org/10.1126/science.1146304

Toth-Zsamboki, E., Oury, C., Cornelissen, H., De Vos, R., Vermylen, J., & Hoylaerts, M. F. (2003). P2X1-mediated ERK2 Activation Amplifies the Collagen-induced Platelet Secretion by Enhancing Myosin Light Chain Kinase Activation. *Journal of Biological Chemistry*, *278*(47), 46661–46667. https://doi.org/10.1074/jbc.M308452200

Trier, D. A., Gank, K. D., Kupferwasser, D., Yount, N. Y., French, W. J., Michelson, A. D., … Yeaman, M. R. (2008). Platelet antistaphylococcal responses occur through P2X1and P2Y12receptor-induced activation and kinocidin release. *Infection and Immunity*, *76*(12), 5706–5713. https://doi.org/10.1128/IAI.00935-08

Trowrridge, E. A., Martin, J. F., & Sio, S. (1982). Evidence for a theory of physical fragmentation of megakaryocytes, implying that all platelets are produced in the pulmonary circulation. *Thrombosis Journal*, *28*(4), 461–475.

Tsuji, M., Ezumi, Y., Arai, M., & Takayama, H. (1997). A Novel Association of Fc Receptor gamma-chain with Glycoprotein VI and Their Co-expression as a Collagen Receptor in Human Platelets. *Journal of Biological Chemistry*, *272*(38), 23528–23531.

Van Amersfoort, E. S., Van Berkel, T. J., & Kuiper, J. (2003). Receptors, mediators, and mechanisms involved in bacterial sepsis and septic shock. *Clin Microbiol Rev*, *16*, 379–414. https://doi.org/10.1128/CMR.16.3.379

van den Boogaard, F. E., Schouten, M., de Stoppelaar, S. F., Roelofs, J. J. T. H., Brands, X., Schultz, M. J., … van der Poll, T. (2015). Thrombocytopenia Impairs Host Defense During Murine Streptococcus pneumoniae Pneumonia. *Critical Care Medicine*, *43*(3), E75–E83. https://doi.org/10.1097/CCM.0000000000000853

Van Heeckeren, A. M., & Schluchter, M. D. (2002). Murine models of chronic Pseudomonas aeruginosa lung infection. *Lab Anim*, *36*(3), 291–312. https://doi.org/10.1258/002367702320162405

Van Heeckeren, A. M., Schluchter, M. D., Xue, W., & Davis, P. B. (2006). Response to acute lung infection with mucoid Pseudomonas aeruginosa in cystic fibrosis mice. *American Journal of Respiratory and Critical Care Medicine*, *173*(3), 288–296. https://doi.org/10.1164/rccm.200506-917OC

Van Heeckeren, A. M., Tscheikuna, J., Walenga, R. W., Konstan, M. W., Davis, P. B., Erokwu, B., … Ferkol, T. W. (2000). Effect of Pseudomonas infection on weight loss, lung mechanics, and cytokines in mice. *American Journal of Respiratory and Critical Care Medicine*, *161*(1), 271–279. https://doi.org/10.1164/ajrccm.161.1.9903019

Van Heeckeren, A., Walenga, R., Konstan, M. W., Bonfield, T., Davis, P. B., & Ferkol, T. (1997). Excessive inflammatory response of cystic fibrosis mice to bronchopulmonary infection with Pseudomonas aeruginosa. *Journal of Clinical Investigation*, *100*(11), 2810–2815. https://doi.org/10.1172/JCI119828

Vanichakarn, P., Blair, P., Wu, C., Freedman, J. E., & Chakrabarti, S. (2008). Neutrophil CD40 enhances platelet-mediated inflammation. *Thrombosis Research*, *122*(3), 346–358. https://doi.org/10.1016/j.thromres.2007.12.019

Venkata, C., Kashyap, R., Farmer, J. C., & Afessa, B. (2013). Thrombocytopenia in adult patients with sepsis: incidence, risk factors, and its association with clinical outcome. *Journal of Intensive Care*, *1*(1), 9. https://doi.org/10.1186/2052-0492-1-9

Von Hundelshausen, P., Koenen, R. R., Sack, M., Mause, S. F., Adriaens, W., Proudfoot, A. E. I., … Weber, C. (2005). Heterophilic interactions of platelet factor 4 and RANTES promote monocyte arrest on endothelium. *Blood*, *105*(3), 924–930. https://doi.org/10.1182/blood-2004-06-2475

Vowinkel, T., Anthoni, C., Wood, K. C., Stokes, K. Y., Russell, J., Gray, L., … Granger, D. N. (2007). CD40-CD40 Ligand Mediates the Recruitment of Leukocytes and Platelets in the Inflamed Murine Colon. *Gastroenterology*, *132*(3), 955–965. https://doi.org/10.1053/j.gastro.2006.12.027

Walker, T. R., & Watson, S. P. (1993). Synergy between Ca2+ and protein kinase C is the major factor in determining the level of secretion from human platelets. *The Biochemical Journal*, *289 (Pt 1*, 277–82. Retrieved from http://www.pubmedcentral.nih.gov/articlerender.fcgi?artid=1132161&tool=pmcentrez&rendertype=abstract

Walsh, T. G., Harper, M. T., & Poole, A. W. (2015). SDF-1α is a novel autocrine activator of platelets operating through its receptor CXCR4. *Cellular Signalling*, *27*(1), 37–46. https://doi.org/10.1016/j.cellsig.2014.09.021

Wang, H. B., Wang, J. T., Zhang, L., Geng, Z. H., Xu, W. L., Xu, T., … Chen, M. (2007). P-selectin primes leukocyte integrin activation during inflammation. *Nature Immunology*, *8*(8), 882–892.

Ward, J. R., Bingle, L., Judge, H. M., Brown, S. B., Storey, R. F., Whyte, M. K. B., … Sabroe, I. (2005). Agonists of toll-like receptor (TLR) 2 and TLR4 are unable to modulate platelet activation by adenosine diphosphate and platelet activating factor. *Thromb Haemost*, *94*, 831–838. https://doi.org/10.1160/TH05-01

Weksler, B., & Coupal, C. (1973). Platelet-dependent generation of chemotactic activity in serum. *J Exp Med*, *137*(6), 1419–30.

Weyrich, A. S., & Zimmerman, G. A. (2013). Platelets in Lung Biology. *Annual Review of Physiology*, *75*(1), 569–591. https://doi.org/10.1146/annurev-physiol-030212-183752

White, J. G. (2005). Platelets are covercytes, not phagocytes: Uptake of bacteria involves channels of

the open canalicular system. *Platelets*, *16*(2), 121–131. https://doi.org/10.1080/09537100400007390

Winokur, R., & Hartwig, J. H. (1995). Mechanism of shape change in chilled human platelets. *Blood*, *85*(7), 1796–804.

Wolf, S. F., Sieburth, D., & Sypek, J. (1994). Interleukin 12: A key modulator of immune function. *Stem Cells*, *12*(2), 154–168. https://doi.org/10.1002/stem.5530120203

Woodfin, A., Reichel, C. A., Khandoga, A., Corada, M., Voisin, M. B., Scheiermann, C., … Nourshargh, S. (2007). JAM-A mediates neutrophil transmigration in a stimulus-specific manner in vivo: Evidence for sequential roles for JAM-A and PECAM-1 in neutrophil transmigration. *Blood*, *110*(6), 1848–1856. https://doi.org/10.1182/blood-2006-09-047431

Worth, R. G., Chien, C. D., Chien, P., Reilly, M. P., McKenzie, S. E., & Schreiber, A. D. (2006). Platelet FcγRIIA binds and internalizes IgG-containing complexes. *Experimental Hematology*, *34*(11), 1490–1495. https://doi.org/10.1016/j.exphem.2006.06.015

Wuescher, L. M., Takashima, A., & Worth, R. G. (2015). A novel conditional platelet depletion mouse model reveals the importance of platelets in protection against staphylococcus aureus bacteremia. *Journal of Thrombosis and Haemostasis*, *13*(2), 303–313. https://doi.org/10.1111/jth.12795

Wurster, A. L., Rodgers, V. L., Satoskar, A. R., Whitters, M. J., Young, D. A., Collins, M., & Grusby, M. J. (2002). Interleukin 21 Is a T Helper (Th) Cell 2 Cytokine that Specifically Inhibits the Differentiation of Naive Th Cells into Interferon γ–producing Th1 Cells. *The Journal of Experimental Medicine*, *196*(7), 969–977. https://doi.org/10.1084/jem.20020620

Xiang, B., Zhang, G., Guo, L., Li, X. A., Morris, A. J., Daugherty, A., … Li, Z. (2013). Platelets protect from septic shock by inhibiting macrophage-dependent inflammation via the cyclooxygenase 1 signalling pathway. *Nat Commun*, *4*, 2657. https://doi.org/10.1038/ncomms3657

Yang, L.-C., Hu, S.-W., Yan, M., Yang, J.-J., Tsou, S.-H., & Lin, Y.-Y. (2015). Antimicrobial activity of platelet-rich plasma and other plasma preparations against periodontal pathogens. *Journal of Periodontology*, *86*(2), 310–8. https://doi.org/10.1902/jop.2014.140373

Yeaman, M. R. (1997). The role of platelets in antimicrobial host defense. *Clinical Infectious Diseases : An Official Publication of the Infectious Diseases Society of America*, *25*(5), 951–970. https://doi.org/10.1086/516120

Yeaman, M. R. (2010). Platelets in defense against bacterial pathogens. *Cellular and Molecular Life Sciences*, *67*(4), 525–544. https://doi.org/10.1007/s00018-009-0210-4

Yeaman, M. R. (2014). Platelets: at the nexus of antimicrobial defence. *Nature Reviews. Microbiology*, *12*(6), 426–37. https://doi.org/10.1038/nrmicro3269

Yeaman, M. R., & Bayer, A. S. (1999). Antimicrobial peptides from platelets Michael. *Drug Resistance Updates*, *2*, 116–126.

Yeaman, M. R., Sullam, P. M., Dazin, P. F., Norman, D. C., Bayer, S., The, S., … Bayer, A. S. (1992). Characterization of Staphylococcus aureus-Platelet Binding by Quantitative Flow Cytometric Analysis. *The Journal of Infectious Diseases*, *166*(1), 65–73.

Yeaman, M. R., Tang, Y. I. Q., Shen, A. J., Bayer, A. S., & Selsted, M. E. (1997). Purification and in vitro activities of rabbit platelet microbicidal proteins. *Infection and Immunity*, *65*(3), 1023–1031.

Yost, C. C., Cody, M. J., Harris, E. S., Thornton, N. L., Mcinturff, A. M., Martinez, M. L., … Zimmerman, G. A. (2015). Impaired neutrophil extracellular trap (NET) formation : a novel innate immune

deficiency of human neonates. *Blood*, *113*(25), 6419–6428. https://doi.org/10.1182/blood-2008-07-171629.An

Yount, N. Y., Waring, A. J., Gank, K. D., Welch, W. H., Kupferwasser, D., & Yeaman, M. R. (2007). Structural correlates of antimicrobial efficacy in IL-8 and related human kinocidins. *Biochimica et Biophysica Acta - Biomembranes*, *1768*(3), 598–608. https://doi.org/10.1016/j.bbamem.2006.11.011

Yount, N. Y., & Yeaman, M. R. (2006). Structural congruence among membrane-active host defense polypeptides of diverse phylogeny. *Biochimica et Biophysica Acta - Biomembranes*, *1758*(9), 1373–1386. https://doi.org/10.1016/j.bbamem.2006.03.027

Youssefian, T., Drouin, A., Massé, J. M., Guichard, J., & Cramer, E. M. (2002). Host defense role of platelets: engulfment of HIV and Staphylococcus aureus ocurs in a specific subcellular compoartmente and is enhanced by platelet activation. *Blood*, *99*(11), 4021–4029. https://doi.org/10.1182/blood-2001-12-0191.Supported

Yun, S.-H., Sim, E.-H., Goh, R.-Y., Park, J.-I., & Han, J.-Y. (2016). Platelet Activation: The Mechanisms and Potential Biomarkers. *BioMed Research International*, 1–5. https://doi.org/10.1155/2016/9060143

Zaidenstein, R., Miller, A., Tal-Jasper, R., Ofer-Friedman, H., Sklarz, M., Katz, D., … Marchaim, D. (2018). Therapeutic Management of Pseudomonas aeruginosa Bloodstream Infection Non-Susceptible to Carbapenems but Susceptible to “Old” Cephalosporins and/or to Penicillins. *Microorganisms*, *6*(1), 9. https://doi.org/10.3390/microorganisms6010009

Zhang, G., Han, J., Welch, E. J., Ye, R. D., Voyno-Yasenetskaya, T. A., Malik, A. B., … Li, Z. (2009). Lipopolysaccharide Stimulates Platelet Secretion and Potentiates Platelet Aggregation via TLR4/MyD88 and the cGMP-Dependent Protein Kinase Pathway. *The Journal of Immunology*, *182*(12), 7997–8004. https://doi.org/10.4049/jimmunol.0802884

Zhang, L., Orban, M., Lorenz, M., Barocke, V., Braun, D., Urtz, N., … Massberg, S. (2012). A novel role of sphingosine 1-phosphate receptor S1pr1 in mouse thrombopoiesis. *The Journal of Experimental Medicine*, *209*(12), 2165–2181. https://doi.org/10.1084/jem.20121090

Zheng, Y., Adams, T., Zhi, H., Yu, M., Wen, R., Newman, P. J., … Newman, D. K. (2015). Restoration of responsiveness of phospholipase Cγ2-deficient platelets by enforced expression of phospholipase Cγ1. *PLoS ONE*, *10*(3). https://doi.org/10.1371/journal.pone.0119739

Zimmerman, T. S., & Kolb, W. P. (1976). Human platelet-initiated formation and uptake of the C5-9 complex of human complement. *J Clin Invest*, *57*(1), 203–211. https://doi.org/10.1172/JCI108261